THE UNIVERSITY *of* EDINBURGH

PHYSICOCHEMICAL AND CRYSTALLOGRAPHIC INVESTIGATIONS INTO THE SALT FORMATION OF TWO HETEROCYCLIC DRUGS

DAVID ELDER

Thesis Presented for the Degree of

Doctor of Philosophy

University of Edinburgh

1992

To the memory of my father, Douglas Elder and my supervisor and friend, Ian Selby.

I heard the voice of Jesus say,
'I am this dark world's light;
Look into me, thy morn shall rise,
And all thy day be bright' :
I looked to Jesus, and I found
In him my Star, my Sun;
And in that light of life I'll walk
Till travelling days are done.

H Bonar, 1808-1889

Declaration

I declare that the work described in this thesis has not been submitted for any other degree and is the original work of the author except where acknowledgement is made by reference. This work was carried out in the Chemistry Department of Edinburgh University under the supervision of Dr R O Gould and at the Syntex Research Centre, Edinburgh under the supervision of the late Dr I A Selby and subsequently Dr J R Langridge.

D P ELDER, BSc, MSc, CChem, MRSC, MIQA

Acknowledgement

I would like to thank my internal supervisor Dr R O Gould for his help and encouragement during this work. Special thanks are due to the late Dr I A Selby, my external supervisor, whose enthusiasm and love of chemistry have made a lasting impression on me. His tragic death has made the world a poorer place and I will miss him as a colleague and friend. Thanks are also due to Dr J R Langridge for useful discussions and for stepping into the breach at the eleventh hour to act as my external supervisor.

I am indebted to my friends and colleagues at Syntex for helpful suggestions and encouragement, to Syntex for their financial support and for the provision of facilities and materials without which this project would not have been possible. I would also like to thank Professor C B Macfarlane for constantly challenging me and for helping to ensure the relevance of all areas of this project.

Worthy of special mention are Mr P J Spencer and Ms L Coleman for their technical assistance in producing graphs and diagrams. Having completed the practical work, the compilation of this manuscript would have been a daunting task without the expert typographical assistance of Ms G Billett and Ms L Donaldson. I am grateful for their humour, patience and hard work.

My thanks go to Drs P Taylor and A J Blake for technical assistance, training and enthusiastic encouragement.

Finally, an undertaking of this size and length, by part time study, required considerable disruption to normal family life. I will be eternally grateful for the understanding and love shown by my wife, Margaret

and children, Matthew and Sarah, which were critical to the completion of this work.

To my Lord, my thanks for your continual presence and love and the knowledge that in death you have given me life eternal.

Abstract

Salt formation provides a means of altering the physicochemical and resultant biological characteristics of a drug entity without modifying its molecular structure. Many published reviews have indicated the importance of the selection of the most appropriate salt form. This work is an investigation into the salt formation of two heterocyclic drugs. This is done by the physicochemical and the crystallographic studies of 19 high resolution single crystal diffraction studies.

The particular targets of the work are the selection of the most appropriate salt forms, investigations into the tautomerism and polymorphism (or pseudo-polymorphism) and an understanding of the interactions most likely between these heterocyclic drugs and their specific receptor sites.

Section 1 describes the effect of protonation on the absorption of drugs, the rationale for using various salt forms and the resultant effect this has on a number of physicochemical properties of the parent compound.

Section 2 is a description of the experimental techniques used in the physicochemical investigations and in crystal structure determination.

In Sections 3 and 7, the preparation and character-isation of the salts and modifications of the two heterocyclic drugs, GU and IM is described.

In Sections 4 and 8, the physicochemical investigations into the hygroscopicity and solid-state stabilities of the salts of GU and IM is described. Van't Hoff solubility studies are used to determine the enthalpies

of solution and where appropriate the relative thermodynamic stabilities of the various phases produced.

The structures of 19 of the salts or modifications of GU and IM, together with their packing and hydrogen bonding interactions is described in Sections 5 and 9.

Sections 6 and 10 describe the ionisation properties of these molecules. Both the guanidine and imidazole moieties of GU and IM, respectively, are tautomeric, the particular form(s) found in these investigations and the effect of protonation is discussed.

The conformations of these structures are discussed and the effect of protonation, especially on the puckering of the piperazine ring, is described.

INDEX

SECTION 1: INTRODUCTION 1
1.1 References 12

SECTION 2: MATERIALS AND METHODS 15
2.1 Materials 16
2.1.1 N^2-[3,5-Dichlorophenyl]-4-[4-hydroxy-2-methoxyphenyl]-1-piperazine carboxamidine (GU) 16
2.1.2 1-[[2-(4-Methylphenyl)-4-Methyl]-3H-imidazol-4-yl-methyl]-5-diphenylmethyl piperazine (IM) 16
2.1.3 Other Materials 20
2.2 Characterisation of Salts 21
2.2.1 Elemental Analysis 21
2.2.2 Karl Fischer Water Content 21
2.2.3 Nuclear Magnetic Resonance Spectroscopy 21
2.2.4 Basic Equivalence Factor 21
2.2.5 Differential Scanning Calorimetry 22
2.2.6 Melting Point 22
2.2.7 Infrared Spectroscopy 22
2.3 Chromatography 22
2.3.1 Liquid Chromatography 23
2.3.2 Liquid Chromatography Methodology for Salts and Modifications of GU and IM 25
2.4 Crystal Structure Determination 27
2.4.1 Introduction 27
2.4.2 X-Rays and X-Ray Diffraction 29
2.4.3 Determination of the Lattice Type and Unit Cell Dimensions 31
2.4.4 Selection and Orientation of a Crystal 31
2.4.5 Cell Dimensions and Density 32
2.4.6 The Deduction of a Trial Structure 33
2.4.7 Refinement of a Trial Structure 36
2.4.8 The Correctness of a Structure 37
2.4.9 Standard Procedures 38
2.5 Water Adsorption/Desorption Isotherms 39

2.6	Stability Studies	40
2.7	Van't Hoff Solubility Studies	40
2.8	References	42
SECTION 3: PREPARATION AND CHARACTERISATION OF SALTS AND MODIFICATIONS OF GU		44
3.1	Introduction	45
SECTION 4: PHYSICOCHEMICAL INVESTIGATIONS INTO SALTS AND MODIFICATIONS OF GU		56
4.1	Hygroscopicity/Efflorescence Studies on Salts and Modifications of GU	57
4.2	Stability Studies on Salts and Modifications of GU	70
4.2.1	Appearance of Stability Samples for Salts and Modifications of GU	70
4.2.2	Solid-State Reaction Kinetics	71
4.3	Van't Hoff Solubility Investigations on Salts and Modifications of GU	93
4.4	Physicochemical Properties of Salts and Modifications of GU	98
4.5	References	106
SECTION 5: CRYSTALLOGRAPHIC DATA FOR GU		108
5.1	GUFBHY	109
5.2	GUFBIP, GUFBIB and GUFBRIB	112
5.2.1	GUFBIP	112
5.2.2	GUFBIB	112
5.2.3	GUFBRIB	113
5.3	GUHFUMET	118
5.4	GUMACEHY	122
5.5	GUMASCHY	126
5.6	GUMHCLHYIP	137
5.7	GUDMES	140

5.8 GUDHCLHY 143
5.9 GUDSULF 146

SECTION 6: GENERAL DISCUSSION OF GU STRUCTURES 150
6.1 Introduction 151
6.2 GU Tautomerism 154
6.3 Guanidinium Cation 158
6.4 GU Conformation 159
6.5 GU Pharmacological Profile 164
6.6 References 172

SECTION 7: PREPARATION AND CHARACTERISATION OF SALTS AND MODIFICATIONS OF IM 178
7.1 Introduction 179

SECTION 8: PHYSICOCHEMICAL INVESTIGATIONS INTO SALTS AND MODIFICATIONS OF IM 190
8.1 Hygroscopicity/Efflorescence Studies on Salts and Modifications of IM 191
8.2 Stability Studies on Salts and Modifications of IM 201
8.2.1 Appearance of Stability Samples for Salts and Modifications of IM 201
8.2.2 Kinetic Modelling of Stability Data 202
8.3 Van't Hoff Solubility Investigations on Salts and Modifications of IM 220
8.4 Physicochemical Properties of Salts and Modifications of IM 229
8.5 References 234

SECTION 9: CRYSTALLOGRAPHIC DATA FOR IM 235
9.1 IMFBTOL 236
9.2 IMMMES 239
9.3 IMMHCLAC 243

9.4 IMTHCLHYA 247
9.5 IMTHCLHYB 251
9.6 IMTHCLHYC 255
9.7 IMTHCLHYD 259
9.8 IMTHCLHYE 263

SECTION 10: GENERAL DISCUSSION OF IM STRUCTURES 270
10.1 Introduction 271
10.2 IM Tautomerism 274
10.3 Imidazolium Cation 279
10.4 IM Conformation 282
10.5 References 285
APPENDIX A 287
APPENDIX B 298

SECTION 1 : INTRODUCTION

1. Introduction

All drugs have to cross cell membranes to be absorbed, distributed and eliminated from the body. The cell membrane is thought to be a bimolecular lipid layer associated with protein. The hydrophobic ends of the lipid molecules are orientated towards the centre of the bilayer and molecules crossing the membrane must first dissolve in the lipid. There are small pores in the membrane through which small water soluble molecules may diffuse through, *eg* Methanol.

There is also believed to be carrier mediated transport across the bilayer, but this is only generally important for drugs resembling some natural substances[1].

An indication of whether or not a drug will be transported across lipid membranes is given by its ability to partition effectively from an aqueous solution into a non-aqueous, organic solution. This is known as the partition coefficient and is usually determined by measuring the partitioning behaviour of a drug between an aqueous buffered solution and an immiscible organic solvent, such as octanol or chloroform at a constant temperature. The partition coefficient (P) is defined as the ratio of the concentrations of the same molecular species between two immiscible liquid phases at equilibrium, normally defined as:

$$P = \frac{[B]_{org}}{[B]_{aq}}$$

For compounds that are not charged, this *in vitro* condition also applies to partitioning within biological systems. Information on partitioning behaviour can be used to predict to what extent a drug might be metabolised, since it is lipid soluble drugs that are liable to undergo extensive metabolism[1].

This simplistic view of partitioning relates to drugs existing as a single molecular species in solution. Most drugs are organic molecules with one or more substituents on them, which confer acidic, basic or amphoteric properties. They exist in solution in equilibrium mixtures among forms of varying degrees of protonation. The terms acidic and basic are used for drugs whose uncharged forms have acidic or basic properties respectively:

Acidic Drug $\quad HA + H_2O \rightleftharpoons H_3O^+ + A^-$

$$Ka = \frac{[H_3O^+][A^-]}{[HA]}$$

Basic Drug $\quad HB^+ + H_2O \rightleftharpoons H_3O^+ + B$

$$Ka = \frac{[H_3O^+][B]}{[HB^+]}$$

Molecules which possess an electrostatic charge are more polar and tend to be hydrophillic. Uncharged molecules tend to be hydrophobic (or lipophilic). The degree of protonation of a drug is, therefore, very important as it dictates the amount of uncharged, lipid soluble drug available for dissolution in the lipid bilayer.

The uncharged form is assumed to be sufficiently lipophilic to transverse the membrane; if it is not, theory predicts that there is no absorption irrespective of pH.

The fraction of charged drug at the absorption site is controlled by both the pH and the pKa, where pKa ≡ -log (Ka), of the drug, according to the Henderson-Hasselbach equation[2]. Thus, for bases

$$pH = pKa + \log \left(\frac{\text{uncharged species concentration}}{\text{charged species concentration}}\right)$$

The pKa(s) is characteristic of a drug and is the pH at which equimolar concentrations of the uncharged and

charged drug exist. For those drugs that can exist as more than one species, at physiological pH, the degree of protonation must be considered when extrapolating *in vitro* partitioning behaviour to *in vivo* distribution of drugs into and across biological membranes. For compounds that protonate, the following relationship can be made:

For Bases $[BH^+]_{aq} \xrightarrow{Ka} [B]_{aq} \xrightarrow{P} [B]_{org}$

where Ka is the dissociation constant and P is the partition coefficient. The greater the degree of protonation, the lower the effective partition coefficient, commonly known as the distribution coefficient (D) given by:

$$D = \frac{[B]_{org}}{[B]_{aq} + [BH^+]_{aq}}$$

Therefore, D is pH dependent and can be calculated from the pKa and P and any pH value:

$$\log D = \log P - \log [1 + \text{antilog } (pKa - pH)]$$

The pH range 1.0 to 8.0 encompasses the changes in pH seen in the gastrointestinal tract and at other absorption sites. This leads to several consequences. First, very weak acids, such as Phenytoin and many barbiturates, whose pKa values are in excess of 7.5, are essentially unaffected by pH and for these acids absorption is independent of pH. Secondly, for acids with pKa values in the range 2.5 to 7.5, the fraction of uncharged species changes dramatically with pH and for these compounds a change in the rate of absorption with pH is expected and has been observed. Thirdly, absorption of very strong acids (pKa less than 2.5) is slow, even under acidic conditions.

A similar analysis indicates that only in very weak bases, eg Caffeine (pKa 0.5), is absorption independent of pH. At the low pH of gastric fluid, most bases exist almost exclusively in the cationic form and for these, gastric absorption should be low. Absorption of these bases should be more rapid from an alkaline environment.

Despite its general appeal, this theory fails to explain certain observations. A variety of quaternary ammonium compounds (charged at all values of pH), elicit systemic effects when given orally. Animal studies also indicate penetration of the charged form of many acids and bases through the intestinal epithelium, though more slowly than the uncharged form. Whether these protonated species transverse the membrane through aqueous pores, through ion specific channels or by carrier mediated transport processes, is not fully understood.

In accordance with predictions of the pH partition theory, weak acids are absorbed more rapidly from the stomach when the pH of the contents is closer to 1 than to 8 and the converse holds for weak bases. Absorption of acids, however, is always much faster from the more alkaline small intestine (pH 5-7) than from the stomach[4].

These apparently conflicting observations can be reconciled if one considers comparative surface area. The total absorptive area of the small intestine has been calculated to be about 200 m^2, with a blood flow of 1 litre.min^{-1}, corresponding estimates for the stomach are 1 m^2 and 0.15 litre.min^{-1}. These increases in surface area and blood flow more than compensate for the decreased fraction of uncharged drug in the small intestine. Indeed, the absorption of all compounds

acidic, neutral or basic is faster from the small intestine.

Absorption following administration of a solid dose form is a two step procedure:

Solid Drug $\xrightarrow{\text{dissolution}}$ Drug in Solution $\xrightarrow{\text{entry into the body}}$ Absorbed Drug

There are two rate-limiting variables affecting absorption, (i) transmembrane rate-limited absorption and (ii) dissolution rate-limited absorption.

In the former case, the drug is very soluble, eg Neomycin and the rate of dissolution >> rate of absorption. In the latter case, the drug is poorly soluble, absorption cannot proceed any faster than the dissolution rate. In this case, changes in dissolution profoundly affect the rate and sometimes the extent of drug absorption.

As a general rule, salts of drugs exhibit higher dissolution rates than the corresponding conjugate acid or base, at equivalent pH, even if the aqueous solubility is comparable. The explanation of this is given by Nernst and Brunner[5] in their diffusion layer model of dissolution:

$$\frac{dw}{dt} = \frac{D\ S\ (C_s - C)}{h}$$

where w is the amount of solute dissolved at time t, dw/dt is the rate of mass transfer per unit time, D is the diffusion coefficient of the solute, S is the surface area of the dissolving solute, C is the concentration of the drug in the bulk solution and C_s is the concentration of the drug in the diffusion layer, h is the thickness of the diffusion layer.

The driving force of the above process is the difference between C_s and C. If the drug is not readily absorbed, then C rapidly increases to the same level as C_s and the rate of dissolution is reduced. Absorption is then said to be transmembrane rate-limited. If the absorption rate is rapid then $C_s >> C$ and the process of absorption is said to be dissolution rate-limited. However, in either case an increase in C_s increases the dissolution rate. Salts increase the value of C_s by acting as their own buffers, altering the pH of the diffusion layer and maximising the solubility of the drug[6]. The salt form of a drug generally has a higher aqueous solubility than the corresponding uncharged form due to strong ion-dipole interactions with water.

Miller and Holland[7] stated that different salts of the same drug rarely differ pharmacologically, the differences are usually based on the physical properties. The salt form is known to influence a number of physicochemical properties of the parent compound including dissolution rate, solubility, stability, melting point and hygroscopicity. These properties in turn affect the processing properties and bioavailability of the drug. Consequently, the pharmaceutical industry has systematically engaged in studies of the physicochemical properties of the uncharged drug and its salts, to determine the most suitable form for drug formulation.

Juncher *et al*[8], demonstrated that the plasma levels of Penicillin V, obtained on administration of three different salts and the free acid, were in the same order as their *in vitro* dissolution rates. Nelson *et al*[9] showed that the *in vitro* dissolution rate of sodium Tolbutamide was 5000x more rapid than the free acid and when plasma levels were compared, these findings were correlated.

Occasionally, some studies show that salt formation can actually decrease the dissolution rate of the drug and its subsequent absorption. This was found for aluminium acetylsalicylate[10], sodium Warfarin[11] and Benzphetamine pamoate[12]. This reduction in dissolution rate was apparently the result of precipitation of an insoluble film on the surface of the tablets, reducing the effective surface area and retarding deaggregation of the particles.

Solubility is also a factor affecting the stability and the formulation of the drug. The solubility of the compound is dependent upon the physical and chemical properties of the solute. For instance, within a series of compounds, a lowered melting point would indicate a decrease in lattice energy and would possibly be reflected in an increase in solubility.

Investigations into the formation of salts of Triamteren indicated that the organic acid salts were more soluble than the corresponding mineral acid salts. In a similar study, the aqueous solubility of a series of 35 salts of the antibacterial Chlorohexidine were investigated[14]. The inorganic salts were poorly soluble. Increasing the hydroxylation (particularly with the sugar acids) of the organic counter ion markedly increasing aqueous solubility.

Several reports showed that the structure of the anion influences the aqueous solubility of the resultant salts. Investigations into the properties of the salts of the weak bases Erythromycin[15] and Lincomycin[16] demonstrated that the aqueous solubility was dependent on the size of alkyl substituents of the anion.

For certain products, such as sustained release dose forms, for suspensions and for taste masking; a reduction in the aqueous solubility is desired. This

may be attained by use of an appropriate salt form. Many problems concerned with the formulation and subsequent stability of topical and oral formulations, containing Bacitracin were overcome by the use of the zinc salt[17]. A substantial advantage over the parent compound is its relative insolubility and consequent lack of taste. A similar approach was used for Propoxyphene[18]; the napsylate is practically water insoluble as compared to the highly water soluble, bitter tasting chloride and can thus be formulated into flavoured, aqueous suspensions. The taste of these suspensions can be markedly improved by the addition of sodium or calcium napsylate, as a common ion to depress solubility further.

Another approach is to select a salt form that will pharmacologically antagonise an unfavourable property (such as taste) of the parent compound. Salts of N-cyclohexylsulphonic acid (cyclamates), have a characteristic sweet taste which can be used to antagonise bitter tasting drugs. The cyclamates of Dextromethorphan and Chlorpheniramine[19,20] exhibit greatly improved bitterness thresholds and enhanced solubility properties, compared to commonly occurring salts.

Systematic investigations of the thermal and photolytic stabilities of the investigative drug candidate and its salts provide essential input towards the choice of the most suitable derivative and dosage form.

Different salt forms impart differing stability characteristics to the parent drug. An orally administered drug must be stable in acidic environments, as generally it must pass intact through the stomach if it is to be absorbed. Erythromycin estolate[21] (lauryl sulphate) has lower solubility and is thus more stable than the free base form. Therefore,

it retains its potency even when exposed to acidic environments for extended periods of time, it can thus be co-administered with food without any decrease in drug plasma levels.

Amorphous calcium Novobiocin is tasteless, yet stable and biologically active in an aqueous suspension. The sodium salt is chemically unstable, while the free acid is not absorbed. The amorphous calcium salt does, however, slowly convert into the non-absorbed, crystalline phase as it is a metastable form[22].

Penicillin G is a therapeutically important drug which is very unstable, with a half-life of <2 weeks at 4°C[23]. Suspensions of the sparingly soluble amine salts, eg procaine, benzathine and hydrabamine salts, improve the stability sufficiently to allow the product(s) to be marketed.

Differences in hygroscopicity of salts will also influence the stability of drugs on storage. This is particularly relevant for drugs, such as Penicillin, which readily undergo hydrolysis. Several studies on the effects of moisture on salts of Penicillin have demonstrated this fact[24,25]. Potassium Penicillin G is much less hygroscopic than the sodium salt and has become the preferred marketed form in the dry state.

For salts of weak bases, the moisture associated with the drug can be very acidic and can potentially cause severe hydrolytic degradation. The stability of the thiamine salts are related to their hygroscopicity, solubility and resultant pH[26,27,28].

Walking *et al*[29] prepared a series of aryl sulphonic acid salts of Xilobam to protect the easily hydrolysed base.

Polar salts have a propensity to be hygroscopic, sometimes in the extreme, through favourable hydrogen bonding interactions with available atmospheric moisture. Thus, the very factors that promote high solubility can result in excessive problems of hygroscopicity and preclude their isolation and use in certain dosage forms. An excellent example is the gluconate salt of Chlorohexidine[14], which although demonstrated the highest attainable solubility, was unuseable due to its low melting point and high hygroscopicity.

A clear compromise of properties for the salt form is thus required, but the difficulty remains of assessing which salt forms are best to screen for a particular drug candidate[30].

1.1 References

1. ROWLAND, M and TOZER, T N in 'Clinical Pharmacokinetics, Concepts and Applications', 16, Lea and Febiger (Philadelphia), 1980

2. ALBERT, A A and SERJEANT, E P in 'The Determination of Ionisation Constants', 5, Chapman and Hall, New York, 1984

3. FLORENCE, A T and ATTWOOD, D in 'Physicochemical Principles of Pharmacy', 334, Macmillan, London, 1981

4. SCHANKER, L S, SHORE, P A, BRODIE, B B and HOGBEN, C A M, J Pharmacol, Exp Ther, 120, 528, 1957

5. NERNST, W and BRUNNER, E, Z Phys Chem, 47, 52, 1904

6. BERGE, S M, BIGHLEY, L D and MONKHOUSE, D C, J Pharm Sci, 66, 1, 1977

7. MILLER, L C and HOLLAND, A H, Mod Med, 28, 312, 1960

8. JUNCHER, H and RAASCHOU, F, Antibiot Med Clin Ther, 4, 497, 1957

9. NELSON, E, KNOECHEL, E L, HAMLIN, W E and WAGNER, J G, J Pharm Sci, 51, 509, 1962.

10. LEVY, G and PROCKNAL, J A, *ibid*, 51, 294, 1962

11. O'REILLY, R A, NELSON, E and LEVY, G, *ibid*, 55, 435, 1966

12. HIGUCHI, W I and HAMLIN, W E, *ibid*, 52, 575, 1963

13. DITTERT, L W, HIGUCHI, T and REESE, D R, *ibid*, 53, 1325, 1964

14. SENIOR, N, J Soc Cosmet Chem, 24, 259, 1973

15. JONES, P H, ROWLEY, E K, WEISS, A L, BISHOP, D L and CHUN, A H C, J Pharm Sci, 58, 337, 1969

16. Chem Abstr, 75, 40421t, 1971

17. GROSS, H M, Drug Cosmet Ind, 75, 612, 1954

18. GRUBER, C M, STEPHENS, V C and TERRILL, P M, Toxicol Appl Pharmacol, 19, 423, 1971

19. CAMPBELL, J A and SLATER, J G, J Pharm Sci, 51, 931, 1962

20. CAMPBELL, J A, *ibid*, 51, 270, 1962

21. STEPHENS, V C, CONINE, J W and MURPHY, H W, J Am Pharm Assoc, Sci Ed, 48, 620, 1959

22. MULLINS, J D and MACK, T J, *ibid*, 49, 245, 1960

23. SCHWARTZ, M A and BUCKWALTER, F H, J Pharm Sci, 51, 1119, 1962

24. WOODWARD, W A, J Pharm Pharmacol, 20, 197, 1947

25. JOHNSON, C A in 'Advances in Pharmaceutical Sciences', Vol 2, Academic Press, New York, 227, 1967

26. Chem Abstr, 67, 102734t, 1967

27. *ibid*, 64, 4874c, 1966

28. BIRD, J C and SHELTON, R S, J Am Pharm Assoc, Sci Ed, 39, 500, 1950

29. WALKING, W D, REYNOLDS, B E, FEGELY, B J and JANICKI, C A , Drug Dev Ind Pharm, 9, 809, 1983

30. GOULD, P L, Int J Pharm, 33, 201, 1986

SECTION 2: MATERIALS AND METHODS

2.1 Materials

2.1.1 N^2-[3,5-Dichlorophenyl]-4-[4-hydroxy-2-methoxyphenyl]-1-piperazine carboxamidine (GU)

GU was synthesised as the hydrate by J C Pascal[1] of Syntex in 1986, as a potential antiarrhythmic agent with class I and class III activities as proposed by Vaughan Williams[2]. Its Syntex code is RS-87337-000 and it is referred to generically here as GU.

A drawing of the molecular structure, together with the numbering system used during the crystallographic investigations, is given as Figure 2.1.1. In each ring, the last digit of the name corresponds to the chemical ring position. The hydrate is a white crystalline powder, melting at 132.0-134.0°C, with decomposition. Its acid/base properties are further discussed in Section 6.1.

2.1.2 1-[[2-(4-Methylphenyl)-4-Methyl]-3H-imidazol-4-yl-methyl]-5-diphenylmethyl piperazine (IM)

Although Elguero *et al*[3] suggest that the numbering of the imidazole ring system should begin with the pyrrole nitrogen, IUPAC still accepts the alternative system of nominating the pyrrole nitrogen by use of 1H or 3H. The latter system was adopted for the present investigations.

The alternative numbering system, *viz* 1-[[2-(4-methylphenyl)-5-methyl]-1H-imidazol-4-yl-methyl]-4-diphenyl methyl piperazine was adopted for the patent application[4]. IM was synthesised by J C Pascal of Syntex in 1989 as the anhydrous free base (-000). It is a novel compound with sodium/calcium ion channel modulating properties, with the potential to prevent neuronal cell death in ischaemic cerebral tissue. It is being developed for the treatment of acute focal cerebral ischaemia (stroke).

It is referred to generically here as IM.
A drawing of the molecular structure, together with the numbering used during the crystallographic investigations, is given as Figure 2.1.1.

The free base can exist as one of two polymorphs dependent upon the nature of the crystallisation solvent used in the final step of the synthesis. Crystallisation from water, produces the metastable lower melting (186°-187°C), Phase B polymorph. Crystallisation from dimethylformamide, produces the stable, higher melting (236°-238°C), Phase A polymorph.
Heating of the Phase B polymorph past its melting point, results in a solid-state phase transition and the production of the more stable Phase A (see Figure 2.1.2).
The monomesylate salt is a white crystalline powder, melting at 203.6-204.0°C.
Similarly, the trichloride salt is a white crystalline powder, melting at 210-213°C, with decomposition.

Its acid/base properties are further discussed in Section 10.1.

Figure 2.1.1 Structure and Numbering System used in Crystallographic Investigations of a) GU b) IM

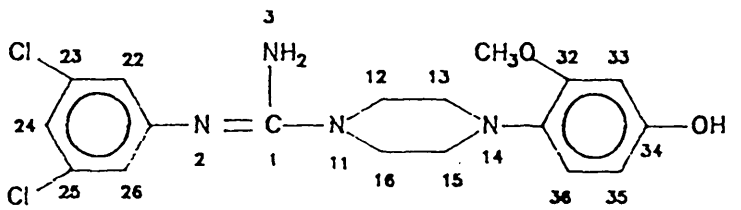

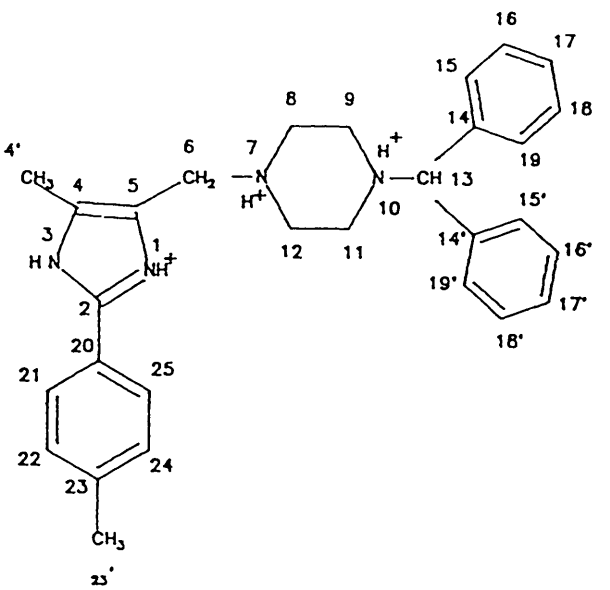

Figure 2.1.2 DSC Heating Curve of (a) IMFBA (b) IMFBB

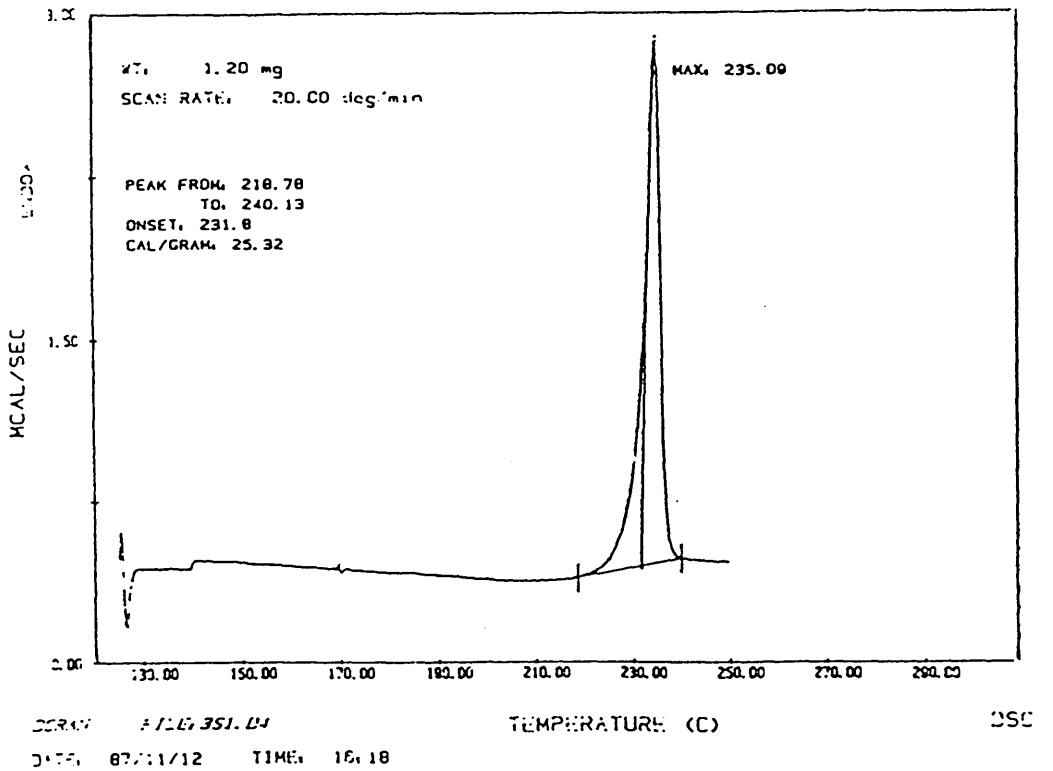

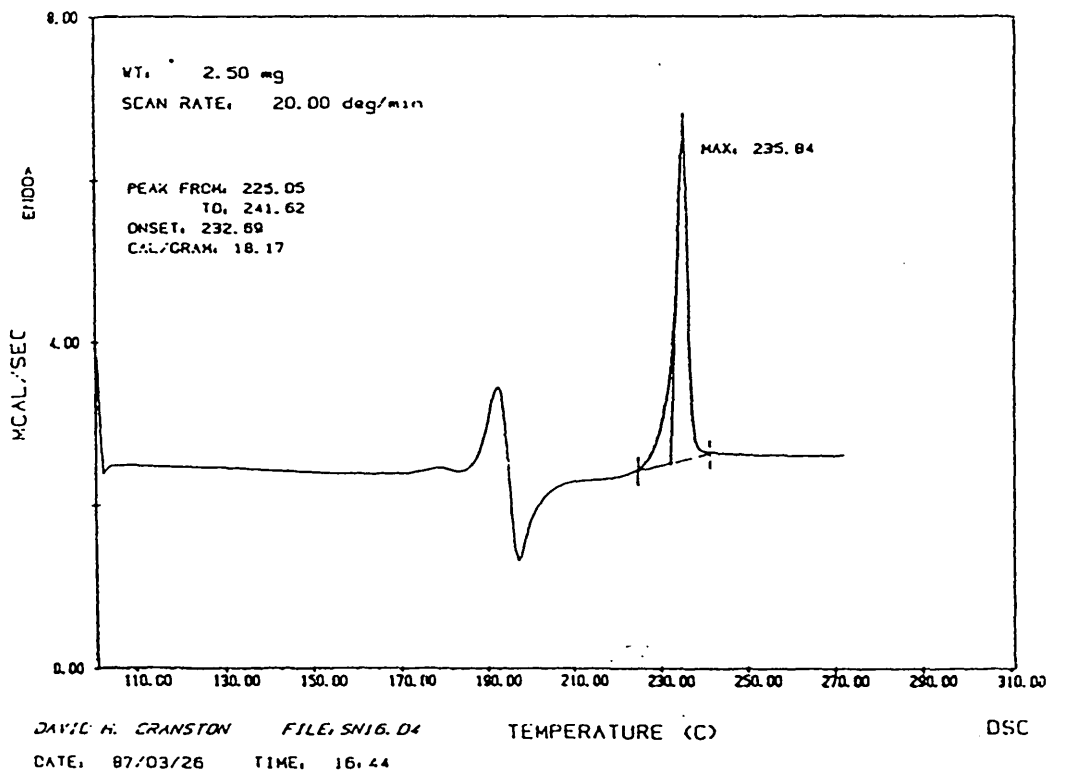

2.1.3 Other Materials

A range of organic and inorganic acids were used in the preparation of a variety of salts of GU and IM. Physico-chemical properties[5] of these acids are summarised in Table 2.1.3.

A wide range of solvents were used. All were of AR or HPLC grade, as appropriate. HPLC grade reagents were supplied by Rathburn Chemicals, Walkerburn, Scotland.

Table 2.1.3 Physico-chemical Properties of Organic and Inorganic Acids Used

Acid		pka(s) at 25°C	Formula	Fw	mp(°C)	Supplier F ≡ Fisons A ≡ Aldrich B ≡ BDH
Organic						
Acetic		4.8	CH_3COOH	60.05	17	F
Ascorbic (L)		4.2	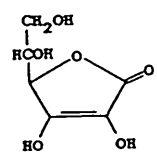	176.12	193(d)	A
Citric	1	3.1	$HO_2C\ CH_2C(OH)$	192.13	153	F
	2	4.8	$(CO_2H)\ CH_2\ CO_2H$			
	3	6.4		90.08	110	A
Lactic	1	3.9	$CH_3\ CH(OH)\ CO_2H$			
Fumaric (trans)	1	3.0	$(:CH.CO_2H)_2$	116.07	286-7(d)	B
	2	4.4				
Maleic (cis)	1	1.9	$(:CH.CO_2H)_2$	116.07	130.5	B
	2	6.2				
Malonic	1	2.9	$CH_2:(CO_2H)_2$	104.06	130-5(d)	B
	2	5.7				
Oxalic	1	1.3	$(CO_2H)_2$	90.04	104-6	A
	2	3.8				
Tartaric (D)	1	3.0	$(CHOH.CO_2H)_2$	150.09	168-170	F
	2	4.4				
Inorganic						
Hydrochloric		-6.1	HCl (*Ca* 31%w/w)	36.46	-15	F
Methane Sulphonic		-1.2	CH_3SO_3H (99%w/w)	96.10	-	F
Nitric		-1.4	HNO_3 (*Ca* 70%w/w)	63.01	-42	F
Ortho-Phosphoric	1	2.1	H_3PO4 (*Ca* 85%w/w)	98.00	-	F
	2	7.2				
	3	12.4				
Sulphuric	1	-3	H_2SO4(98%w/w)	98.08	10	F

2.2 Characterisation of Salts

Each of the individualy prepared salts or solvated forms of the basic drug entity, were characterised using a variety of instrumental techniques.

2.2.1 Elemental Analysis

Samples were analysed by Butterworth Laboratories, 54-56 Waldegrave Road, Teddington, Middlesex, England. Duplicate carbon, hydrogen and nitrogen values (%w/w) were determined simultaneously, by standard procedures, using Perkin Elmer Elemental Analyzers, Model A or C. Found values were compared with the calculated values and are tabulated, in Sections 3.2 and 7.2 respectively, for the various compounds of GU and IM.

2.2.2 Karl Fischer Water Content

Samples (*ca* 200mg) were dissolved in modified Karl Fischer reagent (Fisons, Loughborough, England) and titrated, in duplicate, using a pre-calibrated Metrohm Karl Fischer Automat E-547 Unit. Found values of percent water are compared with calculated values and are tabulated, in Sections 3.2 and 7.2 respectively, for the various compounds of GU and IM.

2.2.3 Nuclear Magnetic Resonance Spectroscopy (NMR)

Salts of GU were prepared in d^6-dimethyl sulphoxide and those of IM in d^4 methanol. The resulting solutions were run on a Bruker WP-200SY, 200MHz NMR spectrometer.

2.2.4 Basic Equivalence Factor

The amount of base (Basic Equivalence Factor) in each of the samples was determined, using the appropriate HPLC

method.
Found values of Base Equivalence Factor are compared with calculated values, and are tabulated in Sections 3.2 and 7.2 respectively, for the various compounds of GU and IM.

2.2.5 Differential Scanning Calorimetry (DSC)

DSC heating curves were obtained on a Perkin Elmer DSC-4, using samples sizes of *ca* 2-3mg, heating rates of 20° min^{-1} and a sensitivity range of 5 $mcal.s^{-1}$.
(≡ *Ca* 21$mJ.s^{-1}$)

2.2.6 Melting Point (mp)

Capillary melting points were performed using a Gallenkamp Melting Point Apparatus, the heating rate being adjusted to 1.0° min^{-1} when the sample reached 10-20° below the anticipated melting point.

2.2.7 Infrared Spectroscopy (IR)

Samples were prepared as potassium bromide discs and run on a Philips PU 9516 Infrared Spectrophotometer, with air as the reference and over the range 4000 to 650 cm^{-1}.

2.3 Chromatography

The general chromatographic procedure requires that a solute undergo distribution between two phases, one of them fixed (*stationary phase*), the other moving (*mobile phase*). It is the mobile phase that transfers the solute through the medium until it emerges, separated from other solutes. Generally, the solute is transported through the separation medium by means of a flowing stream, either liquid (HPLC) or gaseous (GLC), known as the eluant. The stationary phase may act through adsorption as is the case

with activated alumina, silica gel and ion-exchange resins, or it may act by dissolving the solute thus partitioning the latter between the stationary and mobile phases. In the latter process, a liquid coating held on an inert support serves as the stationary phase.

Partitioning is the predominant mechanism of separation in gas-liquid chromatography, paper chromatography and in forms of column chromatography designated as liquid-liquid chromatography. In practice, separations frequently result from a combination of partition and adsorption effects.

2.3.1 Liquid Chromatography (HPLC)

This method is sometimes referred to as HPLC (high performance liquid chromatography). The liquid chromatograph consists of a pumping system, analyte (solute) injection device, chromatographic column, detector and electronic integration system. The high pressure pumping module delivers the mobile phase from a degassed solvent reservoir to the column, via an automated injection system, utilising a Rheodyne loop.

The columns used for analytical separations have small internal diameters (*ca* 2-5mm) and can be obtained in a variety of lengths (*ca* 100-300mm) and are made from stainless steel. Unless otherwise specified in the individual method, the column is maintained at ambient temperatures. Column technology is based on the use of small particle size packings (typically 3-10μm), that allow fast equilibrium between mobile and stationary phases. The use of small particle size stationary phases, thus requires the use of a high pressure pumping system, capable of exerting pressures in the region of 200 bar (2900 psi), to achieve the pre-requisite flow rates of several ml per minute. The stationary phase can be either

a liquid or polymer, either coated or chemically bonded to the surface of the support in a thin film that reduces mass transfer resistance, so that a fast equilibrium can be attained. In partition liquid chromatography, mobile and stationary phases of different polarity are used. If the mobile phase is polar and the stationary phase is non-polar, as is the case with chemically bonded, octadecyl silyl stationary phases (ODS), this is referred to as reverse-phase chromatrography.

Problems of peak asymmetry, encountered with polar drugs, such as alcohols and amines, may be overcome by the use of mobile phase additives for *in-situ* selectivity modification. In this process a mobile phase additive is selectively attracted to the stationary phase and forms a parallel layer. The solutes then partition between the mobile phase and the solvated stationary phase surface. Many additives can be used to affect selectivity and improve the chromatography, they are added as minor components of the mobile phase. For example alkylamines, such as triethylamine, are added to reduce peak tailing and are often referred to as amine modifiers[6,7].

Since analyte (solute) loadings on the column are low, sensitive detectors are required. The most commonly used detectors are the variable wavelength ultra-violet spectrometer, the differential refractometer and the fluorometer; less commonly used are various electro-chemical devices and the mass spectrometer. In general, the signal from the detector is amplified, before being fed to an electronic integration system for the automatic measurement of chromatogram peak areas. Both peak height and peak area (peak response, R_u) can be related to the sample concentration. The detector response may be calibrated by relating peak responses to a known concentration of reference standard (R_s), using either an external or internal standardisation procedure. Only the

former approach was used in this work.

One drawback of the method of external calibration is that accuracy and precision are dependent upon the reproducibility of analyte injection. In all cases the residual standard deviation was always <1%, for the reported data.

2.3.2 Liquid chromatography methodology for Salts and Modifications of GU and IM

The apparatus used included a six figure, pre-calibrated electronic Cahn micro-balance (Model 4700) and a Liquid Chromatograph comprising of a Kontron 420 high pressure pump module, a Kontron MSI 660 auto-injector, a LDC spectromonitor 3100, variable wavelength UV detector and an HP 3392A electronic integrator.

The reference standards were samples of GU or IM, or salts of the above, with a determined purity of 98-102%.

The mobile phase for GU determination was a solution containing 0.025 mol of triethylamine dihydrogen orthophosphate per litre of 38% v/v acetonitrile/water.

For IM determinations, the solution contained 0.04 mol of ammonium acetate and 0.036 mol of triethylamine acetate per litre of 60% v/v acetonitrile/water. The diluent for GU samples was the same as the mobile phase, whilst that for IM omitted the triethylamine acetate. Solutions were equilibrated at room temperature and vacuum degassed. The chromatographic operating conditions are summarised in Table 2.3.3. Duplicate injections of the appropriate reference standard were performed, until satisfactory precision was obtained (typically <1% residual standard deviation). Duplicate injections of the sample solutions, bracketted at regular intervals, with reference standard

injections, were performed. The value of GU or IM in the samples solution was calculated using the mean peak response of the reference standard, before and after the sample solution of interest. Assuming the following convention:

Rs: Peak response for GU or IM in reference standard

Ru: Peak response for GU or IM in sample

Ws: weight (mg) of GU or IM in reference standard

W : weight (mg) of GU or IM in sample

Then, $\frac{Ru \times Ws}{Rs}$ = mg recovered from sample (Wu)

$$\% \text{ label (purity)} = \frac{Wu \times 100}{W}$$

The specificity and statistical validation of these methods have been demonstrated[8,9].

Table 2.3.3 Chromatographic Procedures

Parameter	GU	IM
Reference standard and sample solution	100µg.ml^{-1}	100µg.ml^{-1}
Column Length	150mm	250mm
Column Internal Diameter	4.6mm	4.6mm
Stationary Phase (ODS)	Spherisorb II	Partasil III
Stationary Phase, Particle Size	5µm	10µm
Flow Rate	1.0ml.min^{-1}	1.5ml.min^{-1}
Injection Volume	20µl	20µl
Analyte amount	2µg	2µg
Detector Wavelength	243nm	276nm
Detector Sensitivity	0.2 Absorbance Units Full Scale	

2.4 Crystal Structure Determination

2.4.1 Introduction

A crystalline solid is one whose atoms are disposed in a regular three dimensional array. The atoms in this array are not static; each atom possesses thermal energy and vibrates about its mean position.
For a perfect single crystal, the regular arrangement of atoms in the crystal can be completely described by defining the unit cell, together with its symmetry operations and the positions in the cell of one 'asymmetric unit' of atoms. The asymmetric unit is often a single molecule or the group of molecules and ions making up the formula of the compound being studied.

Each unit cell has three reference axes, with directions being dependent on the symmetry, termed x,y and z. These reference axes are by convention right handed, the unit cell edges parallel to x,y and z are respectively a,b and c and the interaxial angles α, β and γ.
When elements in the unit cell have identical environments except for the orientation of that environment, they are described as symmetry related. The symmetry operators of a finite body must pass through a point (the centre of the body), such a combination of symmetry operators are known as a point group.

Crystallographers use the Hermann-Mauguin system to describe point group symmetries. In this system an n-fold rotation axis is represented simply by the number n and a n-fold rotary inversion axis by $\bar{n}$, the only exception being that $\bar{2}$ is written as m (mirror plane). A two-fold rotation axis indicates that rotation through 180° *i.e.* 360°/2, restores the original environment.
There are ten crystallographic point group symmetry operators which are defined as $1,2,3,4,6,\bar{1},m,\bar{3},\bar{4},\bar{6}$.
The symbol for a point group is obtained by combining the

symbols for the symmetry operators in a prescribed sequence. The combination of a rotation axis and a perpendicular mirror plane is indicated by a slanted line after the number (n) *e.g.*, 2/m.

It is conventional to group the crystallographic point groups into crystal systems, all having some elements of symmetry in common. The three crystal systems accounting for 95% of all organic structures are summarised below:

System	Characteristic Symmetry	Diffraction Symmetry	Lower Symmetry	Unit Cell
Triclinic	One fold symmetry only	1	1	$a\neq b\neq c$ $\alpha\neq\beta\neq\gamma$
Monoclinic	Two fold axis parallel to b	2/m	2 m	$a\neq b\neq c$ $\alpha=\gamma=90°$ $\beta>90°$
Orthorhombic	Three mutually perpendicular two fold axes	mmm	222 mm2	$a\neq b\neq c$ $\alpha=\beta=\gamma=$ 90°

There are additional Bravais lattices that are obtained by adding face-centring (designated F if all faces are centred and A,B or C, if only one pair of faces centred) and body centring (I), of certain of the seven space lattices. The distinguishable lattices for the most common crystal systems are listed below:

Triclinic P

Monoclinic P C

Orthorhombic P C F I

C in monoclinic can alternatively be A or I; C in orthorhombic can be A or B and P designates primitive.

Addition of translational symmetry elements, screw axes and glide planes, to these Bravais lattices gives the 230 crystallographic space groups. Some of these additional symmetry elements, also cause systematic absences in the diffraction pattern. As an example, for a two-fold screw

axis parallel to a, h in the h 0 0 reflections can only be even and for a glide plane perpendicular to a with b/2 translations (a b glide), k in the 0 k l reflections can only be even (the Miller indices, h,k and l are defined in the next section).

2.4.2 X-Rays and X-Ray Diffraction

Studies of the internal structure of crystals depend upon the use of a penetrating radiation that will enter the crystal and will display interference effects, as a result of scattering from the ordered arrays of the crystal lattice. X-rays have the necessary penetrating power and show interference effects since they have wavelengths in the angstrom range (10^{-8}cm). Diffraction effects occur when the crystal interferes with the X-rays, so that some of the scattered radiation is shifted out of phase with respect to other waves. If the crystal lattice did not have a spacing which was the same order of magnitude as the wavelengths of the X-rays, simple reflection and scattering of the X-rays would occur. The reflection is not in fact simple and is greatly disturbed by interference effects and results in both destructive (X-rays out of phase with one another) and constructive interference. The latter occurs whenever the phase of the beams scattered from successive layers is shifted by an integral multiple of wavelengths. This is the basis for Bragg's Diffraction Law where

$$n\,\lambda = 2d(hkl)\,\mathrm{Sin}\Theta \qquad \text{where } n = 1,2,3.....$$

and shows that for a given value of the X-ray wavelength (λ), measurement of Θ (angle between incident X-ray beam and lattice), gives information on the spacing between the lattice planes (d), where h, k and l are Miller Indices and indicate order with respect to x, y and z.

Rearrangement of the Bragg expression to

$$\lambda = \frac{2d}{n}(hkl)\ \text{Sin}\ \Theta$$

shows that the high order reflections from planes with a spacing d, can be treated as if they were due to first order reflections from planes with spacing d/n. Thus each reflection can be labelled using the Miller Indices (hkl) and a spacing d(hkl) can be associated with the reflection. Similar indexing of the reflections in the other layer lines is performed and all of the data is evaluated to deduce the internal structure of the crystal. The phenomenon of X-ray diffraction by crystals may be considered in terms of theory, analogous to diffraction by gratings and extended to 3-dimensions (von Laue) or in terms of reflections from planes through points in the crystal lattice (Bragg). These two treatments are equivalent.

The maximum number of reflections that can be measured for a crystal is $\cong 32\pi V/3\ \lambda^3 n$, where n=1 for a primitive cell, 2 for body or single face centring and 4 for full face centring. The integrated diffraction intensity data may require correction for a geometric factors, absorption and other effects. Atoms that have an absorption edge close to the incident radiation frequency, introduce an additional phase change, which is referred to as Anomalous Scattering. For such atoms the simple scattering factor (F) which is calculated on the basis that the electrons in the atom can be treated as free electrons, has to be modified to take into account the interaction of the incident X-rays with the bound electrons, it is this interaction that produces the absorption edge.

The crystal may also introduce partial polarisation into the unpolarised X-ray beam, as the crystal does not reflect waves vibrating in all directions with equal

efficiency. This causes a reduction in the intensity of the diffracted beam by a factor of $[(1+\cos^2 2\Theta)/2]$. This results in the greatest reductions in intensities for $2\Theta=90°$ and the least reductions for $2\Theta=0°$ or 180°. The intensities for low or high angle data are enhanced relative to those at intermediate levels.

Checks are also required for drift and bad reflections. In addition the amount of time the reciprocal lattice points spend in the reflecting position, the Lorentz Effect, enhances the intensities of high angle relections.

2.4.3 Determination of the Lattice Type and Unit Cell Dimensions

The analysis of a crystal structure consists of three general stages, the first of which is the experimental determination of the lattice type, and includes the determination of the unit cell dimensions.
Two types of experimental data can be derived from measurements of the diffraction pattern:
Firstly the angle or direction of scattering (2Θ) which can be used to measure size and shape of the unit cell. Plus the intensities of the diffracted beam, which give data on the positions of the atoms within the unit cell and eventually related information (such as vibration parameters, fractional occupancies and electron distribution).

2.4.4 Selection and Orientation of a Crystal

The crystal must of necessity be single, to maintain structural uniformity, not cracked or twinned and of an appropriate size (ideally 0.5 to 0.05mm).
The crystal is examined in plane polarised light; for all non-cubic crystals, there will only be certain

orientations of the crystal which do not alter the plane of polarisation. Thus, if a crystal is examined between crossed polars, sharp 'extinction' directions are observed, while multiple crystals display extinction from different parts of the crystal, in different positions.

The crystal is mounted about a suitable axis (usually parallel to a prominent edge) and an oscillation photograph taken. This ensure correct alignment and centring of the crystal about sensible axes and gives an indication of overall crystal quality. Poorly diffracting crystals may be rejected at this stage. Further photographs can be used to determine approximate unit cell dimensions, general symmetry elements and systematic absences. Certain space groups can be uniquely identified at this stage; the use of photographic methods provides good ancillary data and is a useful screening tool for the rejection of sub-standard crystals.

2.4.5 Cell Dimensions and Density

The crystal is then transferred to an automated 2- or 4-circle diffractometer for accurate unit cell dimensions. These are determined from accurately measured 2Θ values, as the 2Θ values are a function only of cell dimensions and wavelength of radiation used.

Given the unit cell volume (V) and the molecular weight (M), the number of molecules (Z) in the unit cell can be established from a knowledge of the density of the crystals, obtained by classical flotation methods. Z must have an integer value. The mass (in g) of the unit cell contents is MZ/N, where M is in daltons and N is Avogadro's Number (6.02×10^{23} mol^{-1}). If the unit cell volume is given in Å^3, then the density (ρ) (g cm^{-3}) is

$$\rho = \frac{MZ}{V} \times 0.1659$$

Conversely, the theoretical density can be determined by substituting different integer values of Z into the above equation, until physically sensible density values are achieved e.g. $\rho \equiv 1.2\text{-}1.5\ g.cm^{-3}$. These can be then compared with the measured or expected density values and discrepancies investigated. For instance, a low theoretical density could be indicative of an under-estimation of the theoretical molecular mass caused by the presence of unsuspected solvation or hydration.

2.4.6 The Deduction of a Trial Structure

The second stage in crystal structure analysis is the deduction of a suggested atomic arrangement. The intensities of the diffraction maxima corresponding to this arrangement can then be calculated and compared with the observed intensities. For the structure, the identity of the atoms present are known, but the positions are not; for the diffraction pattern, the structure amplitudes are known, but the phases and signs are not. The intensity of the diffracted beam is dependent on a number of factors, the amplitude and phase of the scattered wave and this in turn is determined by the arrangement of the atoms, relative to the plane in question. This may be expressed mathmatically for centrosymmetric crystals, by the Structure Factor (Fhkl)

$$Fhkl = \sum_{r=1}^{N} fr \cos 2\pi (hxr+kyr+lzr)\ Tr$$

where fr is the scattering factor for the r^{th} atom.

$2\pi(hxr+kyr+\ell zr)$ is the relative phase for the r^{th} atom.

xr, yr and zr are the atomic fractional coordinates for the r^{th} atom.

Tr is the temperature factor term, which is equivalent to $\exp(-2Br\ Sin^2\Theta/\lambda^2)$ with Br the isotropic temperature factor.

and N is number of atoms in half the unit cell.

Conversely, given a knowledge of the amplitude and phases of the scattered waves in reciprocal space, the electron density (ρ) at any point (x,y,z) in the unit cell of a centrosymmetric crystal may be determined

$$\rho\ (x,y,z) = \sum_h \sum_k \sum_l Fhkl \cos 2\pi\ (hx+ky+lz)$$

The expansion of the electron density distribution, $\rho(x,y,z)$ as a sum of the component density waves is fundamental for the X-ray analysis of complex crystals. Since the intensities can be measured, the relative magnitude of the Fourier coefficients, the structure amplitudes $|F(h,k,l)|$ can be obtained. However, to reconstruct the electron density distribution by adding the component waves, the sign of each F must be known. For non-centrosymmetric crystals, it is required that the amplitudes and their relative phases $\alpha(hkl)$ are known. The latter are not experimentally attainable. In the absence of phase or sign information, it is not known whether each component density wave starts at the origin with a maximum, minimum or some intermediate value. This is the fundamental problem of X-ray analysis - the *phase problem*.

The phase problem is overcome by the deduction of a trial structure, by one of several methods. The intensities of the diffracted maxima corresponding to this postulated arrangement, can then be calculated (Fcalc) and compared with the observed values (Fobs). The two basic approaches are Patterson and Direct Methods. Patterson methods are mainly applicable to structures containing heavy atoms or fragments of known structures.

Direct Methods are a series of analytical techniques which may be utilised to derive an approximate set of phases from which can be calculated a trial electron density map. Direct Methods utilises the facts that structural information is contained in the intensities of

the reflections, that electron density in a real structure cannot be negative and the origin can be fixed.

In practice Direct Methods are carried out on Normalised Structure Factors (E); this takes into account the fall off in the individual scattering factors (f) with increased scattering angle (2Θ). E represents the ratio of F to {F}, where {F} is the r.m.s value of |F| in the given range, $\sin\Theta/\lambda$. Once a table of E values has been produced, only about the strongest 10% are considered. Then a triple product sign relationship is applied, *viz*

$$s(h,k,l).s(h',k',l').s(h-h', k-k', l-l') \propto +1$$

where s is the sign and h,k,l, are all strong reflections.

Here a group of three reflections, all having related indices are selected and since each of the three reflections in a triple phase product has a high E value, the product of their signs are probably positive.

An electron density map (E-map) is then generated using Fourier methods, based on the highest figure of merit. These are numerical quantities used for indicating comparative effectiveness, in this context it is used to indicate an estimate of the average precision in the selection of the phase angles.
The E-map is then interpreted, attempting to elucidate trial structures that make chemical sense. Sometimes, only part of the structure is revealed in an interpretable fashion and the rest is located by iterative procedures.

2.4.7 Refinement of a Trial Structure

After approximate positions have been determined for most, if not all of the atoms; refinement of the structure can proceed. In this procedure the atomic parameters are varied in a systematic fashion, so as to give the best possible agreement of the observed structures factor amplitudes with those calculated for the proposed structure. There are two refinement techniques, one involving Fourier syntheses and the other a Least Squares process. The former is normally only used to complete a partial structure.

The Least Squares procedure utilises the fact that there are many more observations than parameters to be determined, in any crystal structure analysis. Minimising the sum of the squares of the discrepancies between the $|Fobs|$, or $|Fobs|^2$, and those calculated for the trial structure, $|Fcalc|$, produces the best parameters for the model structure.

The discrepancy index (R) is a measure of the correctness of a given structure determination. The smaller the value of R, the better the fit between calculated and observed data.

$$R = \sum_{i=1}^{n} W\ (Yi\ obs - Yi\ calc)^2$$

where W is the weighting factor and is in principle inversely proportioned to σ^2 for each measurement.

The parameters that are normally refined are:

1) Overall scale factor, which relates $|Fobs|$ to $|FCalc|$
2) Atom scattering factor (f), which is related to the atomic number and is normally assumed to be constant.
3) Positional parameters for each atom, with three

parameters per atom, relating to the x,y and z coordinates.
4) Site Occupancy, which for most structures equals one, but may be less if disorder is encountered.
5) Temperature Factors, which show how atoms vibrate and may be treated as isotropic or anisotropic.
In the former, atoms are treated as spheres and a single temperature factor for each atom is required. In the latter, where atoms are treated as ellipsoids, six parameters are required to determine electron density.

For a typical structure, the total number of parameters (M) to be considered is:

$$M = 1 + 3n + n_i + 6n_a$$

(Scale + Number of Atoms + Isotropic Atoms + Anisotropic Atoms)

Relevant chemical knowledge, relating to the geometry of rigid and semi-rigid groups may be employed. For example the geometry of methyl, methylene, methine and aromatic groups are well established and the hydrogens can be constrained to idealised positions.
To complete the structure the hydrogens are located and placed into the trial structure.

2.4.8 The Correctness of a Structure

The following criteria should all be applied
1) The agreement of individual structure factor amplitudes with those calculated for the refined model should be consistent with the estimated precision of the experimental measurements. The R factor must be low.
2) A difference map, phased with final parameters for the refined structure, should reveal no fluctuations in electron density, greater than those expected based on the estimated precision.
3) The refinement must have converged.

4) The model must make chemical sense, with sensible values for bond lengths, bond angles, torsion angles, thermal motion and molecular geometry interactions.

2.4.9 Standard Procedures

The following Standard Procedures were used in all structures, unless otherwise stated in the appropriate Section.
No absorption corrections were applied, scattering factors and anomalous corrections from International Tables for X-Ray Crystallography[10]. Structure solution by Direct Methods (SHELX84 or SHELX86[11,12]), most non-hydrogen atoms being located in the first E-map, and the rest in the first difference Fourier synthesis.
Non-hydrogen atoms refined anisotropically, hydrogen atoms bonded to carbon included in calculated positions and allowed to ride (C-H 1.08Å, geometry constrained to trigonal or tetrahedral as appropriate. Methyl groups were initially placed, where possible, in a fully staggered conformation and sometimes allowed to rotate as a fixed group). Positions of other hydrogen atoms were refined. All hydrogens were assigned a fixed isotropic thermal parameter (U) of 0.05Å^2. Full matrix least-squares refinement (SHELX76[13]), was employed.
Derived bonds, angles and torsion angles obtained using CALC[14]. Perspective drawings of single molecules of GU, projected into the plane of the guanidine group [C(1), N(2), N(3) and N(11)]; together with anions and related solvent molecules (if appropriate), were determined using PLUTO[15].
For IM, the drawings were projected into the plane of the piperazine ring, [N(7), C(9) and C(11)].
Molecular packing diagrams were viewed down an appropriate crystallographic axis and the unit cell was superimposed onto the diagrams, for the sake of clarity.
Fractional Coordinates are given in Appendix A for GU

structures and Appendix B for IM structures.

2.5 Water Adsorption/Desorption Isotherms

The water adsorption (hygroscopicity) and desorption (efflorescence) isotherms of the various salts, were determined gravimetrically.
Samples (*ca* 500mg) were gently ground and pre-dried in a vacuum desiccator, placed in glass weighing crucible(s) of dimensions, d=40mm h=35mm and accurately weighed. The samples were weighed using a Sartorius 2004 MP, electronic, 5 figure, pre-calibrated balance. Based on a 500mg sample size, each weighing should be accurate to +/- 0.002% w/w.
The samples were exposed to different relative humidity (RH) environments in equilibrated hygrostats, using saturated salt solutions to maintain the appropriate humidity[16]. The various relative humidity environments are details below:

25°C/87% RH (saturated sodium carbonate $10H_2O$)
25°C/75% RH (saturated sodium chloride)
25°C/52% RH (saturated magnesium nitrate)
25°C/20% RH (saturated potassium acetate)

The crucibles were weighed on a periodic basis, over a six day period. The % w/w weight gain (loss) at each time point was then calculated.
The efflorescence properties of the various salts were studied by transferring crucibles from one environment to the next lowest environment *ie* 87% RH to 75% RH. The samples were again weighed on a periodic basis, over a seven day period. The % w/w weight gain (loss) at each time point was then determined.
Water adsorption/desorption isotherms were then constructed for all samples.

2.6 Stability Studies

Raw material stability studies were carried out on samples of all of the isolated modifications and salts of GU and IM. The samples were gently ground and pre-dried in a vacuum desiccator. The samples (*ca* 500mg) were placed in small glass containers, which were stoppered for thermal studies and open for the humidity studies. Samples used for light investigations were placed in sealable, clear plastic envelopes. Samples were stored under the following controlled conditions:

1	25°C
2	40°C
3	50°C
4	70°C
5	100°C
6	25°C/87% RH (RH)
7	South Facing Window Light (Lt)
8	Ultra-Violet Light (366nm, Hυ)

The samples were assayed in duplicate, by the appropriate HPLC methodology, on a regular basis. Since the relative stability of the samples were unknown, initially; analyses were carried out after 1,2,3,4,12 and 26 weeks. This sampling interval was later adjusted to, once every 4 weeks, for 24 weeks.
The mean, % label recovery of all samples, at the individual storage conditions and appropriate time points were then plotted as a function of time.

2.7 Van't Hoff Solubility Studies

Van't Hoff[17] demonstrated that the natural logarithm of the molar solubility (ln C_s) varies as a function of the reciprocal of absolute temperature (T) according to the equation:

$$\frac{d(\ln C_s)}{d\ (1/T)} = -\frac{\Delta H_s}{R} \qquad \text{.....Van't Hoff Isochore}$$

Where R is the Universal Gas Constant and ΔH_s is the enthalpy of solution.

This equation can be used to determine the enthalpy of solution (ΔH_s) from the slope of the Van't Hoff plot. Van't Hoff solubility studies were carried out on all salts and modifications of GU and IM. The samples were gently ground and pre-dried in a vacuum desiccator and placed in small, screw topped glass containers with rubber septa and a capacity of *ca* 4ml. The appropriate solvent was added slowly, at the appropriate temperature.

The containers were sealed and mixed for several minutes, additional solute was added until a solid residue was always present. The containers were then placed in an orbital tube rotator at 25 rpm for 72 hours at the appropriate temperature, additional solute being added if total dissolution occurred. Solubilities were determined at 4, 24, 40 and 48°C. Water was the solvent of choice for all GU samples and ethanol for all IM samples. Water was used initially for the IM samples, but the free base modifications were too insoluble ($\leq 100 ng.ml^{-1}$) and the protonated samples were too soluble ($> 10 mg.ml^{-1}$), for this to be a practical proposition.

At the end of the study, aliquots of the supernatant were filtered through a Millipore *Millex*^{R}*-H* 0.45µm filter unit into a pre-tared volumetric flask then diluted and assayed using the relevant HPLC methodology, versus a free base standard. The solubilities thus determined are expressed in terms of the free base and Van't Hoff plots were constructed for all samples.

2.8 References

1. PASCAL, J C, European Patent Application EP 204265 (CI C070295/20), 1986

2. VAUGHAN WILLIAMS, E M, Advances in Drug Res, 9, 69 1974

3. ELGUERO, J, MARZIN, C, KATRITZKY, AK and LUNDA, P (Eds) in 'The Tautomerism of Heterocycles' (Advances in Heterocyclic Chemistry, Supplement 1), 4, 1976, Academic Press, New York

4. PASCAL, J C, LEE, C-H, ALPS, B H, PINHAS, H and WHITING, R L, United States Patent Application 4,829,065, 1989

5. LANGE, N A in 'Handbook of Chemistry, Revised 10th Ed,' 1967, McGraw-Hill, New York

6. COOKE, N H C and OLSEN, K, AM Lab, 11, 451, 1979

7. GOLDBERG, A P and ROWSELL, D G, LC, 2, 736, 1984

8. ELDER, D P and BARRON, M, Personal Communications, 1985

9. SMITH, D, Personal Communications, 1987

10. International Tables for X-Ray Crystallography, Vol IV, 1974, Kynoch Press, Birmingham

11. SHELDRICK, G M, SHELX84, Program for Crystal Structure Solution, University of Göttingen, Federal Republic of Germany, 1984

12. SHELDRICK, G M, SHELX86, *ibid*, 1986

13. SHELDRICK G M, SHELX76, Program for Crystal Structure Determination, University of Cambridge, UK, 1976

14. GOULD, R O and TAYLOR, D, CALC, Interactive Program for Molecular Geometry, University of Edinburgh, UK, 1983

15. MOTHERWELL, W D S and CLEGG, W, PLUTO, Program for Plotting Molecular and Crystal Structures, University of Cambridge, UK, 1978

16. STOKES and ROBINSON, Ind Eng Chem, 41, 2013, 1949

17. ATKINS, P W in 'Physical Chemistry, 2nd Ed', 268, 1982, Oxford University Press, Oxford

SECTION 3 : PREPARATION AND CHARACTERISATION OF SALTS AND MODIFICATIONS OF GU

3.1 Introduction

In this section, the codes used for the salts and modifications of GU that were prepared and subsequently characterised, are as follows.

The first two letters, GU, refer to the guanidine moiety, which is a principal salt forming group in the molecule. The next letter(s), indicate the protonation state of the compound; FB ≡ Free Base, M ≡ Monoprotonated, H ≡ Hemiprotonated, S ≡ Sesquiprotonated, D ≡ Diprotonated and T ≡ Triprotonated.

This is followed, in the case of the protonated compounds, by the code designating the anion; FUM ≡ Fumarate, CIT ≡ Citrate, ACE ≡ Acetate, HCL ≡ Chloride, ASC ≡ Ascorbate, MAL ≡ Maleate, MALN ≡ Malonate, MES ≡ Mesylate, NIT ≡ Nitrate, SULF ≡ Sulphate and PHOS ≡ Phosphate.

Finally, the presence of solvation (or hydration) is indicated by; HY ≡ Hydrate, ET ≡ Ethanol, IP ≡ Isopropanol, SIB ≡ S-Isobutanol, RIB ≡ R-Isobutanol and IPE ≡ Isopentanol.

Some examples are:
GUFBSIB ≡ S-isobutanol solvate of the free base
GUHFUMET ≡ ethanol solvate of the hemifumarate salt
GUMMALNIP ≡ isopropanol solvate of the monomalonate salt
GUDMES ≡ dimesylate salt

Table 3.1 Preparation of Salts and Modifications of GU

Compound	Stoichiometry	Base (mmole)	Acid (mmole)	Solvent	% Yield	Comments
Modifications						
GUFBHY	$C_{18}H_{20}Cl_2N_4O_2.H_2O$	2.42	-	Acetone/Water (50/50 v/v) 25 ml, 60°C	84.0	Crystal quality good enough for structure determination.
GUFBIP	$C_{18}H_{20}Cl_2N_4O_2$ $.2C_3H_8O$	2.42	-	Isopropanol 50 ml, 60°C	76.4	Crystal quality good enough for structure determination.
GUFBIB	$C_{18}H_{20}Cl_2N_4O_2$ $.2C_4H_{10}O$	2.42	-	Isobutanol 50 ml, 80°C	72.7	Crystal quality good enough for structure determination.
GUFBRIB	$C_{18}H_{20}Cl_2N_4O_2$ $.2(R)C_4H_{10}O$	0.48	-	R-Isobutanol 10 ml, 80°C	79.3	Crystal quality allowed a unit cell to be determined, but not good enough for structure determination.
GUFBSIB	$C_{18}H_{20}Cl_2N_4O_2$ $.2(S)C_4H_{10}O$	0.51	-	S-Isobutanol 10 ml, 80°C	71.7	Crystal quality allowed a unit cell to be determined, but not good enough for structure determination.
GUFBIPE	$C_{18}H_{20}Cl_2N_4O_2$ $.2C_5H_{12}O$	2.42	-	Isopentanol 50 ml, 100°C	62.1	Crystallisation only with aid of scratching. Poor quality, small crystals.
GUFBN[1]-Alcohol	$C_{18}H_{20}Cl_2N_4O_2$ $.CH_4O$ - $.C_4H_{10}O$	2.42	-	n-alcohol 50 ml, 60-80°C	-	No product produced.

[1] GUFB formed alcohol solvates with all of the iso-alcohols used, from isopropanol to isopentanol. With the corresponding n-alcohols; methanol, ethanol, n-propanol, n-butanol - no product was produced.

Table 3.1 Preparation of Salts and Modifications of GU (continued)

Compound	Stoichiometry	Base (mmole)	Acid (mmole)	Solvent	% Yield	Comments
Salts						
Monoprotonated						
GUHFUMET	$2(C_{18}H_{21}Cl_2N_4O_2)^+ .C_4H_2O_4^{2-}. 0.25C_2H_6O$	10	10	Ethanol 15 ml, 60°C	68.3	Crystal quality good enough for structure determination.
GUMCITIP	$C_{18}H_{21}Cl_2N_4O_2^+ .C_6H_7O_7^-. 0.5C_3H_8O$	10	10	Isopropanol 15 ml, 60°C	59.6	Crystallisation only with the aid of scratching. Poor quality, small crystals.
GUMACEHY (a)	$C_{18}H_{21}Cl_2N_4O_2^+ .C_2H_3O_2^-. xC_3H_8O$	2.42	17	Isopropanol 50 ml, 60°C	-	Crystal formed at -20°C, good quality but not isolatable - deliquescent.
GUMACEHY (b)	$C_{18}H_{21}Cl_2N_4O_2^+ .C_2H_3O_2^-.H_2O$	2.71	8.3	Ethanol 50 ml, 60°C	72.4	Crystal quality good enough for structure determination.
GUMHCLHYIP	$C_{18}H_{21}Cl_2N_4O_2^+ .Cl^-.H_2O.2C_3H_8O$	12	12	Isopropanol 200 ml, 60°C	65.2	Crystal quality good enough for structure determination.
GUMASCHY	$C_{18}H_{21}Cl_2N_4O_2.^+ .C_6H_7O_6^-.H_2O$	2.42	4.60	Water 50 ml, 60°C	68.2	Crystal quality good enough for structure determination.
GUMMALIP	$C_{18}H_{21}Cl_2N_4O_2^+ .C_4H_3O_4^-.C_3H_8O$	2.42	2.42	Isopropanol 50 ml, 60°C	72.0	Good quality crystals, too small.

Table 3.1 Preparation of Salts and Modifications of GU (continued)

Compound	Stoichiometry	Base (mmole)	Acid (mmole)	Solvent	% Yield	Comments
Monoprotonated						
GUMMALIB	$C_{18}H_{21}Cl_2N_4O_2^+ .C_4H_3O_4^-.C_4H_{10}O$	2.42	2.42	Isobutanol 50 ml, 80°C	86.8	Good quality crystals, too small.
GUMMALNIP	$C_{18}H_{21}Cl_2N_4O_2^+ .C_3H_3O_4^-.C_3H_8O$	2.42	2.42	Isopropanol 50 ml, 60°C	56.4	Good quality crystals, too small.
GUMMALNIB	$C_{18}H_{21}Cl_2N_4O_2^+ .C_3H_3O_4^-.xC_4H_{10}O$	2.42	2.42	Isobutanol 50 ml, 80°C	-	No product produced, even on standing.
GUMMES	$C_{18}H_{21}Cl_2N_4O_2^+ .CH_3SO_3^-$	2.42	2.42	Ethanol/Water (92/8 v/v) 50 ml, 60°C	6.1	Poor quality crystals.
Diprotonated						
GUDHCLHY (a)	$C_{18}H_{22}Cl_2N_4O_2^{2+} .2Cl^-.H_2O$	2.42	4.86	Isopropanol 50 ml, 60°C	86.3	A white precipitate formed immediately.
GUDHCLHY (b)	$C_{18}H_{22}Cl_2N_4O_2^{2+} .2Cl^-.H_2O$	2.42	4.86	Isopropanol/Water (50/50 v/v)	61.3	Poor quality crystals.
GUDHCLHY (c)	$C_{18}H_{22}Cl_2N_4O_2^{2+} .2Cl^-.H_2O$	2.42	4.86	Ethanol/Water (92/8 v/v) 50 ml, 60°C	91.2	A white precipitate formed immediately.

Table 3.1 Preparation of Salts and Modifications of GU (continued)

Compound	Stoichiometry	Base (mmole)	Acid (mmole)	Solvent	% Yield	Comments
Diprotonated						
GUDHCLHY (d)	$C_{18}H_{22}Cl_2N_4O_2^{2+}$ $.2Cl^-.H_2O$	2.42	4.86	Methanol/Ethanol (80/20 v/v) 50 ml, 60°C	80.2	Good quality crystals too small.
GUDHCLHY (e)	$C_{18}H_{22}Cl_2N_4O_2^{2+}$ $.2Cl^-.H_2O$	2.42	4.86	Methanol/Ethanol (60/40 v/v) 50 ml, 60°C	69.3	Crystal quality good enough for structure determination.
GUDMES (a)	$C_{18}H_{22}Cl_2N_4O_2^{2+}$ $.2CH_3SO_3^-$	2.42	9.13	Isopropanol 50 ml, 60°C	92.9	A white precipitate formed immediately.
GUDMES (b)	$C_{18}H_{22}Cl_2N_4O_2^{2+}$ $.2CH_3SO_3^-$	2.42	9.13	Ethanol 50 ml, 60°C	85.2	A white precipitate formed immediately.
GUDMES (c)	$C_{18}H_{22}Cl_2N_4O_2^{2+}$ $.2CH_3SO_3^-$	2.42	9.13	Methanol 50 ml, 50°C	74.1	A white precipitate formed immediately.
GUDMES (d)	$C_{18}H_{22}2Cl_2N_4O_2^{2+}$ $.2CH_3SO_3^-$	2.42	9.13	Isopropanol/Water (50/50 v/v) 50 ml, 60°C	-	Cool to -20°C and leave, but no product produced.
GUDMES (e)	$C_{18}H_{22}Cl_2N_4O_2^{2+}$ $.2CH_3SO_3^-$	2.42	9.13	Isopropanol/Water (76/24 v/v) 50 ml, 60°C	64.2	Cool to -20°C and leave for several weeks. Good quality crystals.

Table 3.1 Preparation of Salts and Modifications of GU (continued)

Compound	Stoichiometry	Base (mmole)	Acid (mmole)	Solvent	% Yield	Comments
Diprotonated						
GUDMES (f)	$C_{18}H_{22}Cl_2N_4O_2^{2+}$ $.2CH_3SO_3^-$	2.42	9.13	Isopropanol/Water (84/16 v/v) 50 ml, 60°C	69.8	Cool to -20°C and leave for several weeks. Crystal quality good enough for structure determination.
GUDNIT	$C_{18}H_{22}Cl_2N_4O_2^{2+}$ $.2NO_3^-$	2.42	7.94	Ethanol/Water (90/10 v/v) 50 ml, 60°C	96.4	Poor quality crystals.
GUDACE (a)	$C_{18}H_{22}Cl_2N_4O_2^{2+}$ $.2C_2H_3O_2^-$	2.42	4.83	Isopropanol 50 ml, 60°C	-	Cool to -20°C and leave, but no product produced.
GUDACE (b)	$C_{18}H_{22}Cl_2N_4O_2^{2+}$ $.2C_2H_3O_2^-$	2.42	4.83	Isopropanol/Water (50/50 v/v) 50 ml, 60°C	-	Cool to -20°C and leave, but no product produced.
GUDACE (c)	$C_{18}H_{22}Cl_2N_4O_2^{2+}$ $.2C_2H_3O_2^-$	2.42	xS	Acetic Acid	-	Cool to -20°C and leave, but no product produced. Evaporate slowly, but a gum forms.
GUSULF (a)	$C_{18}H_{22}Cl_2N_4O_2^{2+}$ $.SO_4^{2-}$	2.42	2.42	Isopropanol 50 ml, 60°C	92.4	A white precipitate formed immediately.
GUSULF (b)	$C_{18}H_{22}Cl_2N_4O_2^{2+}$ $.SO_4^{2-}$	2.42	2.42	Methanol 50 ml, 50°C	85.6	Light purple crystals formed on standing. Poor quality crystals.

Table 3.1 Preparation of Salts and Modifications of GU (continued)

Compound	Stoichiometry	Base (mmole)	Acid (mmole)	Solvent	% Yield	Comments
Diprotonated						
GUSULF (c)	$C_{18}H_{22}Cl_2N_4O_2^{2+}$ $.SO_4^{2-}$	2.42	2.42	Isopropanol/Water (50/50 v/v) 50 ml, 60°C	67.8	Good quality crystals formed at 4°C after three weeks. A unit cell was determined, but not good enough for structure determination.
GUSULFHY	$C_{18}H_{22}Cl_2N_4O_2^{2+}$ $.SO_4^{2-}.H_2O$	2.42	2.42	Ethanol/Water (50/50 v/v) 10 ml, 60°C	91.8	Poor quality crystals.
GUSPHOSHY	$C_{18}H_{22}Cl_2N_4O_2^{2+}$ $.1.5HPO_4^{2-}$	2.42	4.34	Water/Ethanol (95/5 v/v) 65 ml, 90°C	70.8	A fine white precipitate formed over a three day period.
Triprotonated						
GUTHCl	$C_{18}H_{23}Cl_2N_4O_2^{3+}$ $.3Cl^-$	2.42	9.37	Isopropanol/Water (50/50 v/v) 50 ml, 60°C pH* = 1.2	90.0	Crystal quality was very good. Habit was substantially different from GUDHCLHY, but material was characterised as GUDHCLHY from unit cell dimensions.

Table 3.2 Characterisation of Salts and Modifications of GU

Compound	MP (°C)	Elemental Analysis Calc[d].	Elemental Analysis Found	Base Equivalence Factor Calc[d].	Base Equivalence Factor Found	KF Water Content Calc[d].	KF Water Content Found	Comments
Modification								
GUFBHY	132.0-134.2	C 52.31 H 5.36 N 13.56	C 52.31 H 5.40 N 13.54	95.6	95.7	4.36	4.53	NMR, IR, DSC and crystal structure determination used to confirm structure.
GUFBIP	116.6-119.7	C 55.92 H 7.04 N 10.87	C 56.03 H 7.05 N 10.86	76.7	77.0	0	-	NMR, IR and crystal structure determination used to confirm structure.
GUFBIB	82.5-85.5	C 57.45 H 7.42 N 10.31	C 57.52 H 7.49 N 10.39	72.7	73.6	0	-	NMR, IR and crystal structure determination used to confirm structure.
GUFBRIB	82.6-84.6	C 57.45 H 7.42 N 10.31	C 57.42 H 7.36 N 10.35	72.7	73.9	0	-	NMR, IR and DSC used to confirm structure.
GUFBSIB	98.6-100.6	C 57.45 H 7.42 N 10.31	C 57.50 H 7.38 N 10.28	72.7	72.8	0	-	NMR, IR and DSC used to confirm structure.
GUFBIPE	67.1-69.6	C 58.83 H 7.76 N 9.80	C 58.80 H 7.69 N 9.87	69.1	69.5	0	-	NMR, IR and DSC used to confirm structure.

Table 3.2 Characterisation of Salts and Modifications of GU

Compound	MP (°C)	Elemental Analysis Calc[d].	Elemental Analysis Found	Base Equivalence Factor Calc[d].	Base Equivalence Factor Found	KF Water Content Calc[d].	KF Water Content Found	Comments
Monoprotonated								
GUHFUMET	171.1-173.2	C 52.98 H 5.00 N 12.20	C 52.51 H 4.90 N 12.35	86.1	86.5	0	-	NMR, IR and crystal structure determination used to confirm structure.
GUMCITIP	140.0-141.5	C 49.60 H 5.22 N 9.07	C 49.42 H 5.33 N 8.98	64.0	65.2	0	-	NMR and IR used to confirm structure.
GUMACEHY	150.4-151.4	C 50.75 H 5.54 N 11.84	C 50.82 H 5.45 N 11.79	83.5	82.3	3.81	3.89	NMR, IR and crystal structure determination used to confirm structure.
GUMHCLHYIP	235.5-237.5	C 50.58 H 6.90 N 9.83	C 49.76 H 6.68 N 9.87	69.3	71.6	3.16	3.32	NMR, IR and crystal structure determination used to confirm structure.
GUMASCHY	132.1-134.2	C 48.90 H 5.13 N 9.50	C 48.26 H 5.26 N 9.52	67.1	67.9	3.06	3.14	NMR, IR and crystal structure determination used to confirm structure.
GUMMALIP	180.8-182.8	C 52.54 H 5.64 N 9.80	C 52.83 H 5.79 N 9.87	69.2	68.6	0	-	NMR and IR used to confirm structure.

Table 3.2 Characterisation of Salts and Modifications of GU

Compound	MP (°C)	Elemental Analysis Calc[d].	Elemental Analysis Found	Base Equivalence Factor Calc[d].	Base Equivalence Factor Found	KF Water Content Calc[d].	KF Water Content Found	Comments
Monoprotonated								
GUMMALIB	117.9-120.5	C 53.34 H 5.85 N 9.57	C 53.87 H 5.96 N 9.64	67.5	67.0	0	-	NMR and IR used to confirm structure.
GUMMALNIP	114.9-116.9	C 51.53 H 5.76 N 10.01	C 51.74 H 5.89 N 10.14	70.7	70.6	0	-	NMR and IR used to confirm structure.
GUMMES	-	C 50.10 H 4.59 N 10.62	C 50.25 H 4.62 N 10.59	80.1	80.6	0	-	IR used to confirm structure.
Diprotonated								
GUDHCLHY	263.2-265.4	C 44.66 H 5.12 N 11.26	C 44.64 H 5.15 N 11.20	81.3	80.2	3.62	3.69	NMR, IR and crystal structure determination used to confirm structure.
GUDMES	269.1-271.3	C 40.89 H 4.80 N 9.54	C 41.10 H 4.96 N 9.44	66.0	66.4	0	-	NMR, IR and crystal structure determination used to confirm structure.

Table 3.2 Characterisation of Salts and Modifications of GU

Compound	MP (°C)	Elemental Analysis Calc[d]	Elemental Analysis Found	Base Equivalence Factor Calc[d]	Base Equivalence Factor Found	KF Water Content Calc[d]	KF Water Content Found	Comments
Diprotonated								
GUSULF	233.4-235.2	C 43.82 H 4.49 N 11.36	C 43.56 H 4.57 N 11.30	80.1	80.9	0	-	NMR, IR and crystal structure determination used to confirm structure.
GUSULFHY	220.7-223.7	C 42.28 H 4.73 N 10.96	C 40.84 H 4.72 N 10.58	77.3	77.2	3.40	3.72	NMR and IR used to confirm structure.
GUSPHOSHY	240.4-242.4	C 41.04 H 4.69 N 10.64	C 41.38 H 4.85 N 10.80	70.5	69.9	3.21	3.26	IR used to confirm structure.
GUDNIT	177.8-180.4	C 41.45 H 4.26 N 16.13	C 41.04 H 4.12 N 16.03	75.8	75.7	0	-	IR used to confirm structure.
Triprotonated								
GUTHCl	263.8-265.9	C 42.84 H 4.59 N 11.10	C 44.50 H 5.20 N 11.17	75.6	79.9	0	3.72	Although habit was very different, from previous investigations, this was characterised as GUDHCLHY,using unit cell parameters.

SECTION 4: PHYSICOCHEMICAL INVESTIGATIONS INTO SALTS AND MODIFICATIONS OF GU

4.1. Hygroscopicity/Efflorescence Studies on Salts and Modifications of GU

All modifications of the free base were non-hygroscopic under all humidity conditions studied, taking up less than 1% w/w of water. The data are summarised in Figures 4.1.1. to 4.1.4. The samples exhibit Type II adsorption characteristics as classified by Brunauer[1]. This occurs in physical adsorption on nonporous or microporous adsorbent, allowing a multilayer of adsorbate to be bound to the surface. An inflection point is indicative of the first monolayer formation. The moisture adsorption-desorption isotherms show the typically closed hysteresis loop[1,2] which are indicative of the materials having capillary pores. The data are summarised in Figure 4.1.14.

Of the salts studied only the dicarboxcylic acid salts, GUHFUMET and GUMMALNIP and the monochloride salt, GUMHCLHYIP were hygroscopic. GUHFUMET, rapidly adsorbs water under all storage conditions and achieves equilibrium moisture contents after only 24 hours (Figure 4.1.5.), the values equating to between 1.81 (20% RH) and 2.57 (87% RH) moles of water. GUHFUMET exhibits Type I[1] adsorption characteristics. These occur in chemisorption processes and are limited to a few monolayers of adsorbate. The amsymptote is approached when the water molecules occupy all of the available sorption sites. Again the moisture adsorption-desorption isotherms show a closed hysteresis loop (Figure 4.1.15.).

GUMHCLHYIP is only hygroscopic at elevated humidities. After 24 hours at 87%RH the sample has adsorbed 10.09% w/w (≡3.19 moles) of water, but rapidly loses much of this before equilibrating to 6.10% w/w (≡1.93 moles) of water. It equilibrates to a similar level, 6.50% w/w (≡2.05 moles) when stored at 75% RH (Figure 4.1.6.).

GUMHCLHYIP exhibits Type IV[1] adsorption characteristics, these occur on porous surfaces and the inflection point indicates the position of the first monolayer. The moisture adsorption-desorption isotherms show the closed hysteresis loop (Figure 4.1.16.).

GUMMALNIP is deliquescent at 87% RH, it rapidly equilibrates to a level of 6.49% w/w (≡2.01 moles) of water and then gradually deliquesces over the next few days (Figure 4.1.7.). GUMMALNIP is non-hygroscopic when stored at between 20% to 75% RH. It exhibits Type II adsorption characteristics and a closed hysteresis loop (Figure 4.1.15.).

All of the remaining salts are non-hygroscopic (Figures 4.1.8. - 4.1.13.) the majority exhibit Type II adsorption characteristics, the exceptions being GUMACEHY (Type IV, Figure 4.1.8.) and GUMASCHY (Type III, Figure 4.1.9.). Type III adsorption occurs when the heat of adsorption is less than the adsorbate's heat of liquefaction. Thus, additional adsorption is facilitated because the adsorbate's interaction with the monolayer is greater than its interaction with the adsorbent surface.

Only GUMMALIB and GUSULF, exhibit an open hysteresis loop for the adsorption-desorption isotherms (Figure 4.1.15 and 4.1.17). This indicates that these materials have the so-called 'ink-bottle' or narrow neck pores[1,2].

Figure 4.1.1 Hygroscopicity / Efflorescence Studies on GUFBHY

Hygroscopicity Studies

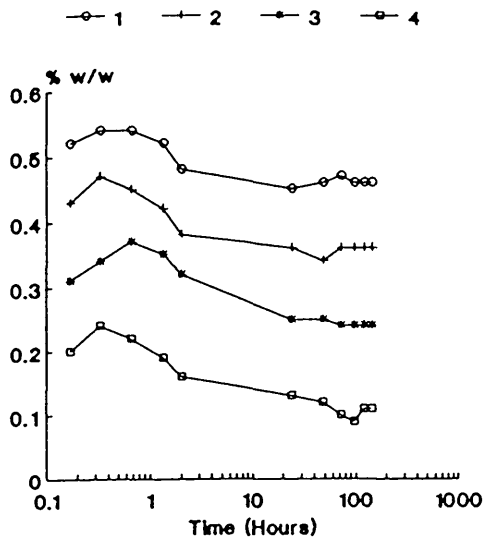

Efflorescence Studies

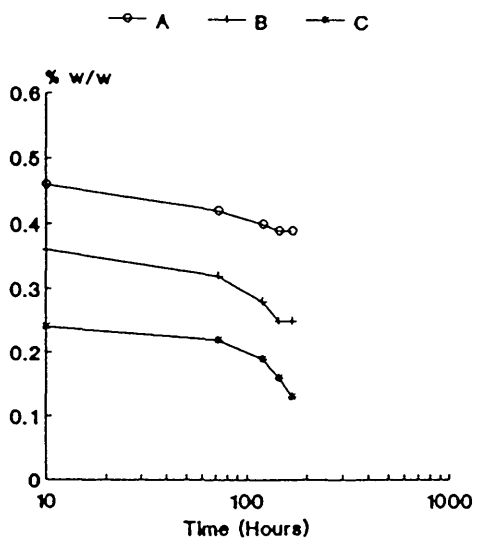

Identifier	Condition
1	87% RH
2	75% RH
3	52% RH
4	20% RH

Identifier	Condition
A	87% RH - 75% RH
B	75% RH - 52% RH
C	52% RH - 20% RH

Figure 4.1.2 Hygroscopicity / Efflorescence Studies on GUFBIP

Hygroscopicity Studies

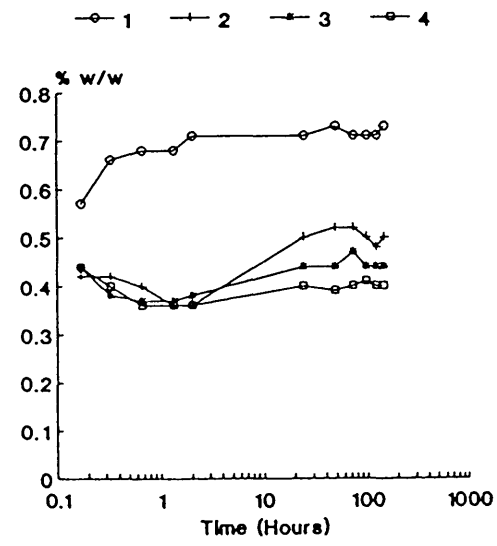

Efflorescence Studies

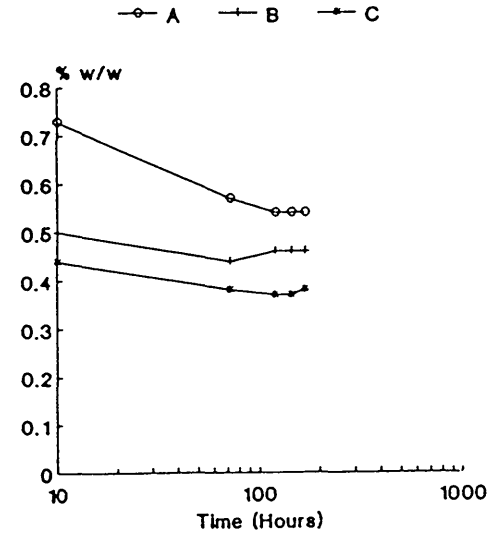

Identifier	Condition
1	87% RH
2	75% RH
3	52% RH
4	20% RH

Identifier	Condition
A	87% RH - 75% RH
B	75% RH - 52% RH
C	52% RH - 20% RH

Figure 4.1.3 Hygroscopicity / Efflorescence Studies on GUFBIB

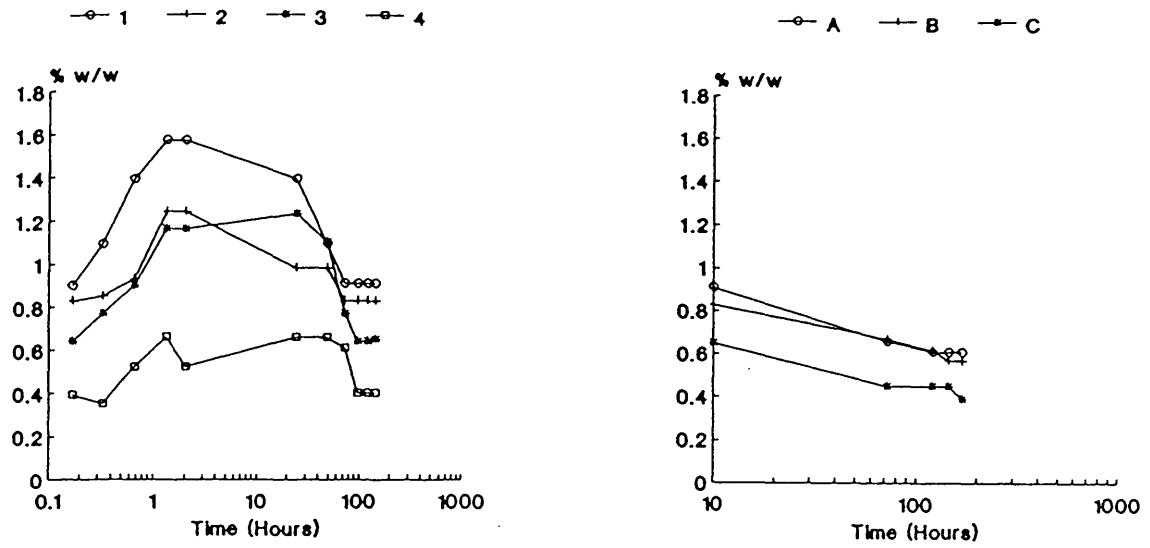

Identifier	Condition
1	87% RH
2	75% RH
3	52% RH
4	20% RH

Identifier	Condition
A	87% RH - 75% RH
B	75% RH - 52% RH
C	52% RH - 20% RH

Figure 4.1.4 Hygroscopicity / Efflorescence Studies on GUFBIPE

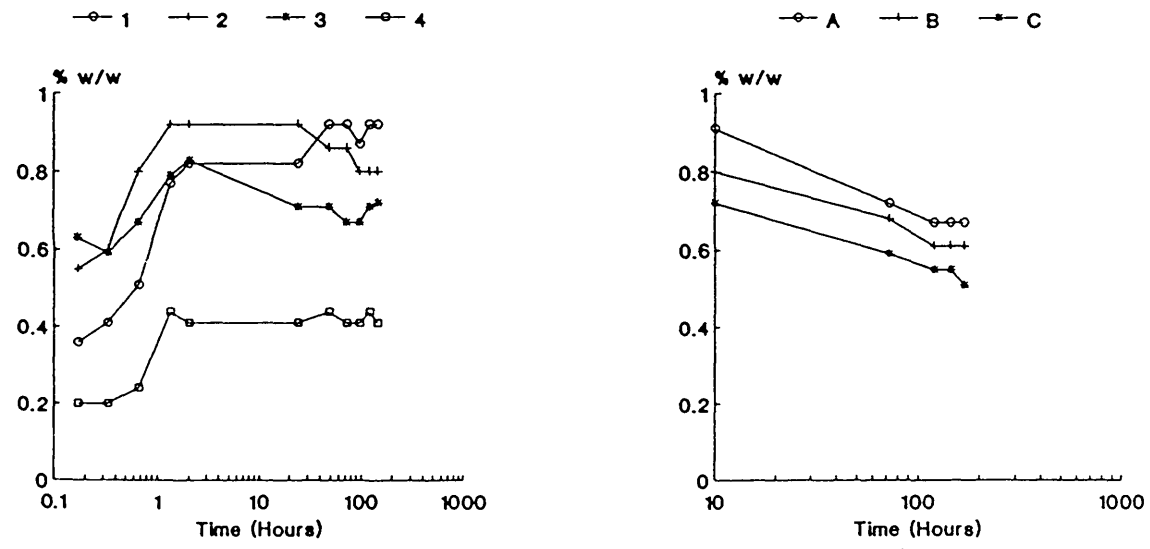

Identifier	Condition
1	87% RH
2	75% RH
3	52% RH
4	20% RH

Identifier	Condition
A	87% RH - 75% RH
B	75% RH - 52% RH
C	52% RH - 20% RH

Figure 4.1.5 Hygroscopicity / Efflorescence Studies on GUHFUMET

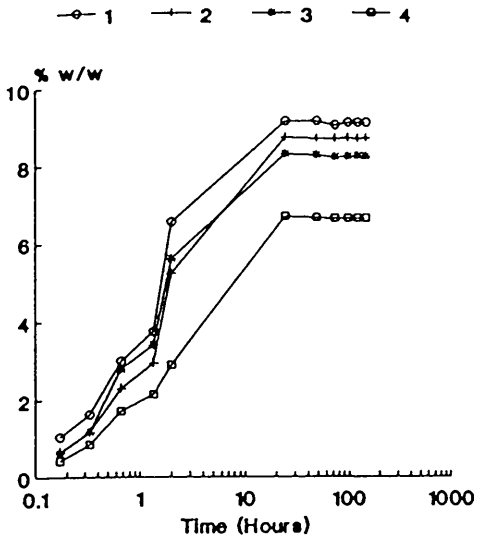

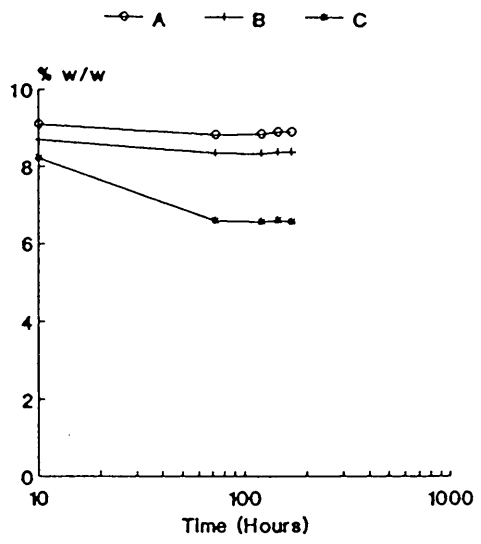

Identifier	Condition
1	87% RH
2	75% RH
3	52% RH
4	20% RH

Identifier	Condition
A	87% RH - 75% RH
B	75% RH - 52% RH
C	52% RH - 20% RH

Figure 4.1.6 Hygroscopicity / Efflorescence Studies on GUMHCLHYIP

Hygroscopicity Studies

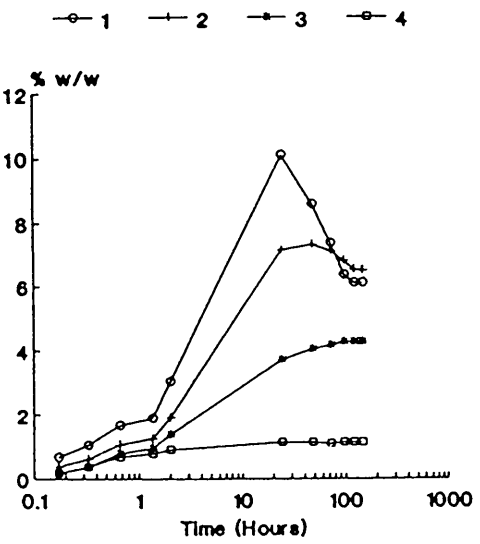

Efflorescence Studies

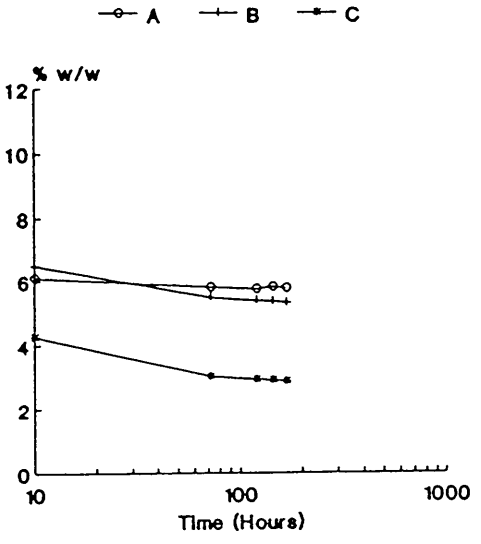

Identifier	Condition
1	87% RH
2	75% RH
3	52% RH
4	20% RH

Identifier	Condition
A	87% RH - 75% RH
B	75% RH - 52% RH
C	52% RH - 20% RH

Figure 4.1.7 Hygroscopicity / Efflorescence Studies on GUMMALNIP

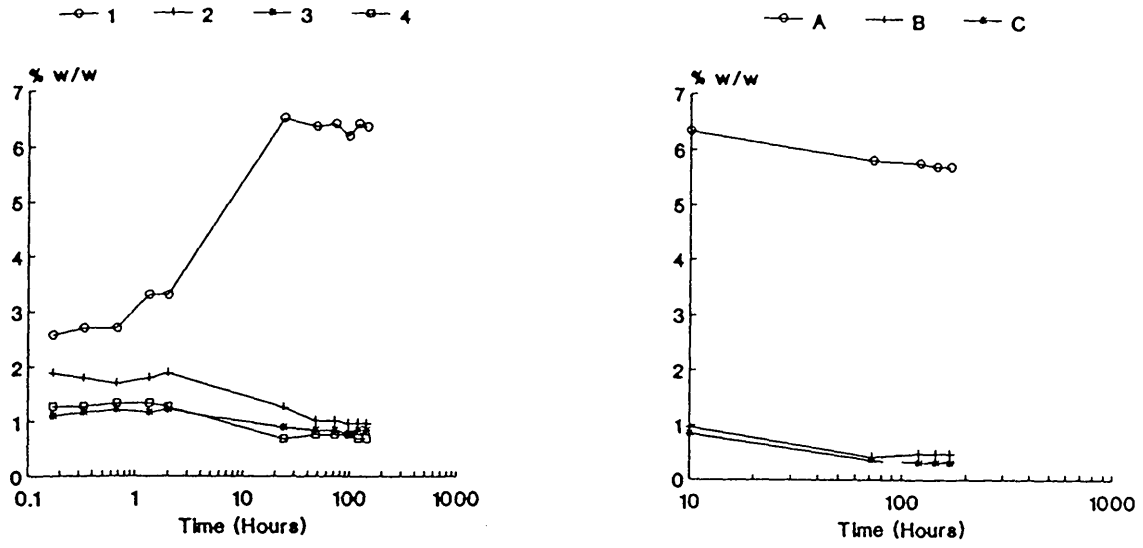

Identifier	Condition
1	87% RH
2	75% RH
3	52% RH
4	20% RH

Identifier	Condition
A	87% RH - 75% RH
B	75% RH - 52% RH
C	52% RH - 20% RH

Figure 4.1.8 Hygroscopicity / Efflorescence Studies on GUMACEHY

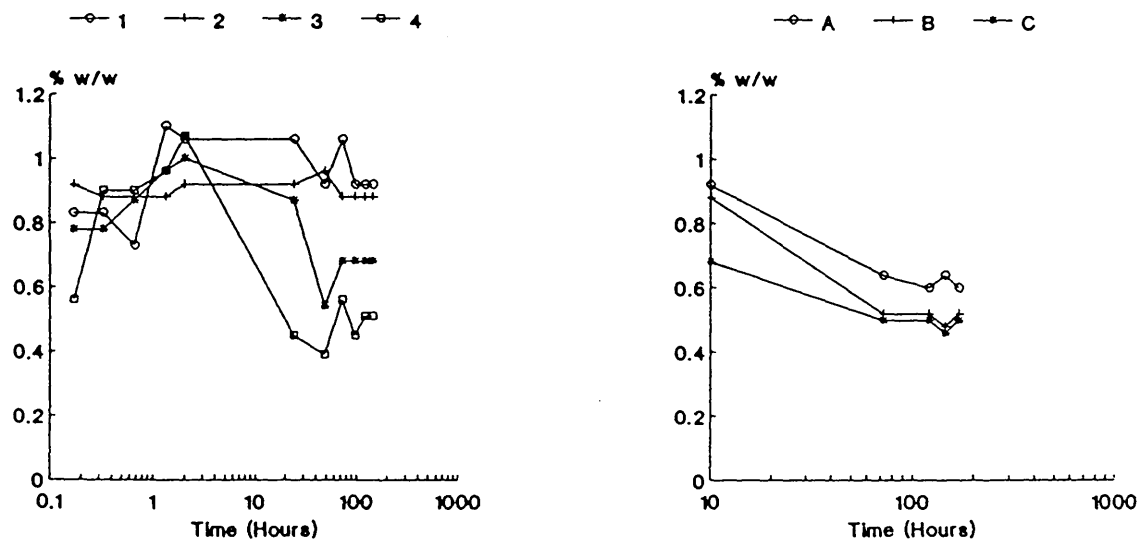

Identifier	Condition
1	87% RH
2	75% RH
3	52% RH
4	20% RH

Identifier	Condition
A	87% RH - 75% RH
B	75% RH - 52% RH
C	52% RH - 20% RH

Figure 4.1.9 Hygroscopicity / Efflorescence Studies on GUMASCHY

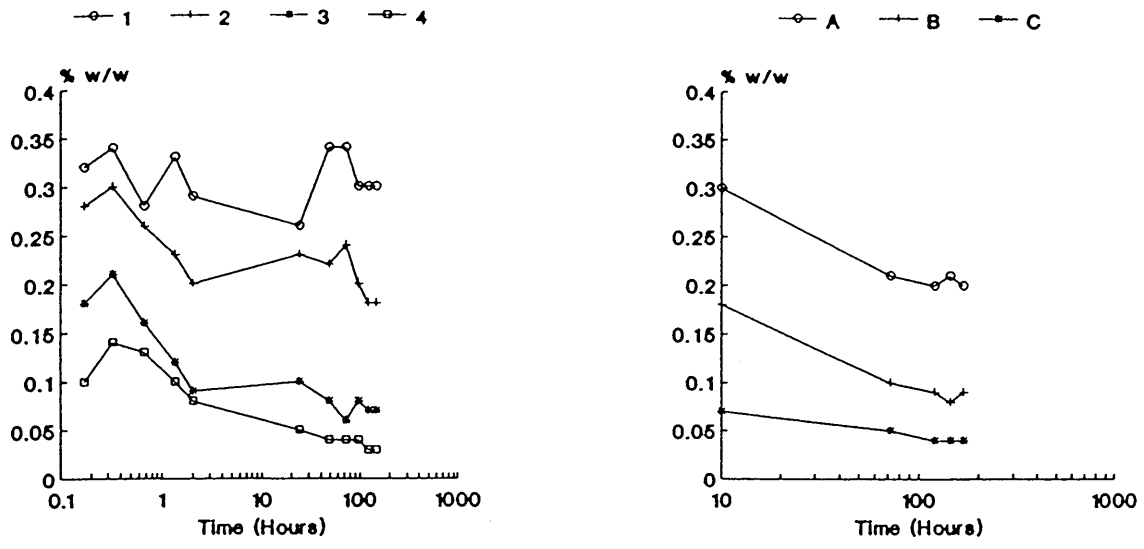

Identifier	Condition
1	87% RH
2	75% RH
3	52% RH
4	20% RH

Identifier	Condition
A	87% RH - 75% RH
B	75% RH - 52% RH
C	52% RH - 20% RH

Figure 4.1.10 Hygroscopicity / Efflorescence Studies on GUMMALIB

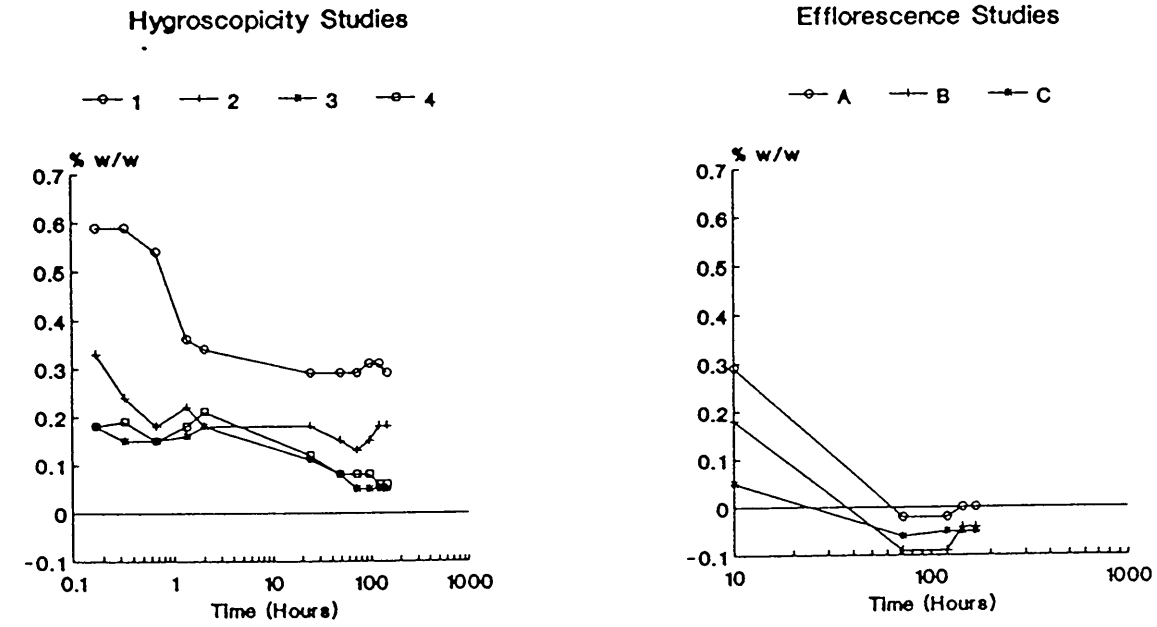

Identifier	Condition
1	87% RH
2	75% RH
3	52% RH
4	20% RH

Identifier	Condition
A	87% RH - 75% RH
B	75% RH - 52% RH
C	52% RH - 20% RH

Figure 4.1.11 Hygroscopicity / Efflorescence Studies on GUSULF

Hygroscopicity Studies

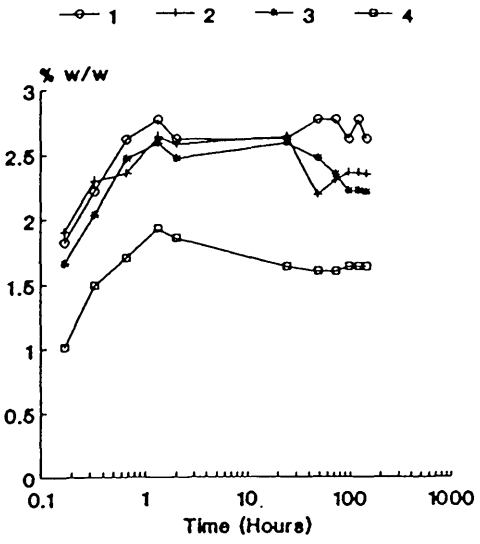

Identifier	Condition
1	87% RH
2	75% RH
3	52% RH
4	20% RH

Efflorescence Studies

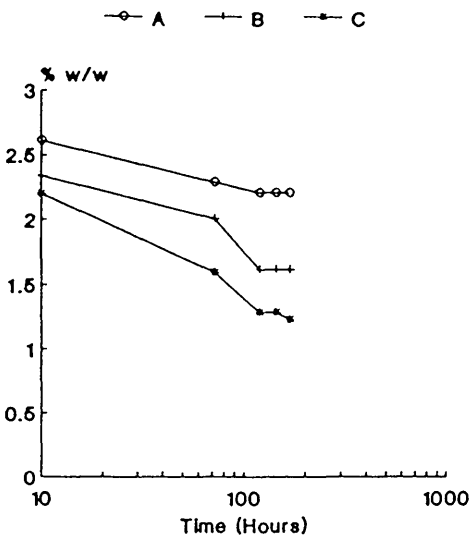

Identifier	Condition
A	87% RH - 75% RH
B	75% RH - 52% RH
C	52% RH - 20% RH

Figure 4.1.12 Hygroscopicity / Efflorescence Studies on GUDHCLHY

Hygroscopicity Studies

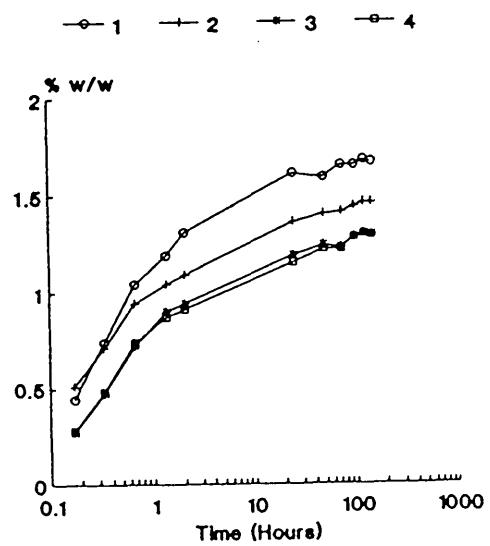

Identifier	Condition
1	87% RH
2	75% RH
3	52% RH
4	20% RH

Efflorescence Studies

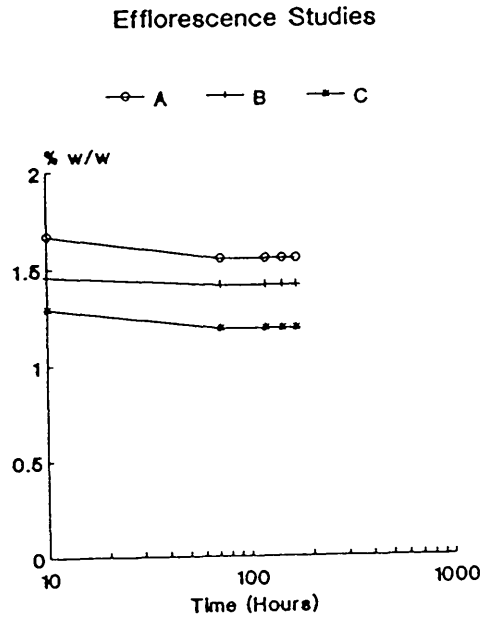

Identifier	Condition
A	87% RH - 75% RH
B	75% RH - 52% RH
C	52% RH - 20% RH

Figure 4.1.13 Hygroscopicity / Efflorescence Studies on GUDMES

Hygroscopicity Studies

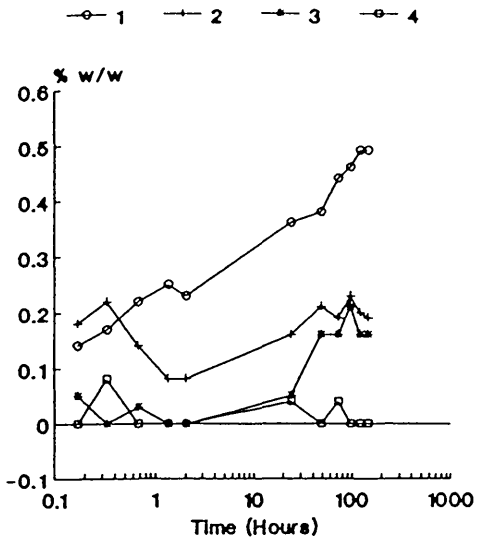

Identifier	Condition
1	87% RH
2	75% RH
3	52% RH
4	20% RH

Efflorescence Studies

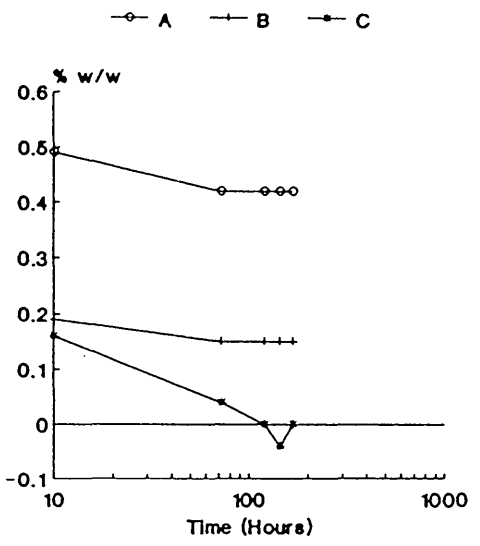

Identifier	Condition
A	87% RH - 75% RH
B	75% RH - 52% RH
C	52% RH - 20% RH

Figure 4.1.14 Adsorption / Desorption Isotherms of Modifications of GU

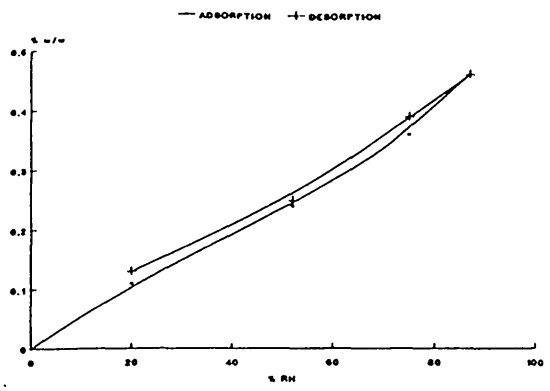

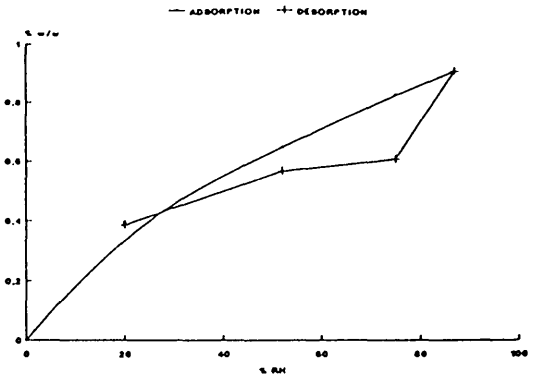

GUFBHY

	HYGROSCOPICITY				EFFLORESCENCE		
	87%RH	75%RH	52%RH	20%RH	75%RH	52%RH	20%RH
% w/w	0.46	0.36	0.24	0.11	0.39	0.25	0.13
Moles $\frac{1}{2}$H O	0.11	0.09	0.06	0.03	0.09	0.06	0.03

GUFBIB

	HYGROSCOPICITY				EFFLORESCENCE		
	87%RH	75%RH	52%RH	20%RH	75%RH	52%RH	20%RH
% w/w	0.91	0.83	0.65	0.40	0.61	0.57	0.39
Moles $\frac{1}{2}$H O	0.27	0.25	0.20	0.12	0.18	0.17	0.12

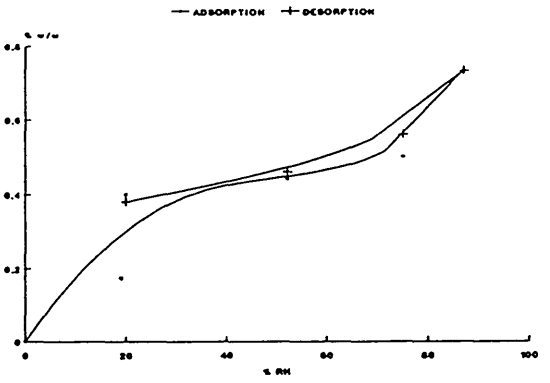

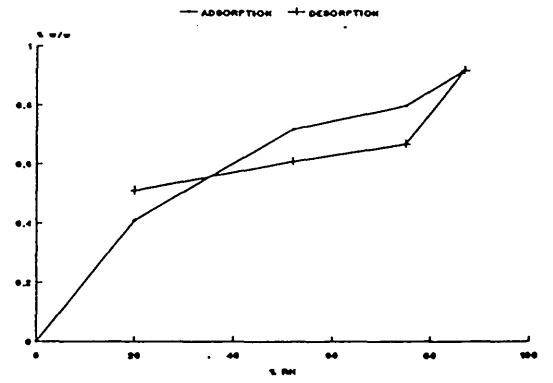

GUFBIP

	HYGROSCOPICITY				EFFLORESCENCE		
	87%RH	75%RH	52%RH	20%RH	75%RH	52%RH	20%RH
% w/w	0.73	0.60	0.44	0.40	0.56	0.46	0.36
Moles $\frac{1}{2}$H O	0.21	0.14	0.12	0.11	0.16	0.13	0.11

GUFBIPE

	HYGROSCOPICITY				EFFLORESCENCE		
	87%RH	75%RH	52%RH	20%RH	75%RH	52%RH	20%RH
% w/w	0.92	0.80	0.72	0.41	0.67	0.61	0.51
Moles $\frac{1}{2}$H O	0.29	0.25	0.23	0.13	0.21	0.19	0.16

Figure 4.1.15 Adsorption / Desorption Isotherms of Monoprotonated Salts of GU

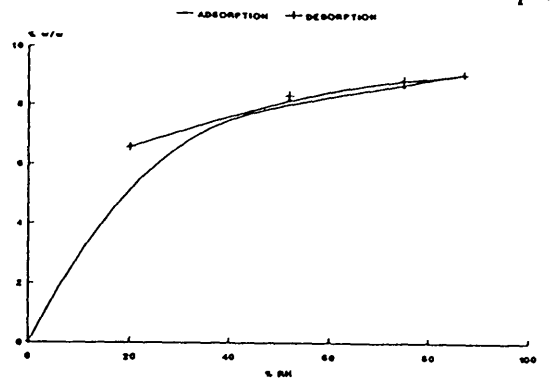

GUHFUMET

	HYGROSCOPICITY				EFFLORESCENCE		
	87%RH	75%RH	52%RH	20%RH	75%RH	52%RH	20%RH
% w/w	9.10	8.70	8.23	6.63	8.92	8.40	6.58
Moles $\frac{1}{2}$H O	2.57	2.44	2.30	1.81	2.51	2.35	1.80

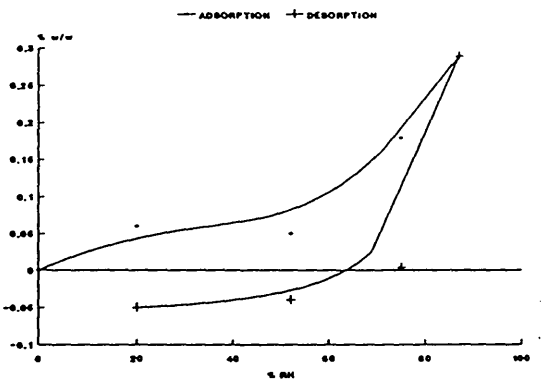

GUMMALIB

	HYGROSCOPICITY				EFFLORESCENCE		
	87%RH	75%RH	52%RH	20%RH	75%RH	52%RH	20%RH
% w/w	0.29	0.18	0.05	0.06	0.00	-0.04	-0.05
Moles $\frac{1}{2}$H O	0.09	0.06	0.02	0.02	0.00	0.00	0.00

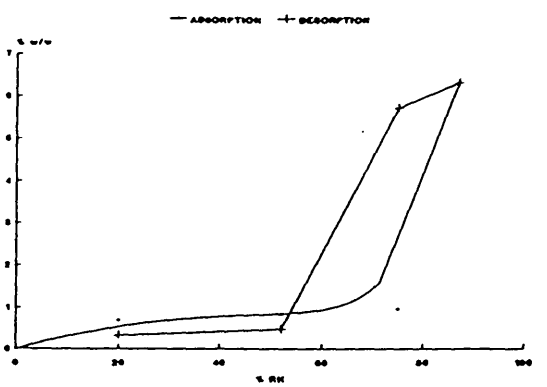

GUMMALNIP

	HYGROSCOPICITY				EFFLORESCENCE		
	87%RH	75%RH	52%RH	20%RH	75%RH	52%RH	20%RH
% w/w	6.33	0.96	0.84	0.69	5.71	0.46	0.32
Moles $\frac{1}{2}$H O	1.97	0.30	0.26	0.21	1.77	0.15	0.10

Figure 4.1.16 Adsorption / Desorption Isotherms of Monoprotonated Salts of GU

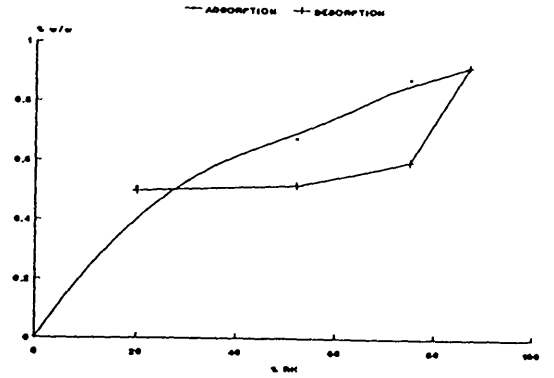

GUMACEHY

	HYGROSCOPICITY				EFFLORESCENCE		
	87%RH	75%RH	52%RH	20%RH	75%RH	52%RH	20%RH
% w/w	0.92	0.88	0.66	0.51	0.60	0.52	0.50
Moles $\frac{1}{2}$H O	0.24	0.23	0.16	0.13	0.16	0.14	0.13

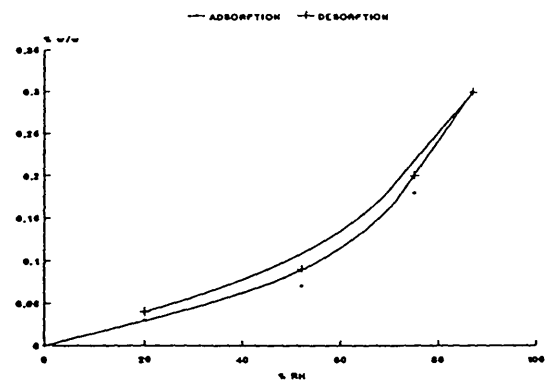

GUMASCHY

	HYGROSCOPICITY				EFFLORESCENCE		
	87%RH	75%RH	52%RH	20%RH	75%RH	52%RH	20%RH
% w/w	0.30	0.18	0.07	0.03	0.20	0.09	0.04
Moles $\frac{1}{2}$H O	0.10	0.06	0.02	0.01	0.06	0.03	0.01

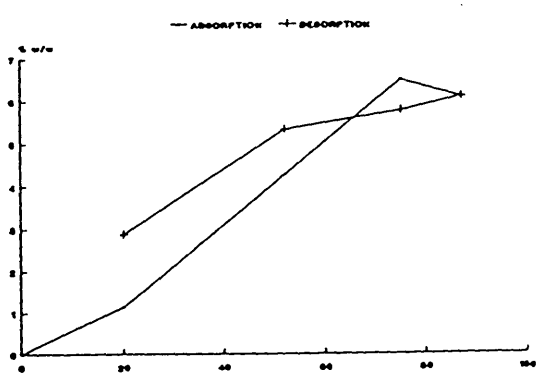

GUMHCLHYIP

	HYGROSCOPICITY				EFFLORESCENCE		
	87%RH	75%RH	52%RH	20%RH	75%RH	52%RH	20%RH
% w/w	6.10	6.50	4.26	1.14	5.77	5.32	2.87
Moles $\frac{1}{2}$H O	1.93	2.03	1.35	0.36	1.82	1.68	0.91

Figure 4.1.17 Adsorption / Desorption Isotherms of Diprotonated Salts of GU

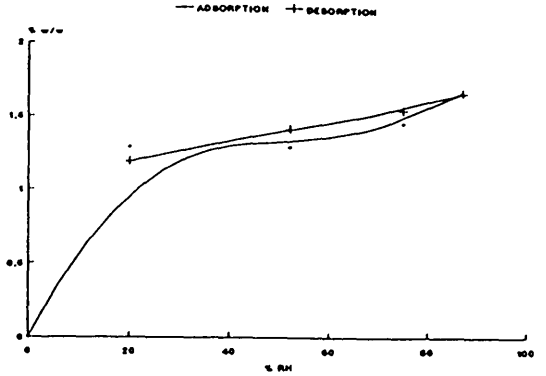

GUDHCLHY

	HYGROSCOPICITY				EFFLORESCENCE		
	87%RH	75%RH	52%RH	20%RH	75%RH	52%RH	20%RH
% w/w	1.67	1.46	1.29	1.29	1.55	1.41	1.19
Moles $\frac{1}{2}$ H O	0.45	0.39	0.35	0.35	0.42	0.38	0.32

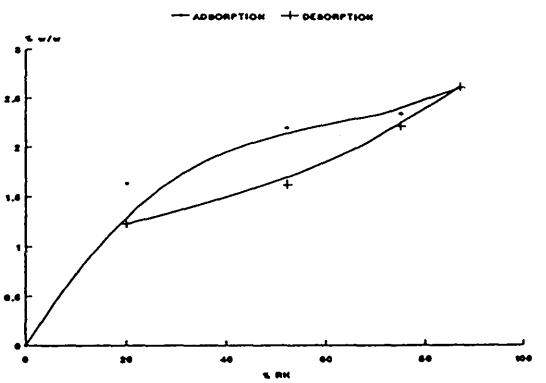

GUSULF

	HYGROSCOPICITY				EFFLORESCENCE		
	87%RH	75%RH	52%RH	20%RH	75%RH	52%RH	20%RH
% w/w	2.61	2.34	2.20	1.63	2.21	1.62	1.23
Moles $\frac{1}{2}$ H O	0.74	0.66	0.62	0.46	0.63	0.46	0.35

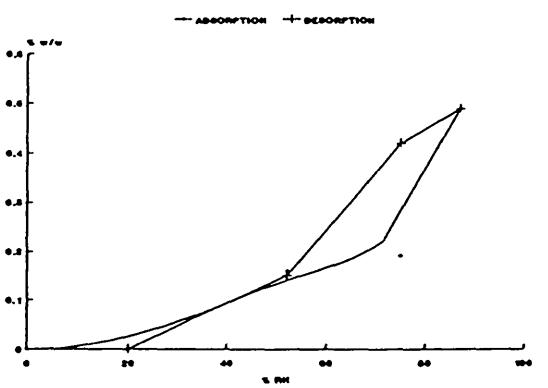

GUDMES

	HYGROSCOPICITY				EFFLORESCENCE		
	87%RH	75%RH	52%RH	20%RH	75%RH	52%RH	20%RH
% w/w	0.49	0.19	0.16	0.00	0.42	0.15	0.00
Moles $\frac{1}{2}$ H O	0.16	0.06	0.05	0.00	0.14	0.05	0.00

4.2 Stability Studies on Salts and Modifications of GU

4.2.1 Appearance of Stability Samples for Salts and Modifications of GU

The appearance of the salts and modifications of GU, at the end of the stability studies are given in Table 4.2.1.

Table 4.2.1 Appearance of Salts and Modifications of GU at the end of the Stability Studies, under the various conditions studied

Salt/ Modification	Condition/Appearance 25°C	40°C	50°C	70°C	100°C	RH*	Lt*	Hv*
GUFBHY	NC	NC	P(1)	P(2)	M,B	NC	F(1)	F(3)
GUFBIP	F(1)	P(1)	P(2)	P(3)	M,B	NC	Br(1)	Br(3)
GUFBIB	F(1)	F(2)	F(4)	Br(4)	M,B	NC	F(1)	Br(2)
GUFBIPE	F(1)	F(2)	F(4)	Br(4)	M,B	NC	F(1)	Br(1)
GUHFUMET	NC	NC	NC	F(1)	M,Br(1)	A,F(1)	F(1)	Br(1)
GUMMALIB	NC	NC	F(1)	F(3)	M,Br(3)	NC	F(4)	P(1)
GUMMALNIP	NC	F(1)	F(3)	Br(2)	M,B	NC	Br(2)	Br(4)
GUMACEHY	NC	NC	F(2)	Br(1)	M,B	NC	Br(1)	Br(3)
GUMASCHY	NC	NC	F(1)	F(3)	M,Br(3)	A,NC	F(1)	F(3)
GUMHCLHYIP	NC	P(1)	P(2)	P(3)	M,Br(3)	A,F(1)	Br(2)	P(5)
GUDMES	NC	NC	F(1)	F(2)	F(4)	A,F(1)	F(1)	F(1)
GUSULFHY	NC	NC	F(1)	F(2)	F(5)	NC	F(1)	F(2)
GUDHCLHY	NC	NC	NC	F(1)	F(3)	NC	NC	F(1)

* see p. 40.

The key to the abbreviations are:

NC No change in colour
F Fawn
B Black
A Aggregates
Br Brown
P Purple
M Melted

Intensities of the colours have been subjectively estimated on a rank order between 1 (least colouration) and 5 (most colouration) and are given in brackets after the abbreviation. The marked colour changes should not be taken as indicative of extensive chemical degradation, although this was certainly observed for some of the samples studied. Both oxidation (to the highly coloured quinone derivative) and photolysis (which is often a precursor to oxidation in the initiation phase, and is usually mediated by free radicals to produce dark-coloured products) may result in colouration of the samples, with only small levels of degradation being present.[3]

Despite a slight darkening in colour, all samples stored between 25° and 50°C and at elevated humidities, demonstrated excellent stability, with no loss in potency over the course of the studies.

4.2.2. Solid-State Reaction Kinetics

The subject of the kinetics of solid-state reactions of drugs and indeed of solid-state reactions in general is not well understood. Solid-state reactions show complex rate behaviour that is not easily modelled and unlike solution reactions cannot be easily fitted to a single kinetic equation.[4]

The kinetics of the solid-state decomposition reactions of drugs have been extensively studied; the objective of most of these studies was to obtain an equation that provided an adequate fit for plots of rate vs. time, to make shelf-life predictions. However the majority of these studies were not aimed at elucidating the molecular details of the reaction under investigation. Solid-state

reactivity is largely controlled by molecular conformation and crystal packing in the particular structure that is involved[5].
In certain cases, the extent of decomposition varies in a sigmoid fashion, the reaction showing an initial rapid change followed by a gradual slowing down (topochemical) or an initial lag phase followed by a rapid change (nucleation).

Topochemical Kinetics

In topochemical or contracting geometry decomposition the solid-state reaction is assumed to be controlled by the advancement of phase boundaries from the outside of the crystal inwards. A series of equations have been derived dependent on whether the advancement of the phase boundary is in 1, 2 or 3 dimensions[6,7].
If the crystal is assumed to react along one direction only, then the rate is a function of time and a zero order rate equation will apply:

$$1 - \alpha = kt \quad \ldots\ldots\ldots\ldots\ldots\ldots\ldots (1)$$

If the reaction is assumed to proceed from the surface of a circular disk (or cylinder) inwardly, then equation (2) will apply:

$$1 - (1-\alpha)^{1/2} = kt \quad \ldots\ldots\ldots\ldots\ldots\ldots (2)$$

And, if the reaction proceeds from the surface of a sphere inwardly in three dimensions, then equation (3) will apply:

$$1 - (1-\alpha)^{1/3} = kt \quad \ldots\ldots\ldots\ldots\ldots\ldots (3)$$

In all case α is the relative amount of decomposition, t is time and k is the rate constant.

Nucleation Kinetics

Nucleation decomposition assumes control by the growth and formation of active nuclei at the surface and inside of the crystals. The formation of decomposition products

initiates strains in the crystal structure which are relieved by crack propogation. Decomposition then continues on these new surfaces and the chain reaction continues.

This situation can be described using the Prout-Tompkins[8] equation:

$$\ln (1/1 - \alpha) = kt \quad \ldots\ldots\ldots\ldots\ldots\ldots (4)$$

This equation has been successfully applied to several inorganic solid-state reactions, including those of mercury fulminate, lead oxalate and nickel formate. The role of crystal defects is also far more important than was first realised. The real solid has surfaces, grain boundaries, dislocations, impurities, occluded solvent *etc.* Molecules at or close to these defects have a higher potential energy than those in the bulk crystal and consequently may be more reactive. In many such reactions the diffusion of a reactant or product is rate controlling and diffusion is only possible by virtue of these lattice defects[6,7].

Diffusion Kinetics

If the rate of reaction is controlled by a 1 dimensional processes then equation (5) will apply:

$$\alpha^2 = kt \quad \ldots\ldots\ldots\ldots\ldots\ldots\ldots (5)$$

and if the reaction is assumed to be controlled by diffusion from a spherical particle then the Jander equation may be applied:

$$[1 - (1-\alpha)^{\frac{1}{3}}]^2 = kt \quad \ldots\ldots\ldots\ldots\ldots\ldots (6)$$

Solid-State reactions of salts and modifications of GU

In an effort to understand the kinetic processes involved in the solid-state stability studies; equations (1) - (6) were applied to the relevant data. Linear regression analyses using a least squares fit program were performed and the correlation coefficients (R^2) are tabulated in Table 4.2.2. This approach was first used to investigate the dehydration of Cytosine monohydrate by Perrier[9].

Table 4.2.2 Solid-State Reaction Kinetics for Salts and Modifcations of GU

Salts/ Modifications	Condition (°C)	Linear Regression Analyses on Kinetic Data (R^2) Topochemical		Nucleation		Diffusion	
		1D	2D	3D	PT	1D	3D
GUFBHY	100	0.937	0.843	0.801	0.706	0.999	0.864
GUFBIP	70	0.935	0.774	0.680	0.709	0.773	0.868
	100	0.723	0.699	0.690	0.675	0.900	0.704
	Lt	0.987	0.964	0.949	0.906	0.957	0.968
	Hv	0.955	0.941	0.935	0.920	0.961	0.943
GUFBIB	70	0.993	0.859	0.739	0.798	0.854	0.956
	100	0.877	0.867	0.850	0.820	0.786	0.861
	Hv	0.884	0.878	0.835	0.824	0.795	0.866
GUFBIPE	70	0.984	0.820	0.701	0.811	0.911	0.925
	100	0.806	0.791	0.786	0.774	0.833	0.794
	Hv	0.754	0.865	0.691	0.740	0.572	0.751
GUHFUMET	100	0.833	0.959	0.878	0.940	0.683	0.960
GUMMALNIP	100	0.764	0.745	0.739	0.727	0.800	0.749
	Hv	0.952	0.939	0.931	0.910	0.934	0.941
GUMACEHY	100	0.889	0.867	0.860	0.843	0.925	0.873
	Hv	0.101	0.088	0.084	0.076	0.122	0.089
GUMASCHY	100	0.628	0.593	0.580	0.554	0.686	0.600
GUMHCLHYIP	100	0.961	0.778	0.684	0.745	0.925	0.876
	Lt	0.981	0.987	0.963	0.873	0.874	0.991
	Hv	0.902	0.719	0.635	0.972	0.966	0.725
GUSULFHY	100	0.869	0.724	0.655	0.497	0.971	0.756
GUDHCLHY	100	0.980	0.985	0.964	0.864	0.658	0.967

The stability data are summarised in Figures 4.2.1 to 4.2.13 and the degradation profiles are summarised in Tables 4.2.3 to 4.2.5.

The stability of the various modifications of the free base at 70°C appears to be dependent upon the volatility of the solvent and not the melting point of the sample. There is initially a small increase in potency for the alcohol solvates, the size of this increase being dependent on the volatility of the solvent (GUFBIP, 104.2%; GUFBIB, 104.0% and GUFBIPE, 102.7%). This is followed by a reasonably linear decrease in potency as a function of time (Figures 4.2.2 - 4.2.4).
The kinetics are either pseudo zero order ot due to 1D advancement of a phase boundary.
The solvates all show a complex degradation profile with several (*ca* 10) more polar and three less polar, degradation products. The hydrate is very stable over the whole study period, exhibiting only a small drop in potency (95% label), accompanied by several more polar degradation products (Figure 4.2.1).

The free base, 100°C samples all show similar decomposition profiles (Figure 4.2.14). There is no increase in potency after 4 weeks as the rate of decomposition is greater than the rate of de-solvation for all of the samples. The hydrate (GUFBHY) had in fact melted after only 1 weeks storage (in line with the other samples), even though it was stored at some 30°C below its melting point. The DSC heating curve (Figure 4.2.17) helps to explain this, by showing a very broad melting endotherm between 101.0 and 137.8°C, followed by decomposition. There is no separate dehydration endotherm. Thus storage at 100°C leads to loss of water and premature melting. The kinetics best fit a 1D diffusion model for GUFBHY and GUFBIP, but none of the models studied gave a good correlation for the data. The

degradation profiles (Table 4.2.3) are again very complex, but appear similar to the 70°C profiles.

With the exception of GUFBIP (84.6%), light stability is good. Although the volatility of the isopropanol solvent appears to be the favoured explanation for the reduced light stability, it should be noted that the photolytic degradation profile (Table 4.2.4 and Figure 4.2.15) is not identical with the thermal degradation profile. The kinetics are confusing and gave acceptable correlations for all of the models studied.

The stability of the free base samples are reduced when stored under UV light, as compared with window light. The degradation profiles (Table 4.2.5 and Figure 4.2.16) are similar, GUFBIP is again the least stable modification and GUFBHY, the most stable. The kinetic profiles for GUFBIP gave acceptable correlations, whilst those for GUFBIB and GUFBIPE gave poor correlations, for the models studied.

The stability of the dicarboxcylate salts of GU are again not solely dependent on the values of their melting points. The fumarate (GUHFUMET) has the highest melting point, while the maleate and malonate salts have similar melting points, but vastly different thermal stabilities. The maleate (GUMMALIB, Figure 4.2.5) is the most stable of the three salts, even when stored at 100°C. It initially shows an almost quantitative desolvation at 100°C, resulting in the loss of the isobutanol solvent and a resulting increase in potency (111.8% ≡ 97.6% loss of isobutanol). This is followed by a gradual loss in potency to 106.0%, with the concurrent increase in the degradation product at RRt 0.68 to a final level of 4.6% (Table 4.2.3). The fumarate (GUHFUMET, Figure 4.2.4) has a half-life of about 25 weeks, when stored at 100°C. There is a marked change in the rate of the reaction

after 12 weeks, possibly as a result of a phase change, although this could not be confirmed due to the high levels of degradation present (Table 4.2.3). The kinetic data gave good correlation for three of the models studied, the 3D diffusion, nucleation and a 2D topochemical model. The malonate salt (GUMMALNIP, Figure 4.2.6) is the least stable of the dicarboxcylate salts, having a half-life of 4 weeks at 100°C. Part of the explanation may again be the volatility of the isopropanol solvent. The degradation profile (Table 4.2.3) is again very complex and the data gave poor correlations in all of the kinetic models studied. All of the salts demonstrated good light stability with quantitative recoveries and low levels of degradation (Table 4.2.4). The stability under UV light was identical for GUMMALIB, but was reduced for GUHFUMET (93.7%) and GUMMALNIP (83.6%). The degradation profiles were similar for all three dicarboxcylate salts (Table 4.2.5).

The monoacetate (GUMACEHY) and monoascorbate (GUMASCHY) salts show excellent light and thermal stability up to 70°C (Figures 4.2.8 and 4.2.9, respectively). On storage at 100°C, both salts exhibited premature melting. This was caused by loss of the water of crystallisation followed by melting of the anhydrate form. Similar behaviour was previously observed for GUFBHY. The anhydrate forms rapidly degrade with half-lives of 28 and 7 days respectively, for GUMACE and GUMASC. The degradation profiles are summarised in Table 4.2.3. As there are two reactions occurring, desolvation and decomposition, it is not surprising that the kinetic models gave poor correlations.

Although melting point is in general an important parameter in assessing salt stability, for the mono and diprotonated chlorides the presence of solvent again appears to be more critical. The hydrated dichloride,

GUDHCLHY has a high melting point (263.2 - 265.4°C) and it demonstrates excellent stability (Figure 4.2.12). The hydrated, isopropanol solvate of the monochloride GUMHCLHYIP, also has a high melting point (235.5 - 237.5°C), but the presence of volatile isopropanol solvent reduces the light and thermal stability at 100°C, quite markedly (Figure 4.2.10). The data for the monochloride salt can be fitted to several kinetic models. For the 100°C data a pseudo zero order or 1D phase advancement model gives the best correlations. For the light data all models except the nucleation and 1D diffusion model, gave good correlations. Conversely for the UV light data, the nucleation and 1D diffusion models gave the best correlations.

For the mesylate (GUDMES, Figure 4.2.11) and the hydrated sulphate (GUSULFHY, Figure 4.2.13), although the geometry of the anions are similar the presence of solvent appears to be the critical factor. GUDMES shows excellent stability at all conditions and likewise GUSULFHY shows good stability at all but the 100°C station. Here, as has previously been observed, dehydration followed by degradation of the anhydrate, results in a half-life of only 12 weeks at 100°C. A 1D diffusion model gave the best treatment of the data.

Table 4.2.3 Degradation Profiles for Salts and Modifications of GU, when stored at 100°C

Salt/ Modifications	Degradation Peaks, RRt (% Area Normalised)															
	NR	More Polar										Less Polar				
	<0.38	0.42	0.44	0.49	0.53	0.56	0.62	0.66	0.68	0.77	0.86	1.0	1.21	1.35	1.45	1.86
GUFBHY	5.7	1.3		2.0		1.8	3.9				3.4	45.4	0.1	0.8	5.2	3.7
GUFBIP	18.9		0.7	1.3				0.3		0.1	0.2	45.4			3.0	3.1
GUFBIB	10.3	0.6	0.4	0.9				0.1		0.7		40.2			2.1	0.1
GUFBIPE	17.9	2.8		3.2			0.1	0.2		1.4	0.3	38.6			2.7	0.3
GUHFUMET	4.7			1.4	0.7	1.5	1.0	4.8		1.0	1.8	55.7	0.5	0.6	0.3	0.3
GUMMALIB	0.2				0.1			3.4			0.1	106.0				
GUMMALNIP	11.4	0.5		1.6	0.6	1.3				0.7		53.6		2.1	4.2	
GUMASCHY	15.6	5.6							9.0			52.8				
GUMACEHY	4.3	0.5		0.5	0.9		0.6		0.4	0.1	0.1	51.8			0.5	
GUMHCLHYIP	1.4		0.4	0.8	0.3	0.8	0.6	1.2	0.6	1.2	0.2	81.8	0.4			0.4
GUDMES	0.8											97.0				
GUSULFHY	5.0											49.8				
GUDHCLHY	1.9											94.4				

Notes: NR ≡ Not retained, RRt 1.0 = Rt of Gu. In all cases, degradation profiles are compiled at the timepoint nearest to the half-life. In cases where the half-life was not reached, profiling was determined at the end of the study.

Table 4.2.4 Degradation Profiles for Salts and Modifications of GU, when stored under window light

Salt/ Modifications	Degradation Peaks, RRt (% Area Normalised)															
	NR	More Polar											Less Polar			
	<0.38	0.42	0.44	0.49	0.53	0.56	0.62	0.66	0.68	0.77	0.86	1.0	1.21	1.35	1.45	1.86
GUFBHY	1.0											98.7				
GUFBIP	1.2	0.6	0.3	0.6	0.2	0.6	0.2		1.5		0.1	84.6				
GUFBIB	0.5		0.1	0.2				0.1				101.2				
GUFBIPE	0.4	0.1		0.3								100.0				
GUHFUMET	0.6		0.1	0.2		0.4						97.1				
GUMMALIB	0.1					0.1		0.1				99.6				
GUMMALNIP	0.4			0.1				0.1				97.8				
GUMASCHY												98.7				
GUMACEHY	6.4											97.1				
GUMHCLHYIP	1.2		0.3	0.5	0.1	0.8		0.9		0.1		88.2				
GUDMES	0.6											99.8				
GUSULFHY	0.5											99.0				
GUDHCLHY	0.4											101.4				

Notes: In all cases, degradation profiles were compiled at the timepoint nearest to the half-life. In cases where the half-life was not reached, profiling was determined at the end of the study.

Table 4.2.5 Degradation Profiles for Salts and Modifications of GU, when stored under UV Light

Salt/ Modifications	Degradation Peaks, RRt (% Area Normalised)															
	NR	More Polar										Less Polar				
	<0.38	0.42	0.44	0.49	0.53	0.56	0.62	0.66	0.68	0.77	0.86	1.0	1.21	1.35	1.45	1.86
GUFBHY	0.9											97.0				
GUFBIP	2.3	0.5		0.8	0.6	0.3		2.4	1.5		0.1	81.5				
GUFBIB	0.7		0.1	0.2				1.0				94.6				
GUFBIPE	0.9	0.3		0.4			0.1	0.9				86.8				
GUHFUMET	0.2			0.2		0.3	0.6	0.2				93.7				
GUMMALIB	0.1					0.1		0.1				100.4				
GUMMALNIP	1.9			0.4		0.4		2.4				83.6			0.5	
GUMASCHY				2.0								97.2				
GUMACEHY	12.1			0.5								92.6				
GUMHCLHYIP	0.9		0.3	0.4	1.2			1.5			0.1	87.0		0.1	0.3	0.2
GUDMES	0.9											98.4				
GUSULFHY	0.6											97.4				
GUDHCLHY	0.5											99.5				

Notes: In all cases, degradation profiles were compiled at the timepoint nearest to the half-life. In cases where the half-life was not reached, profiling was determined at the end of the study.

Figure 4.2.1 Stability Data for GUFBHY

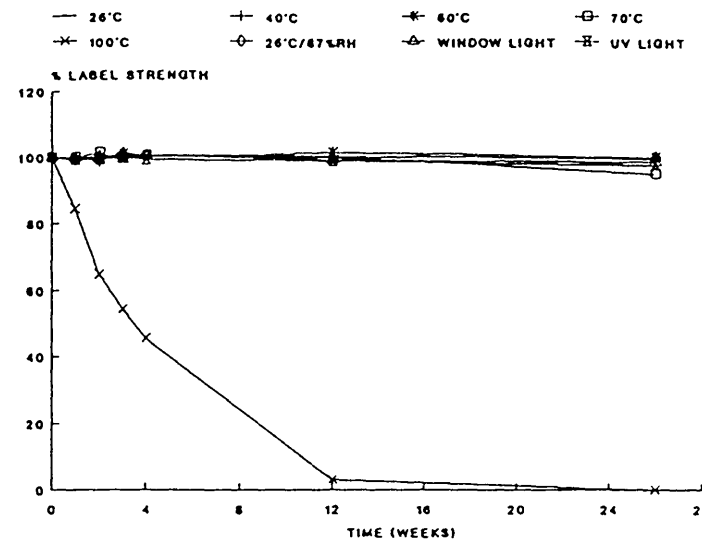

TIMEPOINT	CONDITION (% Label)							
(Weeks)	25	40	50	70	100	RH	Lt	Hν
1	99.0	100.2	98.9	100.0	84.4	99.8	99.4	99.2
2	99.1	98.2	100.2	101.4	64.7	99.7	100.4	99.2
3	100.4	101.5	101.1	99.6	54.4	101.2	99.0	99.5
4	100.1	100.7	100.2	100.6	45.4	100.4	100.3	99.2
12	100.4	100.6	101.6	100.0	3.0	99.8	99.2	98.8
26	99.9	99.5	100.4	95.0	0.0	100.4	98.7	97.7

Figure 4.2.2 Stability Data for GUFBIP

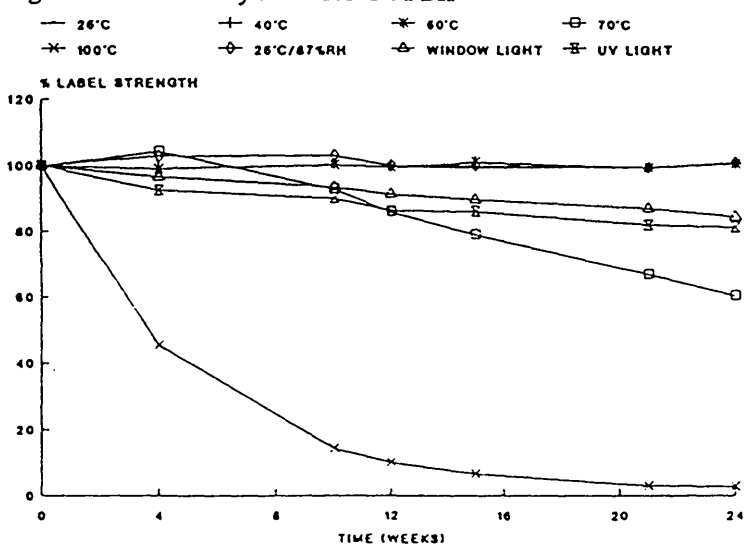

TIMEPOINT	CONDITION (% Label)							
(Weeks)	25	40	50	70	100	RH	Lt	Hν
4	98.9	98.9	98.9	104.2	45.4	102.8	96.6	92.5
10	100.2	100.2	100.2	92.8	14.4	102.9	93.5	90.1
12	99.4	99.4	99.4	85.8	10.2	100.0	91.2	86.3
15	99.2	100.7	101.2	79.1	6.7	99.8	89.6	86.0
21	99.4	99.4	99.4	67.0	3.0	99.4	87.1	82.1
25	100.5	100.5	100.5	60.5	2.9	101.0	84.6	81.5

Figure 4.2.3 Stability Data for GUFBIB

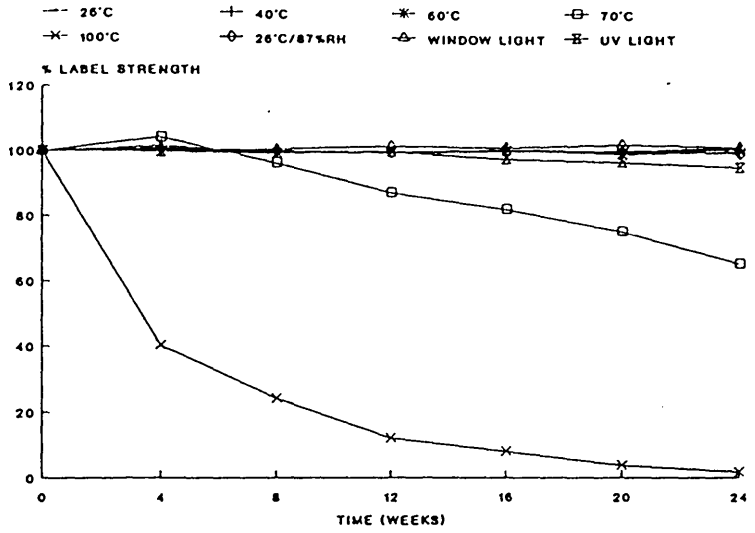

TIMEPOINT	CONDITION (% Label)							
(Weeks)	25	40	50	70	100	RH	Lt	Hν
4	99.9	100.0	101.3	104.0	40.2	100.6	100.3	99.4
8	99.3	98.9	99.2	95.8	24.1	99.8	100.4	99.0
12	99.3	99.6	99.6	86.8	12.1	99.2	101.2	99.3
16	100.2	100.0	100.2	81.8	8.1	99.7	101.0	97.3
20	100.0	99.4	98.8	75.0	3.8	100.0	101.7	96.2
24	100.9	100.4	99.6	65.2	1.9	98.9	101.2	94.6

Figure 4.2.4 Stability Data for GUFBIPE

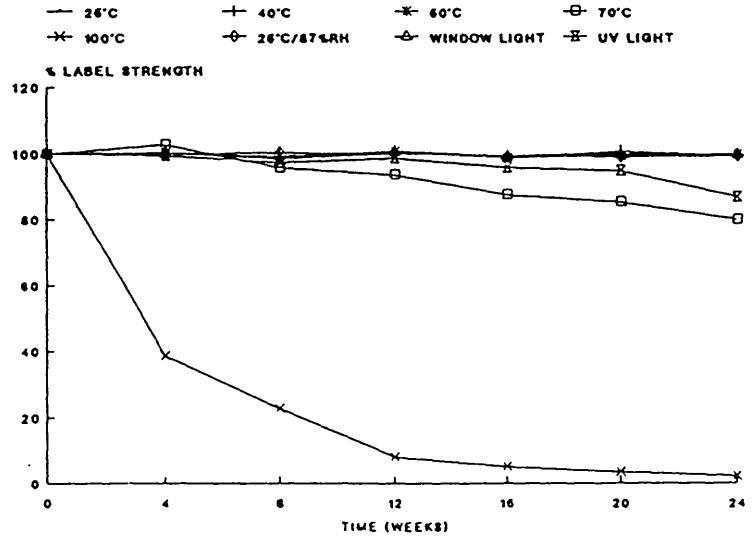

TIMEPOINT	CONDITION (% Label)							
(Weeks)	25	40	50	70	100	RH	Lt	Hν
4	100.2	99.7	100.2	102.7	38.6	100.4	100.2	99.4
8	99.2	99.0	99.4	95.6	22.8	98.4	100.4	97.4
12	99.8	101.0	100.5	93.5	8.0	100.2	100.4	98.6
16	99.6	99.0	98.8	87.4	5.0	99.2	99.0	95.6
20	100.0	100.8	99.2	85.2	3.4	98.7	99.5	94.6
24	99.6	99.4	99.8	80.0	2.2	99.2	100.0	86.8

Figure 4.2.5 Stability Data for GUHFUMET

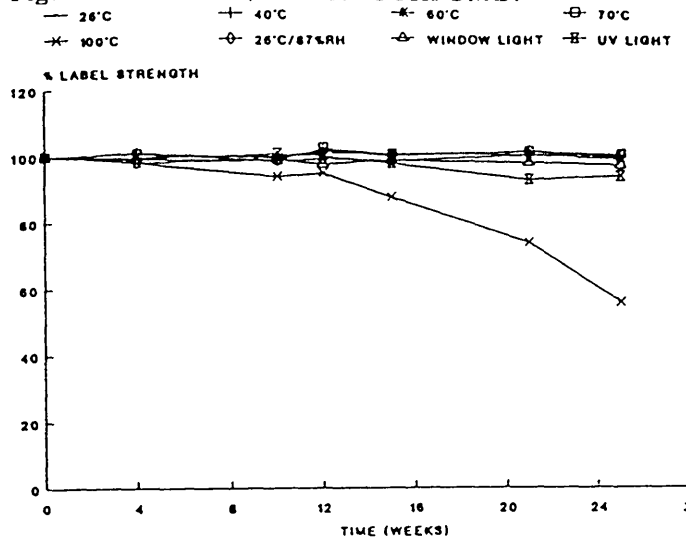

TIMEPOINT	CONDITION (% Label)							
(Weeks)	25	40	50	70	100	RH	Lt	Hν
4	99.7	101.2	100.7	100.8	98.0	98.1	99.0	99.3
10	99.9	99.4	99.5	98.6	93.7	98.6	98.7	100.8
12	100.6	101.4	101.7	102.4	94.6	99.2	97.5	100.0
15	100.5	99.8	100.4	100.4	87.5	98.6	98.4	97.6
21	100.2	101.4	101.2	101.2	73.8	99.9	97.9	92.6
25	98.7	100.2	99.3	100.4	55.7	100.2	97.1	93.7

Figure 4.2.6 Stability Data for GUMMALIB

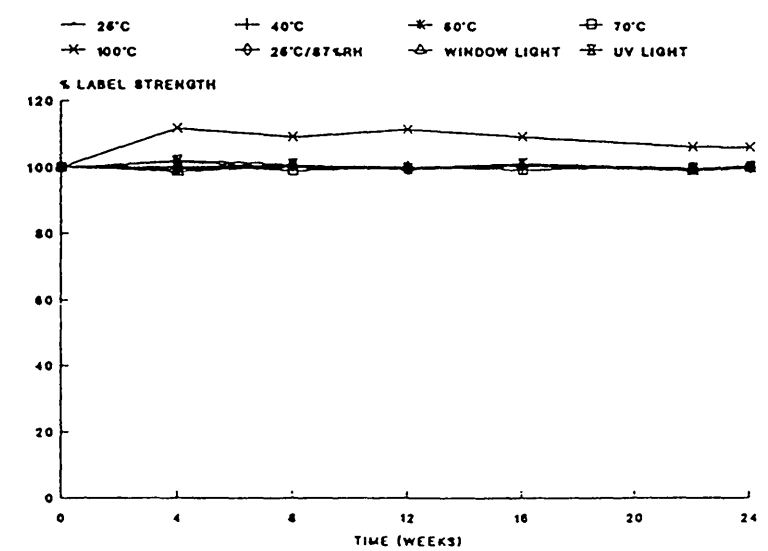

TIMEPOINT	CONDITION (% Label)							
(Weeks)	25	40	50	70	100	RH	Lt	Hν
4	99.4	100.3	101.6	100.0	111.8	99.4	98.6	102.2
8	99.9	100.1	100.2	99.0	109.1	100.8	100.0	100.9
12	99.2	99.5	100.2	99.8	111.4	100.4	100.0	99.4
16	100.3	100.2	101.4	99.2	109.1	100.8	100.3	101.2
22	99.6	99.9	99.9	99.9	106.2	100.0	98.8	99.2
24	100.7	100.2	99.8	99.9	106.0	99.8	99.6	100.4

Figure 4.2.7 Stability Data for GUMMALNIP

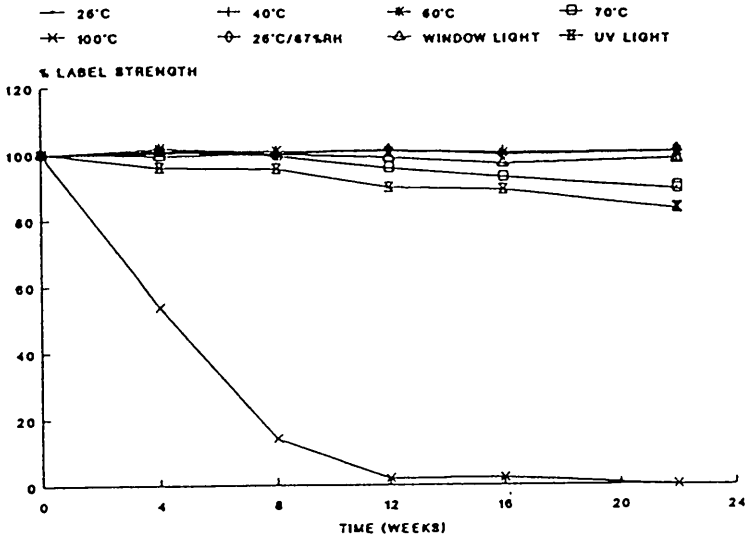

TIMEPOINT (Weeks)	CONDITION (% Label) 25	40	50	70	100	RH	Lt	Hυ
4	100.0	100.8	101.6	100.6	53.6	100.8	99.2	95.6
8	100.8	100.8	100.7	99.1	14.0	100.0	99.7	95.2
12	101.0	101.0	100.6	95.5	2.1	101.2	98.8	89.6
16	100.2	100.4	100.0	92.7	2.2	99.4	96.8	88.8
22	100.3	100.6	100.6	89.1	0.0	100.3	98.4	83.0
24	100.0	100.4	99.2	90.0	0.0	101.2	97.8	83.6

Figure 4.2.8 Stability Data for GUMACEHY

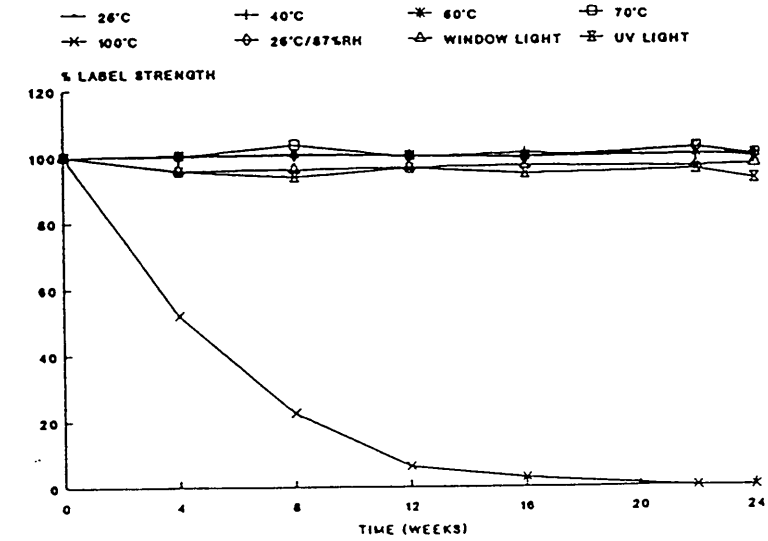

TIMEPOINT (Weeks)	CONDITION (% Label) 25	40	50	70	100	RH	Lt	Hυ
4	100.5	100.2	100.2	100.2	51.8	99.8	95.6	95.2
8	100.3	100.2	100.8	103.4	22.4	100.3	95.9	93.6
12	99.7	100.0	100.1	99.8	6.2	100.2	96.4	96.0
16	99.4	100.8	99.5	99.7	2.8	99.1	97.0	94.4
22	100.0	100.0	100.4	102.4	0.0	102.0	96.5	95.5
24	100.0	100.4	99.2	100.2	0.0	99.8	97.1	92.6

Figure 4.2.9 Stability Data for GUMASCHY

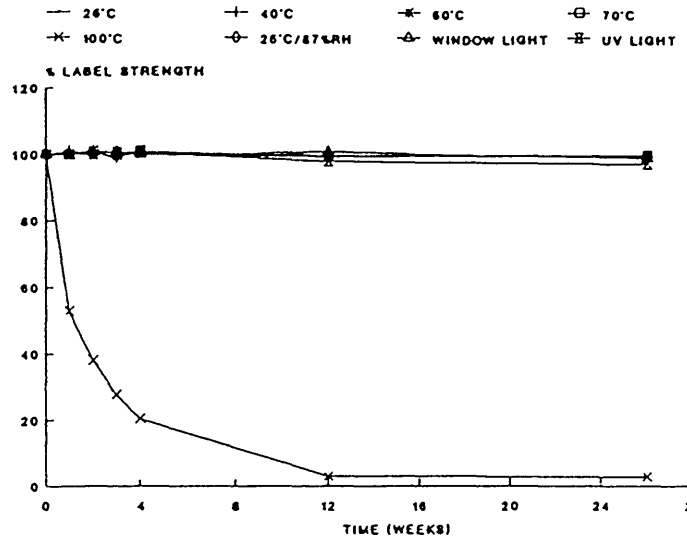

TIMEPOINT	CONDITION (% Label)							
(Weeks)	25	40	50	70	100	RH	Lt	Hν
1	100.0	101.0	100.2	99.9	52.8	100.2	99.6	99.8
2	100.8	100.4	101.2	100.6	38.0	1002.	100.3	99.7
3	100.8	98.8	100.5	100.6	27.6	100.8	100.6	99.6
4	99.6	100.5	100.4	100.9	20.4	100.6	100.0	100.2
12	99.3	99.1	99.3	99.3	3.0	99.6	100.8	97.8
26	100.0	99.6	99.4	99.7	2.9	99.6	98.7	97.2

Figure 4.2.10 Stability Data for GUMHCLHYIP

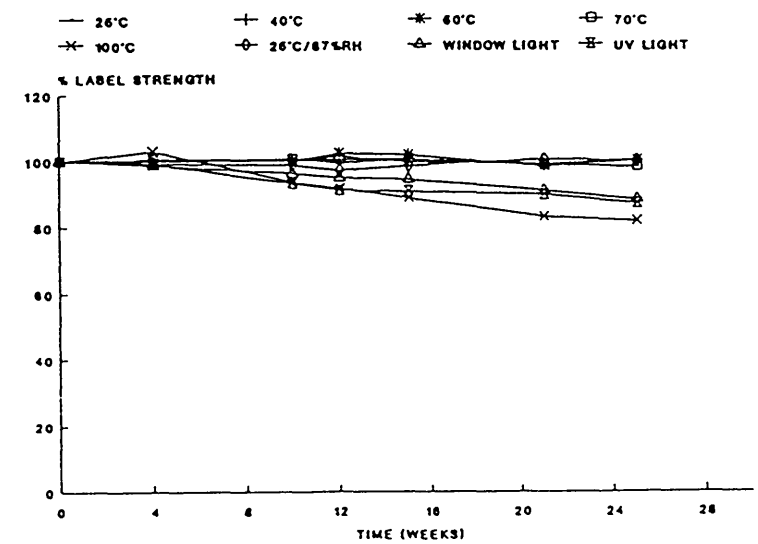

TIMEPOINT	CONDITION (% Label)							
(Weeks)	25	40	50	70	100	RH	Lt	Hν
4	99.9	100.0	100.6	100.5	102.9	99.2	98.6	99.2
10	100.6	100.3	100.2	100.6	93.6	98.8	96.2	93.0
12	99.4	101.4	102.4	100.4	91.6	97.2	94.9	91.1
15	100.4	99.5	101.8	100.5	88.7	98.4	94.2	90.7
21	98.5	99.0	98.2	98.6	83.0	100.4	90.8	89.6
25	98.2	100.2	100.2	98.2	81.8	100.2	88.2	87.0

Figure 4.2.11 Stability Data for GUDMES

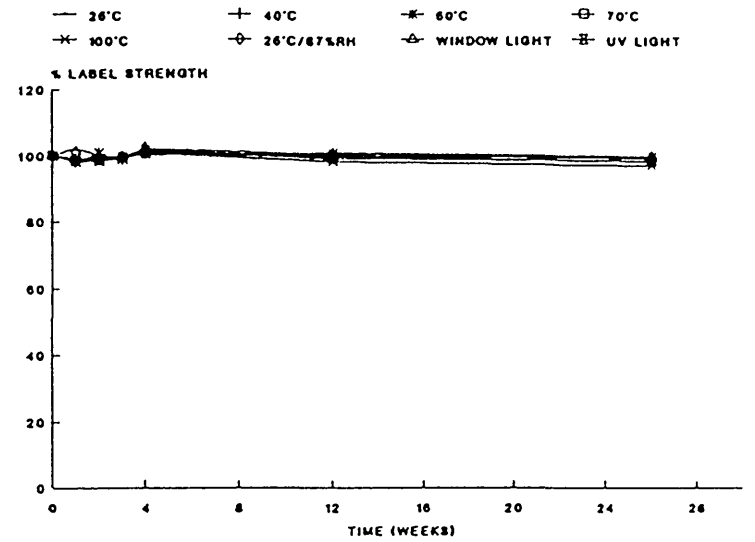

TIMEPOINT	CONDITION (% Label)							
(Weeks)	25	40	50	70	100	RH	Lt	Hv
1	102.4	97.9	98.3	100.0	98.0	98.1	98.8	99.2
2	100.1	100.3	100.8	98.4	98.2	98.8	99.3	99.0
3	99.8	99.6	98.7	99.3	99.0	99.2	99.8	99.6
4	99.9	100.5	100.6	100.4	100.6	101.2	102.4	101.5
12	101.0	99.4	100.5	99.6	98.0	100.0	100.3	98.8
26	99.9	98.3	99.5	98.2	97.0	99.2	99.8	98.4

Figure 4.2.12 Stability Data for GUDHCLHY

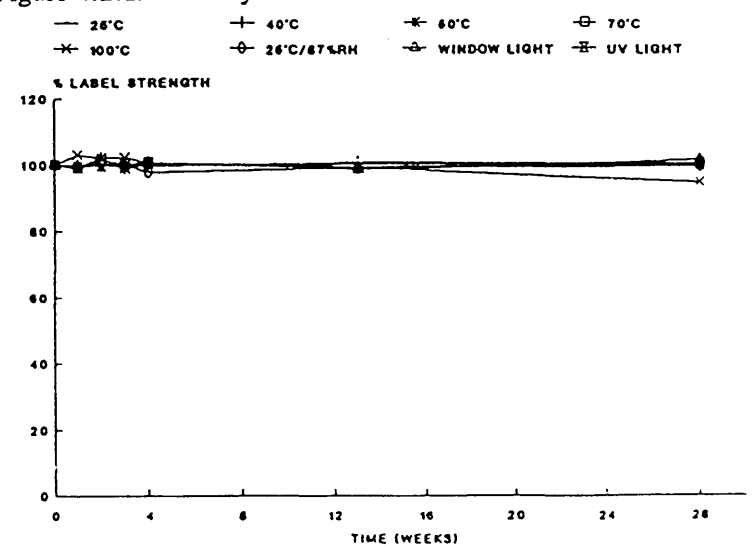

TIMEPOINT	CONDITION (% Label)							
(Weeks)	25	40	50	70	100	RH	Lt	Hv
1	100.4	99.6	99.5	98.8	103.0	99.3	100.0	99.3
2	100.0	101.3	102.1	101.4	102.1	100.2	100.5	99.6
3	99.8	100.2	98.8	100.6	102.2	99.8	99.7	99.4
4	99.6	99.6	100.2	100.7	100.8	97.8	100.8	100.4
13	100.2	100.8	99.4	99.2	98.9	98.8	98.3	99.2
28	100.0	100.4	100.2	100.1	94.4	99.1	101.4	99.5

Figure 4.2.13 Stability Data for GUSULFHY

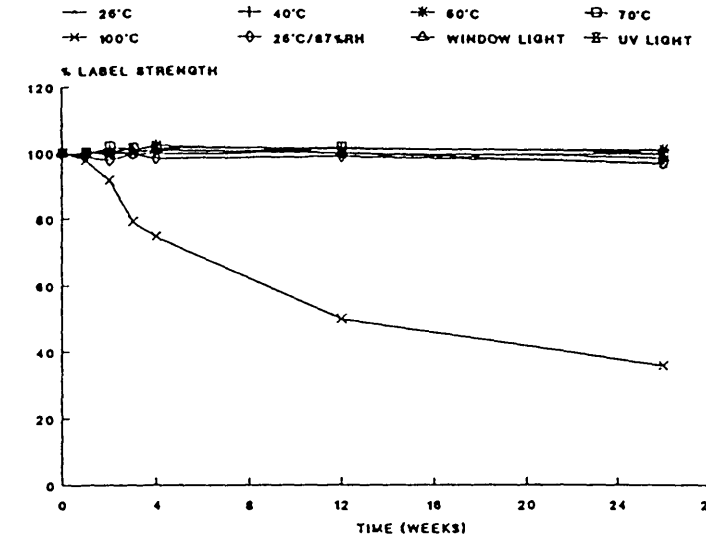

TIMEPOINT	CONDITION (% Label)							
(Weeks)	25	40	50	70	100	RH	Lt	Hv
1	99.8	99.9	99.6	100.0	97.7	98.8	100.0	100.2
2	99.6	100.7	100.4	101.8	91.7	97.8	99.9	99.9
3	100.1	101.0	101.2	101.4	79.2	99.6	100.2	99.8
4	100.7	100.5	102.4	101.6	74.8	98.4	101.0	99.7
12	100.0	101.2	101.2	101.7	49.8	99.0	100.2	99.9
26	100.0	101.2	101.5	100.3	35.8	97.1	99.0	97.4

Figure 4.2.14 Comparison of thermal Stability (100°C) of Salts and Modifications of GU

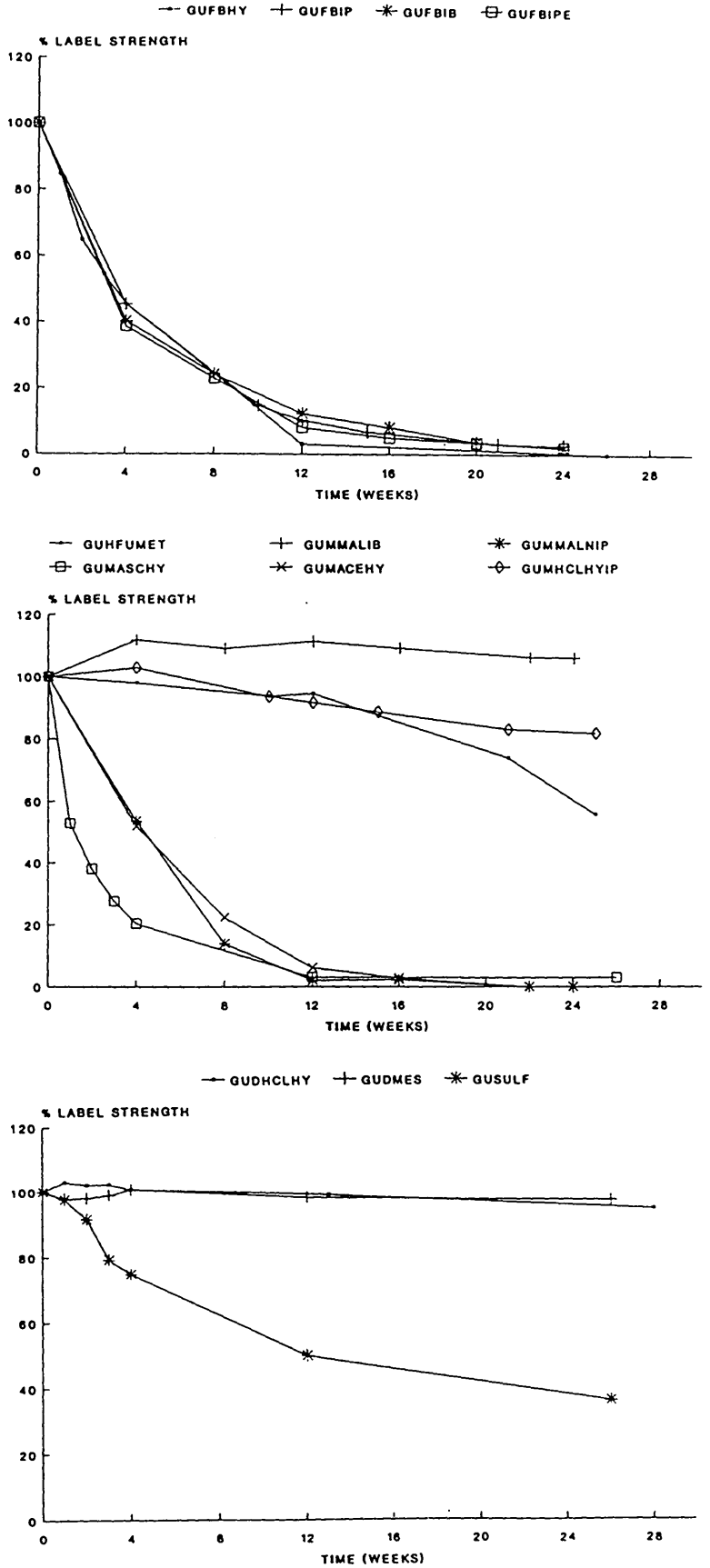

Figure 4.2.15 Comparison of window light Stability of Salts and Modifications of GU

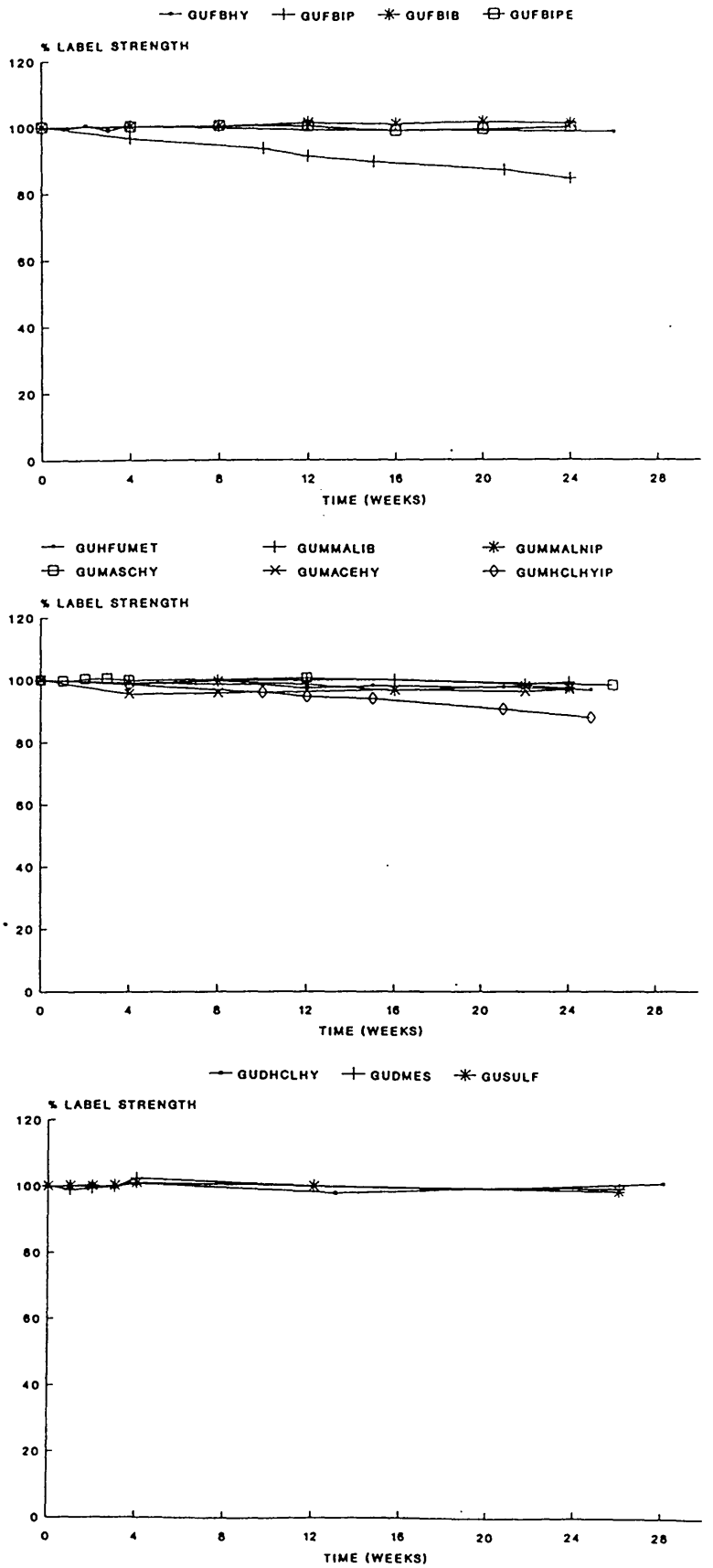

Figure 4.2.16 Comparison of UV Light Stability of Salts and Modifications of GU

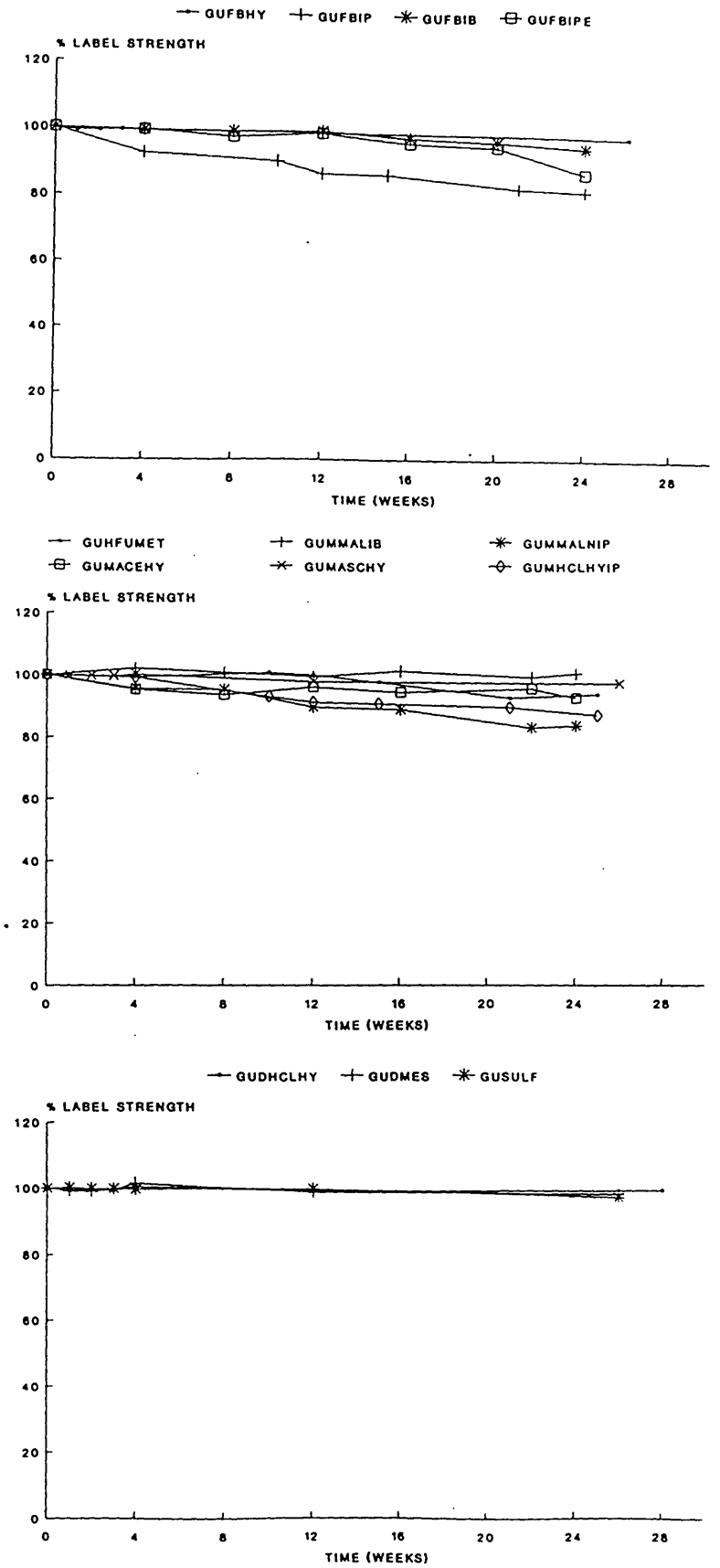

Figure 4.2.17 DSC heating curve for GUFBHY

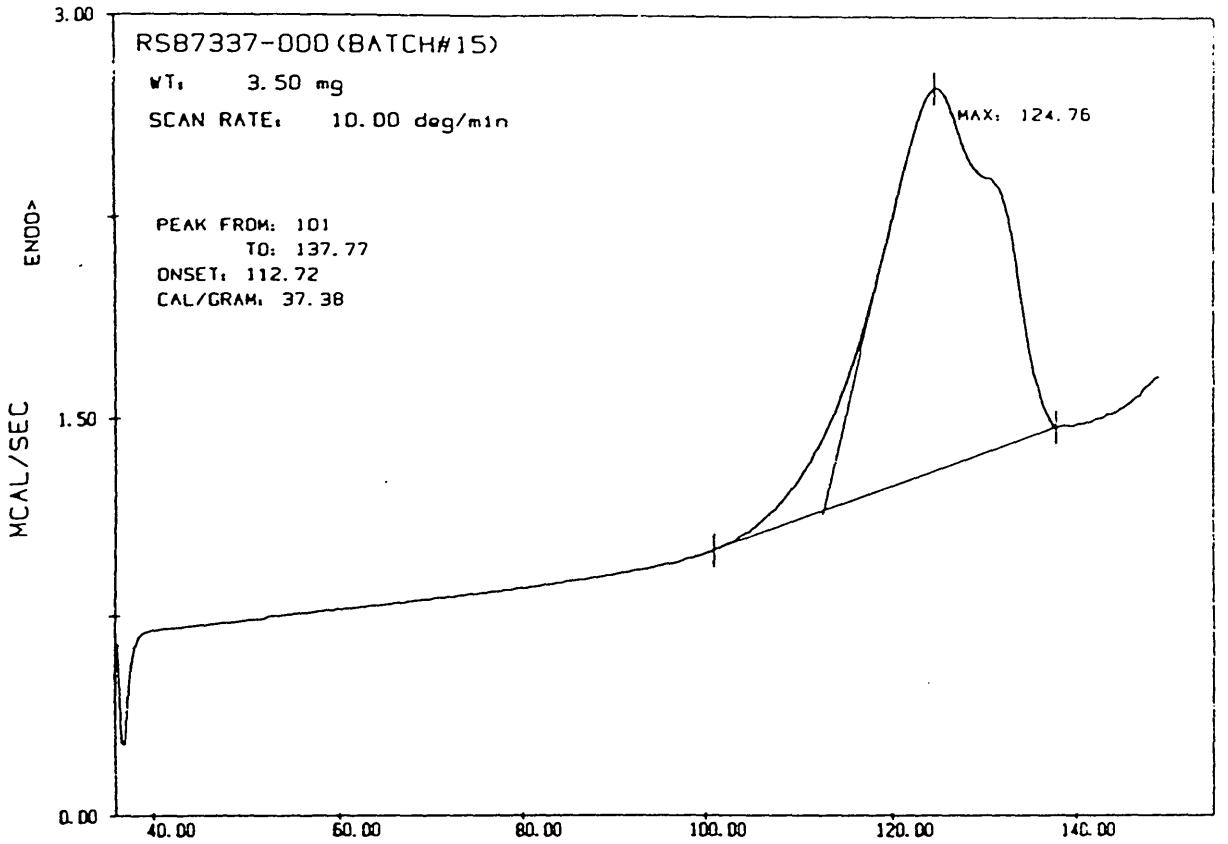

4.3 Van't Hoff Solubility Investigations on Salts and Modifications of GU

The data and Van't Hoff Solubility plots are summarised in Figures 4.3.1 and 4.3.2, respectively, for the mono and diprotonated salts of GU. Due to the low aqueous solubility (<0.001mg.ml^{-1}) of the free base solvates, Van't Hoff solubility investigations could not be carried out for them.

Linear regression analyses (using least squares fit) were performed on the data, the correlation coefficients (R^2) were good, only GUMACEHY gave an R^2 value of <0.9 (0.845).

These data together with the heat of solution (ΔHs) values are given in Table 4.3.1.

Table 4.3.1 Summary of linear regression and Heats of Solution (ΔHs) data for salts of GU

Salts of GU	Linear Regression Analyses R^2	a	b	ΔHs KJ.Mol^{-1}
GUMACEHY	0.845	-8.343	1068.7	- 8.89
GUMASCHY	0.914	4.530	-2180.0	18.13
GUMMALIB	0.999	2.286	-2123.9	17.66
GUMHCLHYIP	0.996	-0.943	-1318.5	10.96
GUSULF	0.999	3.058	-2707.1	22.51
GUDMES	0.982	-11.278	2763.6	-22.98
GUSPHOS	0.990	2.555	-2410.7	20.04
GUDNIT	0.986	2.230	-2225.8	18.51
GUDHCLHY	0.934	-2.283	- 859.0	7.14

a ≡ intercept, b ≡ slope of graph

Only two of the salts studied gave an inverse relationship between natural logarithm of molar concentration (ln Cs) and the inverse of absolute temperature (T^{-1}). The monoacetate (GUMACEHY, ΔHs = -8.89 $KJ.mol^{-1}$) and the dimesylate (GUDMES, ΔHs =-22.98 $KJ.mol^{-1}$) salts, both demonstrated exothermic heat of solution which implies an extensive solute - solvent interaction[10].

This behaviour is in contrast to that observed for most drugs[10,11], where a rise in temperature results in a corresponding increase in drug solubility and results in an endothermic heat of solution.

Cyclosporin A[12] was recently reported to exhibit an exothermic heat of solution. This work was in accord with the previous investigations of Loosli *et al*[13], who suggested that at higher temperatures the intramolecular hydrogen bonds are stronger and the molecule adopts a conformation corresponding to an isolated, rather than a solvated molecule. As the temperature decreases the intramolecular hydrogen bonds weaken and the solubility increases.

Both the dimesylate (GUDMES) and the monoacetate (GUMACEHY) salts show evidence of intramolecular associations in solid phase. GUDMES exhibits a unique intramolecular hydrogen bond between the piperazine nitrogen, N(14) and the methoxy oxygen, O (32). (see Table 5.7)

Although GUMACEHY is not capable of exhibiting this type of intramolecular association, due to its protonation state (only the diprotonated salts possess a proton on the piperazine nitrogen, N(14)); it can achieve a similar bonding arrangement, by using a water molecule as a key intermediate. The water molecule exhibits a

bifurcated hydrogen bond to the piperazine nitrogen, N(14) and to the methoxy oxygen, O (32) of the same molecule (see Table 5.4).

The remainder of the salts all gave positive relationships and endothermic heat of solution.

Figure 4.3.1. Van't Hoff solubility Plots for Monoprotonated Salts of GU

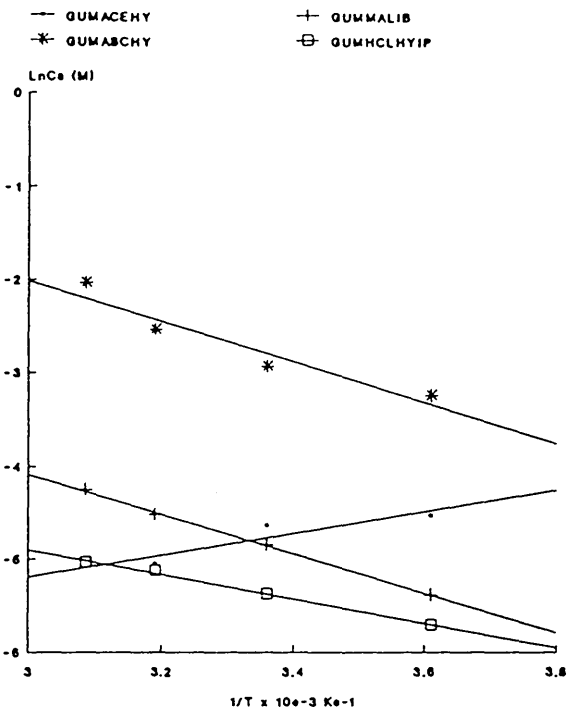

SALT	10^3 Inverse of Absolute Temperature (K^{-1}) 3.61	3.36	3.19	3.086
GUMACEHY	-4.63	-4.64	-6.00	NA
GUMASCHY	-3.24	-2.94	-2.64	-2.04
GUMMALIB	-6.38	-4.84	-4.61	-4.26
GUMHCLHYIP	-6.71	-6.37	-6.12	-6.03

Figure 4.3.2. Van't Hoff solubility Plots for Diprotonated Salts of GU

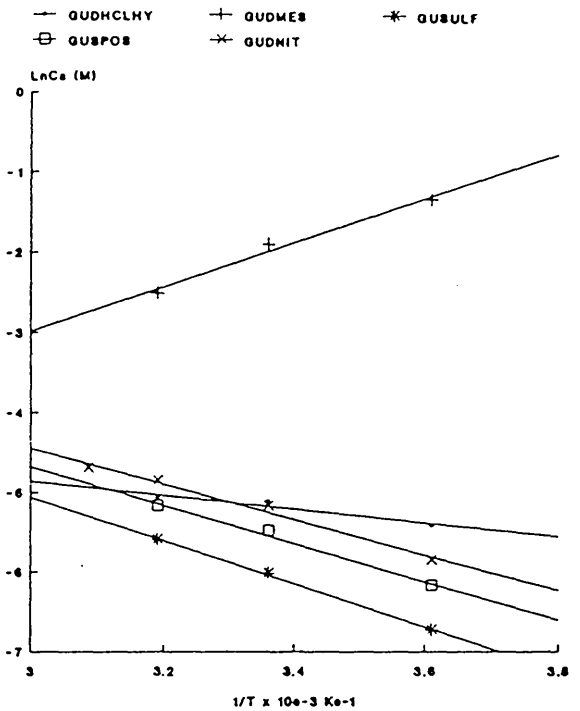

10^3 Inverse of Absolute Temperature (K^{-1})

SALT	3.61	3.36	3.19	3.086
GUSULF	-6.72	-6.02	-6.69	NA
GUDMES	-1.34	-1.90	-2.62	NA
GUSPHOS	-6.17	-6.48	-6.17	NA
GUDNIT	-6.80	-6.17	-4.86	-4.89
GUDHCLHY	-6.41	-6.11	-6.06	NA

4.4 Physicochemical Properties of Salts and Modifications of GU

Salt formation provides a means of altering the physicochemical and resultant biological characteristics of a drug entity without modifying its molecular structure[14]. Many published reviews[14,15,16] have indicated the importance of the selection of the most appropriate salt form. In making this selection, the variables under consideration are yield, rate and quality of the crystallisation process, availability and cost of the process, solubility, hygroscopicity, stability of the salt form and the toxicological effects of chronic and acute dosing of the drug and its conjugate acid. These requirements are in many ways conflicting and salt selection tends to be a semi-empirical process.

The most important considerations for salt formation are the relative pka of the basic drug (HB^+) and of the acid of the proposed counterion (HA). Salt formation requires that the equilibrium lie well to the right

$$B + HA \rightleftharpoons HB^+ + A^-$$

Since log k for this reaction is, pka (HB^+) - pka (HA), it is essential that the pka (HB^+) > pka (HA). A secondary consideration is that of relative toxicity of the conjugate acid. A compilation of salts used in pharmaceutical products marketed in the US up to 1974 is given in Table 4.4.1.

The physicochemical properties of the salts and modifications of GU studied are summarised in Table 4.4.2. Clearly the very low aqueous solubility and intrinsic toxicity of the solvate alcohols, will restrict the use of the modifications of the free base of GU. The deliquescent nature of GUMMALNIP and GUMACEIP would

prevent the use of these monoprotonated salts, whilst the moderate hygroscopicity of GUMHCLHYIP could lead to processing difficulties during solid oral dose form development.
Due to the strength of hydrochloric acid (pka < 0), the resulting aqueous solutions tend to be very acidic (< pH 2[17]). This can limit the utility of chloride salts in certain parenteral dosage forms and lead to processing or packaging incompatibilities.

In addition, although the aqueous solubilities of the monoprotonated (GUMHCLHYIP) and diprotonated (GUDHCLHY) salts are adequate, 1.8 and 2.4 $mg.ml^{-1}$, respectively; the solubility in gastric fluid is likely to be much reduced. This is based on the effect of the common chloride ion on the equilibrium product in gastric fluid:

$$BH^{+}Cl^{-}_{(s)} \underset{\leftarrow}{\overset{Ksp}{\rightleftharpoons}} BH^{+}_{(aq)} + Cl^{-}_{(aq)}$$

This reduction in solubility can result in the dissolution rate of the chloride salt(s) falling below that of the free base form[18,19].

The moderate hygroscopicity, allied to the low aqueous solubility would preclude the use of the fumarate (GUHFUMET) salt.
The monocitrate (GUMCITIP) salt could not be readily crystallised, and in addition its low aqueous solubility would again preclude its use.

The intrinsic toxicity of the alcohol solvates of the monomaleate (GUMMALIP and GUMMALIB) would present problems. In addition although GUMMALIB demonstrated excellent stability and moderate aqueous solubility ($3.1mg.ml^{-1}$), the low melting point (117.9-120.5°C) might present problems with processing. Low melting point drugs generally exhibit plastic deformations[20], which can lead

to aggregation of the bulk drug, significantly affecting its flow and compression properties. The melting point also influences the compatibility of the drug with formulation excipients[21], as it affects the eutectic melting point and can produce melting during tabletting, due to the frictional forces encountered.

All of the diprotonated salts studied, gave high melting points, good yields, were non-hygroscopic and demonstrated excellent stability. The solubility of the GUSULFHY was insufficient for further development; however the remainder all gave adequate and in the case of the mesylate (GUDMES) excellent solubility.

Since these salts are all formed from mineral acids, the resulting aqueous solutions tend to be very acidic and as mentioned previously, this can limit their use in parenteral dosage forms. These problems are not insurmountable, in that the dosage form can be buffered to an appropriate pH (3.5-4.0) and the consequent reduction in solubility compensated for by the addition of appropriate co-solvents.

However the two most promising salts are the monoascorbate (GUMASCHY) and monoacetate (GUMACEHY) salts. Both are non-hygroscopic, have moderate melting points and demonstrate good stability. Both the acetate (pka 4.76) and ascorbate (pka 4.21) salts produce aqueous solutions of acceptable pH.
The ascorbate has superior aqueous solubility ($20.9 mg.ml^{-1}$, *cf* $3.8 mg.ml^{-1}$ for GUMACEHY) and in addition the ascorbate's anti-oxidant and low toxicity[22] properties, greatly facilitated its selection as the salt of choice. However it is not easily synthesised (see Table 3.1) or isolated.

Therefore based on the cost, non-hygroscopicity and good stability, the free base hydrate (GUFBHY) was selected for development. The ascorbate salt was subsequently prepared, *in situ* during formulation, by the addition of equimolar quantities of the base and ascorbic acid.

One striking feature of these salt selection investigations are the propensity of the salts and modifications of GU to form solvates (pseudopolymorphs). Perhaps this is not too surprising given the widespread nature of the phenomenon of polymorphism and solvation. Indeed Dunitz[5] speculated that almost all compounds are polymorphic, if the right conditions for crystallisation, are produced.

Table 4.4.1 FDA APPROVED COMMERCIALLY MARKETED SALTS

Anion	Percent[a]	Anion	Percent
Acetate	1.26	Iodide	2.02
Benzenesulfonate	0.25	Isothionate[i]	0.88
Benzoate	0.51	Lactate	0.76
Bicarbonate	0.43	Lactobionate	0.13
Bitartrate	0.63	Malate	0.13
Bromide	6.58	Maleate	3.03
Calcium edetate	0.25	Mandelate	0.38
Camsylate[b]	0.25	Mesylate	2.90
Carbonate	0.38	Methylbromide	0.76
Chloride	47.56	Methylnitrate	0.38
Citrate	3.03	Mucate	0.13
Edetate	0.25	Napsylate	0.25
Edisylate[c]	0.38	Nitrate	0.64
Estolate[d]	0.13	Pamoate (Embonate)	1.01
Esylate[e]	0.13	Pantothenate	0.25
Fumarate	0.25	Phophate/ diphosphate	3.16
Gluceptate[f]	0.18	Polygalacturonate	0.13
Gluconate	0.51	Salicylate	0.88
Glutamate	0.25	Stearate	0.25
Glycollylarsnilate[g]	0.13	Subacetate	0.38
Hexylresorcinate	0.13	Succinate	0.38
Hydrabamine[h]	0.25	Sulphate	7.46
Hydroxynaph-thoate	0.25	Tannate	0.88
		Tartrate	3.54
		Teoclate[j]	0.13
		Triethiodine	0.13

Cation	Percent[a]	Cation	Percent
Organic:		*Metallic:*	
Benzathine[k]	0.66	Aluminium	0.66
Chloroprocaine	0.33	Calcium	10.49
Choline	0.33	Lithium	1.64
Diethanolamine	0.98	Magnesium	1.31
Ethylenediamine	0.66	Potassium	10.82
Meglumine[l]	2.29	Sodium	61.97
Procaine	0.66	Zinc	2.95

[a] Percent is based on total number of anionic or cationic salts in use through 1974.
[b]Camphorsulphonate. [c]1,2- Ethanedisulphenate. [d]Laurylsulphate. [e]Ethanesulphonate. [f]Glucoheptonate. [g]p-Glycollamidophenylarsonate. [h]N,N' Di(dehydroabietyl)ethylenediamine[i]. 2-Hydroxyethanesulphate[j]. 8-Chlorotheophyllinate. [k]N,N' Dibenzylethylenediamine. [l]N-Methylglucamine.

Table 4.4.2 Comparison of physicochemical data of salts of GU

Salt/ Modification	mp (°C)	% Yield	Hygroscopicity[A]	Adsorption Desorption Isotherms	Stability[B]	Ambient Solubility ($mg.ml^{-1}$)	Comments
Modification							
GUFBHY	132.0-134.2	84.0	All 1	II, closed	25-70,RH,Lt,Hv (5),100(1)		Low aqueous solubility and toxicity of solvate alcohols are a problem
GUFBIB	82.5- 85.5	72.7	All 1	II, closed	25-50,RH,Lt,Hv (5),70(3);100(1)		
GUFBIP	116.6-119.7	76.4	All 1	II, closed	25-50,RH,(5),Lt Hv,(4),70(3),100 (1)	All < 0.001	
GUFBRIB	82.6- 84.6	79.3	-	-	-		
GUFBSIB	98.4-100.6	71.7	-	-	-		
GUFBIPE	67.1- 69.6	62.1	All 1	II, closed	25-50,RH,Lt(5) 70,Hv(4);100(1)		
Monoprotonated							
GUHFUMET	171.1-173.2	68.3	All 2	I, closed	25-70,RH,Lt,Hv (5),100(3)	<0.1	Low aqueous solubility
GUMMALIP	180.8-182.8	72.0	-	-	-	-	Toxicity of solvate alcohols are a problem
GUMMALIB	117.9-120.5	86.8	All 1	II, open	All 5	3.1	

Table 4.4.2 Comparison of physicochemical data on salts of GU

Salt/ Modification	mp (°C)	% Yield	Hygroscopicity[A]	Adsorption Desorption Isotherms	Stability[B]	Ambient Solubility ($mg.ml^{-1}$)	Comments
GUMMALNIP	114.9-116.9	56.4	87%,deliquescent (2),75°-20%(1)	II, closed	25-70,RH,Lt,Hv (5),100(1)	-	Deliquescent at high RH, toxicity of solvate alcohols are a problem
GUMCITIP	140.0-141.5	59.6	-	-	-	<0.1	Low aqueous solubility
GUMACEIP	-	-	87%-52% deliquescent	-	-	-	Deliquescent at medium to high RH
GUMACEHY	150.4-154.4	72.4	All 1	IV, closed	25-70,RH,Lt Hv(5),100(1)	3.8	Good
GUMASCHY	132.1-134.2	68.2	All 1	III, closed	25-70,RH,Lt, Hv(5),100(1)	20.9	Excellent, synthesis a problem
GUMHCLHYIP	235.5-237.5	65.2	85%,75%,(2) 52%,20%,(1)	IV, closed	25-70,RH(5) 100,Lt,Hv(4)	1.8	Hygroscopicity and toxicity of solvate alcohols are a problem
Diprotonated							
GUDHCLHY	263.2-265.4	69.3	All 1	II, closed	All 5	2.4	Good
GUDMES	269.1-271.3	69.8	All 1	II, closed	All 5	59.1	Excellent

Table 4.4.2 Comparison of physicochemical data on salts of GU

Salt/ Modification	mp (°C)	% Yield	Hygroscopicity[A]	Adsorption Desorption Isotherms	Stability[B]	Ambient Solubility ($mg.ml^{-1}$)	Comments
GUSULFHY	220.7-223.7	91.8	-	· -	25-70,RH,Lt Hv(5),100(2)	<0.1	Low aqueous solubility
GUSULF	233.4-235.2	67.8	All 1	II, open	-	1.0	Good
GUSPHOS	240.4-242.4	70.8	-	-	-	1.6	-
GUDNIT	177.8-180.4	95.0	-	-	-	2.2	-

Table 4.4.2 Notes

A. Hygroscopicity classed as follows:
1. 0% - 5% w/w; Non-hygroscopic
2. 5% -10% w/w; Moderate hygroscopicity
3.10% -20% w/w; Medium hygroscopicity
4.>20% w/w; High hygroscopicity

B. Stability classed as follows:
1. 0% - 20% label; Very poor stability
2. 20% - 50% label; Poor stability
3. 50% - 80% label; Moderate stability
4. 80% - 90% label; Medium stability
5. 90% -100% label; Good stability

4.5 References

1. BRUNAUER, S, DEMING, L S, DEMING, W E and TELLER, E, J Amer Chem Soc, 62, 1723, 1940

2. UMPRAYN, K and MENDES, R W, Drug Dev Ind Pharm, 13, 653, 1987

3. WELLS, J I in 'Pharmaceutical Preformulation' (the physicochemical properties of drug substances), 170, 1988, Ellis Horwood, Chichester

4. CARSTENSEN, J T in 'Theory of Pharmaceutical Systems' 295, 1973 Academic Press, New York

5. DUNITZ, J D, in 'X-Ray Analysis and the Structure of Organic Molecules', 319, 1979, Cornell University Press, Ithica

6. LAIDLER, K J in 'Chemical Kinetics', 316, 1973, Tata McGraw Hill, New Delhi

7. SHARP, J H, BRINDLEY, G W and NARAHARIACHAR, B N, J Am Ceramic Society, 49, 379, 1966

8. PROUT, E and TOMPKINS, F, Trans Faraday Soc, 40, 448, 1944

9. PERRIER, P, (1980) through Polymorphs and Solvates of Drugs, RSC Course, University of Bradford, 1989

10. SOKOLOSK; T D in 'Solutions and Phase Equilibria' (Eds. Osol, A *et al*), 19, 248, Mack, Easton, Pennsylvania.

11. MACHERAS, P E, Koupparis, M A, Antimisiaris, S A, Pharm Res, 7, 537, 1990

12. ISMAILORS, G, REPPAS, C, DRESSMAN, J B and MACHERAS, P E, J Pharm Pharmacol, 43, 287, 1991

13. LOOSLI, H-R, OSCHKINAT, H, WEBER, H-P, PETCHER, T J and WIDMER, A, Helv Chim Acta, 68, 682, 1985

14. GOULD, P L, Int J Pharm, 33, 201, 1986

15. BERGE, S M, BIGHLEY, L D and MONKHOUSE, D C, J Pharm Sci, 66, 1, 1977

16. AGHARKAR, S, LINDENBAUM, S and HIGUCHI, T, *ibid*, 65, 747, 1976

17. NUDELMAN, A, McCAULLY, R J and BELL, S C, *ibid*, 63, 1880, 1974

18. MIYAZAKI, S, OSHIBA, M and NADAI, T, Int J Pharm, 6, 77, 1980

19. MIYAZAKI, S, OSHIBA, M and NADAI, T, J Pharm Sci, 70, 594, 1981

20. JONES, T M, Drug Cosmet Ind, 124, 40, 103, 1979

21. LI WAN PO, A and MROSO, P V, Int J Pharm, 18, 287, 1984

22. Handbook of Pharmaceutical Excipients, 6, 1986, published by American Pharmaceutical Society and The Pharmaceutical Society of Great Britain, London

SECTION 5 : CRYSTALLOGRAPHIC DATA FOR GU

5.1 GUFBHY

Crystal Data

Colourless rods from 50% aqueous acetone, 0.34 x 0.19 x 0.10 mm.

$C_{18}H_{20}Cl_2N_4O_2.H_2O$, M = 413.3, monoclinic, $P2_1/c$ (No.14), a = 9.055(3), b = 9.078(8), c = 23.945(8)Å, β = 93.72(2)°, V = 1964.2Å^3, Z = 4, V/Z = 491 Å^3. Lattice parameters refined from setting angles for 18 reflections with θ between 8.8 and 11.0°.

Dc = 1.40 g cm^{-3}, μ = 3.55 cm^{-1}, F(000) = 864, T=290K.

Data Collection and Processing

Stoë STADI-2 diffractometer, MoK_α, λ=0.71073Å. 2584 independent data ($2 < \theta < 25°$, $-10 \leq h \leq 10$, $0 \leq k \leq 9$, $0 \leq l \leq 28$) yielding 1536 data with $I \geq 2.5\sigma(I)$. No measurable crystal decay or movement.

Structure Solution and Refinement

Solution by direct methods (SHELX84).

$\varpi^{-1} = \sigma^2(F) + 0.00023F^2$, R = 0.047, wR = 0.046, S = 1.14 based on 262 parameters. Maximum shift/esd on last cycle = 0.06. Maximum and minimum ripple in difference electron density map : 0.33 and -0.38 e.Å^{-3}.

Structure Discussion

Selected bond lengths, angles and torsion angles are given in Tables 5.10.1-5.10.3. The molecular perspective and molecular packing diagrams (as viewed along the b-axis) are shown in Figure 5.1. It is dominated by hydrogen bonding and ring stacking.

The water molecule is central to the hydrogen bonding, being joined to three different drug molecules. One of its donor bonds appears to be bifurcated, the hydrogen atom being equally directed towards N(14) and O(32) of the same molecule. These distances are summarised in Table 5.1, together with some of the close inter-

molecular contacts. The main hydrophobic interactions involve atoms of the methoxy phenyl ring 3 interacting with the piperazine ring of the molecules related to it by the inversion centres at ½, 1, 0 and 0, 1, 0.

Table 5.1 Hydrogen Bonding and Other Close Intermolecular Contacts

a) Hydrogen Bonding

Donor	Acceptor	Symmetry	D-H	H...A	D...A
N(2)-H(2A)....	O(34)	-x,2-y,-z	1.00(5)	2.12(5)	3.102(6)
N(2)-H(2B)	(none)		0.83(5)		
O(34)-H(34)...	O(1W)	-x,2-y,-z	0.95(5)	1.67(5)	2.605(5)
O(1W)-H(1W)...	N(14)	-x,1-y,-z	0.74(6)	2.49(6)	3.193(5)
...	O(32)	-x,1-y,-z		2.65(6)	3.094(5)
O(1W)-H(2W)...	N(3)	1+x,y,z	0.89(5)	1.99(5)	2.863(6)

b) C...C Contacts Shorter than 3.75Å

C(16).....C(35)	-1-x,2-y,-z	3.523(7)
C(16).....C(34)	-1-x,2-y,-z	3.529(7)
C(12).....C(12)	-x,1-y,-z	3.537(7)
C(15).....C(35)	-1-x,2-y,-z	3.623(7)
C(1).....C(35)	x,-1+y,z	3.627(7)
C(12).....C(34)	-x,2-y,-z	3.681(7)
C(15).....C(36)	-1-x,2-y,-z	3.687(7)
C(13).....C(35)	-x,2-y,-z	3.713(7)
C(13).....C(34)	-x,2-y,-z	3.736(7)

c) C...N Contacts Shorter than 3.75Å

C(12).....N(2)	-x,1-y,-z	3.547(6)
C(3M).....N(2)	-x,1-y,-z	3.725(7)

c) C...O Contacts Shorter than 3.75Å

C(16).....O(1W)	-1+x,y,z	3.298(6)
C(24).....O(34)	x,1½-y,½+z	3.375(6)
C(34).....O(1W)	-x,2-y,-z	3.400(6)
C(35).....O(1W)	-x,2-y,-z	3.537(6)
C(12).....O(1W)	-x,1-y,-z	3.571(6)

Figure 5.1 Molecular Perspective and Molecular Packing Diagrams (viewed along the b-axis) of GUFBHY

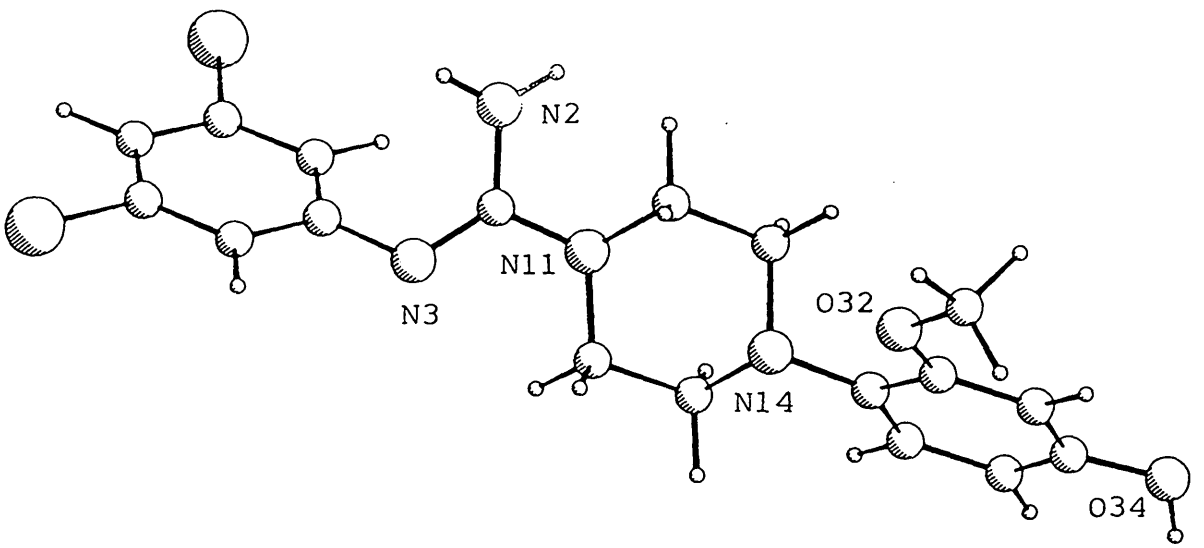

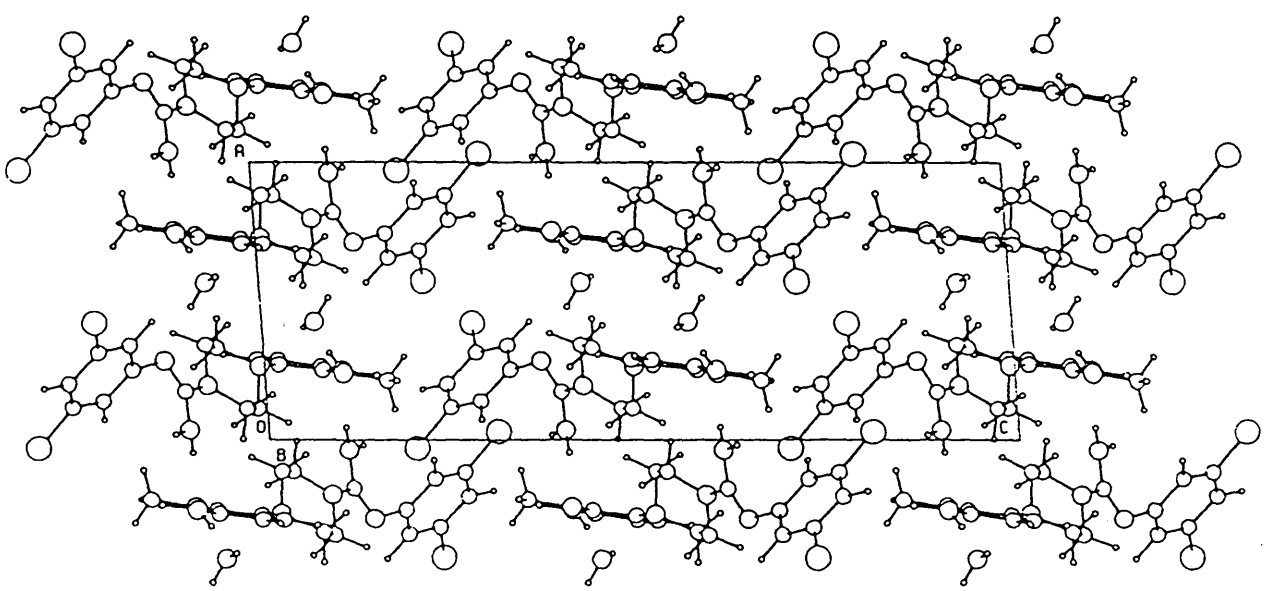

5.2 GUFBIP, GUFBIB and GUFBRIB

5.2.1 GUFBIP

Crystal Data

Colourless plates from isopropanol, 0.32 x 0.20 x 0.04 mm.

$C_{18}H_{20}Cl_2N_4O_2.2C_3H_8O$, M = 515.5, triclinic, $P\bar{1}$ (No.2),

a = 10.256 (7), b = 11.755 (6), c = 12.644 (8) Å,

α = 110.02 (4), β = 94.20 (4), γ = 104.30 (3)°,

V = 1366.9 Å^3, Z = 2, V/Z = 683 Å^3.

Lattice parameters refined from accurately measured 2Θ values (18.4 - 21.4°) for 27 reflections

Dc = 1.25 g cm^{-3}, μ = 2.70 cm^{-1}, F(000) = 548,

T = 193K.

Data Collection and Processing

Stoë STADI-4 diffractometer with Oxford Cryosystem attachment, MoK_α, λ = 0.71073 Å. 3568 independent data ($2 < \Theta < 22°$, $-10 \leq h \leq 10$, $-12 \leq k \leq 12$, $0 \leq l \leq 13$) yielding 1744 data with $I \geq 3\sigma(I)$. No measurable crystal decay or movement.

Structure Solution and Refinement

Solution by direct methods (SHELX 86).

$w^{-1} = \sigma^2(F) + 0.00023F^2$, R = 0.049, wR = 0.054,

S = 1.15 based on 340 parameters. Maximum shift/esd on last cycle = 0.07. Maximum and minimum ripple in difference electron density map : 0.24 and -0.24 e.Å^{-3}.

5.2.2 GUFBIB

Colourless plates from isobutanol, 0.4 x 0.5 x 0.08 mm.

$C_{18}H_{20}Cl_2N_4O_2.2C_4H_{10}O$, M = 543.5, triclinic, $P\bar{1}$ (No.2),

a = 10.328 (2), b = 11.767 (2), c = 12.884 (3) Å,

α = 107.51 (1), β = 96.37 (2), γ = 103.45 (1)°,

V = 1424.4Å^3, Z = 2, V/Z = 712 Å^3.

Lattice parameters refined from accurately measured 2θ values (15.0 - 21.2°) for 31 reflections.
Dc = 1.27 $g.cm^{-3}$, μ = 2.62 cm^{-1}, F(000) = 580,
T = 193 K.

Data Collection and Processing

Stoë STADI-4 diffractometer with Oxford Cryosystem attachment, MoK_α, λ = 0.71073 Å. 3588 independent data ($2 < \theta < 22°$, $-10 \leq h \leq 10$, $-12 \leq k \leq 12$, $0 \leq l \leq 13$) yielding 2008 data with $I \geq 3\sigma(I)$. No measurable crystal decay or movement.

Structure Solution and Refinement

Solution by direct methods (SHELX 86).
$\varpi^{-1} = \sigma^2(F) + 0.00059F^2$, R = 0.057, wR = 0.068,
S = 1.23 based on 328 parameters. Maximum shift/esd on last cycle = 0.09. Maximum and minimum ripple in difference electron density map : 0.40 and -0.30 $e.Å^{-3}$.

Substantial disorder was apparent in solvent molecules. In molecule 1, two positions were refined isotropically with half site occupancy for the terminal methyl group, C(4A') and C(4A"). In molecule 2, it was necessary to consider two alternative chains and four atoms with half site occupancy. The two carbon chains consist of C(1B')-C(2B)-C(3B')-C(4B') and C(1B")-C(2B)-C(3B")-C(4B"), where C(1B") and C(3B') effectively occupy the same position. In this molecule only O(2B) was refined anisotropically.

5.2.3 GUFBRIB

Colourless plates from R isobutanol, 0.4 x 0.5 x 0.08 mm.
$C_{18}H_{20}Cl_2N_4O_2.2C_4H_{10}O$, M = 543.5, triclinic, P1 (No.1),
a = 10.42 (2), b = 11.90 (1), c = 13.06 (2) Å,
α = 107.0 (1), β = 96.6 (1), γ = 103.9 (1)°,
V = 1473.76 $Å^3$, Z = 2, V/Z = 737 $Å^3$.

Lattice parameters refined from accurately measured 2θ values (20.2 - 21.0) for 15 reflections.
Dc = 1.22 $g.cm^{-3}$, T = 193 K.

Data Collection and Processing

Stoë STADI-4 diffractometer with Oxford Cryosystem attachment, MoK_α, λ = 0.71073 Å. Crystal not good enough to collect data.

Structure Discussions

The three compounds are essentially isomorphous, the cell volumes of GUFBIB and GUFBRIB being extended (mainly by elongation of c) by 57$Å^3$ and 107$Å^3$ respectively, in order to accommodate four extra CH_2 groups in the solvent molecules. The cell volume of GUFBRIB is larger than its achiral analogue, GUFBIB, due to increased disorder and reduced packing efficiency in the non-centrosymmetric cell.

Selected bond lengths, angles and torsion angles are given in Tables 5.10.1-5.10.3.

The molecular perspective diagrams of GUFBIP and GUFBIB, together with the molecular packing diagram of GFUBIP are shown in Figure 5.2.1. One of the solvent molecules forms a unique donor hydrogen bond with N(3) in both GUFBIP and GUFBIB, while the other is bifurcated, giving closest contact with O(32) and slightly more distant contact with N(14) of the same molecule; a contact of the same type was found in GUFBHY. These contacts are shown in Figure 5.2.2 and the distances are summarised in Table 5.2, together with some of the close intermolecular contacts.

Table 5.2 Hydrogen Bonding and Other Close Intermolecular Contacts

a) Hydrogen Bonding

			GUFBIP			GUFBIB		
Donor	Acceptor	Symmetry	D-H	H...A	D...A	D-H	H...A	D...A
N(2)-H(2A)	O(34)	-x,-y,1-z	0.92(7)	2.17(7)	3.068(8)	0.82(7)	2.17(7)	3.084(8)
N(2)-H(2B)	O(2B)	-x,1-y,1-z	0.81(7)	2.22(7)	2.998(9)	0.95(7)	2.08(7)	3.005(9)
O(34)-H(34)	O(2A)	1-x,-y,1-z	0.78(8)	1.92(8)	2.694(7)	0.83(7)	1.87(7)	2.695(7)
O(2A)-H(2AO)	N(3)	1-x,1-y,1-z	0.88(8)	1.95(8)	2.813(7)	0.97(7)	1.83(7)	2.794(7)
O(2B)-H(2BO)	O(32) x,y,z		0.78(8)	2.51(8)	3.185(7)	0.76(8)	2.61(8)	3.160(7)
	N(14) x,y,z		2.54(8)	3.238(8)		2.50(8)	3.220(8)	

b) C...C Contacts Closer than 3.75Å (excluding partially occupied sites in GUFBIB)

C(24).....C(36)	1-x,1-y,1-z	3.566(10)	3.602(10)
C(16).....C(2A)	1-x,1-y,1-z	3.569(11)	3.579(12)
C(12).....C(22)	-x,1-y,1-z	3.597(9)	3.558(9)
C(12).....C(34)	-x,-y,1-z	3.610(9)	3.607(9)
C(15).....C(25)	1-x,1-y,1-z	3.670(10)	3.680(10)
C(23).....C(3M)	-x,1-y,1-z	3.707(10)	3.664(10)
C(24).....C(3M)	-x,1-y,1-z	3.728(10)	3.707(10)
C(1).....C(12)	-x,1-y,1-z	[3.800(9)]	3.715(9)

c) C...N Contacts Closer than 3.75Å

C(1A).....N(3)	1-x,1-y,1-z	3.563(10)	3.696(10)

Figure 5.2.1 Molecular Perspective Diagrams of GUFBIP and GUFBIB and Molecular Packing Diagram (viewed along the b-axis) of GUFBIP

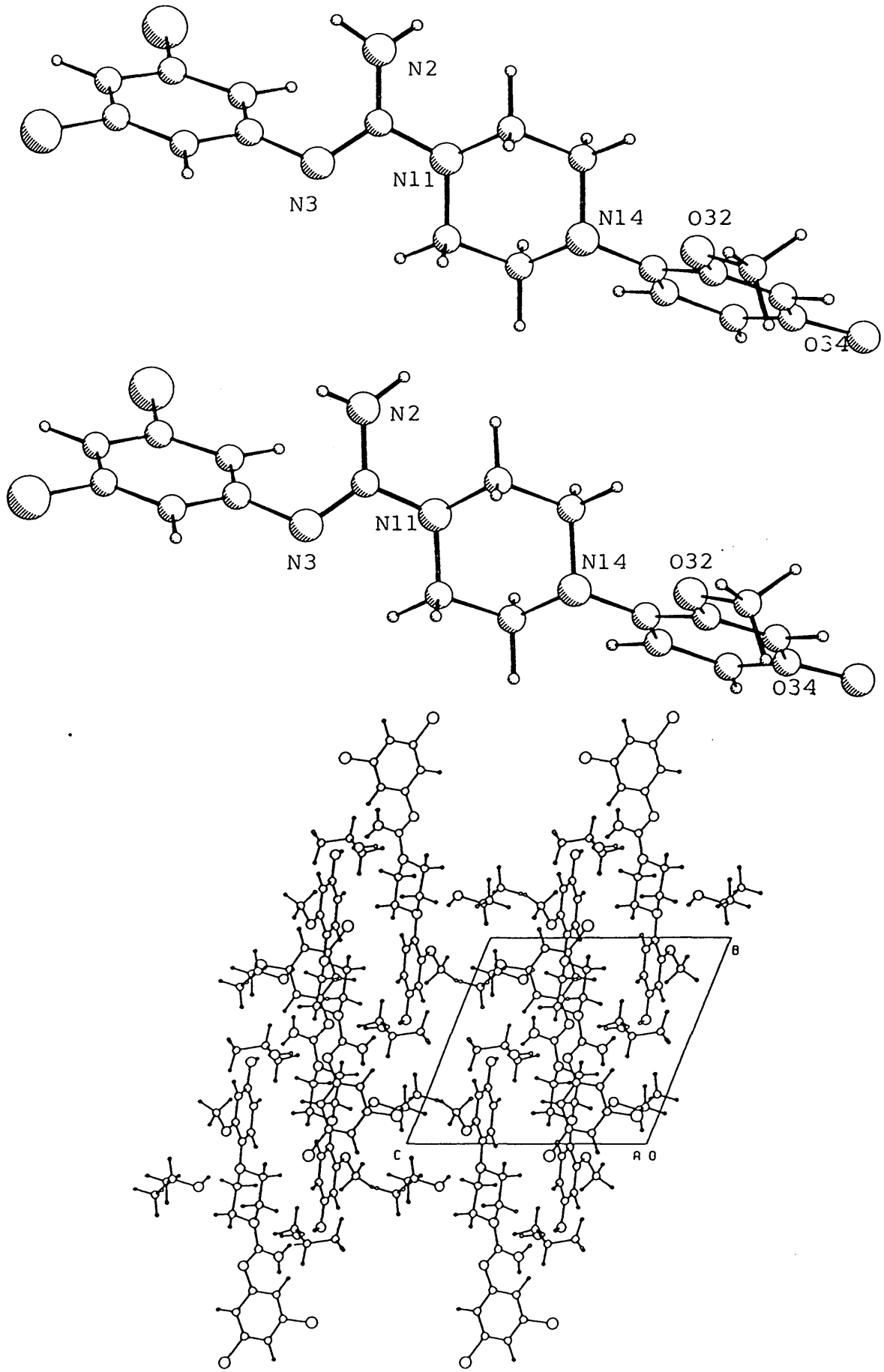

Figure 5.2.2 Perspective View of the Molecule of GUFBIP together with Associated Solvent Molecules and Showing the Numbering Scheme

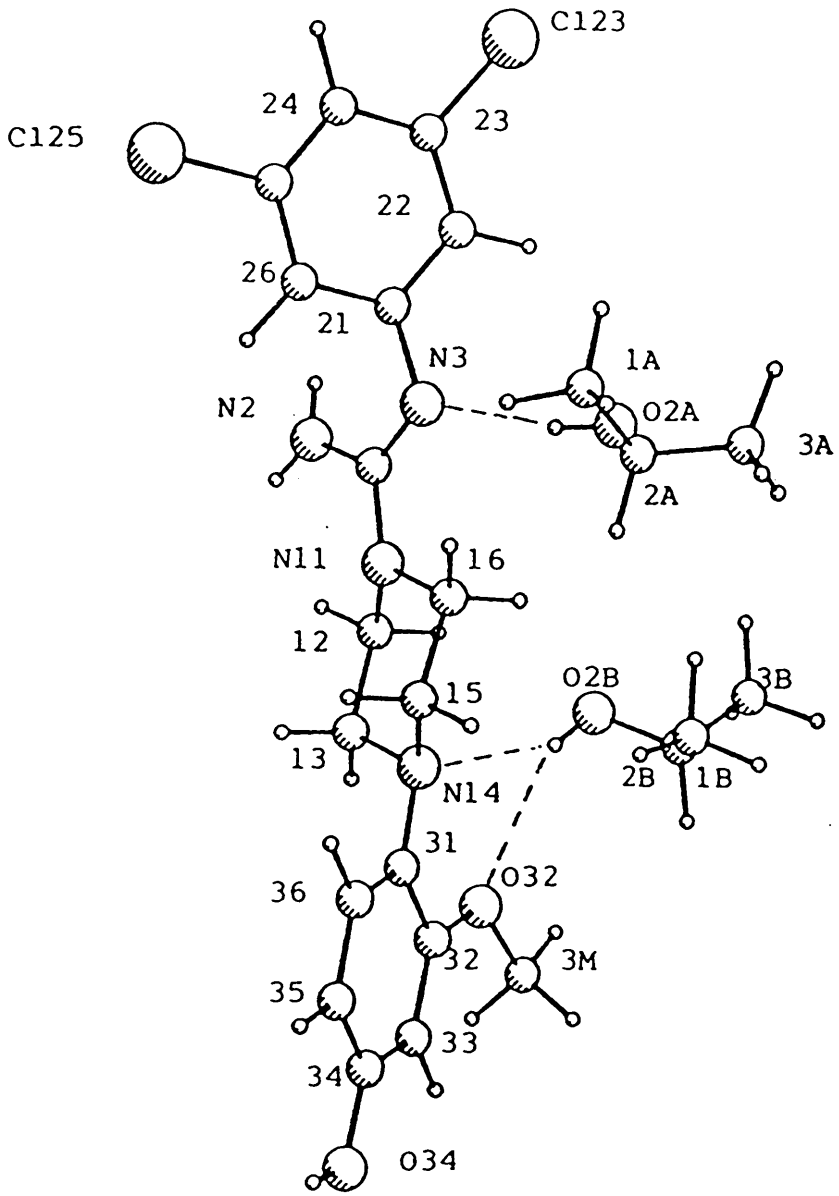

5.3 GUHFUMET

Crystal Data

Small hexagonal plates from ethanol, 0.23 x 0.13 x 0.05 mm.

2 $(C_{18}H_{21}Cl_2N_4O_2)^+.C_4H_2O_4^{2-}.C_2H_6O$, M = 476.2, monoclinic, $P2_1/n$ (alternative setting of $P2_1/c$, No.14),

a = 14.449 (19), b = 11.240 (9), c = 16.239 (16) Å,

β = 111.09 (8)°, V = 2460.7 Å^3, Z = 4, V/Z = 615 Å^3.

Lattice parameters refined from setting angles for 20 reflections with 2θ between 30 and 35°.

Dc = 1.28 g cm^{-3}, μ = 26.80 cm^{-1}, F(000) = 1096,

T = 290 K.

Data Collection and Processing

Stoë STADI-4 diffractometer, CuK_α, λ = 1.54178 Å. 2742 independent data ($2 < \theta < 60°$, $0 \leq h \leq 16$, $0 \leq k \leq 12$, $-8 \leq l \leq 18$) yielding 1294 data with $I \geq 2.5\sigma(I)$. No measurable crystal decay or movement.

Structure Solution and Refinement

Solution by direct methods (SHELX 86).

$\varpi^{-1} = \sigma^2(F) + 0.00040F^2$, R = 0.065, wR = 0.067,

S = 1.337 based on 312 parameters. Maximum shift/esd in the last cycle was 0.177, this was associated with a badly disordered ethanol fragment. Maximum and minimum ripple in difference electron density map : 0.29 and -0.31 e.Å^{-3}.

Substantial disorder was apparent in solvent molecules and it was necessary to consider two alternative alkyl chains and four atoms with partial site occupancy (C(1S):0.386/C(2S):0.724 and C(3S):0.712/C(4S):0.467). In this molecule, only O(1S) was refined anisotropically and no hydrogens were located.

Structure Discussion

Selected bond lengths, angles and torsion angles are

given in Tables 5.10.1-5.10.3. The molecular perspective diagram and the molecular packing (as viewed along the b-axis) are shown in Figure 5.3. It is dominated by hydrogen bonding and ring stacking and comprises of parallel interleaved sheets of methoxyphenyl ring systems forming parallel bilayers. The dichlorophenyl rings sit on the edge of the bilayer with one chlorine projecting into the layer and one outwith. The anions straddle the resulting channel between the parallel bilayers with the double bond being located on a special position, the remainder of the channel being occupied by water and disordered ethanol molecules (the latter were omitted from the packing diagram for clarity). The hydrogen bonding and other close intermolecular contacts are summarised in Table 5.3. The phenolic oxygen, O(34) forms a bifurcated hydrogen bond with the fumarate oxygens, giving closest contact with O(1C) and slightly more distant contact with O(2C) of the same molecule. A similar bifurcated hydrogen bond is formed between the guanidino nitrogen, N(3) and the fumarate oxygen, O(2C) and the phenolic oxygen, O(34); giving closest contact to the former and longer contact with the latter atoms of the same molecule.

Table 5.3 Hydrogen Bonding and Other Close Intermolecular Contacts

a) Hydrogen Bonding

Donor	Acceptor	Symmetry	D-H	H...A	D...A
O(34)-H(34)...	O(1C)	x,y,z	0.76	1.91(10)	2.670(11)
...	O(2C)	x,y,z	0.76	2.79(10)	3.300(11)
O(1C)-H(2A)...	N(2)*	½-x,-½+y,1½-z	1.22	1.77(8)	2.977(11)
N(2)-H(2B)....	O(1S)	½+x,½-y,-½+z	0.97	1.94(9)	2.905(11)
O(1S)-H	O(2C)	x,y,z	-	-	2.733(11)
N(3)-H(3).....	O(2C)	-x,1-y,1-z	1.34	1.51(13)	2.799(11)
.....	O(34)	-x,1-y,1-z	1.34	2.66(13)	3.205(11)

* salt H-bond

b) C...C Contacts Shorter than 3.75Å

C(2C).....C(1C)	-x,1-y,2-z	2.47(2)
C(3M).....C(1S)	½ + x,1 ½-y,-½ + z	3.19(4)
C(1).....C(4S)	-x,1-y,1-z	3.40(3)
C(23).....C(2S)	½ + x,½-y,-½ + z	3.55(3)
C(22).....C(2S)	½ + x,½-y,-½ + z	3.57(3)
C(24).....C(32)	-½ + x,½-y,-½ + z	3.62(2)
C(23).....C(4S)	½ + x,½-y,-½ + z	3.67(3)
C(24).....C(1S)	-½ + x,½-y,-½ + z	3.68(4)
C(16).....C(34)	-x,1-y,1-z	3.69(2)
C(1).....C(2S)	-x,1-y,1-z	3.70(3)
C(25).....C(1S)	½ + x,½-y,-½ + z	3.71(4)
C(26).....C(3M)	x,-1 + y,z	3.72(2)
C(23).....C(13)	½ + x,½-y,½ + z	3.72(2)

c) C...N Contact Shorter than 3.75Å

C(4S).....N(2)	-x,1-y,1-z	3.48(3)
C(3M).....N(2)	x,1 + y,z	3.58(1)
C(3S).....N(3)	-x,1-y,1-z	3.66(2)
C(2S).....N(11)	-x,1-y,1-z	3.68(2)
C(4S).....N(11)	-x,1-y,1-z	3.70(3)

d) C...O Contacts Shorter than 3.75Å

C(1C).....O(1C)	-x,1-y,2-z	2.96(2)
C(1S).....O(32)	-½ + x,1 ½-y,½ + z	3.02(4)
C(13).....O(34)	½-x,-½ + y,1 ½-z	3.14(2)
C(21).....O(34)	-x,1-y,1-z	3.31(1)
C(2C).....O(34)	x,y,z	3.33(2)
C(16).....O(2C)	-x,1-y,1-z	3.34(1)
C(1C).....O(1S)	x,y,z	3.34(2)
C(2S).....O(2C)	x,y,z	3.38(2)
C(12).....O(1C)	½-x,-½ + y,1 ½-z	3.37(1)
C(3S).....O(2C)	x,y,z	3.41(2)
C(1C).....O(2C)	-x,1-y,2-z	3.45(2)

Figure 5.3 Molecular Perspective and Packing Diagrams (viewed along the b-axis) of GUHFUMET

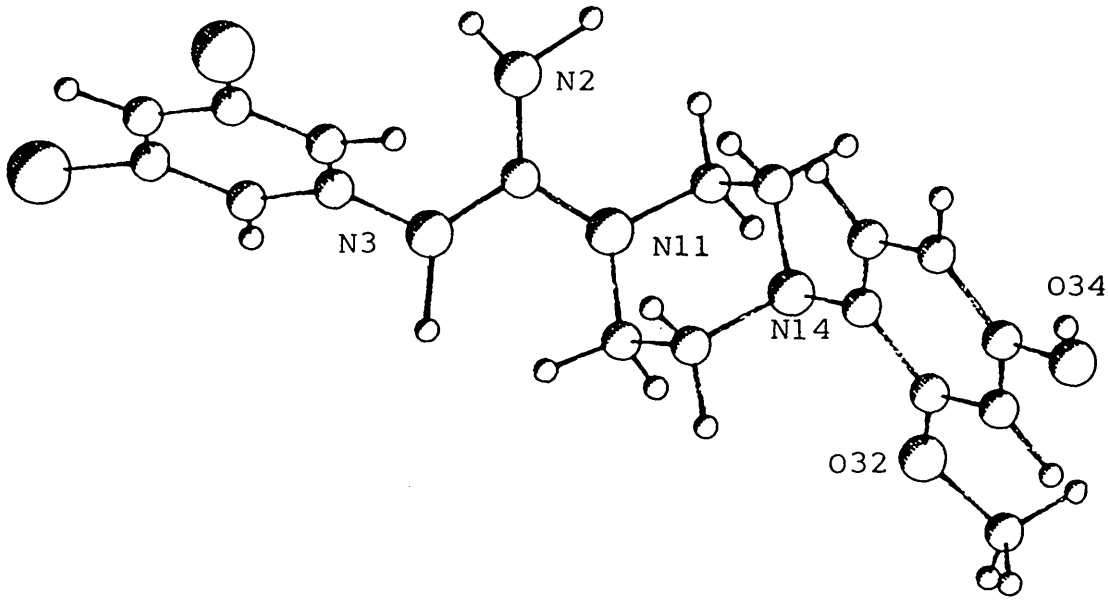

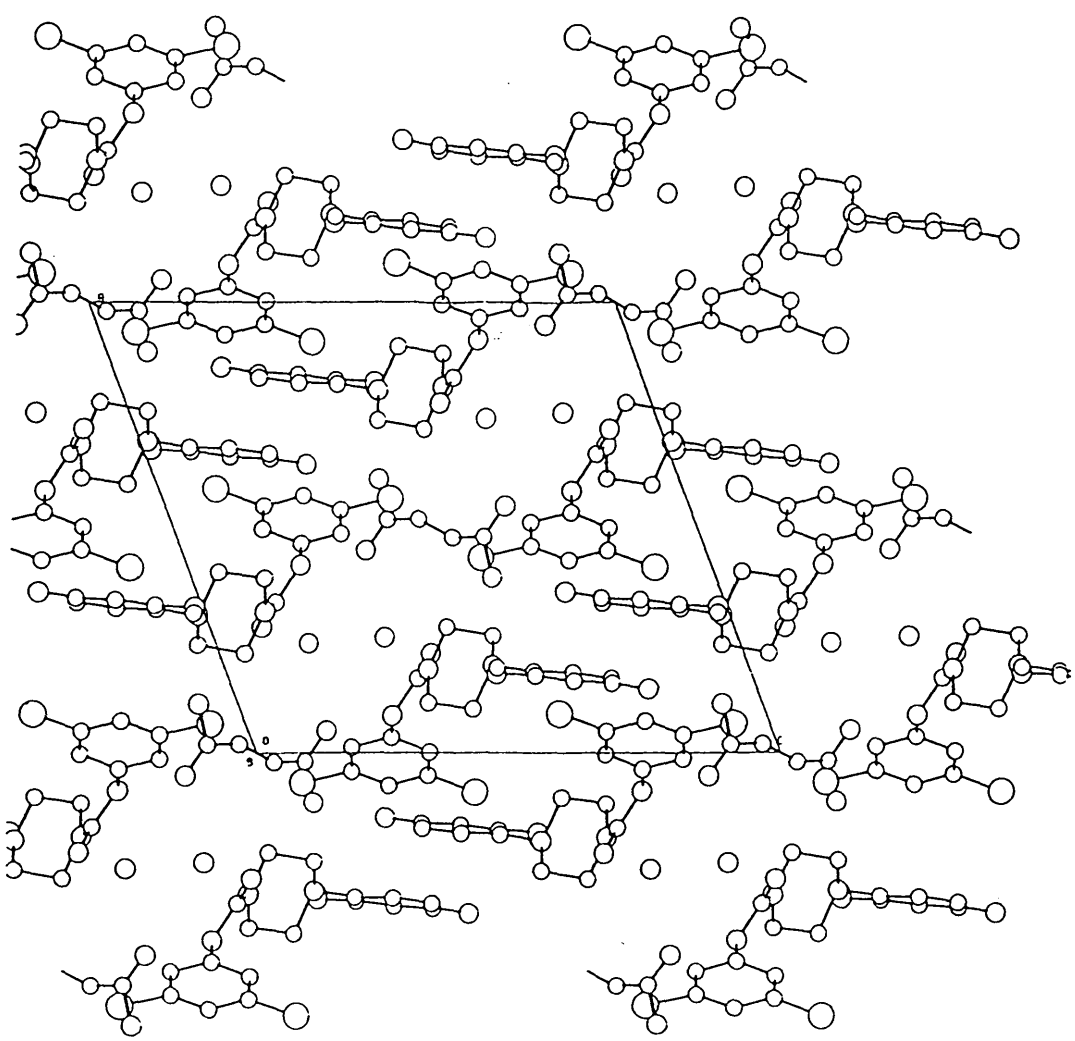

5.4 GUMACEHY

Crystal Data

Colourless plates from 95% aqueous ethanol, 0.20 x 0.15 x 0.03 mm.

$C_{18}H_{21}Cl_2N_4O_2^+.C_2H_3O_2^-.H_2O$, M = 455.3, monoclinic, $P2_1/c$ (No.14), a = 8.918 (1), b = 11.322 (2), c = 22.362 (3) Å, β = 93.82 (1)°, V = 2252.7 Å^3, Z = 4, V/Z = 563 Å^3. Lattice parameters refined from accurately measured 2Θ values (24.8 - 31.6°) for 24 reflections.

Dc = 1.395 g cm^{-3}, μ = 2.78 cm^{-1}, F(000) = 984, T = 290 K.

Data Collection and Processing

Stoë STADI-4 diffractometer, MoK_α, λ = 0.71069 Å. 3119 independent data ($2 < \Theta < 25°$, $-10 \leq h \leq 10$, $-13 \leq k \leq 13$, $-8 \leq l \leq 26$) yielding 2026 data with $I \geq 2.5\sigma(I)$.

Structure Solution and Refinement

Solution by direct methods (SHELX 86).

$w^{-1} = \sigma^2(F) + 0.000116F^2$, R = 0.0505, wR = 0.0505, S = 1.128 based on 301 parameters. Maximum shift/esd in the last cycle = -0.053. Maximum and minimum ripple in difference electron density map : 0.23 and -0.24 e.Å^{-3}.

Structure Discussion

Selected bond lengths, angles and torsion angles are given in Tables 5.10.1-5.10.3. The molecular perspective and packing diagrams (as viewed along the b-axis) are shown in Figure 5.4. GUMACEHY shows major conformational differences from the majority of GU structures. Instead of the extended conformation, it demonstrates a folded conformation, mainly involving rotations about the single non-ring bonds at N(3) and N(11), as evidenced by the torsion angle, N(11)-C(1)-N(3)-C(21) = 37.05(7)°.

The water molecule is central to the hydrogen bonding, being joined to three different drug molecules.

As with previous structures, one of its donor bonds appears to be bifurcated, giving closest contact with N(14) and a long contact with O(32) of the same molecule. The strength of these bifurcated hydrogen bonds, is the inverse of that observed with the isomorphous alcohol solvates, GUFBIP and GUFBIB. These distances are summarised in Table 5.4, together with some close intermolecular contacts.

Table 5.4 Hydrogen Bonding and Other Close Intermolecular Contacts

a) Hydrogen Bonding

Donor	Acceptor	Symmetry	D-H	H...A	D...A
N(2)-H(2B)...	O(1W)	1-x,½+y,½-z	0.86	2.00(5)	2.855(6)
O(1W)-H(1W)...	N(14)	x,y,z	0.98	1.94(5)	2.811(5)
...	O(32)	x,y,z	0.98	2.98(5)	3.330(5)
O(1W)-H(2W)...	O(34)	1+x,y,z	0.82	1.97(5)	2.786(5)
O(34)-H(34)...	O(1S)	1+x,y,z	0.85	1.77(5)	2.613(5)
O(1S)-H(2A)...	N(2)*	x,-1+y,z	0.96	1.95(5)	2.901(6)
N(3)-H(3).....	O(2S)	x,-1+y,z	0.92	1.88(5)	2.742(5)

* salt H-bond

b) C...C Contacts Shorter than 3.75Å

C(3M).....C(1S)	x,y,z	3.486(9)
C(24).....C(3M)	1-x,1-y,1-z	3.490(9)
C(24).....C(1S)	-x,-y,1-z	3.574(7)
C(24).....C(1S)	-x,1-y,1-z	3.603(7)
C(25).....C(21)	-x,-y,1-z	3.633(7)
C(3M).....C(25)	x,y,z	3.674(9)
C(22).....C(25)	-x,-y,1-z	3.676(7)
C(24).....C(21)	-x,-y,1-z	3.676(7)
C(25).....C(3M)	1-x,1-y,1-z	3.681(9)
C(23).....C(26)	-x,-y,1-z	3.712(7)

c) C...N Contacts Shorter than 3.75Å

C(1S).....N(11)	x,1 + y,z	3.435(7)
C(1S).....N(3)	x,1 + y,z	3.505(7)

d) C...O Contacts Shorter than 3.75Å

C(13).....O(1W)	x,y,z	3.108(6)
C(13).....O(1W)	1-x,-½ + y,½-z	3.210(6)
C(12).....O(1W)	1-x,-½ + y,½-z	3.221(6)
C(12).....O(1W)	x,y,z	3.248(6)
C(15).....O(2S)	1-x,1-y,1-z	3.289(6)
C(16).....O(2S)	1-x,1-y,1-z	3.320(6)
C(1S).....O(1W)	x,y,z	3.401(6)
C(2S).....O(34)	-1 + x,y,z	3.411(7)
C(1S).....O(34)	-1 + x,y,z	3.427(6)
C(34).....O(1S)	1 + x,y,z	3.465(6)
C(1).....O(2S)	x,-1 + y,z	3.493(6)
C(24).....O(1S)	-x,1-y,1-z	3.550(6)
C(13).....O(34)	2-x,-½ + y,0.5-z	3.564(6)
C(26).....O(2S)	x,-1 + y,z	3.567(6)
C(23).....O(1S)	1 + x,y,z	3.576(6)

Figure 5.4.1 Molecular Perspective and Packing Diagrams (viewed along the b-axis) of GUMACEHY

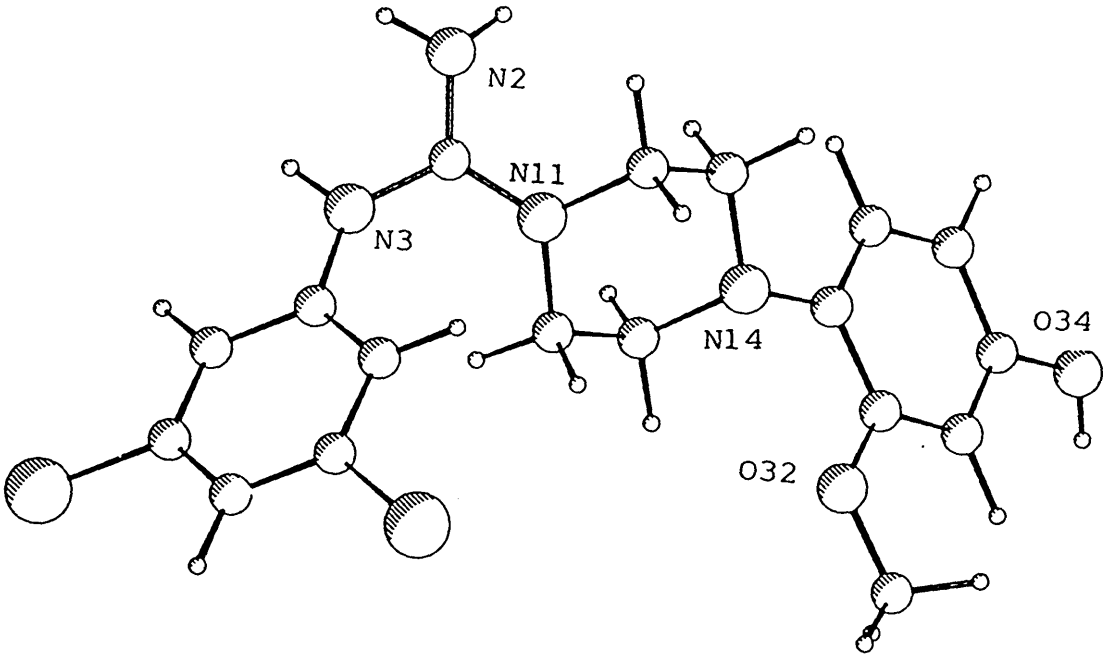

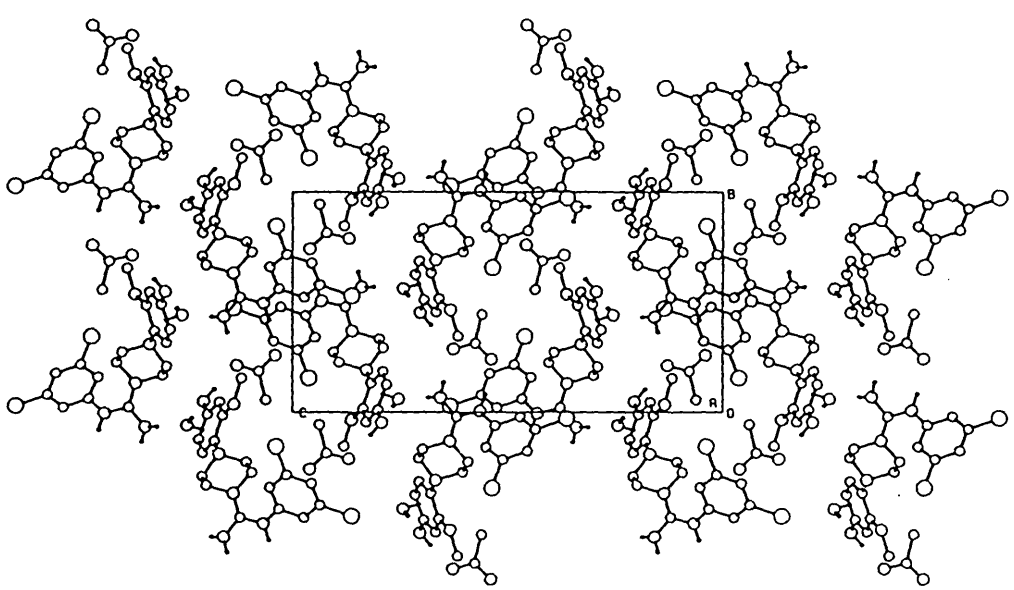

5.5 GUMASCHY

Crystal Data

Colourless, misshapen, triangular plates from water, 0.25 x 0.25 x 0.1 mm.

$C_{18}H_{21}Cl_2N_4O_2^+.C_6H_9O_6^-.H_2O$, M = 591.5, triclinic, P1 (No.1), a = 7.748 (5), b = 9.347 (4), c = 19.419 (7) Å, α = 86.19 (4), β = 86.84 (6), γ = 65.61 (5)°, V = 1279.3 Å^3, Z = 2, V/Z = 640 Å^3.

Lattice parameters refined from accurately measured 2Θ values (16.7 - 31.1°) for 15 reflections.

Dc = 1.535 g cm^{-3}, μ= 2.64 cm^{-1}, F(000) = 616.0, T = 290 K.

Data Collection and Processing

Enraf-Nonius CAD-4 diffractometer, MoK$_\alpha$, λ = 0.71073 Å. 4513 independent data ($2 < \Theta < 25°$, $-9 \leq h \leq 9$, $-11 \leq k \leq 11$, $0 \leq l \leq 16$) yielding 2837 data with $I \geq 2.5\sigma(I)$. No measurable crystal decay or movement.

Structure Solution and Refinement

Solution by direct methods (SHELX84).

$w^{-1} = \sigma^2(F) + 0.000584F^2$, R = 0.045, wR = 0.0440, S = 1.117 based on 250 parameters. Maximum shift/esd 0.84. Maximum and minimum ripple in difference electron density map : 0.29 and -0.28 e.Å^{-3}. Due to the presence of two crystallographically independent molecules within the unit cell, the molecule was refined in three separate parts (cation 1, cation 2 and all anions plus water molecules) each part refined in separate consecutive cycles.

Structure Discussion

Selected bond lengths, angles and torsion angles are given in Tables 5.10.1-5.10.3. The molecular perspective diagrams of the two crystallographically independent molecules within the unit cell are shown in Figure 5.5.1. Due to the presence of the chiral anion

the structure must be non-centrosymmetric (with space group P1), however, the N(Z) test indicates a high pseudo-centrosymmetric character:

Z	HKL	Centro	Non-Centro
0.1	24.60	24.81	9.52
0.2	34.04	34.53	18.13
0.3	39.73	41.87	25.92
0.4	45.53	47.38	32.97
0.5	50.74	52.05	39.35
0.6	56.06	56.14	45.12
0.7	59.79	59.72	50.34
0.8	62.50	62.89	55.07
0.9	65.27	65.72	59.34
1.0	67.82	68.33	63.21

A pseudo-centre of inversion was determined between each pair of atoms and meaned over the whole structure (x = 0.7539, y = 0.8747 and z = 1.4009); the deviation of the atom pairs from the pseudo-centre of inversion (Å) was then determined and is tabulated in Table 5.5.1.

Table 5.5.1 Deviation of Centroid of Atom Pairs from Pseudo-Centre of Inversion in Å

Pseudo centre of Inversion at:		0.75390	0.87474	1.40093
C21	C61	0.0827	-0.0729	-0.0443
C22	C62	0.0679	-0.0499	-0.0710
C23	C63	0.0456	-0.0479	-0.0374
CL23	CL63	0.0607	-0.0379	-0.0453
C24	C64	0.0584	0.0012	-0.0370
C25	C65	0.0463	-0.0364	-0.0469
CL25	CL65	0.0308	-0.0312	-0.0459
C26	C66	0.0307	-0.0093	-0.0426
N3	N3'	0.0361	-0.0565	-0.0264
C1	C1'	-0.0306	-0.0845	-0.0302
N2	N2'	-0.0661	-0.1629	0.0970
N11	N51	-0.0301	-0.0116	-0.0757

C12	C52	0.0264	0.0018	-0.1344
C13	C53	-0.0721	0.0786	-0.0747
C15	C55	-0.0246	-0.0378	0.0144
C16	C56	0.0409	-0.0130	-0.0264
N14	N54	0.0071	0.0106	0.0058
C31	C71	-0.0476	0.0417	0.0373
C32	C72	0.0561	0.0112	0.0165
O32	O72	0.0545	0.0778	0.0082
C3M	C7M	0.1131	0.1420	-0.0041
C33	C73	-0.0255	0.0355	0.1021
C34	C74	-0.1030	0.0522	0.1313
O34	O74	-0.0940	0.0321	0.1764
C35	C75	-0.1378	0.0905	0.0949
C36	C76	-0.1249	0.0791	0.0530
ESDS of Centre		0.00863	0.00684	0.00391

In order to accomodate the chiral anions the conformations of the cations are significantly altered (see Figure 5.5.1), mainly involving rotations about the single non-ring bonds at N(3), N(11) and N(14), also previously observed with GUMACEHY.

The cations, as a result, pack in a very efficient manner, with the dichlorophenyl rings twisted *ca* 80° out of the plane of the remainder of the molecule. These rings stack up in interleaved layers; with considerable dipolar interaction between ring systems, on adjacent sides of the resulting hydrophobic channel. This is particularly well illustrated when viewed along the a-axis (Figure 5.5.2).

The molecular packing as viewed along the b-axis, is shown in Figure 5.5.2, also serves to illustrate the hydrophobic and hydrophilic channels. The latter channel is occupied by the more polar functionalities of the cation; the guanidinium and methoxy groups, protruding into the channel, with the anions and water molecules occupying the remaining volume.

The ^1H NMR of GUMASCHY (see Table 5.5.2) suggests that the ascorbate anion is present as the resonance hybrid of the two forms a and b.

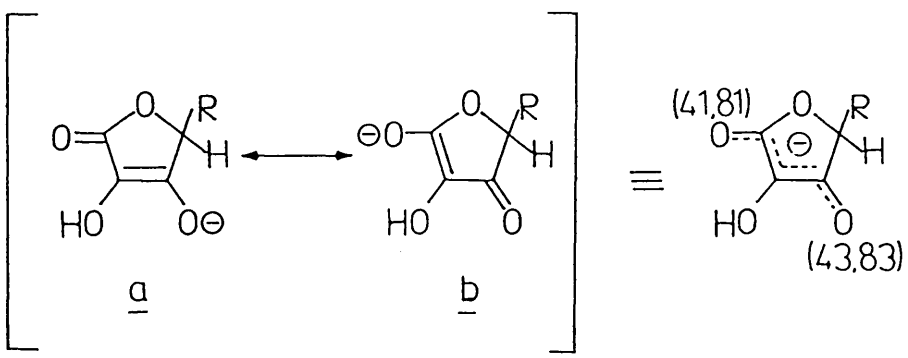

Where R = $CH(OH)CH_2OH$

Thus, it is possible for the anion to form salts using either O(41/81) or O(43/83) as the donating oxygen. Interestingly, in the crystal structure each of the independent anions utilises a different acidic oxygen atom to form a salt with the cation. The hydrogen bonding scheme in Figure 5.5.4, shows that anion I utilises O(43) for salt formation, whereas anion II utilises O(81) for salt formation.

The molecular packing is dominated by hydrogen bonding with the two independent water molecules being central to the whole scheme, each being joined to three different drug molecules.

One of the donor bonds from N(2') appears to be bifurcated, the hydrogen atom being equally directed

towards O(80) and O(2W); similarly, the donor bond from O(85) is bifurcated giving closest contact with O(41) and a long contact with O(40) of the same molecule.

These distances are summarised in Table 5.5.3, together with some of the close intermolecular contacts.

Table 5.5.3 Hydrogen Bonding and Other Close Intermolecular Contacts

a) Hydrogen Bonding

Donor	Acceptor	Symmetry	D-H	H...A	D...A
O(34)-H(34)...	O(43)	-1+x,1+y,1+z	0.88	1.95(8)	2.646(7)
N(3)-H(3).....	O(43)	1+x,y,1+z	0.77	2.61(9)	3.167(8)
O(43)-H(2A)*..	N(2)	1+x,y,1+z	0.88	1.71(8)	2.766(8)
N(2)-H(2B).....	O(1W)	1+x,y,1+z	1.15	2.08(8)	3.017(9)
O(1W)-H(1WZ)..	O(83)	x,y,z	0.74		2.639(9)
O(45)-H(45)....	O(83)	1+x,y,z	0.87	1.91(9)	2.742(8)
O(42)-H(42)...	O(1W)	1+x,-1+y,z	1.11	1.86(8)	2.792(9)
O(1W)-H(1W1)...		O(46)	x,y,z	0.63	2.29(9)
2.891(9)					
O(46)-H(46)...	O(32)	x,y,1+z	1.25	1.57(7)	2.741(7)
O(82)-H(82)...	O(2W)	-1+x,y,z	0.50	2.45(13)	2.688(11)
O(2W)-H(2W1)...		O(86)	x,-1+y,z	0.64	2.11(9)
2.742(8)					
O(86)-H(86)...	O(46)	x,1+y,z	0.94	1.88(8)	2.751(8)
O(74)-H(74)...	O(81)	1+x,-1+y,z	1.23	1.41(7)	2.647
(7)N(3')-H(3).....	O(81)	-1+x,y,z	0.96	2.00(7)	2.972(8)
O(81)-H(2B')*.	N(2')	-1+x,y,z	0.95	2.52(8)	3.024(9)
N(2')-H(2A')..	O(80)	-1+x,y,z	0.74	2.28(8)	2.890(8)
..	O(2W)	-1+x,-1+y,z	0.74	2.03(8)	2.936(9)
O(2W)-H(2W2)...		O(41)	x,-1+y,z	0.64	2.669(8)
O(85)-H(85)...	O(41)	1+x,y,z	1.09	1.84(8)	2.815(8)
...	O(40)	1+x,y,z	1.09	2.49(8)	3.339(8)

* salt H-bond

b) C...C Contacts Shorter than 3.75Å

C23.....C65	2+x,y,z	3.471(10)
C24.....C63	2+x,y,z	3.472(10)

C62.....C75	-1+x,1+y,z	3.499(10)
C24.....C63	2+x,y,z	3.511(10)
C23.....C64	2+x,y,z	3.522(10)
C62.....C74	-1+x,1+y,z	3.534(10)
C22.....C35	1+x,-1+y,z	3.540(9)
C15.....C34	1+x,y,z	3.587(9)
C41.....C85	1+x,y,z	3.602(11)
C24.....C64	2+x,y,z	3.604(11)
C16.....C34	1+x,y,z	3.609(9)
C56.....C74	-1+x,y,z	3.610(10)
C3M.....C42	x,1+y,1+z	3.649(11)
C33.....C42	-1+x,1+y,1+z	3.649(10)
C7M.....C81	x,-1+y,z	3.653(11)
C24.....C62	2+x,y,z	3.655(10)
C33.....C43	-1+x,1+y,1+z	3.659(11)
C22.....C34	1+x,-1+y,z	3.666(9)
C12.....C45	x,y,1+z	3.667(10)
C22.....C64	2+x,y,z	3.669(10)

c) C...N Contacts Shorter than 3.75Å

C(81).....N(2')	1+x,y,z	3.354(10)
C(43).....N(2)	-1+x,y,-1+z	3.415(10)
C(44).....N(2)	-1+x,y,-1+z	3.540(10)
C(71).....N(2')	1+x,y,z	3.640(9)
C(45).....N(14)	x,y,-1+z	3.714(8)

d) C...O Contacts Shorter than 3.75Å

C(16).....O(42)	x,1+y,1+z	3.017(9)
C(85).....O(41)	-1+x,y,z	3.064(9)
C(46).....O(86)	x,1+y,z	3.175(10)
C(3M).....O(46)	x,y,1+z	3.239(10)
C(3M).....O(45)	-1+x,1+y,1+z	3.254(10)
C(56).....O(82)	x,-1+y,z	3.262(11)
C(24).....O(74)	x,1+y,z	3.279(9)
C(15).....O(42)	x,1+y,1+z	3.303(9)
C(15).....O(34)	1+x,y,z	3.314(8)
C(46).....O(83)	1+x,y,z	3.319(10)

C(86).....O(72)	x,y,z	3.374(10)
C(55).....O(74)	-1+x,y,z	3.397(9)

Figure 5.5.1 Molecular Perspective Diagrams of GUMASCHY (Molecules 1 and 2)

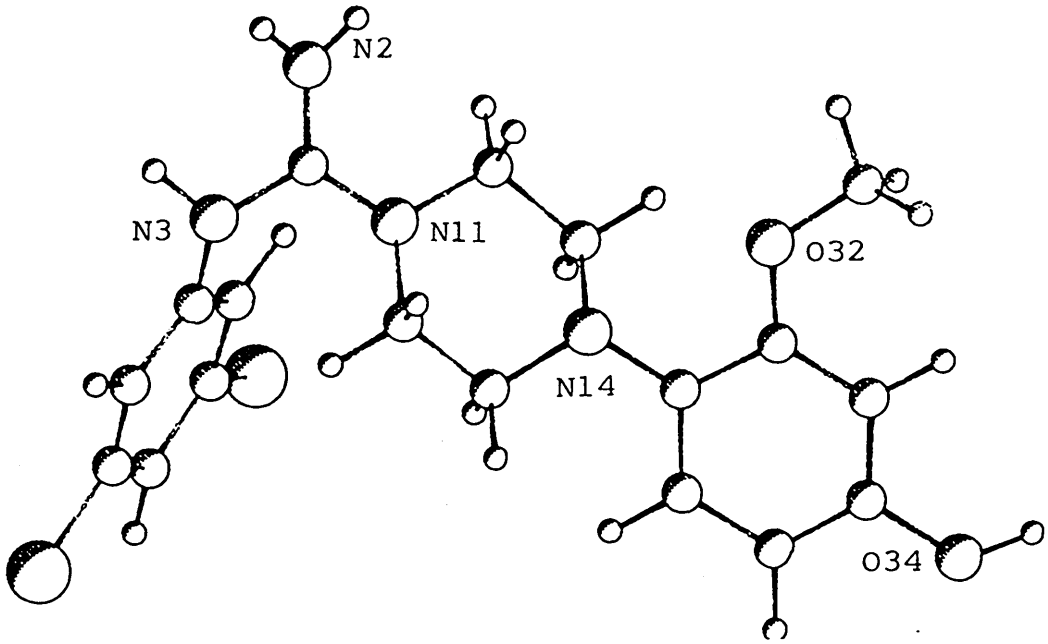

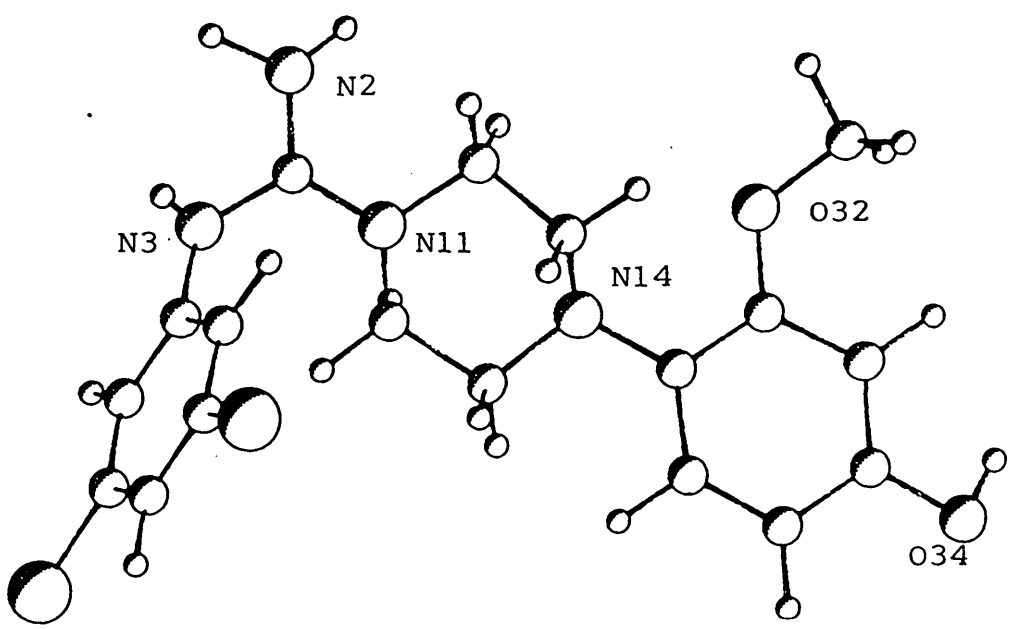

Figure 5.5.2 Molecular Packing Diagrams (viewed along the a- and b-axes) of GUMASCHY

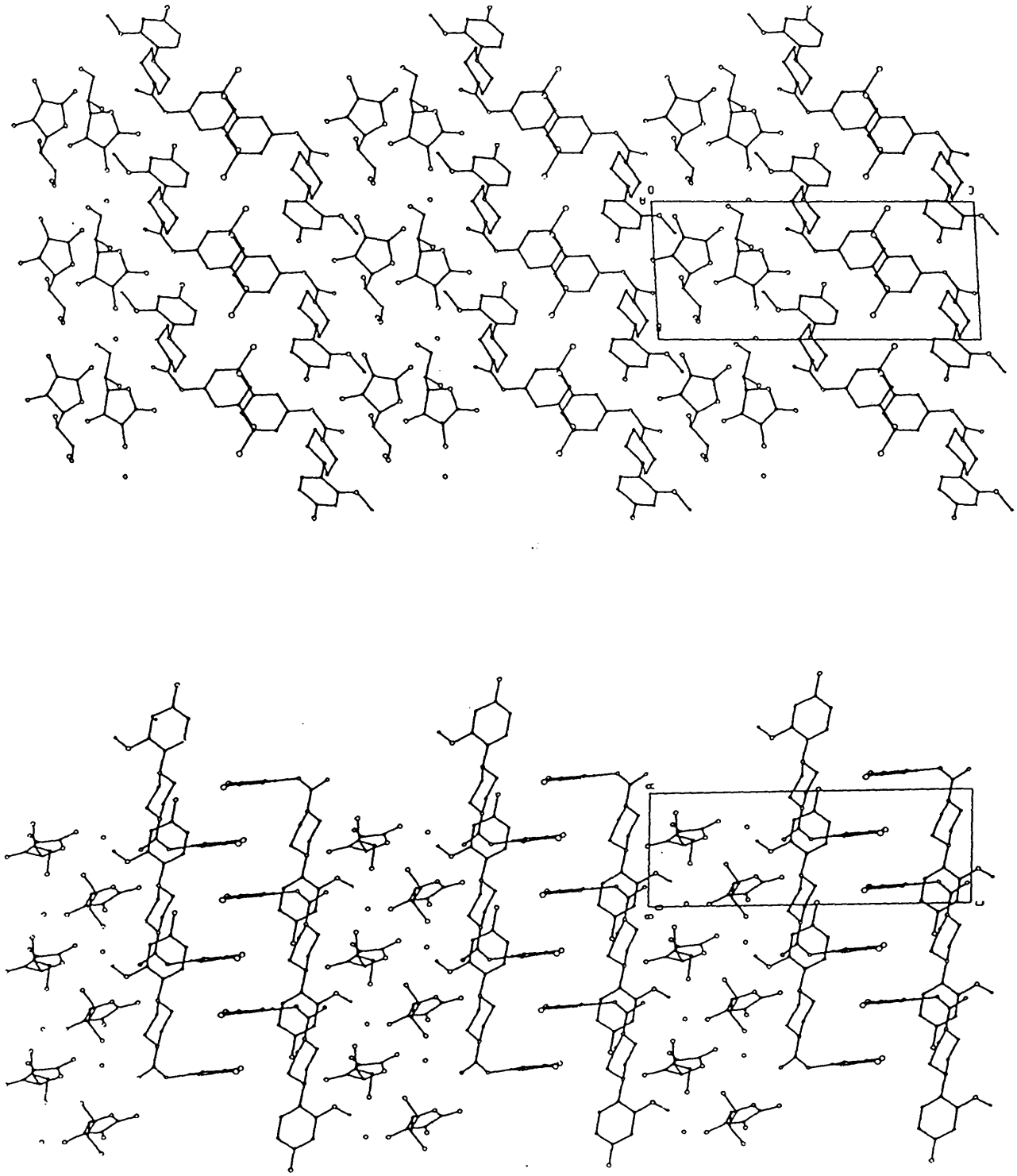

Table 5.5.2 ^{1}H NMR Spectral Data for GUMASCHY

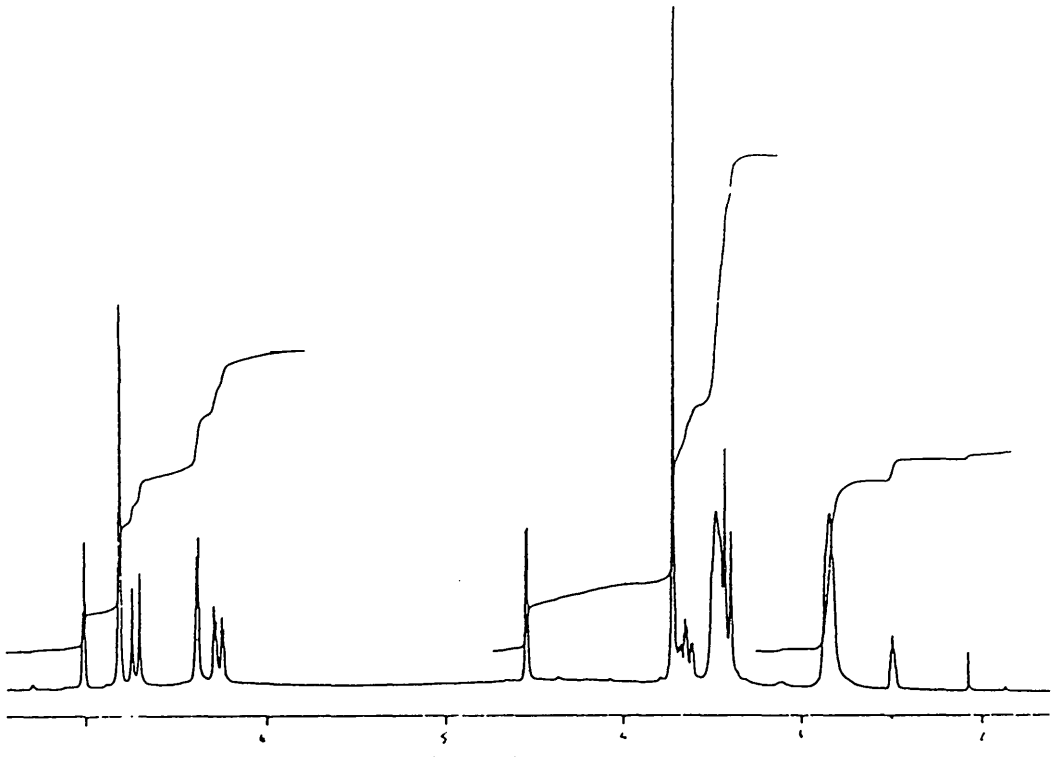

Chemical Shift (δ)	Multiplicity (M)	Integral	Assignment
2.84	m,b	4	NCH_2
3.41	d superimposed on	2	C(46)H_2-OH
3.48	m,b	4	NCH_2
3.65	d,d superimposed on	1	C(45)H-OH
3.70	s	3	OCH_3
4.54	d	1	O40-C(41)H
6.27	dd	1	H(35)
6.38	d	1	H(33)
6.72	d	1	H(36)
6.80	d	2	H(22)/H(26)
7.01	t	1	H(24)
9.00	s,b	1	OH
3-7	s,v,b	~5	NH_2, OH x 3

m = multiplet, d = doublet, s = singlet, t = triplet, dd = double doublet, b = broad, vb = very broad

Figure 5.5.3 Hydrogen Bonding Scheme for GUMASCHY

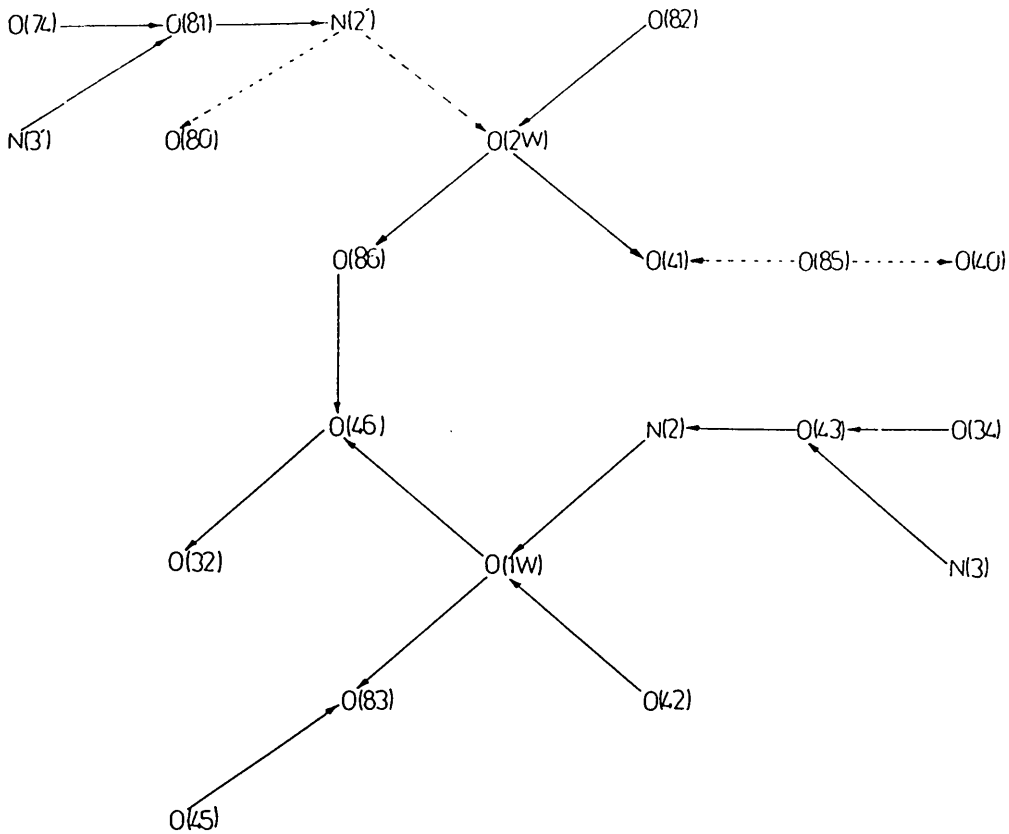

5.6 GUMHCLHYIP

Crystal Data

Colourless plates from isopropanol, 0.42 x 0.21 x 0.07 mm.

$C_{18}H_{21}Cl_2N_4O_2^+.Cl^-.H_2O.2C_3H_8O$, M = 569.9, triclinic, $P\bar{1}$ (No.2), a = 9.690 (1), b = 12.352 (2), c = 13.562 (2) Å, α = 103.83 (1), β = 90.02 (6), γ = 108.54 (1)°, V = 1489.2 Å^3, Z = 2, V/Z = 745 Å^3.

Lattice parameters refined from accurately measured 2θ values (30-35°) for 28 reflections.

Dc = 1.27 g cm^{-3}, μ = 29.8 cm^{-1}, F(000) = 604, T = 290 K.

Data Collection and Processing

Stoë STADI-4 diffractometer, CuK_α, λ = 1.54183 Å. 4233 independent data ($3 < \theta < 60°$, $-10 \leq h \leq 10$, $-13 \leq k \leq 12$, $0 \leq l \leq 15$) yielding 2402 data with $I \geq 2.5\sigma(I)$. No measurable crystal decay and a maximum drift correction of 1.10 applied.

Structure Solution and Refinement

Solution by direct methods (SHELX86).

$\varpi^{-1} = \sigma^2(F) + 0.00049F^2$, R = 0.081, wR = 0.099, S = 1.33 based on 355 parameters. Maximum shift/esd in the last cycle = 0.20. Maximum and minimum ripple in difference electron density map : 0.58 and -0.52 e.Å^{-3}.

Structure Discussion

Selected bond lengths, angles and torsion angles are given in Tables 5.10.1-5.10.3. The molecular perspective and packing diagrams as viewed along the b-axis is shown in Figure 5.6. It is dominated by hydrogen bonding and ring stacking. These distances are summarised in Table 5.6.

Table 5.6 Hydrogen Bonding and Other Close Intermolecular Contacts

a) Hydrogen Bonding

Donor	Acceptor	Symmetry	D-H	H...A	D...A
N(2)-H(2A)....	O(5S)	x,y,z	1.00(5)*	1.88(5)	2.863(10)
N(2)-H(2B)....	Cl(1)#	1-x,-y,-z	1.00(5)*	2.29(5)	3.273(7)
N(3)-H(3).....	O(2S)	x,y,z	1.00(6)*	1.81(6)	2.792(10)
O(34)-H(34)...	Cl(1)	x,-1+y,z	1.00(6)*	2.20(6)	3.174(6)
O(1W) ...	Cl(1)	-x,-y,-z			3.297(17)
O(1W) ...	N(14)	-x,-y,-z			3.082(18)
O(1W) ...	O(32)	-x,-y,-z			3.038(18)
O(2S)-H(2S)...	Cl(1)	-x,-y,-z	1.00(6)*	2.20(6)	3.120(7)
O(5S)-H(5S)...	O(1W)	1+x,y,z	0.99(6)*	2.55(6)	2.716(18)

* constrained

salt H-bond

b) C...C Contacts Shorter than 3.75Å

C(15).....C(35)	2-x,2-y,1-z	3.622(11)
C(12).....C(12)	1-x,1-y,1-z	3.666(11)
C(15).....C(34)	2-x,2-y,1-z	3.722(11)
C(1S).....C(4S)	2-x,1-y,-z	3.726(24)
C(16).....C(34)	2-x,2-y,1-z	3.732(11)
C(13).....C(22)	1-x,1-y,1-z	3.740(11)
C(3S).....C(6S)	1-x,1-y,-z	3.749(25)

c) C...N Contacts Shorter than 3.75Å

C(1S).....N(3)	x,y,z	3.664(17)

d) C...O Contacts Shorter than 3.75Å

C(26).....O(1W)	x,y,z	3.308(19)
C(22).....O(5S)	x,y,z	3.354(10)
C(4S).....O(1W)	1+x,y,z	3.387(24)
C(12).....O(2S)	x,y,z	3.403(10)
C(5S).....O(1W)	1+x,y,z	3.433(23)
C(21).....O(5S)	x,y,z	3.502(10)
C(1).....O(2S)	x,y,z	3.556(11)
C(26).....O(2S)	x,y,z	3.576(11)

Figure 5.6 Molecular Perspective and Molecular Packing Diagrams (viewed along the b-axis) of GUMHCLHYIP

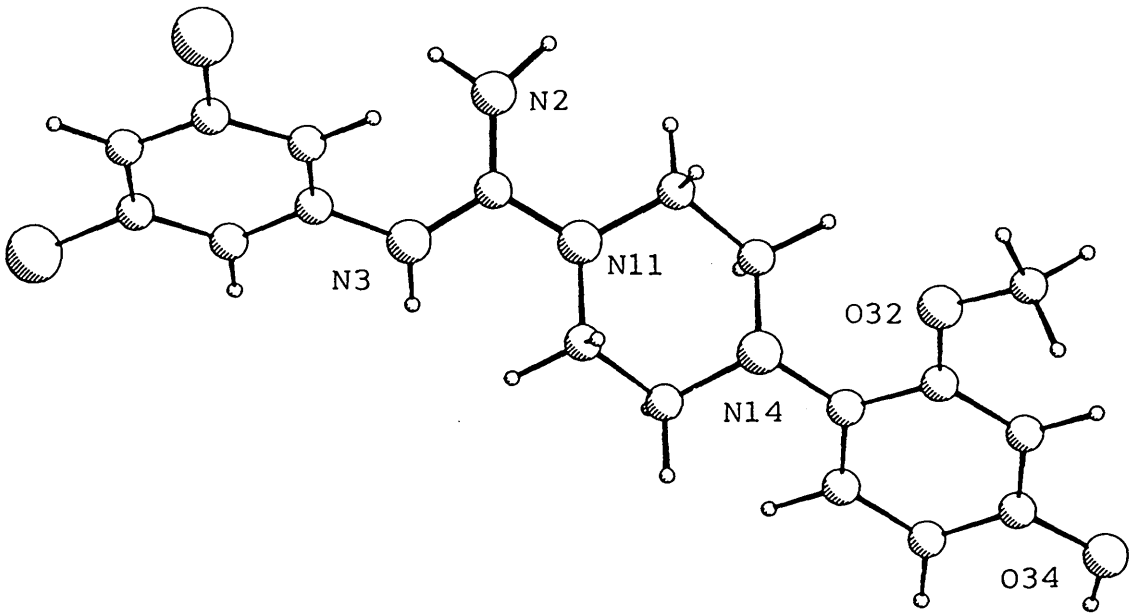

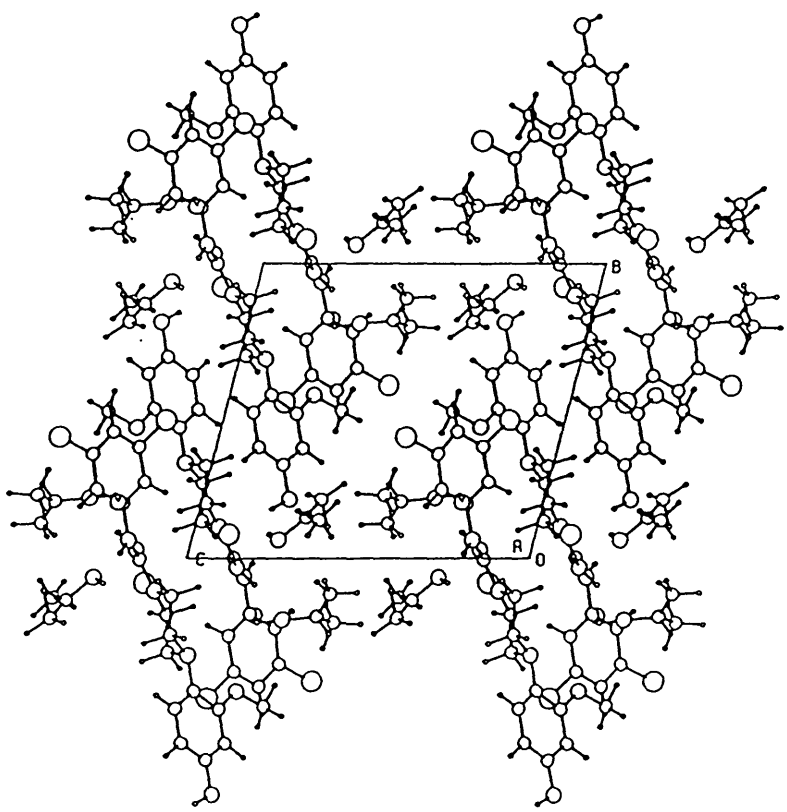

5.7 GUDMES

Crystal Data

Colourless plates from 16% aqueous isopropanol, 0.36 x 0.24 x 0.12 mm.

$C_{18}H_{22}Cl_2N_4O_2^{2+}.2CH_3SO_3^-$, M = 587.5, triclinic, $P\bar{1}$ (No.2),

a = 14.034 (5), b = 8.315 (3), c = 12.222 (6) Å,

α = 102.52 (7), β = 109.95 (8), γ = 91.17 (6)°,

V = 1301.8 Å^3, Z = 2, V/Z = 651 Å^3.

Lattice parameters refined from accurately measured 2Θ values (9.4-25.1°) for 10 reflections.

Dc = 1.498 g cm^{-3}, μ = 4.5 cm^{-1}, F(000) = 612.0,

T = 290 K.

Data Collection and Processing

Stoë STADI-4 diffractometer, MoKα, λ=0.71069Å. 3395 independent data ($2 < \Theta < 25°$, $-15 \leq h \leq 15$, $-8 \leq k \leq 8$, $0 \leq l \leq 12$) yielding 1810 data with $I \geq 2.5\sigma(I)$.

Structure Solution and Refinement

Solution by direct methods (SHELX86).

$w^{-1} = \sigma^2(F) + 0.000296F^2$, R = 0.0525, wR = 0.0494,

S = 1.252 based on 349 parameters. Maximum shift/esd in the last cycle = 0.076. Maximum and minimum ripple in difference electron density map : 0.38 and -0.32 e.Å^{-3}. The chlorines (Cl(23) and Cl(25)) and one of the mesylate oxygens (O(3S)) showed evidence of some thermal disorder.

Structure Discussion

Selected bond lengths, angles and torsion angles are given in Tables 5.10.1-5.10.3. The molecular perspective and packing diagrams as viewed along the b-axis are shown in Figure 5.7. It is dominated by hydrogen bonding and ring stacking. The ring systems stack up in interleaved pairs, alternating between dichlorophenyl and methoxyphenyl pairs. There is a unique intra-molecular hydrogen bond formed between the

piperazine nitrogen, N(14) and the methoxy oxygen, O(32). These distances are summarised in Table 5.7, together with some of the close intermolecular contacts.

Table 5.7 Hydrogen Bonding and Other Close Intermolecular Contacts

a) Hydrogen Bonding

Donor	Acceptor	Symmetry	D-H	H...A	D...A
O(1S)-H(2A)...	N(2)*	x,1+y,1+z	0.82	2.03(8)	2.827(9)
N(2)-H(2B)....	O(34)	x,y,1+z	0.97	1.93(7)	2.855(9)
O(34)-H(34)...	O(2S)	x,y,z	0.80	1.83(8)	2.626(7)
O(4S)-H(14)...	N(14)*	x,1+y,z	0.90	1.91(7)	2.747(8)
N(14)-H(14)...	O(32)#	x,y,z	0.90	2.33(7)	2.650(8)
N(3)-H(3).....	O(55)	x,y,z	0.71	2.08(8)	2.777(8)

* salt H-bonds

\# intra-molecular H-bond

b) C...C Contacts Shorter than 3.75Å

C(23).....C(35)	x,y,1+z	3.452(11)
C(24).....C(35)	x,y,1+z	3.453(12)
C(23).....C(23)	-x,1-y,2-z	3.567(13)
C(24).....C(36)	x,y,1+z	3.638(12)
C(23).....C(24)	-x,1-y,2-z	3.641(13)
C(22).....C(24)	-x,1-y,2-z	3.717(12)
C(35).....C(3M)	x,1+y,z	3.725(11)
C(25).....C(34)	x,y,1+z	3.752(12)
C(36).....C(3M)	x,1+y,z	3.752(12)

c) C...N Contacts Shorter than 3.75Å

C(34).....N(2)	x,y,-1+z	3.684(10)

d) C...O Contacts Shorter than 3.75Å

C(12).....O(5S)	x,y,z	3.137(9)
C(12).....O(4S)	x,1+y,z	3.165(9)
C(16).....O(1S)	x,1+y,1+z	3.188(8)
C(13).....O(6S)	-x,1-y,1-z	3.189(10)

Figure 5.7 Molecular Perspective and Molecular Packing Diagrams (viewed down the b-axis) of GUDMES

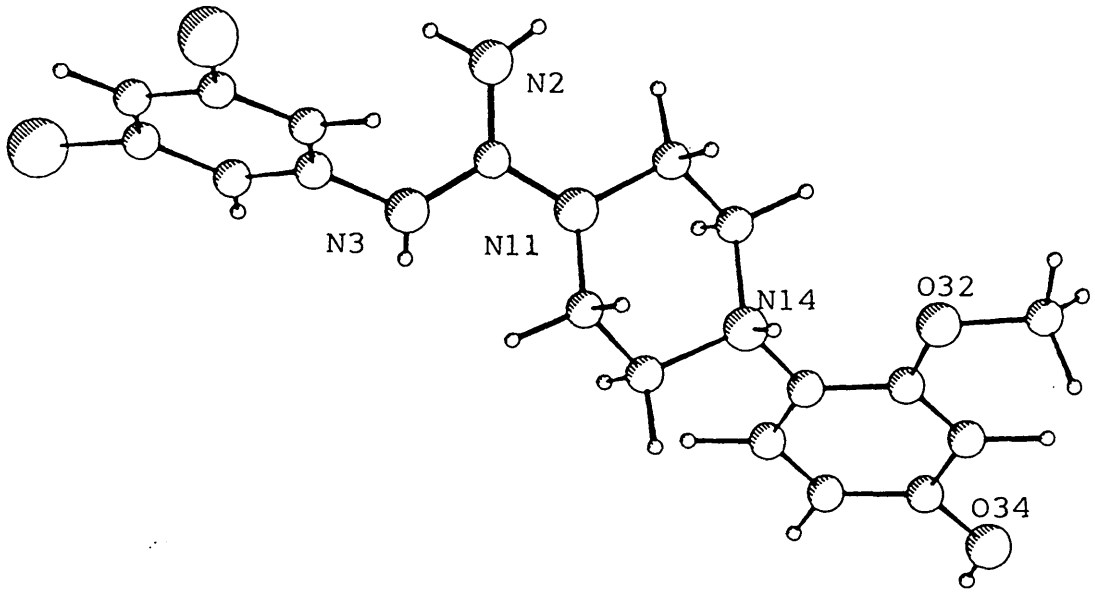

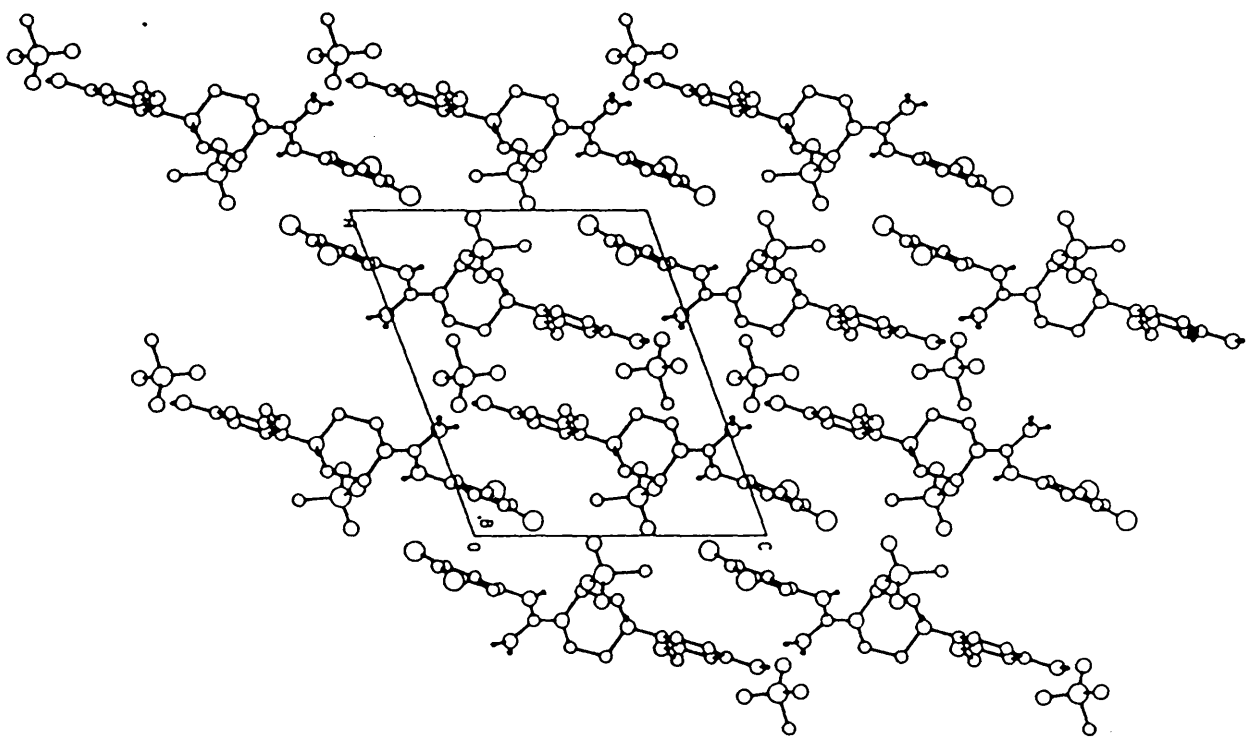

5.8 GUDHCLHY

Crystal Data

Colourless plates from methanol, 0.38 x 0.12 x 0.08 mm. $C_{18}H_{22}Cl_2N_4O_2^{2+}.2Cl^-.H_2O$, M = 486.2, monoclinic, $P2_1/c$ (No.14), a = 8.782 (1), b = 16.638 (3), c = 15.432 (3) Å, β = 97.03 (2)°, V = 2237.9 Å^3, Z = 4, V/Z = 560 Å^3. Lattice parameters refined from accurately measured 2θ values (20-30°) for 25 reflections.
Dc = 1.44 g cm^{-3}, μ = 5.56 cm^{-1}, F(000) = 1008,
T = 290 K.

Data Collection and Processing

Stoë STADI-4 diffractometer, MoK_α, λ = 0.71073 Å. 3058 independent data ($3 < 2\theta < 45°$, $-9 \leq h \leq 9$, $0 \leq k \leq 17$, $0 \leq l \leq 16$) yielding 1232 data with $I \geq 2.5\sigma(I)$. No measurable crystal decay and a maximum drift correction of 1.01 applied.

Structure Solution and Refinement

Solution by direct methods (SHELX86).
$\varpi^{-1} = \sigma^2(F) + 0.00016F^2$, R = 0.052, wR = 0.059,
S = 1.16 based on 283 parameters. Maximum shift/esd in the last cycle = 0.01. Maximum and minimum ripple in difference electron density map : 0.31 and -0.26 e.Å^{-3}.

Structure Discussion

Selected bond lengths, angles and torsion angles are given in Tables 5.10.1-5.10.3. A major conformational difference occurs in GUDHCLHY relative to most of the protonated and free base structures. The C(1)-N(11) bond is short and it may no longer be described as being equatorial to the piperazine ring, the two exocyclic torsion angles having a mean absolute value of 118.4°. This indicates an increase in the double bond character of the bond and the change in conformation is clear in Figure 5.8.

The molecular packing as viewed along the b-axis is also shown in Figure 5.8. It is dominated by hydrogen bonding and ring stacking. These distances are summarised in Table 5.8. Unlike GUDMES, there is no internal hydrogen bond between the piperazine nitrogen N(14) and the methoxy oxygen, O(32).

Table 5.8 Hydrogen Bonding and Other Close Intermolecular Contacts

a) Hydrogen Bonding

Donor	Acceptor	Symmetry	D-H	H...A	D...A
N(2)-H(2A)...	Cl(1)	1+x,1½-y,1½+z	1.31(8)	1.88(8)	3.122(9)
N(3)-H(3)....	Cl(1)*	1+x,y,z	0.92(9)	2.22(9)	3.135(9)
N(14)-H(14)..	Cl(2)*	1+x,y,z	1.39(8)	1.65(8)	3.027(8)
O(34)-H(34)..	O(1W)	x,½-y,z-½	0.93(9)	1.82(10)	2.697(11)
O(1W)-H(1W)..	Cl(1)	-x,1-y,-z	1.01(9)	2.79(10)	3.123(9)
O(1W)-[H(2W)].	Cl(2)	x,½-y,½+z			3.215(9)
N(14)-H(14)...	O(32)	x,y,z	1.39(8)		2.821(10)

* salt H-bonds

b) C...C Contacts Shorter than 3.75Å

C(16).....C(35)	-1-x,1-y,-z	3.731(13)

c) C...N Contacts Shorter than 3.75Å

C(33).....N(2)	1+x,1½-y,½+z	3.557(13)
C(34).....N(2)	1+x,1½-y,½+z	3.701(13)

d) C...O Contacts Shorter than 3.75Å

C(34).....O(1S)	x,½-y,-½+z	3.482(13)
C(35).....O(1S)	x,½-y,-½+z	3.507(13)
C(3M).....O(1S)	-x,1-y,1-z	3.617(14)
C(13).....O(1S)	-1+x,½-y,-½-z	3.677(13)

Figure 5.8 Molecular Perspective and Molecular Packing Diagrams (viewed along the b-axis) of GUDHCLHY

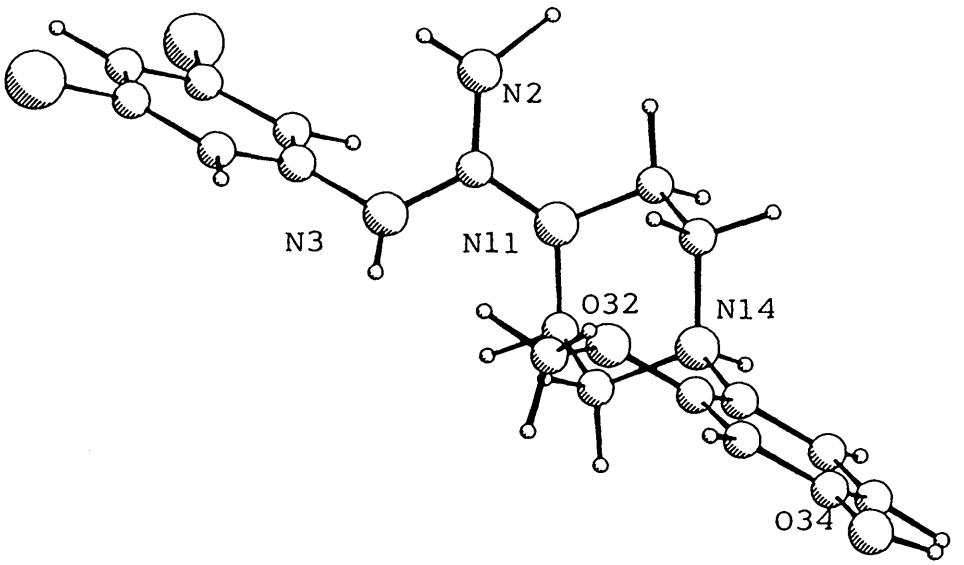

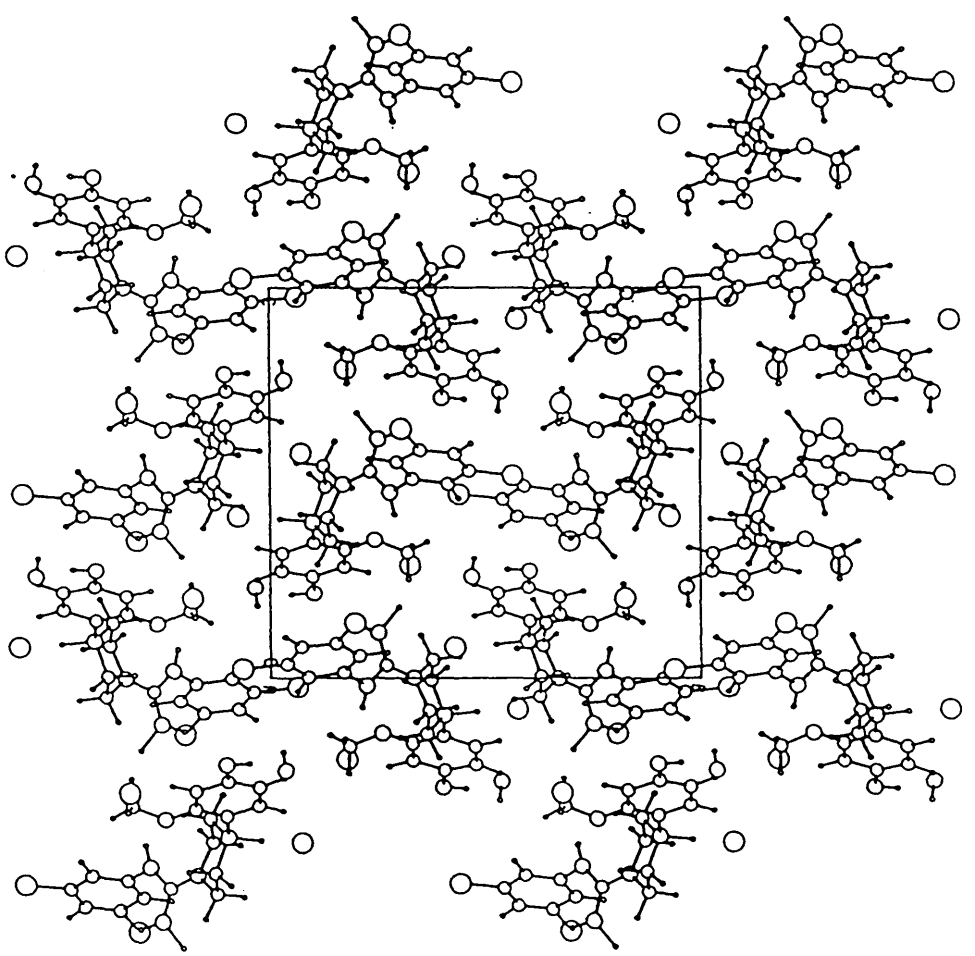

5.9 GUDSULF

Crystal Data

Small colourless plates from 50% w/v aqeuous isopropanol, 0.2 x 0.1 x 0.01 mm.

$C_{18}H_{22}Cl_2N_4O_2^{2+}.SO_4^{2-}$, M = 493.2, monoclinic, space group not identified, a = 14.29 (2), b = 8.35(2), c = 20.08 (4) Å, β = 97.44 (15)°, V = 2376.4 Å^3, Z = 4, V/Z = 594 Å^3.

Lattice parameters refined from setting angles for 7 reflections with θ between 3.9 and 6.2°.

Dc = 1.38 g.cm^{-3}.

Data Collection and Processing

Stoë STADI-4 diffractometer with Oxford Cryosystem attachment, MoK_α, λ = 0.71073 Å. Crystal not good enough to collect data set.

Table 5.10.1 Selected Bond Lengths for All GU Structures

	FBHY	FBIP	FBIB	HFUM	MACE	MASC1	MASC2	MHCL	DMES	DHCL
C(1) - N(2)	1.380(7)	1.364(9)	1.337(9)	1.328(13)	1.321(7)	1.314(9)	1.281(9)	1.318(10)	1.308(10)	1.329(13)
C(1) - N(3)	1.308(6)	1.298(9)	1.313(8)	1.364(13)	1.348(6)	1.364(9)	1.374(9)	1.334(10)	1.345(10)	1.339(13)
C(1) - N(11)	1.372(6)	1.375(9)	1.377(8)	1.329(13)	1.340(6)	1.331(9)	1.312(8)	1.361(10)	1.331(9)	1.334(12)
N(3) - C(21)	1.415(6)	1.404(9)	1.403(8)	1.424(14)	1.405(6)	1.430(9)	1.417(9)	1.423(10)	1.420(10)	1.430(13)
N(11) - C(12)	1.475(6)	1.459(8)	1.469(8)	1.447(12)	1.470(6)	1.477(8)	1.449(9)	1.477(9)	1.457(9)	1.463(12)
N(11) - C(16)	1.476(6)	1.462(8)	1.453(8)	1.485(13)	1.475(6)	1.467(9)	1.494(8)	1.484(9)	1.451(9)	1.452(12)
C(12) - C(13)	1.525(7)	1.519(9)	1.515(9)	1.518(14)	1.519(6)	1.497(9)	1.518(10)	1.527(11)	1.518(10)	1.529(13)
C(13) - N(14)	1.474(6)	1.487(8)	1.464(8)	1.461(13)	1.463(6)	1.478(8)	1.472(9)	1.474(10)	1.505(9)	1.506(12)
N(14) - C(15)	1.472(6)	1.458(8)	1.466(8)	1.483(13)	1.473(6)	1.459(8)	1.461(9)	1.466(10)	1.508(9)	1.528(12)
N(14) - C(31)	1.443(6)	1.428(8)	1.440(8)	1.443(14)	1.445(6)	1.436(8)	1.393(9)	1.434(10)	1.474(9)	1.503(12)
C(15) - C(16)	1.526(7)	1.516(9)	1.530(9)	1.504(14)	1.519(7)	1.530(9)	1.482(9)	1.529(11)	1.521(10)	1.518(13)
C(21) - C(22)	1.396(7)	1.384(10)	1.392(9)	1.394(17)	1.386(7)	1.358(9)	1.398(10)	1.391(11)	1.368(11)	1.390(14)
C(21) - C(26)	1.403(7)	1.405(9)	1.394(9)	1.398(17)	1.400(7)	1.396(9)	1.368(10)	1.367(12)	1.391(11)	1.401(14)
C(22) - C(23)	1.386(7)	1.385(10)	1.380(9)	1.409(18)	1.376(7)	1.382(10)	1.379(10)	1.389(12)	1.407(12)	1.375(15)
C(23) - Cl(23)	1.749(6)	1.735(7)	1.748(7)	1.748(15)	1.739(5)	1.732(8)	1.732(7)	1.740(9)	1.732(9)	1.705(12)
C(23) - C(24)	1.395(8)	1.368(10)	1.377(10)	1.377(21)	1.383(7)	1.388(11)	1.375(10)	1.358(13)	1.381(13)	1.397(16)
C(24) - C(25)	1.377(8)	1.378(10)	1.364(10)	1.374(20)	1.377(7)	1.349(11)	1.413(10)	1.381(13)	1.358(13)	1.358(16)
C(25) - Cl(25)	1.751(5)	1.737(7)	1.742(7)	1.715(14)	1.737(5)	1.726(8)	1.710(8)	1.731(10)	1.737(10)	1.765(11)
C(25) - C(26)	1.381(7)	1.383(10)	1.373(10)	1.380(18)	1.379(7)	1.351(10)	1.382(10)	1.390(13)	1.372(12)	1.394(15)
C(31) - C(32)	1.411(7)	1.400(9)	1.393(9)	1.396(16)	1.399(6)	1.374(9)	1.433(9)	1.399(11)	1.391(10)	1.379(14)
C(31) - C(36)	1.392(7)	1.393(9)	1.388(9)	1.394(16)	1.387(6)	1.381(9)	1.387(10)	1.379(11)	1.361(10)	1.393(14)
C(32) - O(32)	1.380(6)	1.364(8)	1.381(8)	1.370(14)	1.376(6)	1.368(8)	1.360(8)	1.377(10)	1.365(9)	1.365(13)
C(32) - C(33)	1.391(7)	1.380(9)	1.384(9)	1.364(16)	1.396(7)	1.423(10)	1.367(9)	1.382(12)	1.375(10)	1.416(14)
O(32) - C(3M)	1.420(7)	1.420(9)	1.423(8)	1.427(13)	1.406(8)	1.431(9)	1.399(9)	1.394(12)	1.424(10)	1.427(14)
C(33) - C(34)	1.388(7)	1.387(10)	1.397(9)	1.402(16)	1.371(7)	1.382(9)	1.371(10)	1.386(12)	1.386(10)	1.386(14)
C(34) - O(34)	1.382(6)	1.370(9)	1.376(8)	1.360(14)	1.376(6)	1.369(8)	1.388(9)	1.380(10)	1.354(9)	1.383(13)
C(34) - C(35)	1.381(7)	1.364(10)	1.366(9)	1.381(16)	1.384(7)	1.363(9)	1.365(10)	1.372(12)	1.378(10)	1.366(14)
C(35) - C(36)	1.411(7)	1.391(10)	1.387(9)	1.384(16)	1.392(7)	1.392(9)	1.382(10)	1.402(12)	1.372(11)	1.410(14)

Table 5.10.2 Selected Bond Angles for All GU Structures

	FBHY	FBIP	FBIB	HFUM	MACE	MASC1	MASC2	MHCL	DMES	DHCL
N(2) - C(1) - N(3)	124.9(4)	124.5(6)	124.5(6)	120.0(9)	116.6(4)	116.8(6)	118.9(6)	121.5(7)	119.5(7)	120.0(9)
N(2) - C(1) - N(11)	114.5(4)	115.7(6)	117.7(6)	121.6(9)	120.7(4)	122.0(6)	123.2(6)	121.1(7)	120.9(7)	120.8(9)
N(3) - C(1) - N(11)	120.5(4)	119.9(6)	117.8(6)	118.4(9)	122.7(4)	121.2(6)	117.9(6)	117.4(7)	119.6(7)	119.2(9)
C(1) - N(3) - C(21)	119.0(4)	118.7(6)	119.4(5)	122.2(9)	129.0(4)	122.4(6)	121.8(6)	126.0(7)	124.7(7)	121.7(8)
C(1) - N(11)- C(12)	120.2(4)	122.6(5)	121.6(5)	123.3(8)	122.6(4)	117.5(5)	118.2(5)	120.6(6)	122.0(6)	123.6(8)
C(1) - N(11)- C(16)	119.1(4)	117.3(5)	118.6(5)	124.0(8)	124.7(4)	118.3(5)	121.5(5)	120.4(6)	121.7(6)	125.0(8)
C(12)- N(11)- C(16)	114.4(3)	112.5(5)	112.4(5)	112.0(7)	112.5(3)	116.5(5)	113.8(5)	114.1(6)	114.5(5)	111.4(7)
N(11)- C(12)- C(13)	111.5(4)	110.6(5)	110.2(5)	108.4(8)	109.8(4)	109.7(5)	112.3(5)	110.2(6)	109.6(5)	109.2(7)
C(12)- C(13)- N(14)	109.5(4)	111.2(5)	110.6(5)	109.0(8)	109.1(4)	108.5(5)	110.6(5)	111.1(6)	111.1(5)	110.1(7)
C(13)- N(14)- C(15)	108.7(3)	108.4(5)	109.4(5)	110.1(8)	109.2(3)	108.3(5)	108.9(5)	108.6(6)	110.6(5)	113.0(7)
C(13)- N(14)- C(31)	110.5(4)	111.5(5)	112.1(5)	116.0(8)	114.8(3)	114.4(5)	113.4(5)	111.1(6)	109.7(5)	111.2(7)
C(15)- N(14)- C(31)	116.4(4)	114.3(5)	112.7(5)	111.3(8)	112.0(3)	114.1(5)	116.9(5)	114.5(6)	112.6(5)	112.2(7)
N(14)- C(15)- C(16)	108.4(4)	110.2(5)	109.4(5)	111.0(8)	111.8(4)	110.4(5)	110.0(5)	108.7(6)	110.3(6)	108.0(7)
N(11)- C(16)- C(15)	111.2(4)	109.8(5)	109.8(5)	110.8(8)	110.5(4)	111.7(5)	112.0(5)	110.4(6)	109.2(6)	110.3(7)
N(3) - C(21)- C(22)	118.6(4)	119.7(6)	118.8(6)	117.9(10)	117.0(4)	119.5(6)	118.4(6)	120.2(7)	119.7(7)	120.9(9)
N(3) - C(21)- C(26)	122.4(4)	121.2(6)	122.4(6)	120.9(10)	123.4(4)	119.9(6)	119.3(6)	118.6(7)	118.0(7)	117.5(9)
C(22)- C(21)- C(26)	118.9(4)	118.9(6)	118.5(6)	121.0(11)	119.5(4)	120.6(6)	122.1(7)	121.0(7)	122.3(7)	121.5(9)
C(21)- C(22)- C(23)	119.6(5)	119.7(6)	118.9(6)	116.8(11)	120.0(4)	118.6(6)	116.7(6)	117.3(7)	116.1(7)	120.3(10)
C(22)- C(23)-Cl(23)	120.0(4)	119.0(5)	118.5(5)	117.0(10)	119.6(4)	119.9(6)	119.0(5)	117.1(6)	116.8(7)	119.5(8)
C(22)- C(23)- C(24)	122.4(5)	122.5(7)	123.5(6)	122.2(13)	121.8(5)	121.3(7)	124.6(7)	124.0(8)	123.4(8)	119.7(10)
Cl(23)- C(23)- C(24)	117.7(4)	118.5(5)	118.1(5)	120.8(11)	118.5(4)	118.8(6)	116.3(5)	119.0(7)	119.8(7)	120.8(9)
C(23)- C(24)- C(25)	116.6(5)	117.3(7)	116.0(6)	119.7(14)	117.2(4)	118.1(7)	115.5(7)	116.5(8)	116.9(9)	118.5(10)
C(24)- C(25)-Cl(25)	118.8(4)	119.2(5)	118.3(5)	120.4(11)	118.9(4)	118.7(6)	118.5(6)	118.8(7)	118.1(7)	118.6(9)
C(24)- C(25)- C(26)	123.1(5)	122.5(7)	123.4(7)	120.1(13)	123.1(4)	122.5(7)	122.3(7)	122.5(9)	123.1(9)	124.5(10)
Cl(25)- C(25)- C(26)	118.1(4)	118.3(5)	118.2(5)	119.4(10)	118.1(4)	118.8(6)	119.1(6)	118.7(7)	118.7(7)	116.9(8)
C(21)- C(26)- C(25)	119.3(4)	119.1(6)	119.6(6)	120.2(11)	118.4(4)	118.9(6)	118.5(7)	118.7(8)	118.2(7)	115.4(9)
N(14)- C(31)- C(32)	117.6(4)	119.9(6)	119.4(5)	119.5(10)	118.2(4)	117.6(5)	118.7(6)	118.9(7)	116.9(6)	121.4(8)
N(14)- C(31)- C(36)	124.7(4)	122.7(6)	123.1(6)	122.5(10)	124.2(4)	125.2(6)	123.5(6)	123.7(7)	123.3(6)	116.9(8)
C(32)- C(31)- C(36)	117.7(4)	117.5(6)	117.5(6)	118.0(10)	117.6(4)	117.1(6)	117.7(6)	117.4(7)	119.7(7)	121.6(9)
C(31)- C(32)- O(32)	115.9(4)	115.3(6)	115.2(5)	116.1(10)	116.1(4)	118.8(6)	115.1(6)	115.4(7)	115.6(6)	118.7(9)
C(31)- C(32)- C(33)	121.0(4)	121.0(6)	121.8(6)	120.8(10)	121.2(4)	120.9(6)	120.3(6)	121.4(7)	119.3(7)	119.2(9)
O(32)- C(32)- C(33)	123.0(4)	123.6(6)	122.9(6)	123.2(10)	122.8(4)	120.3(6)	124.6(6)	123.2(7)	125.0(7)	122.1(9)
C(32)- O(32)- C(3M)	118.7(4)	116.7(5)	116.9(5)	117.9(8)	117.9(4)	120.1(5)	117.3(5)	118.6(7)	117.9(6)	120.4(8)
C(32)- C(33)- C(34)	120.0(4)	119.6(6)	118.6(6)	120.6(10)	119.5(4)	119.1(6)	119.6(6)	119.4(8)	120.1(7)	117.7(9)
C(33)- C(34)- O(34)	117.8(4)	116.5(6)	115.9(5)	116.0(10)	121.2(4)	121.5(6)	120.2(6)	116.7(7)	117.6(6)	114.5(9)
C(33)- C(34)- C(35)	120.6(4)	120.8(6)	120.7(6)	119.4(10)	121.0(4)	121.1(6)	121.8(6)	121.2(8)	120.2(7)	124.0(10)
O(34)- C(34)- C(35)	121.6(4)	122.7(6)	123.3(6)	124.6(10)	117.8(4)	117.4(6)	117.9(6)	122.1(7)	122.2(6)	121.5(9)
C(34)- C(35)- C(36)	119.1(4)	119.3(6)	119.6(6)	119.4(11)	118.9(4)	118.2(6)	119.5(6)	118.2(8)	118.8(7)	117.7(9)
C(31)- C(36)- C(35)	121.6(4)	121.6(6)	121.6(6)	121.7(11)	121.9(4)	123.6(6)	121.0(6)	122.4(7)	121.7(7)	119.6(9)

Table 5.10.3 Selected Torsion Angles for All GU Structures

	FBHY	FBIP	FBIB	HFUM	MACE	MASC1	MASC2	MHCL	DMES	DHCL
N(2) -C(1) -N(3) -C(21)	22.7(7)	19.1(10)	19.9(10)	21.1(14)	-143.9(5)	139.9(7)	133.0(7)	-22.0(12)	-21.2(11)	-19.8(14)
N(11)-C(1) -N(3) -C(21)	-161.8(4)	-160.5(6)	-159.4(6)	-157.6(9)	37.0(7)	-40.9(10)	-46.5(9)	158.1(7)	159.8(7)	159.8(9)
N(2) -C(1) -N(11)-C(12)	29.2(6)	34.1(9)	35.2(9)	12.9(15)	18.4(7)	-7.1(9)	-6.5(10)	0.1(11)	-11.3(11)	-13.3(14)
N(2) -C(1) -N(11)-C(16)	179.8(4)	-178.7(6)	-177.0(6)	-156.7(9)	-155.8(4)	141.4(7)	143.2(7)	154.1(7)	152.8(7)	165.0(9)
N(3) -C(1) -N(11)-C(12)	-146.8(4)	-146.2(6)	-145.5(6)	-168.4(8)	-162.6(4)	173.7(6)	173.0(6)	-179.9(7)	167.7(6)	167.1(8)
N(3) -C(1) -N(11)-C(16)	3.8(6)	1.0(9)	2.3(9)	21.9(14)	23.2(7)	-37.8(9)	-37.3(9)	-25.9(10)	-28.2(10)	-14.6(14)
C(1) -N(3) -C(21)-C(22)	-139.8(5)	-133.4(7)	-133.8(7)	-131.0(11)	-170.0(5)	140.7(7)	146.9(7)	-37.3(11)	128.7(8)	118.8(11)
C(1) -N(3) -C(21)-C(26)	43.6(7)	52.6(9)	52.2(9)	55.2(15)	12.3(8)	-38.7(9)	-37.0(10)	147.8(8)	-53.0(10)	-63.0(13)
C(1) -N(11)-C(12)-C(13)	-160.5(4)	-157.8(6)	-155.7(6)	-111.3(10)	-118.6(4)	-162.7(6)	-161.6(6)	-155.2(7)	-137.2(7)	-119.6(9)
C(16)-N(11)-C(12)-C(13)	47.6(5)	53.6(7)	54.8(7)	59.5(10)	56.2(5)	48.2(7)	46.4(7)	49.2(8)	57.6(7)	61.9(9)
C(1) -N(11)-C(16)-C(15)	158.6(4)	153.7(6)	153.4(6)	115.6(10)	122.5(5)	168.1(6)	160.6(6)	152.5(7)	135.9(7)	117.2(10)
C(12)-N(11)-C(16)-C(15)	-49.1(5)	-56.0(7)	-56.0(7)	-55.1(10)	-52.1(5)	-43.1(7)	-48.5(7)	-51.9(8)	-58.8(7)	-64.3(9)
N(11)-C(12)-C(13)-N(14)	-54.3(5)	-54.9(7)	-56.1(7)	-62.7(10)	-60.8(4)	-59.1(6)	-53.0(7)	-54.2(8)	-54.2(7)	-55.2(9)
C(12)-C(13)-N(14)-C(15)	64.2(5)	58.8(7)	60.1(6)	61.4(10)	62.1(4)	68.1(6)	60.9(7)	62.9(7)	55.0(7)	53.0(9)
C(12)-C(13)-N(14)-C(31)	-166.9(4)	-174.5(5)	-174.2(5)	-171.1(8)	-171.2(4)	-163.4(5)	-167.1(5)	-170.3(6)	179.9(5)	-179.8(7)
C(13)-N(14)-C(15)-C(16)	-65.3(4)	-61.1(6)	-60.9(6)	-56.8(10)	-59.0(5)	-62.6(6)	-62.9(7)	-64.3(7)	-56.1(7)	-53.5(9)
C(31)-N(14)-C(15)-C(16)	169.1(4)	173.8(5)	173.7(5)	173.2(8)	172.7(4)	168.7(5)	166.9(6)	171.0(6)	-179.3(6)	179.8(7)
C(13)-N(14)-C(31)-C(32)	74.5(5)	80.4(7)	80.2(7)	143.2(10)	158.1(4)	66.3(7)	67.8(8)	77.6(8)	87.6(7)	-62.6(11)
C(13)-N(14)-C(31)-C(36)	-104.0(5)	-100.6(7)	-98.3(7)	-35.5(14)	-21.8(6)	-117.0(7)	-116.8(7)	-103.7(8)	-88.0(8)	114.5(9)
C(15)-N(14)-C(31)-C(32)	-160.9(4)	-156.2(6)	-155.9(6)	-89.9(12)	-76.6(5)	-168.2(6)	-164.2(6)	-159.0(7)	-148.7(6)	65.0(11)
C(15)-N(14)-C(31)-C(36)	20.5(6)	22.7(9)	25.6(8)	91.3(12)	103.4(5)	8.5(9)	11.3(9)	19.7(10)	35.7(9)	-117.9(9)
N(14)-C(15)-C(16)-N(11)	57.1(5)	60.0(7)	58.8(7)	52.3(11)	53.3(5)	49.5(7)	56.2(7)	58.5(7)	56.6(7)	57.7(9)
N(3) -C(21)-C(22)-C(23)	-178.1(5)	-175.8(6)	-175.9(6)	-175.9(11)	-176.4(4)	-179.1(6)	179.4(6)	-176.7(7)	177.1(7)	-179.0(9)
C(26)-C(21)-C(22)-C(23)	-1.5(7)	-1.6(10)	-1.6(10)	-2.2(18)	1.3(7)	0.3(10)	3.4(10)	-1.9(12)	-1.1(12)	2.8(16)
N(3) -C(21)-C(26)-C(25)	178.8(4)	175.8(6)	175.5(6)	176.5(11)	178.8(4)	-179.6(6)	-176.5(6)	175.9(8)	-178.2(7)	179.9(9)
C(22)-C(21)-C(26)-C(25)	2.2(7)	1.7(10)	1.5(10)	3.0(19)	1.2(7)	1.0(10)	-0.6(11)	1.1(12)	0.1(12)	-1.8(15)
C(21)-C(22)-C(23)-Cl(23)	-179.8(4)	-179.1(5)	-179.5(5)	-178.1(9)	179.5(4)	178.1(5)	176.7(5)	-179.6(6)	178.4(6)	177.0(8)
C(21)-C(22)-C(23)-C(24)	0.9(8)	1.0(11)	1.2(10)	1.5(20)	-1.8(7)	-1.0(11)	-3.3(11)	0.9(13)	0.6(13)	-2.2(16)
C(22)-C(23)-C(24)-C(25)	-1.1(8)	-0.5(11)	-0.4(10)	-1.6(22)	-0.2(7)	0.6(11)	0.3(11)	0.9(14)	1.0(14)	0.7(16)
Cl(23)-C(23)-C(24)-C(25)	179.6(4)	179.7(5)	-179.8(5)	178.0(11)	178.5(4)	-178.6(6)	-179.7(5)	-178.6(7)	-176.7(7)	-178.5(9)
C(23)-C(24)-C(25)-Cl(25)	-176.8(4)	178.8(5)	178.1(5)	179.6(11)	-175.7(4)	-177.6(6)	-177.8(5)	-179.5(7)	-179.2(7)	-178.6(8)
C(23)-C(24)-C(25)-C(26)	1.9(8)	0.6(11)	0.2(11)	2.3(21)	2.9(7)	0.8(12)	2.9(11)	-1.8(14)	-2.2(14)	0.3(17)
C(24)-C(25)-C(26)-C(21)	-2.6(8)	-1.2(11)	-0.7(11)	-3.0(20)	-3.4(7)	-1.5(11)	-2.7(11)	0.8(14)	1.8(13)	0.3(16)
Cl(25)-C(25)-C(26)-C(21)	176.2(4)	-179.4(5)	-178.6(5)	179.6(10)	175.2(4)	176.9(5)	177.9(6)	178.6(7)	178.7(6)	179.1(8)
N(14)-C(31)-C(32)-O(32)	4.1(6)	2.3(9)	4.4(8)	0.1(15)	-1.5(6)	-1.4(9)	-1.1(9)	0.2(11)	-1.6(9)	-3.9(14)
N(14)-C(31)-C(32)-C(33)	-177.5(4)	-177.0(6)	-176.5(6)	-179.1(10)	178.4(4)	177.2(6)	179.2(6)	-178.4(7)	-178.7(6)	175.2(8)
C(36)-C(31)-C(32)-O(32)	-177.3(4)	-176.7(6)	-177.1(5)	178.8(10)	178.4(4)	-178.3(6)	-176.8(6)	-178.6(7)	174.2(7)	179.2(9)
C(36)-C(31)-C(32)-C(33)	1.2(7)	4.0(10)	2.1(9)	-0.3(17)	-1.7(7)	0.3(9)	3.5(10)	2.8(12)	-3.0(11)	-1.8(15)
N(14)-C(31)-C(36)-C(35)	177.5(4)	178.9(6)	177.5(6)	179.1(10)	-179.6(4)	-176.7(6)	-176.0(6)	179.1(7)	177.5(7)	-176.6(8)
C(32)-C(31)-C(36)-C(35)	-1.1(7)	-2.1(10)	-1.0(10)	0.4(17)	0.5(7)	0.1(10)	-0.6(10)	-2.2(12)	2.0(11)	0.5(15)
C(31)-C(32)-O(32)-C(3M)	-177.3(4)	171.4(6)	168.1(6)	-166.1(10)	-177.7(5)	-161.5(6)	-164.1(6)	173.7(7)	-178.8(6)	-166.0(9)
C(33)-C(32)-O(32)-C(3M)	4.3(7)	-9.4(9)	-11.0(9)	13.1(15)	2.4(7)	19.9(9)	15.6(9)	-7.7(12)	-1.8(10)	15.0(14)
C(31)-C(32)-C(33)-C(34)	0.3(7)	-2.4(10)	-0.1(10)	-1.0(17)	1.4(7)	-1.1(10)	-3.8(10)	-0.8(12)	0.9(11)	1.2(14)
O(32)-C(32)-C(33)-C(34)	178.6(4)	178.4(6)	179.0(6)	179.8(10)	-178.7(4)	177.4(6)	176.5(6)	-179.4(7)	-176.0(7)	-179.8(9)
C(32)-C(33)-C(34)-O(34)	175.8(4)	177.5(6)	176.6(6)	-179.3(10)	178.8(4)	179.7(6)	-178.8(6)	178.2(7)	-179.3(7)	179.9(9)
C(32)-C(33)-C(34)-C(35)	-1.9(7)	-1.2(10)	-3.1(10)	2.3(17)	0.2(7)	1.7(10)	1.2(11)	-1.8(13)	2.2(11)	0.6(15)
C(33)-C(34)-C(35)-C(36)	2.0(7)	3.1(10)	4.2(10)	-2.2(17)	-1.3(7)	-1.4(10)	1.8(11)	2.4(13)	-3.1(11)	-1.9(16)
O(34)-C(34)-C(35)-C(36)	-175.6(4)	-175.6(6)	-175.6(6)	179.6(11)	-179.9(4)	-179.5(6)	-178.2(6)	-177.6(7)	178.4(7)	178.9(9)
C(34)-C(35)-C(36)-C(31)	-0.5(7)	-1.4(10)	-2.1(10)	0.8(18)	1.0(7)	0.6(10)	-2.0(11)	-0.3(12)	1.0(11)	1.3(14)

SECTION 6: GENERAL DISCUSSION OF GU STRUCTURES

6.1 Introduction

GU is a N,N' disubstituted amidine, (in pursuance of Jen *et al* [1], the term amidine is used here to include the system -N-C(X)=N, in which X=C,N,O and S). More specifically GU may be viewed as a N,N' disubstituted guanidine. GU is capable of existing as a monoanion (pKa 11.5), neutral species (pKa 8.6), monocation (pKa 4.1) and dication. Under strongly acidic conditions it is potentially capable of existing as a trication. Only the neutral and cationic species were studied during these investigations. In solution GU can exist as an equilibrium mixture of all of these species; in practice the relative proportions, depends both on the ionisation constants and the pH of the media considered. The sites and order of protonation are shown in Figure 6.1.1. All attempts to produce the trication failed and the reasons for this are worthy of further discussion.

Guanidine is a symmetrical amidine and has many unique chemical properties.
The neutral species is the strongest organic base known (pka 13.6) approaching the hydroxide ion in its proton affinity[2]. The monocation is one of the most stable carbonium ions ever isolated, being stable to boiling water. Pauling[3] used valence bond theory to explain this great stability, calculating the resonance energy of the guanidine free base as ~197 $kJ.mol^{-1}$ and indicating that the monocation had a resonance energy of between 163-172 $kJ.mol^{-1}$ (*cf* benzene 126-146 $kJ.mol^{-1}$) *ie* a resonance stabilisation energy of 25-34 $kJ.mol^{-1}$.

In terms of the Hückel[4] molecular orbital theory the calculated delocalisation energy (DE) for the guanidinium ion is 1.60β (~110.5 $kJ.mol^{-1}$). A proton may be removed from the guandinium ion in the plane of the molecule,

orthogonal to the pi electron system, thus perturbing, but not fundamentally altering the 6 pi electron system. The resulting orbitals for guanidine reflect the loss of symmetry of the molecule, but retain most of the Y aromaticity[2,5] with a DE of 1.20β (82.8 $kJ.mol^{-1}$). This is a loss of delocalisation energy of ~0.4β or 27.6 $kJ.mol^{-1}$ on deprotonation of the guanidinium ion, in good agreement with Pauling's estimate of 25-34 $kJ.mol^{-1}$.

However, Y-delocalised systems with more or less than 6 pi electrons are decidedly less stable. BO_3^{2-}, CO_3^{-}, and $CN_3H_6^{2+}$ are only stable under special conditions[6,7]. The corresponding 4 pi electron systems are generally even less stable, being present as postulated intermediates or being stable only at extremely low temperatures.

This then explains the reluctance of the substituted guanidinium ion to undergo additional protonation and move away from the highly stable 6 pi electron system.

Figure 6.1.1 Sites and Order of Protonation of GU

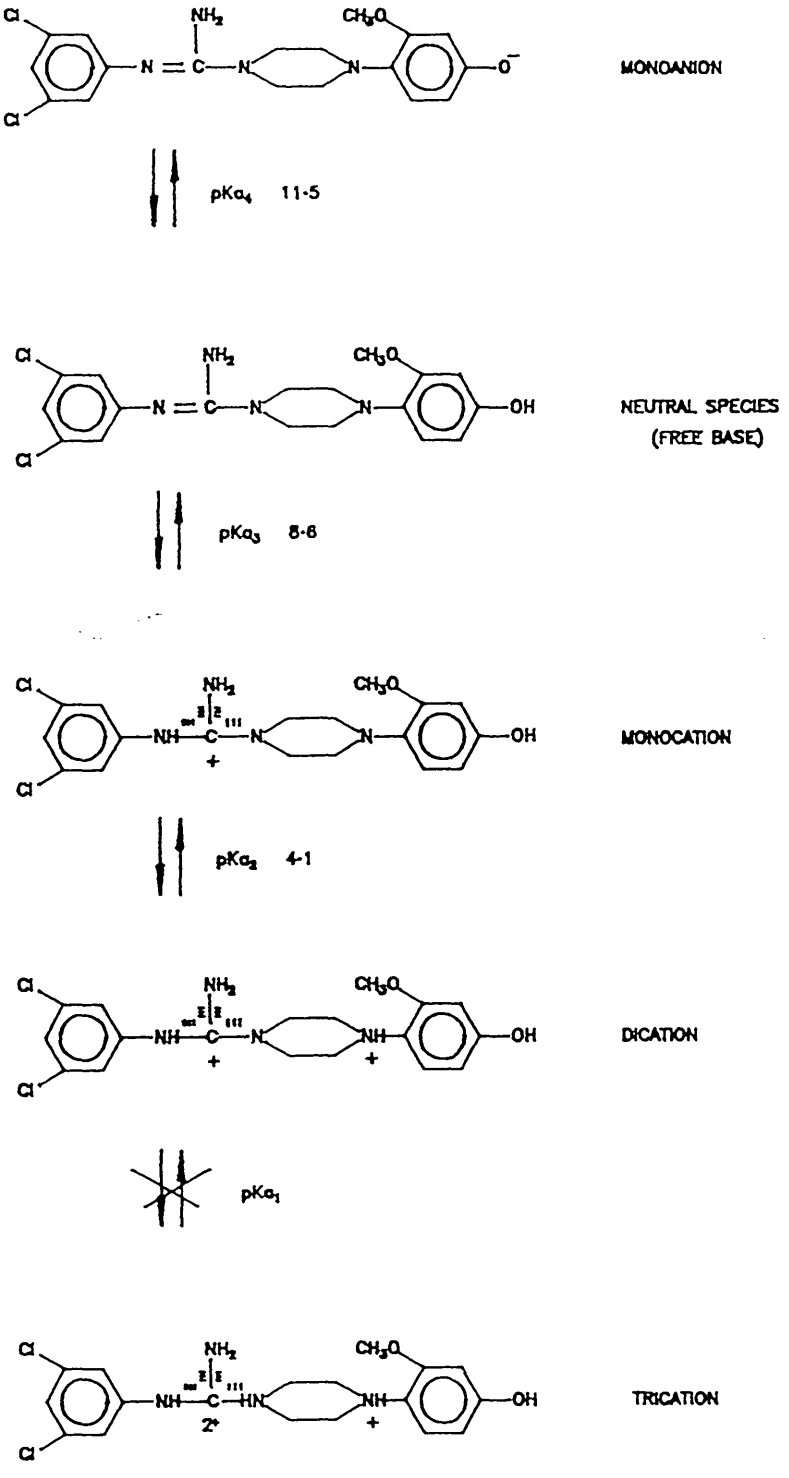

6.2 GU Tautomerism

Whilst the guanidinium ion has three equivalent resonance forms, the free base exhibits three non-equivalent resonance structures, two of which are energetically, unfavoured as they involve separate charges.
N monosubstituted and N,N′ disubstituted amidines and guanidines display prototropic tautomerism:

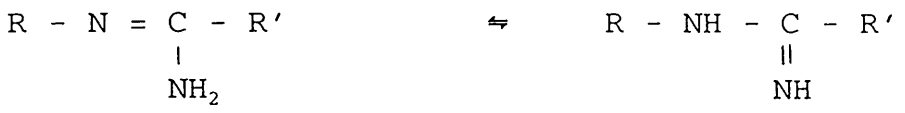

(where R' is a substituted amino group in guanidines)

The tautomeric equilibrium depends on the effects of the substituents at the nitrogen atoms[8,9].

The monoalkyl amidines and guanidines and N,N dialkyl amidines and guanidines should be weaker bases than the parent compound, as the replacement of one or two hydrogens of a primary amine group by alkyl groups tends to prevent double bond character from accumulating on this group. This is because, as carbon is more electro-negative than hydrogen, it resists the build up of a positive charge on the adjacent nitrogen. In consequence, the double bond resonance is restricted to the two other nitrogen atoms. This causes a decrease in basic strength toward that found in an imidine group, the decrease being twice as great for the N,N dialkyl guanidines as for the monoalkyl guanidines. A very much larger effect would be expected for the N,N′ dialkyl guanidines and indeed was observed for GU (pKa 8.6). The alkyl groups on two of the nitrogens would tend to force the double bond onto the third nitrogen, consequently the resonance hybrid:

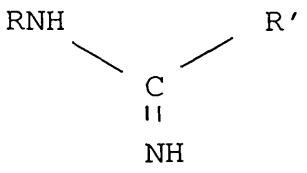

(where R′ is a substituted amino group in guanidines)

is more important than the other two forms. This would have little tendency to add a proton and the substance would be a weak base[3].

Prevorsek[10,11] investigating the IR spectra of N mono-substituted and N,N′ disubstituted amidines showed that alkyl groups tend to prefer attachment to the amino nitrogen of the amidine group, confirming Pauling's theories. However they found that the reverse was true for aryl groups; these conclusions were in agreement with earlier work on N aryl amidines by Pyman[12,13] and was supported later by Moritz[14].

For N aryl amidines, Prevorsek found two N-H bands at 3500 and 3400cm^{-1}, in close agreement with those found in formamide[15] at 3533 and 3411cm^{-1}, indicating a terminal amino group.

Whereas the introduction of a phenyl moiety on the amino group reduces the basicity by a factor of *ca* 10, introduction of a phenyl on the imino group reduces basicity by *ca* 1000. The explanation for the drastic effects on basicity is that the imino phenyl is not

interacting with the pi system of the amidine, since it is twisted out of plane. Consequently the phenyl pi system is orientated so that it may overlap with the lone pair of the sp^2 hybridised imino nitrogen[9].

Charlton's[16] pioneering paper on the tautomeric preference among substituted guanidines argued qualitatively that protonation would be expected on the nitrogen most able to support a positive charge. The tautomeric ratio in 4-methylthiazol-2-yl guanidine, a model guanidine heterocyclic was studied by Button *et al*[17].
They concluded that the aryl imino tautomer, $RN{=}C(NH_2)_2$ was very dominant and evidence was produced arguing that this conclusion may be general for the guanidino heterocyclics. X-Ray diffraction studies on the crystal structure of 2-(phenylimino) thiazolidine thiazine and its 2,6-dimethyl substituted analogues also showed the preference for these compounds to adopt the aryl imino structure.

In the free base structures of GU studied, the hydrate (GUFBHY)[18] and the isomorphous alcohol solvates (GUFBIP and GUFBIB)[19]; all showed unambigously, the aryl imino tautomer, $PhN{=}C(-NH_2)NR'$. In all cases, the two hydrogen atoms were located and refined on the central nitrogen, N(2) and C(1)-N(3) was significantly shorter than C(1)-N(2), 0.072(8) Å and 0.066(9)Å for GUFBHY and GUFBIP respectively. In GUFBIB the difference of 0.024(9)Å is not significant, this may be related to the greater degree of disorder in this structure or may indicate the presence of the energetically unfavoured resonance structure, $(PhN{=}C(-NH_2)-NR_2)$.

$$\overset{\delta-}{\quad}\qquad\overset{\delta+}{\quad}$$

The relevant crystallographic data are summarised in Table 6.2.1.

Table 6.2.1 Guanidine Bond Lengths, Tautomeric Preference and Dihedral Angle between Guanidine and Dichlorophenyl Ring in Free Base Structures of GU

Structures	Bond Lengths (Å)				Tautomer	Dihedral
	C(1)-N(3)	C(1)-N(2)	C(1)-N(11)	x̄C-N		Angle(ø°)
GUFBHY	1.308(6)	1.380(7)	1.372(6)	1.353(39)	Imino	55.5
GUFBIP	1.298(9)	1.364(9)	1.375(9)	1.346(42)	Imino	61.8
GUFBIB	1.313(8)	1.337(9)	1.377(8)	1.342(32)	Imino	62.2
x̄C-N	1.306(8)	1.360(22)	1.375(3)			x̄60(3)

It may be seen from Table 6.2.1, that the dichlorophenyl groups are twisted by a mean value of 60(3)°, out of the plane of the guanidine group. Thus allowing efficient overlap of the phenyl pi system, with that of the lone pair of N(3), the imino nitrogen.
The ionisation constant for GU (pka_3) provides good supportive evidence for the tautomeric preference. The pka value of 8.6 for GU is in good agreement with other N imino phenyl structures, such as Mifentidine, pKa = 8.88[20].

That this tautomer is also prevalent in solution is confirmed by Jackman and Jen[21]. They used ^1H and ^{13}C NMR on some cyclic amidines, guanidines and related structures. The authors confirmed that in all tautomeric systems studied, the predominant tautomer was the imino form [PhN = C (NHR) R'] rather than the amino form [PhNH-C(=NR) R']. Clement and Kämpchen[22] studied the tautomeric equilibria of N monosubstituted amidines and N,N' diphenyl guanidines using ^{15}N NMR. They concluded that in all compounds studied, the C=N double bond is 'conjugated' with the phenyl group. In another recent study, Oszczapowicz[23] using substituent induced chemical shifts in ^{13}C NMR spectra of N^2-phenyl formamidines, acetamidines and guanidines; confirmed that in the 65 compounds studied, all exist with an imino (N^2) nitrogen adjacent to the phenyl group.

In a series of papers on unsymmetrically and symmetrically substituted amidines[24] and N aryl amidines[25]; the authors demonstrated using pKa measurements that N aryl amidines exist predominantly as the imino tautomer and that levels of the amino tautomer were negligible.

The ^1H NMR spectrum in d^6 dimethyl sulphoxide solution of GUFBHY[18] shows a single broad resonance at δ = 5.8ppm. That this single resonance is not the result of rapid exchange of the two NH protons of the alternative tautomer is suggested by the fact that other exchangeable protons present (phenolic OH, solvent water) give separate discrete signals, implying slow proton exchange. The 5.8 ppm peak is thus most likely due to the NH_2 protons of the aryl imino tautomer.

6.3 Guanidinium Cation

Protonation of the tautomerising amidine or guanidine yields only one cation, the conjugate acid (BH+) of both tautomeric bases (B1 and B2)[25]. Considering specifically the guanidinium ion, some of the structural consequences of its 6 pi-electron, pseudo-aromatic character are three essentially equivalent C-N bonds and the strictly planar geometry of the cation[26].

The C-N bond length, inter-planar angle (ϕ) of the phenyl and guanidinium groups and the root mean square deviation (σ) of the guanidinium groups, from planarity, for all GU cations studied are summarised in Table 6.3.1.

Table 6.3.1 Guanidinium Bond Lengths, Planarity (σ) and Dihedral Angle between Guanidinium and Dichlorophenyl Ring in Protonated Structures of GU

Structures	C(1)-N(3)	C(1)-N(2)	C(1)-N(11)	$\bar{x}$ C-N	Planarity (σ,Å)	Dihedral Angle (ø,°)
Monoprotonated						
GUHFUMET	1.364(13)	1.328(13)	1.329(13)	1.340(21)	0.0008	66.3
GUMASCHY	1.364(9)	1.314(9)	1.331(9)	1.336(25)	0.0023	68.3
	1.374(9)	1.281(9)	1.312(8)	1.322(46)	0.0012	71.8
GUMACEHY	1.348(6)	1.321(7)	1.340(6)	1.336(14)	0.0027	45.2
GUMHCLHYIP	1.334(10)	1.318(10)	1.361(10)	1.338(22)	0.0008	51.6
Diprotonated						
GUDMES	1.345(10)	1.308(10)	1.331(9)	1.328(19)	0.0028	66.2
GUDHCLHY	1.339(13)	1.329(13)	1.334(12)	1.331(13)	0.0012	73.8
	$\bar{x}$1.352(15)	$\bar{x}$1.314(16)	$\bar{x}$1.334(15)	$\bar{x}$1.333(19)		64(10)

The guanidinum groups are essentially planar in all structures. Although individual C-N bond lengths demonstrate some divergence; the mean C-N bond lengths are equivalent, with a mean value of 1.333(19)Å. The dihedral (inter-planar) angles, range from 45.2 to 73.8°, but the mean value of 64°, is similar to that observed for the free base structures[18,19] [60(3)°] and demonstrates that ø is essentially independent of the ionisation state.

6.4 GU Conformation

GU can exist in either an extended or folded conformation and with respect to the position of the amino and methoxy moieties, be either cis or trans. In the extended conformation the torsion angles, N(11)-C(1)-N(3)-C(21) are *ca* 160°, but in the folded

conformation the absolute values are nearer 40°. When GU exists in the cis conformation, the absolute values of the torsion angles N(2)-N(11)-N(14)-O(32) and N(2)-C(1)-C(31)-O(32) are in the region of 0-90° and for the trans conformation this increases to between 90°-180°. These values are summarised in Table 6.4.1.

Table 6.4.1 GU Molecular Conformational Summary

Structure	Torsion Angles			Comments
	N(2)-N(11)-N(14)-O(32)	N(2)-C(1)-C(31)-O(32)	N(11)-C(1)-N(3)-C(21)	
Free Base				
GUFBHY	46.41(5)	64.74(4)	-161.79(4)	Extended cis
GUFBIP	56.29(8)	73.86(5)	-160.53(6)	Extended cis
GUFBIB	59.80(7)	75.92(5)	-159.41(6)	Extended cis
Monoprotonated				
GUHFUMET	172.43(5)	-144.50(7)	157.62(9)	Extended trans
GUMASCHY	8.94(6)	- 10.35(5)	40.86(9)	Folded cis
	2.98(7)	20.01(6)	- 46.54(9)	Folded cis
GUMACEHY	174.07(2)	159.33(3)	37.05(7)	Folded trans
GUMHCLHYIP	25.12(8)	40.27(6)	158.07(7)	Extended cis
Diprotonated				
GUDMES	51.60(9)	50.96(7)	159.77(7)	Extended cis
GUDHCLHY	57.77(8)	86.31(8)	-159.78(9)	Extended cis

The majority of the structures studied exist in the extended cis conformation, the exceptions being GUHFUMET (extended trans), GUMASCHY (folded cis) and GUMACEHY (folded trans).
All phenyl rings are planar within experimental error.

Table 6.4.2 GU Puckering Parameters and In-ring Piperazine Torsion Angles

Structure	Puckering Parameters					Torsion Angles	
	Q	q2	q3	Ø°	ϴ°	$\bar{x}$ N (11)	$\bar{x}$ N (14)
Free Base							
GUFBHY	0.578	0.122	0.565	8.8	32.4	48.3	64.8
GUFBIP	0.577	0.053	0.574	33.0	5.2	54.8	60.0
GUFBIB	0.580	0.044	0.579	24.5	4.4	55.4	60.5
						$\bar{x}$ 53(4)	$\bar{x}$62(3)
Monoprotonated							
GUHFUMET	0.584	0.064	0.581	75.1	6.3	57.2	59.1
GUMASCHY	0.571	0.156	-0.549	23.3	15.9	45.2	65.4
	0.552	0.107	0.541	29.9	11.2	47.4	62.2
GUMACEHY	0.577	0.066	-0.574	-46.0	6.6	54.2	60.5
GUMHCLHYIP	0.580	0.098	0.571	17.2	9.7	50.6	63.6
						$\bar{x}$ 51(5)	$\bar{x}$62(2)
Diprotonated							
GUDMES	0.565	0.017	0.565	75.6	1.7	58.2	55.6
GUDHCLHY	0.583	0.050	0.581	17.5	4.9	63.1	53.2
						$\bar{x}$ 61(3)	$\bar{x}$54(2)

The piperazine ring exists in a half-chair conformation significantly flattened towards N(11) in the free base and monoprotonated structures, and toward N(14) in the diprotonated structures. This is illustrated using the absolute in-ring torsion angles about N(11) [but excluding N(14)] and about N(14), [but excluding N(11)], these values are summarised in Table 6.4.2, together with the puckering parameters of Cremer and Pople[27] (starting from either nitrogen atom and reducing ø and Θ to first quadrant angles). The mean torsion angles (for structures of a particular protonation state), illustrate that there is no significant difference, between the free base and monoprotonated structures. This can be explained in that the 'aromatic', planar guanidinium cation, extensively

delocalises the positive charge over the whole of the cation. This results in marginal positive charge being present on the piperazine nitrogen, N(11). Thus the monoprotonated structures closely resemble the free base structures in terms of flattening of the piperazine ring towards N(11). In the diprotonated structures, the presence of a second positive charge on the other piperazine nitrogen, N(14), results in a flattening towards N(14), as the ring tries to maximise the separation of the two positive charges. This flattening of the ring is accompanied by significant lengthening of both the in-ring and out-ring C-N(14) bond lengths, as shown in Table 6.4.3.

Table 6.4.3 GU In-ring and Out-ring Piperazine Bond Lengths

Structure	Out-Ring Bond Lengths (Å)	In-Ring Bond Lengths (Å)		
	N(14)-C(31)	x̄N(11)-C(12)/C(16)	x̄N(14)-C(13)/C(15)	C(12)-C(13) x̄C(15)-C(16)
Free Base				
GUFBHY	1.443	1.476	1.473	1.526
GUFBIP	1.428	1.460	1.472	1.518
GUFBIB	1.440	1.461	1.465	1.522
	x̄1.437	x̄1.466	x̄1.470	x̄1.522
Monoprotonated				
GUHFUMET	1.443	1.466	1.472	1.511
GUMASCHY	1.436	1.472	1.468	1.514
	1.393	1.472	1.466	1.500
GUMACEHY	1.445	1.472	1.468	1.519
GUMHCLHYIP	1.434	1.480	1.470	1.528
	x̄1.430	x̄1.472	x̄1.469	x̄1.514
Diprotonated				
GUDMES	1.474	1.454	1.506	1.520
GUDHCLHY	1.503	1.458	1.517	1.524
	x̄1.489	x̄1.456	x̄1.512	x̄1.522

In order to determine whether the tautomers found in solution correspond to those in the crystal structures, the ^1H NMR spectra of a free base (GUFBHY), and selected monoprotonated (GUMHCLHYIP) and diprotonated (GUDHCLHY) salts were measured in d^6 dimethyl sulphoxide solution. The assignments for hydrogen atoms bonded to carbon are shown in Table 6.4.4.

In the spectrum of GUFBHY, a single broad resonance at δ 5.8 ppm could be attributed to two protons attached to N(2), and ruled out protons on N(2) and N(3). In the salts, the positions of the resonances due to the replaceable protons were less well defined, but the effects on others were clear.

Conversion of GUFBHY into GUMHCLHYIP gives major shifts at centres near N(3) [H(22), H(24) and H(26)] and negligible effects on the resonances of other protons. In GUDHCLHY, these resonances change very little, while there are major shifts to the protons bonded to C(13), C(15) and C(36). It thus appears that the tautomeric forms of the ions in dimethyl sulphoxide solution are the same as those in the crystal[28], and confirms the order of protonation.

Table 6.4.4 ^1H NMR Spectra for the Free Base (GUFBHY) Monoprotonated (GUMHCLHYIP) and Diprotonated (GUDHCLHY) Salts in d^6 dimethyl sulphoxide solution. (Values given are δ in ppm relative to tetramethylsilane)

Protons	GUFBHY	GUMHCLHYIP	GUDHCLHY
H(12A),H(12B),H(16A),H(16B)	3.46	3.69	3.72
H(13A),H(13B),H(15A),H(15B)	2.84	2.96	4.08
H(22),H(26)	6.69	7.39	7.43
H(24)	6.89	7.37	7.38
H(33)	6.39	6.45	6.68
H(35)	6.28	6.32	6.50
H(36)	6.71	6.71	7.61
H(3M1),H(3M2),H(3M3)	3.73	3.73	3.87

6.5 GU Pharmacological Profile

A number of cyclic amidines possess interesting pharmacological properties[29,1].
Previous investigations have shown that slight changes in the structure of cyclic amidines could have profound consequences with respect to their pharmacological activity[1,30]. Several physicochemical properties of these compounds have been considered to be related to this phenomenon. In particular, steric and electronic requirements have been suggested as being of prime importance[31,32,30]. There is strong evidence that some cyclic amidines interact with α-adrenergic receptors[33] and, in particular, the antihypertensive effect of Clonidine is thought to be mediated by stimulation of central α-adrenergic receptor sites[34,35]. The α-adrenergic receptor appears to pose very strict structural demands on those interacting compounds, which ultimately elicit a pharmalogical response. With the advanced receptor labelling techniques available[36] it is now possible to assess these structural requirements at the receptor level. These can be expressed in terms of their equilibrium affinity or dissociation constants (pki) based on their ability to displace ^{3}H Clonidine from its α-adrenergic receptor sites in rat brain homogenate.

Structural differences between molecules should be reflected in their affinity for these receptors and hence comparisons of these receptor affinities should give insight into the structural features required for efficient receptor- complex formation[37]. In current representations of the interaction of Clonidine, related phenyl imidazoles and phenyl guanidines with the α-adrenergic receptor(s), it is generally accepted that the phenyl ring and the heterocyclic or open chain derivative are not co-planar[38,39]. The inter-planar torsion angle (ϕ) is assumed to be either 60°, 75° or 90°. The knowledge of

the conformational characteristics of the phenyl imidazoles is important for the considerations of a topological analogy of these class of compounds with the phenylethylamine type drugs. This includes the natural andrenergic ligands and, in consequence, of whether both types of drug interact with the same receptor site or not[40,41]. Moreover, the assumed conformation of the phenyl imidazoles is important for HOMO and LUMO energies, since the calculated orbital energies are strongly dependent on ϕ.

The evidence for the conformation of the phenyl imidazoles stems from x-ray diffraction studies, conformational energy calculations, UV photoelectron spectroscopy and NMR work. In Xylometazoline[42], the methyl substituents at the ortho position of the phenyl ring, lead to the stabilisation of the nearly mutually perpendicular arrangement of the two ring systems (ϕ = 85°). A similar ring conformation has been found in other ortho di-substituted compounds of this series eg Clonidine Hydrochloride[43] and Clonidine Phosphate[44]. But in Tolonidine Nitrate[45] which has only one ortho substituent, ϕ is close to 60°. Carpy *et al*[39] using crystallographic and quantum mechanical calculations and Jackman *et al*[21] using NMR techniques, both predicted that the solution state conformation would have a nearly perpendicular arrangement of the two ring systems (or two planar moieties in the case of the open ring guanidines and thioguanidines). The driving force for this, was postulated to be steric; in which compounds with large di-ortho substituents would be forced to adopt non-planar conformations to avoid mesomeric interactions within the molecule[30].

However, UV photoelectron spectroscopic measurements in combination with CNDO/S quantum mechanical calculations suggest that di-ortho, mono-ortho and unsubstituted

phenyl imidizoles all prefer a perpendicular conformation of their ring systems[38]. That steric requirements only are not selective enough to explain observed differences was amply demonstrated by Léger *et al*[46]. The authors determined the crystal structure of 1-[(3-methyl-4-isothiazolyl)methyl] guanidinium hemisulphate and found that the two crystallographically independent molecules adopted two different conformations with the inter-planar angles being 83° for molecule 1 and 65° for molecule 2.

Carpy *et al*[39] postulated a model for the interaction of phenyl imidazole-like compounds with the α-adrenoreceptor sites.

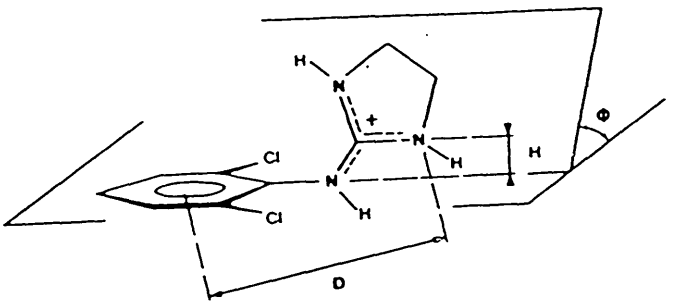

The model proposed the following requirements for efficient ligand-receptor interaction.
(*a*) electrostatic attraction between the positively charged amidine function and a negatively charged site on the α-adrenoreceptor.
(*b*) hydrophobic interaction between the aromatic nucleus and an electron deficient area of the α-adrenoreceptor and
(*c*) the possible additional formation of a hydrogen bond between the receptor and the exocyclic NH. The distance (D) of the nitrogen (furthest from the phenyl ring) and the centre of the phenyl ring and the height (H) of this nitrogen atom above the phenyl ring are thought to be of considerable significance for the α-adrenergic agents[47,48,49]. The available data have been summarised for all of the structures of GU (Table 6.5.1) and for the phenyl imidazole type compounds (Table 6.5.2).

Table 6.5.1 Summary of Crystallographic Data for all GU structures on the basis of the Pharmacophore Model of Carpy *et al*[39]

Structure	Pharmacophore Model Parameters D(Å)	H(Å)	ϕ
Free Base			
GUFBHY	4.93	0.43	55.5
GUFBIP	4.90	-0.43	61.8
GUFBIB	4.92	-0.36	62.2
Monoprotonated			
GUHFUMET	4.93	-0.37	66.3
GUMASCHY*	4.80	-0.02	68.3
	4.75	0.01	71.8
GUMACEHY*	4.86	0.08	45.2
GUMHCLHYIP	4.97	0.03	51.6
Diprotonated			
GUDMES	4.92	-0.42	66.2
GUDHCLHY	4.85	-0.82	73.8

* folded conformation, ø = dihedral angle between phenyl and guanidine groups

Structures exhibiting the folded conformation, (GUMASCHY and GUMACEHY) will be omitted from the subsequent discussions; as the most common conformation, occurring in 70% of the structures studied, is the extended one. The values of D obtained for the various structures of GU are very similar, with a mean value of 4.92(4)Å and a range of 4.85Å to 4.97Å.

The value of D is also independent of the protonation state of GU; free base (4.92Å), monoprotonated (4.95Å) and diprotonated (4.88Å). These values compare favourably with those cited in Table 6.5.2, for other α-adrenergic compounds. Where the structures studied do deviate markedly from this model is in the value of H. Typical absolute values of H obtained were 0.4(2)Å with a range of 0.43Å to -0.82Å, this is significantly less than the

typical value of 1.0Å for other α-adrenergic compounds.

Table 6.5.2 Summary of Crystallographic Data for α-Adrenergic Compounds of the Basis of the Pharmacophore Model of Carpy *et al*[39]. Key on p. 171

Structure	References	Pharmacophore Model Parameters		
		D(Å)	H(Å)	φ
Imidazolines				
Clonidine HCl	50	5.00	1.03	75.8
Clonidine HCl	43	5.00	1.03	75.6
Clonidine PO4	44	4.98	1.31	89.4
Xylazine PO4	51	4.84	1.04	81.0
Tiamenidine HCl	52	5.08	0.85	77.0
IPRO-4 HCl	53	5.01	0.82	77.0
Lofexidine HCl	54	5.07	0.72	-
Tolonidine NO_3	45	4.93	0.84	53.0
Xylometazoline HCl	42	4.96	1.32	95.0
CG-8345-60	46	5.29	0.80	97.0
		5.70	-2.64	65.0
ICI-101187	55	4.85	0.61	87.0
Nebidrazine	56	5.06	0.15	-
Guanabenz (MNDO)	57	5.11	2.04	39.7
Indanidine HCl	58	5.31	1.12	63.0
Phentolamine HCl	59	5.12	-1.57	88.0
RX-781094	60	4.27	2.08	87.0
RS-21361	60	5.53	-2.17	63.0
WY-26392	61	5.57	-	-
Phenylethylamines				
COR-3441	62	5.66	-	-
BE-2254	63	5.23	0.25	-
Oxypertine	64	5.72	1.83	-

The validity of this model has been questioned by several researchers in this field. Diamont *et al*[57] studied the conformation and pharmacological activity of the specific α-adrenergic agonist drug, Guanabenz. They observed that in the crystal state, the dihedral angle between the two planar moieties was only 39.7°, as compared with about 76° in Clonidine[50,43]. Using PCILO calculations they were

able to show that Clonidine is rotationally restricted as compared with Guanabenz and that the dihedral angle is about 60° in the former, but 0° in the latter. Similarly using MNDO calculations they were able to calculate the charge distribution for the two molecules.

At physiological pH (7.4), both molecules exist predominantly in the protonated form, Guanabenz (pKa 8.1, 83.4% protonated) and Clonidine (pKa 8.05, 82.9% protonated). The authors found that on protonation the additional positive charge is distributed in Clonidine, over the aromatic nucleus (+0.243), imino spacer group (+0.590) and the remainder of the imidazole ring (+0.165), In contrast, the charge distribution in Guanabenz shows a small fraction over the aromatic nucleus (+0.094), the majority residing on the guanidinium (+0.814) with the remainder being present in the imino spacer group (+0.095).

Interestingly the 1,2,4-triazole-4-amine analogue (Nebidrazine,[56]) of Guanabenz also gave an almost planar arrangement of the two rings (8°), in agreement with the PCILO calculations for Guanabenz. CNDO charge distribution calculations were performed on the triazole ring only, so that comparison with Guanabenz are not possible.

Charge distribution and its effect on binding affinity to receptor sites has been the subject of previous reports[42]. When considered as a class, the imidazolines have higher affinities for the α-adrenergic receptor than the phenylethylamines[65].
Ghose *et al*[42] postulated that one of the reasons for this observation may be that the dispersed charge arrangement within the imidazole moiety helps it to achieve better interaction with the α-adrenergic receptor. This may not be possible in the phenylethylamines since the positive charge is concentrated at the nitrogen atom in the

protonated forms of these molecules. The α-adrenergic receptor-ligand model of Carpy *et al*[39] appears not to model the phenylethylamines very effectively as can be seen from the values obtained for COR-3441[62], BE-2254[63], and Oxypertine[64] in Table 6.5.2.

Kaliszan *et al*[66] suggested that an additional parameter that should be considered for this model, was that of breadth (B) of the anchoring fragment of aromatic ring. They studied a series of pyrazine imidazolines and concluded that the general steric features of D ~ 5Å and the angle between the planes of the hydrophobic and imidazoline fragment of about 75°, were in accord with those suggested by Carpy *et al*[39]. However, pyrazine, as compared to benzene, was not lipophilic enough to provide sufficient hydrophobic binding of the ligand to the receptor.
Introduction of hydrophobic substituents to the pyrazine system can result in compounds with sufficient affinity for the ligand, provided the steric requirements are fulfilled. It is the substituent rather than the pyrazole that provides binding affinity for the receptor. Whereas the total molecular hydrophobicity influences the affinity of the ligand for the receptor, the specificity could be related to the breadth of the hydrophobic 'anchoring' moiety. Substances having anchoring fragments below 7.23Å show antagonist properties if their geometry and lipophilicity are appropriate. Analogously, compounds having anchoring fragments above 6.03Å behave as partial agonists.

Thus far the discussion relating to the pharmacology of GU have centred around its α-adrenergic receptor affinity, which is closely linked with the dichlorophenyl guanidine moiety. The remainder of the molecule is also pharmacologically active, 2-methoxyphenyl piperazine has been shown to have potent hypotensive effects in man[67].

Like other phenyl piperazine derivatives[68,69] it enhances central 5-hydroxytryptaminergic (5-HT) transmission[70] and recent ligand binding studies show that it behaves as a selective 5-HT agonist, displaying affinity for the 5-HT, binding site comparable with that of the recognised 5-HT agonist, 1-(3-trifluoromethylphenyl) piperazine[71]. Indeed, the 2-methoxyphenyl piperazine moiety has been incorporated into the structure of many pharmacologically unrelated compounds, which can form 2-methoxyphenyl piperazine by metabolic cleavage of their side chain[32].

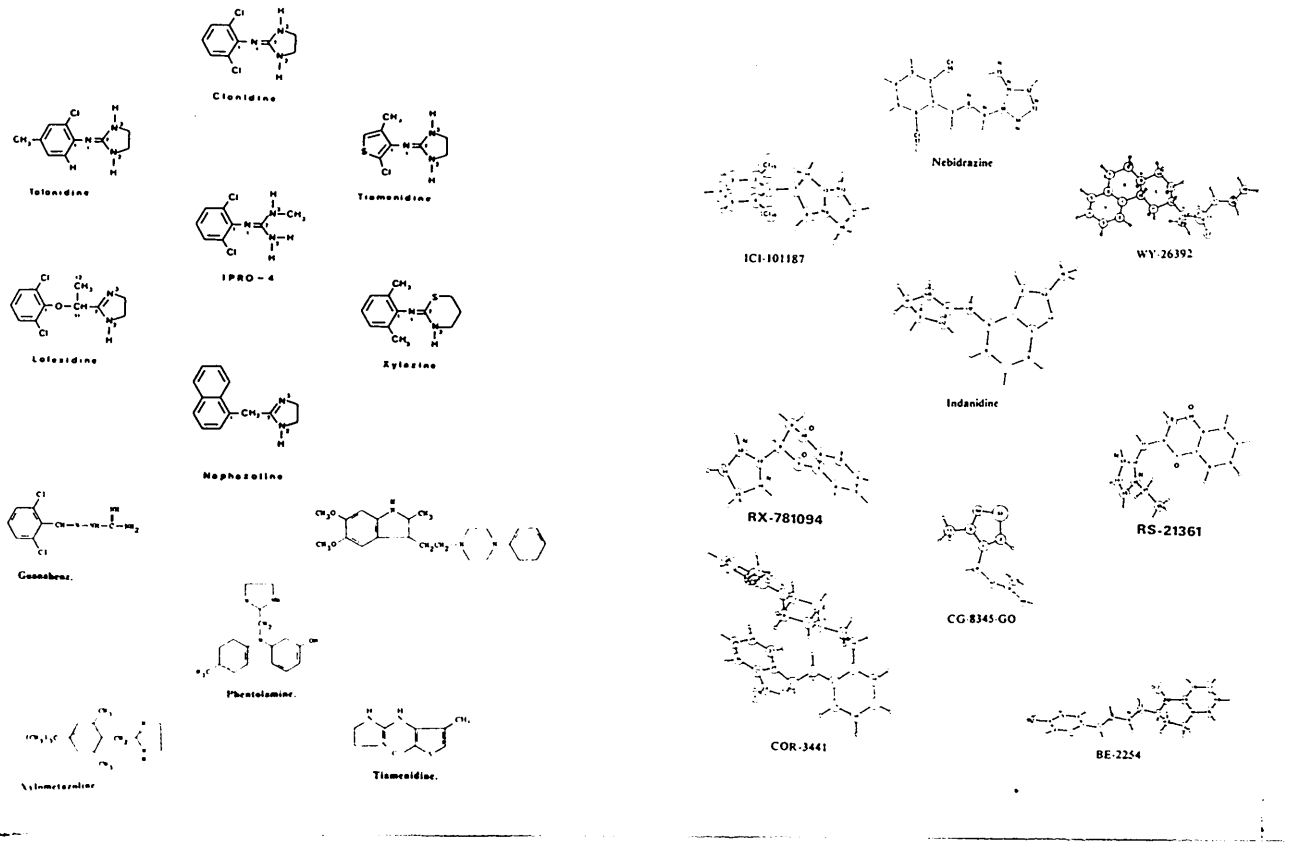

6.6 References

1. JEN, T, VAN HOEVEN, H, GROVES, W, McLEAN, R A and LOEV, B, J Med Chem 18, 90, 1975

2. GUND, P, J Chem Educ, 49, 100, 1972

3. PAULING, L, in 'The Nature of the Chemical Bond', 3rd Edition, 286, 1960, Cornell University Press, New York

4. HÜCKEL, E, Z PHYSIK, 70, 204, 1931

5. KLEIN, J, Tetrahedron, 39, 2733, 1983

6. SOLOWAY, S, ROSENSTOCK, H M and SANTORO, A J, J Org Chem, 23, 1042, 1958

7. TAYLOR, P C, GRISCOM, D L and BRAY, P J, J Chem Phys, 5, 748, 1971

8. SCHRINER, R L and NEUMANN, F W, Chem Rev, 35, 351, 1944

9. HÄFELINGER, G in 'The Chemistry of Aminidines and Imidates', ed S Patai, 53, 1974, J Wiley, London

10. PREVORSÈK, D C, Bull Soc Chim Fr, 0, 788, 1958

11. PREVORSÈK, D C, J Phys Chem, 66, 769, 1962

12. PYMAN, F L, J Chem Soc 367, 3359, 1923

13. PYMAN, F L, and CHEW, C, J Chem Soc, 2318, 1927

14. MORITZ, A G, Spectrochimica Acta, 20, 1555, 1964

15. ORVILLE-THOMAS, W J and PARSON A E, Trans Faraday Soc, 54, 460, 1958

16. CHARLTON, M J, Org Chem, 30, 969, 1965

17. BUTTON, R G, CAIRNS, J P and TAYLOR, P J J Chem Soc Perkin Trans, II, 1555, 1985

18. ELDER D P, SELBY, I A, Taylor, D and GOULD, R O, submitted for publication, Acta Cryst, 1991

19. ELDER D P, SELBY, I A, BLAKE, A J and GOULD, R O, submitted for publication, *ibid*, 1991

20. BAZZANO, C, VANOI, P C, MONDONI, M, GALLAZZI, A, CEREDA, E and DONETTI, A, Eur J Med Chem-Chim Ther, 21, 27, 1986

21. JACKMAN, L M and JEN, T, J Amer Chem Soc, 97, 10, 1975

22. CLEMENT, B and KÄMPCHEN, T, Chem Ber, 119, 1101, 1986

23. OSZCZAPOWICZ, J, RACZYŃSKA, E W and OSEK, J, Magnetic Resonance in Chemistry, 24, 9, 1986

24. RACZYŃSKA, E W and OSZCZAPOWICZ, J, Tetrahedron, 41, 5175, 1985

25. RACZYŃSKA, E W, J Chem Soc Perkin Trans II, 1189, 1986

26. COTTON, F A, DAY, V W, HAZEN, E E and LARSEN, S, J Amer Chem Soc, 95, 4834, 1973

27. CREMER, D and POPLE, J A, *ibid*, 97, 1354, 1975

28. ELDER D P, SELBY, I A and GOULD, R O, submitted for publication, Acta Cryst, 1991

29. SCHLITTER, E, Handb Exp Pharmacol, 39, 13, 1977

30. TIMMERMANS, P and VAN ZWIETEN, P A, J Med Chem, 20, 1636, 1977

31. STRUYKER BOUDIER, H, De BOER, J, SMEETS, G, LIEN, E J and VAN ROSSUM, J M, Life Sci, 17, 377, 1975

32. ROUOT, B, LECLERC, G, WERMUTH, C G, MIESCH, F and SCHWARTZ, J, J Med Chem 19, 1049, 1976

33. MUJIC, M and VAN ROSSUM, J M, Arch Int Pharmacodyn, 155, 432, 1965

34. SCHMITT, H, Handb Exp Pharmacol, 39, 299, 1977

35. KOBINGER, W, Rev Physiol Biochem Pharmacol 81, 39, 1978

36. U'PRICHARD, D C and SYNDER, S H, Life Sci, 24, 79, 1979

37. De JONG, A P and SOUDIJN, W, Eur J Pharmacol, 69, 175, 1981

38. De JONG, A P and VAN DAM, H, J Med Chem 23, 889, 1980

39. CARPY, A, LÉGER, J-M, LECLERC, G, DECKER, N, ROUOT, B and WERMUTH, C G, Molecular Pharmacol, 21, 400, 1982

40. RUFFOLO, R R, WADDEL, J E and YADEN, E L, J Pharmacol Exp Ther, 213, 267, 1980

41. RUFFOLO, R R in 'Adrenoceptors and Catecholamine Action' (G Kunos, Ed), 1982, J Wiley and Sons, New York

42. GHOSE, S and DATTAGUPTA, J K, Acta Cryst, C42, 1524, 1986

43. CODY, V and DETITTA, G T, J Cryst Mol Struct, 9, 33, 1979

44. CARPY, A, HICKEL, D and LÉGER, J-M, Cryst Struct Commun, 8, 433, 1979(a)

45. CARPY, A, Hickel, D and LÉGER, J-M, *ibid*, 8, 945, 1979 (c)

46. LÉGER, J-M, COLLETER, J-C and CARPY, A, Acta Cryst, C41, 622, 1985

47. DATTAGUPTA, J K, MEYER E F and MUKHOPADHYAY, B P, *ibid*, B38, 2830, 1982

48. DATTAGUPTA, J K, PATTANAYEK, R R and SAHA, N N, *ibid*, B37, 1439, 1981

49. PULLMAN, B, COUBEILS, J L, COURRIERE, P and GERVOIS, J P, J Med Chem 15, 17, 1972

50. BYRE, G, MOSTAD, A, and RØMMING, C, Acta Chem Scand, B30, 843, 1976

51. CARPY, A, GADRET, M and LÉGER, J-M, Acta Cryst, B35, 994, 1979 (b)

52. CARPY, A, LÉGER, J-M, WERMUTH, C G and LECLERC, G, *ibid*, B37, 885, 1981 (a)

53. CARPY, A, HICKEL, D and LÉGER, J-M, Cryst Struct Commun, 10, 13, 1981 (b)

54. CARPY, A, HICKEL, D and LÉGER, J-M, *ibid*, 9, 43, 1980

55. CARPY, A, LÉGER, J-M and COLLETER, J-C, Acta Cryst, C39, 1426, 1983

56. CARPY, A, SAUX, M and MONTAGUT, M, *ibid*, C40, 1265, 1984 (b)

57. DIAMONT, S, AGRANAT, J, GOLDBLUM, A, COHEN, S and Atlas, D, Biochem Pharmacol, 34, 491 1985

58. H'NAÏFI, A, LÉGER, J-M and CARPY, A, Acta Cryst, C42, 339, 1986

59. LÉGER, J-M, DUBOST, J-P, COLLETER, J-C and CARPY, A, *ibid*, C39, 1430, 1983 (b)

60. CATTIER-HUMBLET, C and CARPY, A, Eur J Med Chem-Chim Ther, 20, 251, 1985

61. CARPY, A, H'NAÏFI, A and LÉGER, J-M, Acta Cryst, C40, 1965, 1984 (c)

62. CARPY, A, FENIOU, C, H'NAÏFI, A and COLLETER, J-C, *ibid*, C40, 1970, 1984 (d)

63. CARPY, A, LÉGER, J-M and COLLETER, J-C, *ibid*, C40, 154, 1984 (a)

64. LÉGER, J-M, SAUX, M, and CARPY, A, *ibid*, C39, 1428, 1983 (a)

65. RUFFOLO, R R, DILLARD, R D, YADEN, E L and WADDELL, J E, J Pharmacol Exp Ther, 211, 74, 1979

66. KALISZAN, R, FOKS, H, DAMASIEWICZ, B, NASAL, A, RADWAŃSKA, A, KUŹMIERKIEWICZ, W, PANCECHOWSKA-KSEPKO, D, RUDNICKA, W and WISTEROWICZ, K, Pol J Pharmacol Pharm, 37, 79, 1985

67. PAGE, I H, WOLFORD, R W and CORCORAN, A C, Arch Int Pharmacodyn Ther, 119, 214, 1959

68. FULLER, R W, SNODDY, H D, MARSON, N R, HEMRICK-LUECKE, S K and CLEMENS, J A, J Pharmacol Exp Ther, 218, 636, 1981

69. MAJ, J and LEWANDOWSKA, A, Pol J Pharmacol Pharm, 32, 495, 1980

70. POWLOWSKI, L, *ibid*, 35, 319, 1983

71. LYON, R A, TITELER, M, McKENNEY, J, MAGEE, P S and GLENNON, R A, J Med Chem, 29, 630, 1986

72. BENFENATI, E, CACCIA, S and DELLA VEDOVA, F, J Pharm Pharmacol, 39, 312, 1987

Abbreviations used are:

HOMO	Highest Occupied Molecular Orbital
LUMO	Lowest Unoccupied Molecular Orbital
MNDO	Modified Neglect of Differential Overlap
PCILO	Perturbation Configuration Interaction using Localised Orbitals
CNDO	Complete Neglect of Differential Overlap

SECTION 7 : PREPARATION AND CHARACTERISATION OF SALTS AND MODIFICATIONS OF IM

7.1 Introduction

In this section, a similar coding system to that used in Section 3, is adopted.

The first two letters of IM refer to the imidazole moiety, which is one of the salt forming groups of the molecule. The next letter(s) indicated the protonation state of the compound; FB ≡ Free Base, M ≡ Monoprotonated, H ≡ Hemiprotonated, S ≡ Sesquiprotonated, D ≡ Diprotonated and T ≡ Triprotonated.

This is followed, in the case of the protonated compounds, by the code designating the anion; FUM ≡ Fumarate, CIT ≡ Citrate, ACE ≡ Acetate, HCL ≡ Chloride, ASC ≡ Ascorbate, MAL ≡ Maleate, MALN ≡ Malonate, MES ≡ Mesylate, NIT ≡ Nitrate, SULF ≡ Sulphate, PHOS ≡ Phosphate, LAC ≡ Lactate, TAR ≡ Tartrate, OXA ≡ oxalate and SUC ≡ succinate.

The presence of solvation (or hydration) is indicated by; HY ≡ Hydrate, Et ≡ Ethanol, IP ≡ Isopropanol, IB ≡ Isobutanol, AC ≡ Acetone and TOL ≡ Toluene.

Finally, a series of polymorphic modifications of a particular compound are designated by the suffixed letters A, B, C.

Some examples are:
IMFBA, IMFBB and IMFBC ≡ A, B and C polymorphic modifications of the free base
IMFBTOL ≡ toluene solvate of the free base
IMMHCLAC ≡ acetone solvate of the monochloride salt
IMDMES ≡ dimesylate salt
IMTHCLHYA, IMTHCLHYB, IMTHCLHYC ≡ A, B and C polymorphic modifications of the hydrated trichloride salt

Table 7.1 Preparation of Salts and Modifications of IM

Compound	Stoichiometry	Base (mmole)	Acid (mmole)	Solvent	% Yield	Comments
Modifications						
IMFBA	$C_{29}H_{32}N_4$	2.29	-	Ethanol 10 ml, 60°C	92.4	Poor quality[1] crystals.
IMFBB	$C_{29}H_{32}N_4$	2.29	-	DMF 10 ml, 100°C	90.6	Poor quality[1] crystals.
IMFBC	$C_{29}H_{32}N_4$	22.9	-	Ethanol 10 ml, 25°C	93.1	Poor quality[2] crystals.
IMFBTOL	$C_{29}H_{32}N_4$ C_7H_8	0.23	-	Toluene 20 ml, 110°C	67.8	Crystal quality good enough for structure determination.

1. IMFBA was crystallised from the following solvents: all normal (n-) and secondary (iso-) alcohols (up to pentanol), water, acetone, methyl ethyl ketone, ethyl acetate, butyl acetate, acetonitrile, 1,4-dioxan and dichloromethane. Also crystallised from the following mixed solvents: methanol/water, isopropanol/water, dimethylformamide/water, acetone/water and tetrahydrofuran/water.

   All of these solvents produced gums or poor quality crystals. The best crystals were produced from isopropanol/water, but on microscopic examination were found to be twinned.

2. IMFBC was prepared by producing a supersaturated solution of the free base in ethanol and agitating at room temperature, until a copious precipatate of IMFBC separated.

3. IMMHCLHY was crystallised from the following solvents: all normal (n-) and secondary (iso-) alcohols (up to pentanol), ethyl acetate, isooctane, acetone, water. Also crystallised from the following solvent mixtures: hexane/acetonitrile, ethyl acetate/methanol, water/methanol, isooctane/methanol, acetone/methanol, ethyl acetate/methanol and ethyl acetate/dichloromethane. With the exception of acetone/methanol which yielded diffraction grade crystals of IMMHCLAC, all produced very small, poor quality crystals.

Table 7.1 Preparation of Salts and Modifications of IM

Compound	Stoichiometry	Base (mmole)	Acid (mmole)	Solvent	% Yield	Comments
Salts						
Monoprotonated						
IMMHCLHY	$C_{29}H_{33}N_4^+.Cl^-.H_2O$	2.29	2.29	Ethanol 20 ml, 60°C	82.3	Poor quality[3] crystals.
IMMHCLAC	$C_{29}H_{33}N_4^+.Cl^-.C_3H_6O$	2.29	2.29	Acetone/Methanol (50/50 v/v) 20ml, 60°C	61.9	Crystal quality good enough for structure determinations.
IMMMES (a)	$C_{29}H_{33}N_4^+.CH_3SO_3^-$	2.29	2.11	Ethanol 20 ml, 60°C	85.6	Poor quality[4] crystals.
IMMMES (b)	$C_{29}H_{33}N_4^+.CH_3SO_3^-$	2.29	2.30	Ethyl Acetate/ Methanol (95/5 v/v) 20 ml, 60°C	64.8	Crystals were large plates of sufficient quality for structure determinations.
Diprotonated						
IMDMES	$C_{29}H_{34}N_4^{2+}.2CH_3SO_3^-$	1.14	2.29	Ethyl Acetate/Methanol (90/10 v/v) 50 ml, 80°C		No crystals produced even at -20°C. Evaporated slowly, but a gum was formed.

4. IMMMES was crystallised from the same solvents and solvent mixtures as detailed in 3. Again, with the exception of ethyl acetate/methanol, which yielded diffraction grade crystals of IMMMES, all produced small or poor quality crystals.

Table 7.1 Preparation of Salts and Modifications of IM

Compound	Stoichiometry	Base (mmole)	Acid (mmole)	Solvent	% Yield	Comments
Diprotonated						
IMDHCL (a)	$C_{29}H_{34}N_4^{2+}.2Cl^-$	2.29	4.60	Isopropanol 50 ml, 60°C	-	No crystals produced even at -20°C. Evaporated slowly, but a gum was formed.
IMDHCL (b)	$C_{29}H_{34}N_4^{2+}.2Cl^-$	1.14	2.29	Ethyl Acetate/ Methanol (90/10 v/v) 50 ml, 80°C	85.8	No crystals produced even at -20°C. Evaporated slowly, but a gum was formed. On scratching the gum, poor quality crystals were produced.
IMDACE (a)	$C_{29}H_{34}N_4^{2+}.2C_2H_3O_2^-$	2.29	4.61	Isopropanol 30 ml, 60°C	56.7	No crystals produced even at -20°C. Evaporated slowly, but a gum was formed. On scratching the gum, poor quality crystals were produced. Crystals characterised as Free Base.
IMDACE (b)	$C_{29}H_{34}N_4^{2+}.2C_2H_3O_2^-$	2.29	4.60	Isopropanol/Water (30/70 v/v) 15 ml, 60°C	-	No crystals produced even at -20°C. Evaporated slowly, but a gum was formed.
IMDACE (c)	$C_{29}H_{34}N_4^{2+}.2C_2H_3O_2^-$	2.29	4.60	DMF/Water (50/50 v/v) 35 ml, 100°C	-	No crystals produced even at -20°C. Evaporated slowly, but a gum was formed.

Table 7.1 Preparation of Salts and Modifications of IM

Compound	Stoichiometry	Base (mmole)	Acid (mmole)	Solvent	% Yield	Comments
Triprotonated						
IMTHCLHYA (a)	$C_{29}H_{35}N_4^{3+}.3Cl^-.H_2O$	2.29	6.90	Ethanol 10 ml, 60°C	89.2	Poor quality[6] crystals.
IMTHCLHYA (b)	$C_{29}H_{35}N_4^{3+}.3Cl^-.H_2O$	2.29	6.90	Ethyl Acetate/ Methanol (95/5 v/v) 10 ml, 60°C	61.4	Crystal quality good enough for structure determination.
IMTHCLHYB	$C_{29}H_{35}N_4^{3+}.3Cl^-.2H_2O$	2.29	7.01	Isopropanol 20 ml, 60°C	73.2	Two distinct crystal morphologies were formed. Needle shaped crystals were identified as IMTHCLHYB. Plate shaped were identified as IMTHCLHYE.
IMTHCLHYC	$C_{29}H_{35}N_4^{3+}.3Cl^-.5H_2O$	2.28	7.00	Acetone/Water (95/5 v/v)	69.3	Large plate shaped crystals, quality good enough for structure determination.
IMTHCLHYD (a)	$C_{29}H_{35}N_4^{3+}.3Cl^-.5H_2O$	-	-	Suspend crystals of IMTHCLHYA in water for several months	-	Large plate shaped crystals, quality good enough for structure determination.

5. IMTHCL was crystallised from the same solvents and solvent mixtures detailed in 3. Majority of crystals were small and of poor quality.

Table 7.1 Preparation of Salts and Modifications of IM

Compound	Stoichiometry	Base (mmole)	Acid (mmole)	Solvent	% Yield	Comments
Triprotonated						
IMTHCLHYD (b)	$C_{29}H_{36}N_4^{3+}.3Cl^-.5H_2O$	-	-	Suspend crystals of IMTHCLHYE in water for several months	-	Large plate shaped crystals, quality good enough for structure determination.
IMTHCLHYE	$C_{29}H_{36}N_4^{3+}.3Cl^-.5H_2O$	2.29	7.01	Hexane/Acetonitrile (95/5 v/v) 100 ml, 80°C Also from Isopropanol 20 ml, 60°C	61.4	Large, rectangular shaped crystals, quality good enough for structure determination. Also produced from isopropanol (see IMTHCLHYB).
IMTACE[6]	$C_{29}H_{36}N_4^{3+}.3C_2H_3O_2^-$	2.27	6.99	Water 20 ml, 80°C	-	No crystals produced even at -20°C. Evaporated slowly, but a gum was formed.
IMTLAC	$C_{29}H_{36}N_4^{3+}.3C_3H_6O_3^-$	2.29	7.00	Water 20 ml, 80°C	-	No crystals produced even at -20°C. Evaporated slowly, but a gum was formed.

6. Following nomenclature was adopted for the anions used in these investigations; HCL (chloride), MES (mesylate), ACE (acetate), LAC (lactate), TAR (tartrate), MALN (malonate), SULF (sulphate), OXA (oxalate), ASC (ascorbate), MAL (maleate), FUM (fumarate) and SUC (succinate).

Table 7.1 Preparation of Salts and Modifications of IM

Compound	Stoichiometry	Base (mmole)	Acid (mmole)	Solvent	% Yield	Comments
Triprotonated						
IMTTAR	$C_{29}H_{36}N_4^{3+}.3C_4H_5O_6^-$	2.29	7.01	Water 20 ml, 80°C	-	No crystals produced even at -20°C. Evaporated slowly, but a gum was formed.
IMTMALN	$C_{29}H_{36}N_4^{3+}.3C_3H_3O_4^-$	2.29	7.01	Water 20 ml, 80°C	-	No crystals produced even at -20°C. Evaporated slowly, but a gum was formed.
IMTSULF	$C_{29}H_{36}N_4^{3+}.3HSO_4^-$	2.29	6.69	Water 20 ml, 80°C	61.8	Poor quality crystals.
IMTOXA	$C_{29}H_{36}N_4^{3+}.3C_2HO_4^-$	2.29	6.69	Water 20 ml, 80°C	51.4	Poor quality crystals.
IMTASC	$C_{29}H_{36}N_4^{3+}.3C_6H_7O_6^-$	2.30	7.02	Water 20 ml, 80°C	-	No crystals produced even at -20°C. Evaporated slowly, but a gum was formed.
IMTMAL	$C_{29}H_{36}N_4^{3+}.3C_4H_3O_4^-$	2.31	7.05	Water 20 ml, 80°C	-	No crystals produced even at -20°C. Evaporated slowly, but a gum was formed.

Table 7.1 Preparation of Salts and Modifications of IM

Compound	Stoichiometry	Base (mmole)	Acid (mmole)	Solvent	% Yield	Comments
Triprotonated						
IMTMES	$C_{29}H_{36}N_4^{3+}.3CH_3SO_3^-$	2.29	6.84	Water 20 ml, 80°C	-	No crystals produced even at -20°C. Evaporated slowly, but a gum was formed.
IMTSUC	$C_{29}H_{36}N_4^{3+}.3C_4H_5O_4^-$	2.29	6.93	Water 20 ml, 80°C	48.6	Trituration of the gum with acetone and standing produced excellent crystals. All were twinned.
IMSFUM	$C_{29}H_{36}N_4^{3+}.1.5C_4H_3O_4^-$	2.77	9.47	Tetrahydrofuran/Water (50/50 v/v) 10 ml, 60°C	83.4	Poor quality crystals.

Table 7.2 Characterisation of Salts and Modifications of IM

Compound	MP (°C)	Elemental Analysis Calc[d].	Elemental Analysis Found	Base Equivalence Factor Calc[d].	Base Equivalence Factor Found	KF Water Content Calc[d].	KF Water Content Found	Comments
Modification								
IMFBA	236.1-238.4	C 79.78 H 7.39 N 12.83	C 80.08 H 7.44 N 12.83	100.0	99.8	0	-	NMR, IR and DSC used to confirm the structure.
IMFBB	186.4-188.6	C 79.78 H 7.39 N 12.83	C 79.77 H 7.44 N 12.79	100.0	98.7	0	2.3	NMR, IR and DSC used to confirm the structure.
IMFBC	219.1-220.4	C 79.78 H 7.39 N 12.83	C 80.42 H 7.63 N 12.98	100.0	99.3	0	-	IR and DSC used to confirm the structure.
IMFBTOL	201.8-204.2	C 81.78 H 7.62 N 10.60	C 81.94 H 7.94 N 10.86	82.6	81.8	0	-	IR, DSC and crystal structure determination used to confirm the structure.
Monoprotonated								
IMMHCLHY	175.0-177.8	C 70.92 H 7.18 N 11.41	C 71.41 H 6.98 N 11.46	88.9	88.1	3.67	3.72	NMR and IR used to confirm the structure.

Table 7.2 Characterisation of Salts and Modifications of IM

Compound	MP (°C)	Elemental Analysis Calc[d].	Elemental Analysis Found	Base Equivalence Factor Calc[d].	Base Equivalence Factor Found	KF Water Content Calc[d].	KF Water Content Found	Comments
Monoprotonated								
IMMHCLAC	-	C 72.36 H 7.40 N 10.55	C 72.45 H 7.58 N 10.48	82.2	81.8	0	-	NMR, IR and crystal structure determination used to confirm the structure.
IMMMES	203.0-204.0	C 67.39 H 6.79 N 10.48	C 67.42 H 6.80 N 11.14	81.6	80.9	0	0.2	IR and crystal structure determination used to confirm the structure.
Diprotonated								
IMDHCL	201.5-204.0	-	-	85.6	80.6	0	0.1	NMR and IR used to confirm the structure as the trichloride (IMTHCL) and not IMDHCL.
IMDACE	-	C 71.20 H 7.24 N 10.06	C 80.04 H 7.47 N 12.84	78.4	98.9	0	1.9	NMR and IR used to confirm the structure as the Free Base (IMFB) and not IMDACE.
Triprotonated								
IMTHCLHYA	188.1-190.9	C 61.76 H 6.61 N 9.93	C 61.97 H 6.58 N 10.16	77.4	77.8	3.2	3.0	NMR, IR and crystal structure determination used to confirm the structure.

Table 7.2 Characterisation of Salts and Modifications of IM

Compound	MP (°C)	Elemental Analysis Calc[d].	Elemental Analysis Found	Base Equivalence Factor Calc[d].	Base Equivalence Factor Found	KF Water Content Calc[d].	KF Water Content Found	Comments
Triprotonated								
IMTHCLHYB	-	-		-		-		Crystal structure determination used to confirm the structure. Not enough material isolated for additional characterisation.
IMTHCLHYC	189.8-191.8	C 54.76 H 7.13 N 8.81	C 55.06 H 7.19 N 8.98	68.6	69.3	14.2	13.7	Crystal structure determination used to confirm the structure.
IMTHCLHYD	-	-		-		-		Crystal structure determination used to confirm the structure. Not enough material isolated for additional characterisation.
IMTHCLHYE	209.7-210.8	C 54.76 H 7.13 N 8.81	C 54.97 H 7.01 N 8.94	68.6	67.4	14.2	14.8	Crystal structure determination used to confirm structure.
IMSFUM	-	C 68.84 H 6.27 N 9.17	C 69.04 H 6.49 N 9.01	71.5	70.8	0	-	Acidic Equivalence Factor, Calc[d]: 28.5% Found: 29.8%

SECTION 8 : PHYSICOCHEMICAL INVESTIGATIONS INTO SALTS AND MODIFICATIONS OF IM

8.1 Hygroscopicity/Efflorescence Studies on Salts and Modifications of IM

All modifications of the free base were non-hygroscopic under all humidity conditions studied. The data are summarised in Figures 8.1.1 to 8.1.3.

The two polymorphic phases of the free base studied (IMFBA and IMFBB), both exhibited Type I adsorption[1,2] characteristics and the typically closed hysteresis loop for the moisture adsorption-desorption isotherms. The metastable IMFBB adsorbs about 4 times the level of water compared to the stable IMFBA. The data are summarised in Figure 8.1.10.

In contrast, the toluene solvate (IMFBTOL) exhibited Type II adsorption characteristics, with a negative inflection point and a closed hysteresis loop for the moisture adsorption-desorption isotherms.

All of the chloride salts were hygroscopic. IMMHCLHY, rapidly adsorbs water under all humidity conditions and achieves equilibrium moisture levels after about 24 hours (Figure 8.1.4). At ambient and elevated relative humidities the salt is hygroscopic and only when stored at 20% relative humidity is the water uptake < 5% w/w. IMMHCLHY exhibits Type II adsorption characteristics and the atypical open hysteresis loop for moisture adsorption-desorption isotherms (Figure 8.1.11).

The trichloride salts (IMTHCLHYA, IMTHCLHYC and IMTHCLHYE) were all extensively hygroscopic at ambient and elevated relative humidities (Figures 8.1.7-8.1.9). The monohydrated IMTHCLHYA was the least hygroscopic, equilibrating to 11.45% w/w (≡ 3.59 moles water) and the pentahydrated IMTHCLHYC was the most hygroscopic, equilibrating to 20.66% w/w (≡ 7.30 moles water).

However, even at these elevated levels of water uptake, there was no indication of deliquescent behaviour.

Both IMTHCLHYA and IMTHCLHYC exhibited Type II behaviour (Figure 8.1.12). All three phases, in common with the monoprotonated chloride salt, exhibited the atypical open hysteresis loop for the moisture adsorption-desorption isotherms.

The remaining mesylate (IMMMES) and fumarate (IMSFUM) salts were non-hygroscopic (Figures 8.1.5 and 8.1.6) under all humidity conditions studied. Both salts exhibited Type II adsorption and the typical closed hysteresis loops for moisture adsorption-desorption (Figure 8.1.11).

Figure 8.1.1 Hygroscopicity/Efflorescence Studies on IMFBA

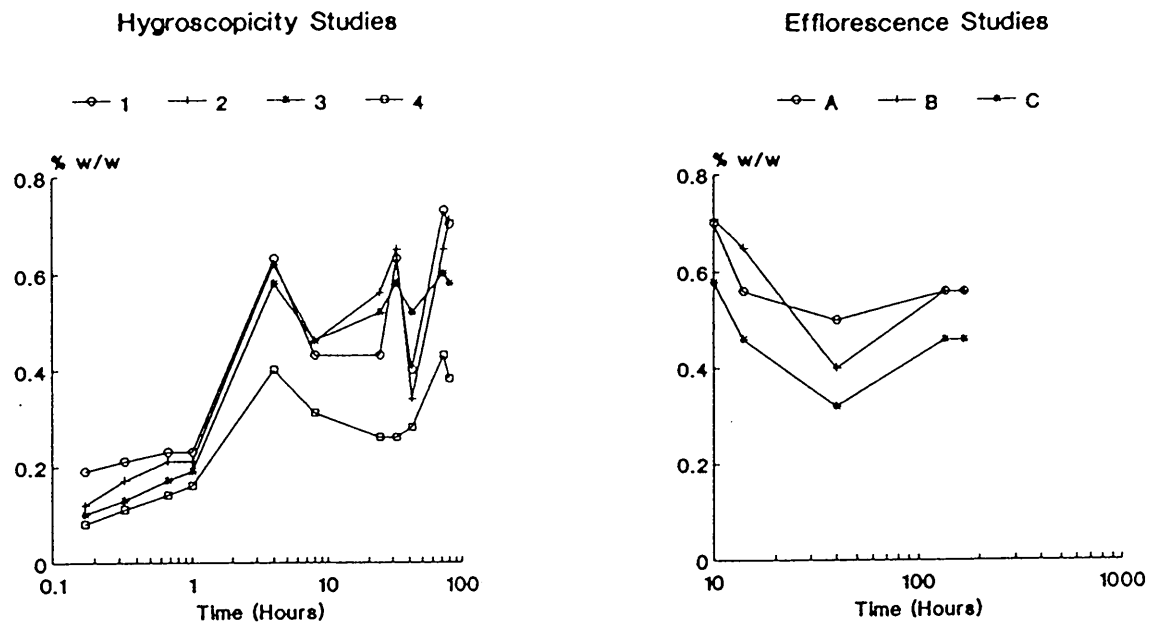

Identifier	Condition
1	87% RH
2	75% RH
3	52% RH
4	20% RH

Identifier	Condition
A	87% RH - 75% RH
B	75% RH - 52% RH
C	52% RH - 20% RH

Figure 8.1.2 Hygroscopicity/Efflorescence Studies on IMFBB

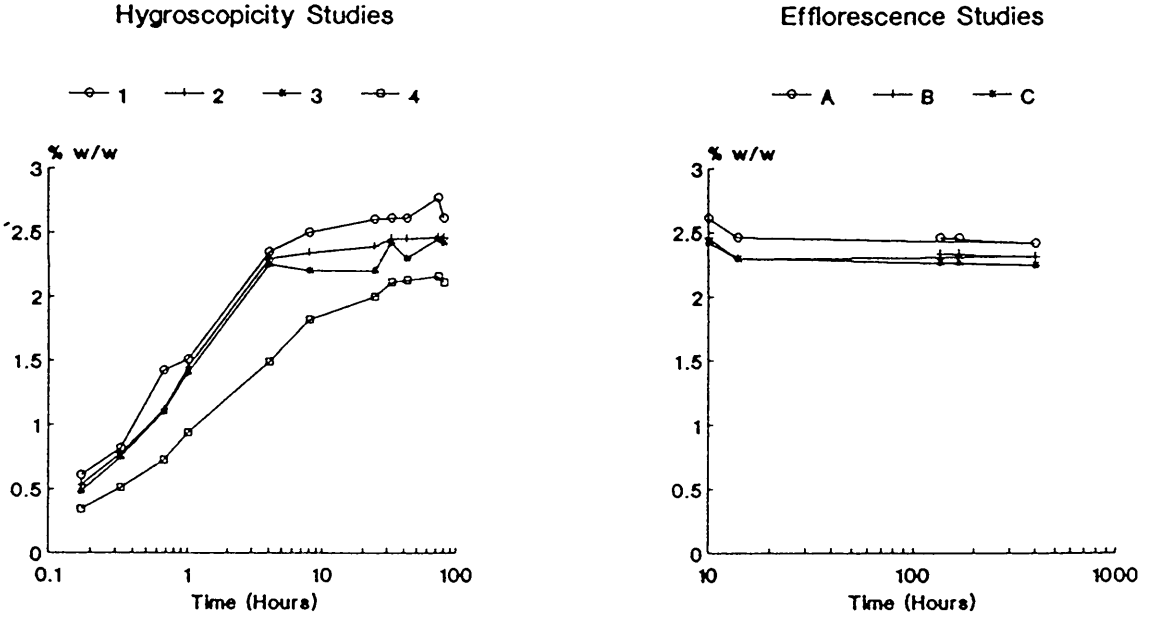

Identifier	Condition
1	87% RH
2	75% RH
3	52% RH
4	20% RH

Identifier	Condition
A	87% RH - 75% RH
B	75% RH - 52% RH
C	52% RH - 20% RH

Figure 8.1.3 Hygroscopicity/Efflorescence Studies on IMFBTOL

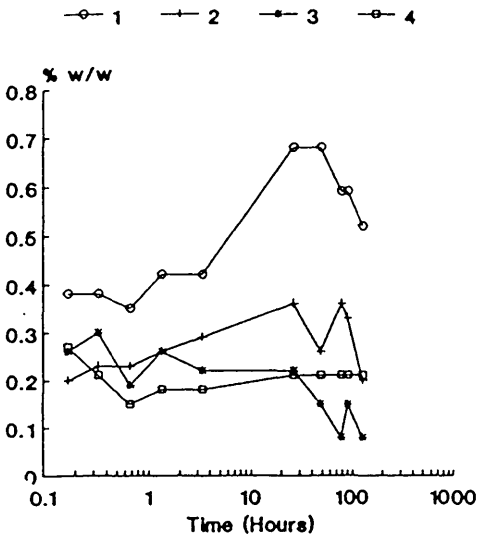

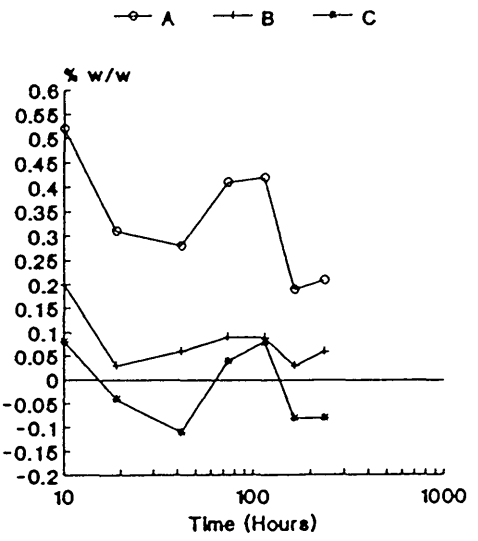

Identifier	Condition
1	87% RH
2	75% RH
3	52% RH
4	20% RH

Identifier	Condition
A	87% RH - 75% RH
B	75% RH - 52% RH
C	52% RH - 20% RH

Figure 8.1.4 Hygroscopicity/Efflorescence Studies on IMMHCLHY

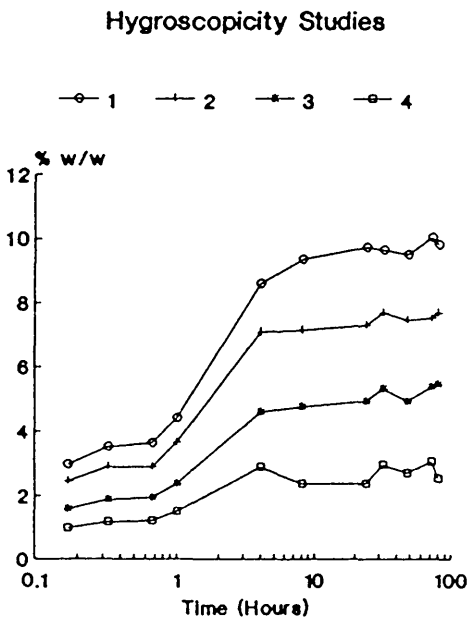

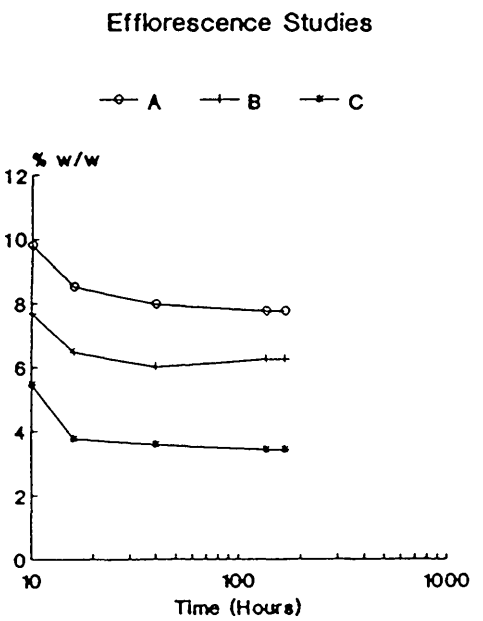

Identifier	Condition
1	87% RH
2	75% RH
3	52% RH
4	20% RH

Identifier	Condition
A	87% RH - 75% RH
B	75% RH - 52% RH
C	52% RH - 20% RH

Figure 8.1.5 Hygroscopicity/Efflorescence Studies on IMMMES

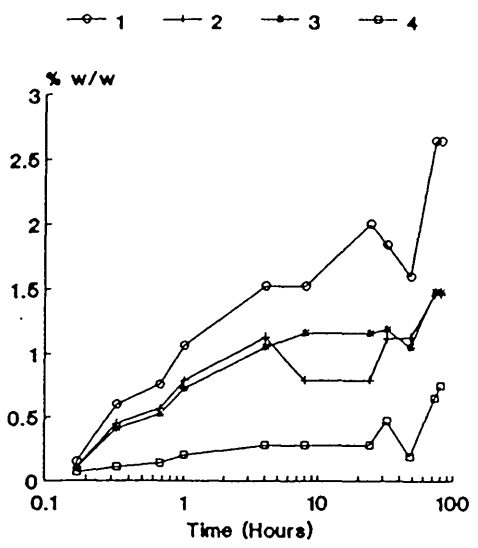

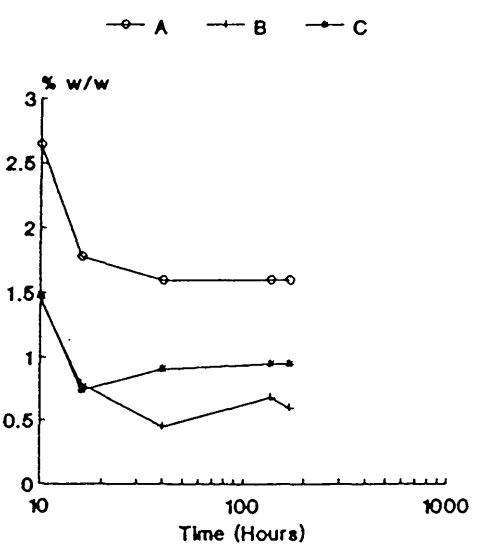

Identifier	Condition
1	87% RH
2	75% RH
3	52% RH
4	20% RH

Identifier	Condition
A	87% RH - 75% RH
B	75% RH - 52% RH
C	52% RH - 20% RH

Figure 8.1.6 Hygroscopicity/Efflorescence Studies on IMSFUM

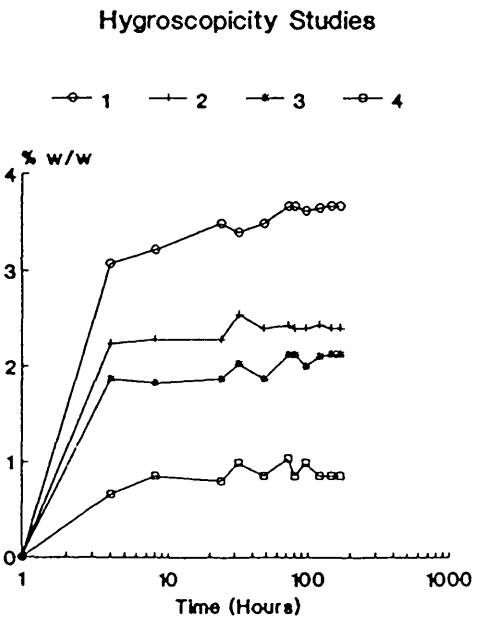

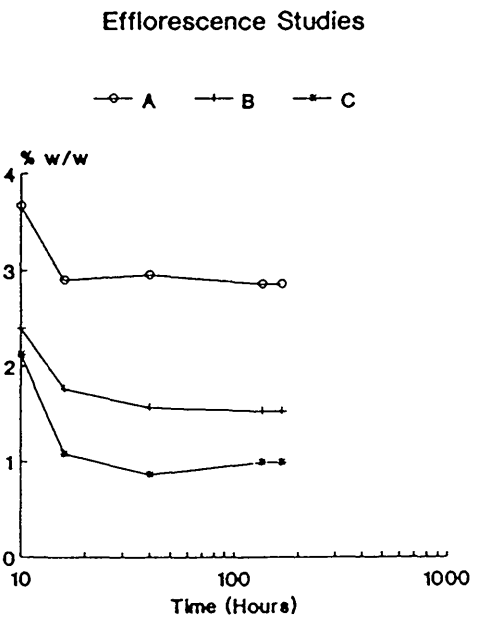

Identifier	Condition
1	87% RH
2	75% RH
3	52% RH
4	20% RH

Identifier	Condition
A	87% RH - 75% RH
B	75% RH - 52% RH
C	52% RH - 20% RH

Figure 8.1.7 Hygroscopicity/Efflorescence Studies on IMTHCLHYA

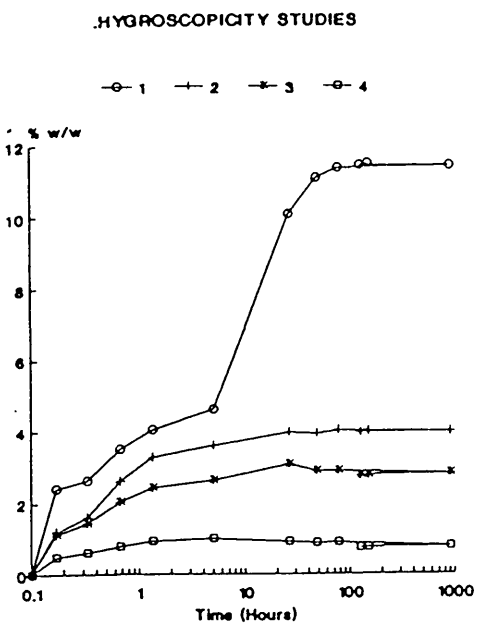

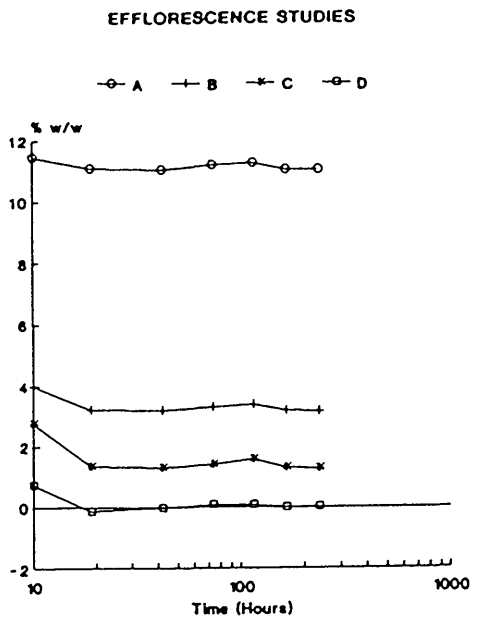

Identifier	Condition
1	87% RH
2	75% RH
3	52% RH
4	20% RH

Identifier	Condition
A	87% RH - 75% RH
B	75% RH - 52% RH
C	52% RH - 20% RH
D	20% RH - 0% RH

Figure 8.1.8 Hygroscopicity/Efflorescence Studies on IMTHCLHYC

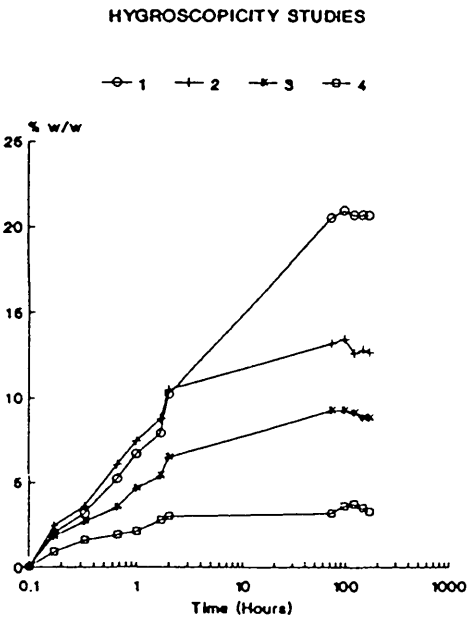

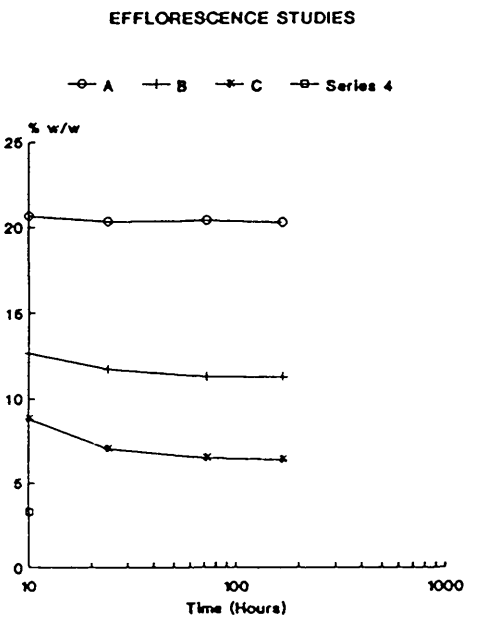

Identifier	Condition
1	87% RH
2	75% RH
3	52% RH
4	20% RH

Identifier	Condition
A	87% RH - 75% RH
B	75% RH - 52% RH
C	52% RH - 20% RH

Figure 8.1.9 Hygroscopicity/Efflorescence Studies on IMTHCLHYE

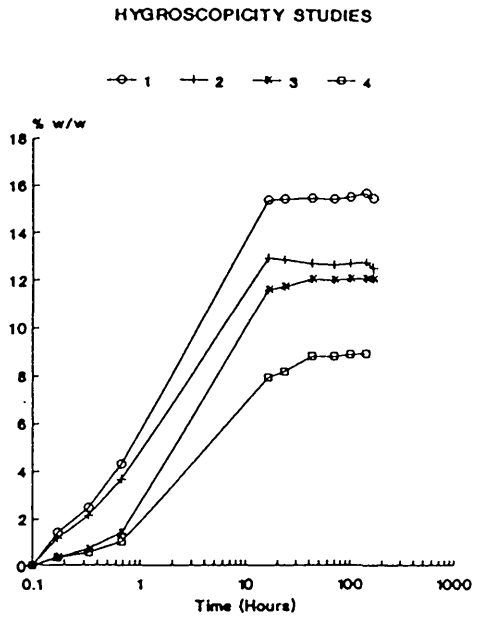

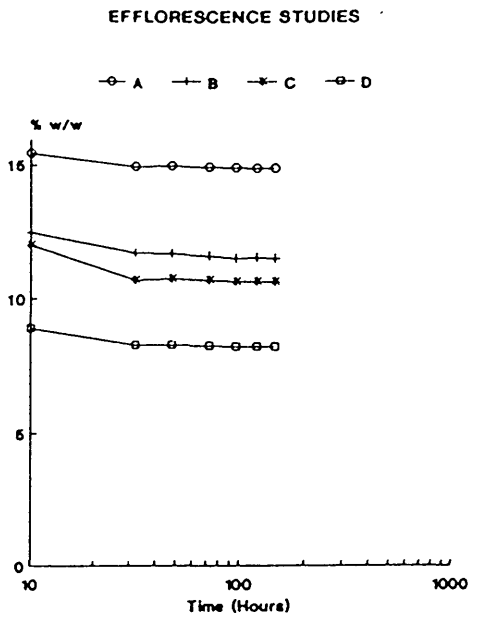

Identifier	Condition
1	87% RH
2	75% RH
3	52% RH
4	20% RH

Identifier	Condition
A	87% RH - 75% RH
B	75% RH - 52% RH
C	52% RH - 20% RH
D	20% RH - 0% RH

Figure 8.1.10 Adsorption/Desorption Isotherms of Modifications of IM

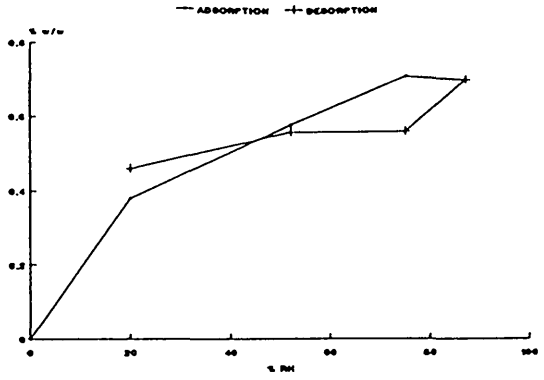

IMFBA

	HYGROSCOPICITY				EFFLORESCENCE		
	87%RH	75%RH	52%RH	20%RH	75%RH	52%RH	20%RH
% w/w	0.70	0.71	0.58	0.36	0.56	0.56	0.46
Moles $\frac{1}{2}$H O	0.17	0.17	0.14	0.09	0.14	0.14	0.11

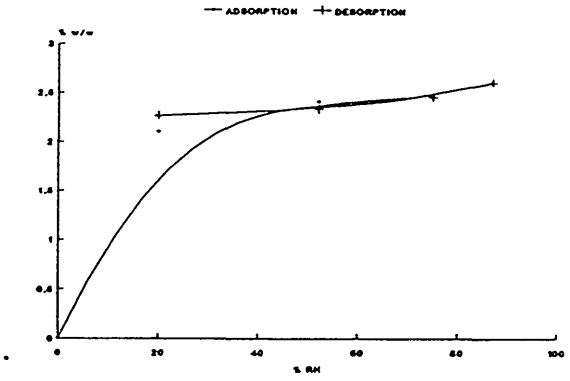

IMFBB

	HYGROSCOPICITY				EFFLORESCENCE		
	87%RH	75%RH	52%RH	20%RH	75%RH	52%RH	20%RH
% w/w	2.61	2.46	2.42	2.11	2.46	2.34	2.27
Moles $\frac{1}{2}$H O	0.63	0.60	0.59	0.51	0.60	0.57	0.55

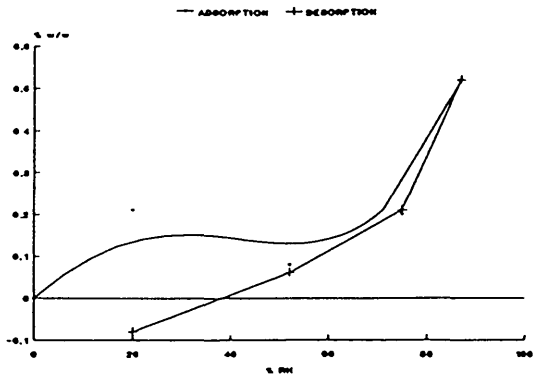

IMFBTOL

	HYGROSCOPICITY				EFFLORESCENCE		
	87%RH	75%RH	52%RH	20%RH	75%RH	52%RH	20%RH
% w/w	0.52	0.20	0.08	0.21	0.21	0.06	-0.06
Moles $\frac{1}{2}$H O	0.15	0.06	0.02	0.06	0.06	0.02	0.00

Figure 8.1.11 Adsorption/Desorption Isotherms of Salts of IM

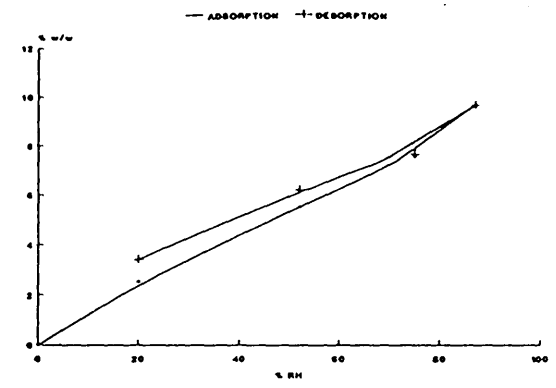

IMMHCLHY

	HYGROSCOPICITY				EFFLORESCENCE		
	87%RH	75%RH	52%RH	20%RH	75%RH	52%RH	20%RH
% w/w	9.80	7.68	5.56	2.54	7.75	6.25	3.43
Moles $\frac{1}{2}$H O	2.67	2.10	1.52	0.69	2.11	1.70	0.93

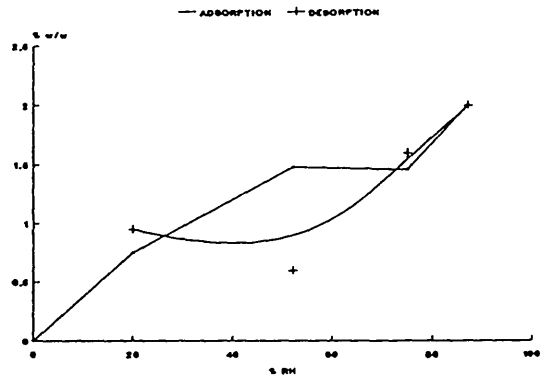

IMMMES

	HYGROSCOPICITY				EFFLORESCENCE		
	87%RH	75%RH	52%RH	20%RH	75%RH	52%RH	20%RH
% w/w	2.00	1.46	1.46	0.75	1.60	0.60	0.95
Moles $\frac{1}{2}$H O	0.59	0.43	0.44	0.22	0.47	0.18	0.28

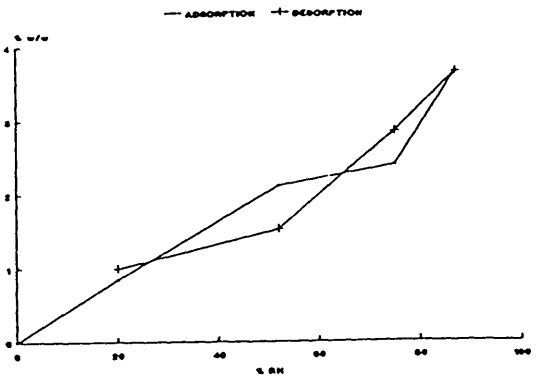

IMSFUM

	HYGROSCOPICITY				EFFLORESCENCE		
	87%RH	75%RH	52%RH	20%RH	75%RH	52%RH	20%RH
% w/w	3.67	2.40	2.12	0.86	2.86	1.53	1.00
Moles $\frac{1}{2}$H O	1.25	0.81	0.72	0.29	0.97	0.52	0.34

Figure 8.1.12 Adsorption/Desorption Isotherms of Salts of IM

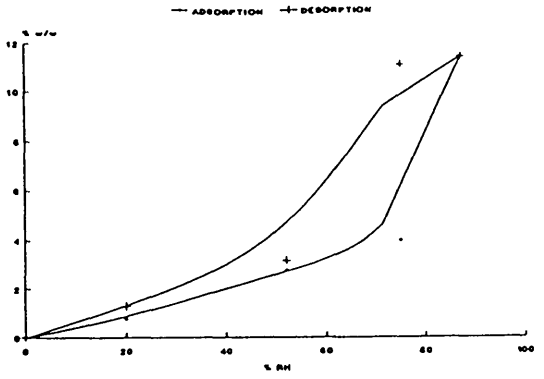

IMTHCLHYA

	HYGROSCOPICITY				EFFLORESCENCE		
	87%RH	75%RH	52%RH	20%RH	75%RH	52%RH	20%RH
% w/w	11.45	3.98	2.76	0.74	11.07	3.17	1.28
Moles $\frac{1}{2}$H O	3.59	1.25	0.86	0.23	3.47	0.99	0.40

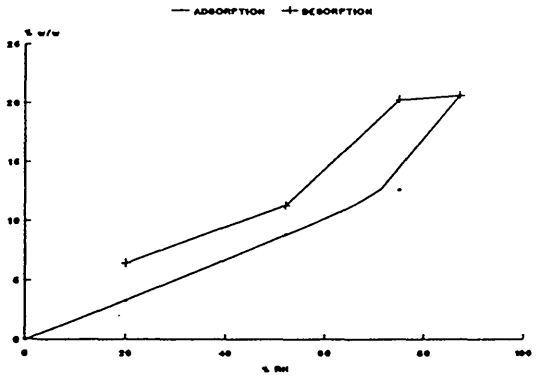

IMTHCLHYC

	HYGROSCOPICITY				EFFLORESCENCE		
	87%RH	75%RH	52%RH	20%RH	75%RH	52%RH	20%RH
% w/w	20.66	12.66	6.82	3.26	20.31	11.29	6.43
Moles $\frac{1}{2}$H O	7.30	4.47	3.12	1.15	7.18	3.99	2.27

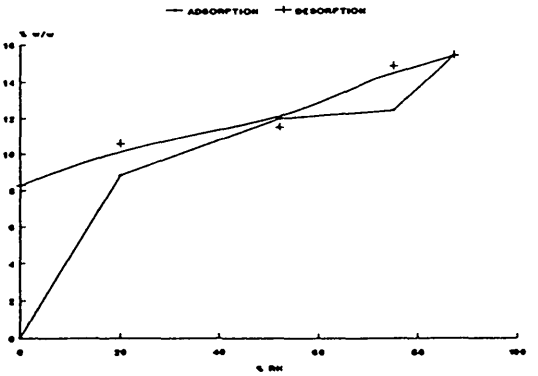

IMTHCLHYE

	HYGROSCOPICITY				EFFLORESCENCE		
	87%RH	75%RH	52%RH	20%RH	75%RH	52%RH	20%RH
% w/w	15.44	12.48	12.01	8.91	14.87	11.52	10.65
Moles $\frac{1}{2}$H O	5.46	4.41	4.24	3.15	5.25	4.07	3.76

8.2 Stability Studies on Salts and Modifications of IM

8.2.1 Appearance of Stability Samples for Salts and Modifications of IM

As with the stability samples of GU (see Section 4.2.1), considerable changes in appearance and especially colour, were observed throughout the course of these studies. These findings are summarised in Table 8.2.1. Although subjective in nature, the appearance of the samples are classified into various categories and intensities of colour, descriptive notes relating to textural changes, such as aggregation and melting are also included, if appropriate.

Table 8.2.1 Appearance of Stability Samples for Salts and Modifications of IM

Salt/ Modification	Condition (Appearance)							
	25°C	40°C	50°C	70°C	100°C	RH	Lt	Hv
IMFBA	NC	F(2)	F(3)	F(4)	O(4)	NC	Y(4)	O(4)
IMFBB	NC	F(1)	F(2)	F(3)	O(3)	NC	Y(3)	O(3)
IMFBC	NC	NC	F(1)	F(2)	O(2)	NC	Y(2)	O(3)
IMFBTOL	NC	NC	F(1)	F(2)	M,O(5)	NC	Y(1)	Y(4)
IMMHCLHY	NC	NC	NC	F(1)	O(5)	A,F(1)	Y(2)	O(4)
IMMMES	NC	NC	NC	F(1)	O(4)	NC	Y(4)	O(4)
IMTHCLHYA	NC	NC	NC	NC	Y(2)	A,NC	NC	Y(4)
IMTHCLHYC	NC	Y(1)	Y(2)	Y(4)	M,O(5)	A,NC	Y(5)	O(4)
IMTHCLHYE	NC	NC	NC	Y(1)	Y(3)	A,NC	NC	Y(4)

NC - No change in colour
A - Aggregated
M - Melted
F - Fawn
Y - Yellow
O - Orange

Intensity of colour is given in brackets, with 5 being the most intense and 1, the least intense.

8.2.2 Kinetic Modelling of Stability Data

Samples that showed appreciable levels of decomposition were analysed using the six solid-state kinetic models, previously described in Section 4.2.2. Linear regression analyses, using least-squares fit, were performed and the data are summarised in Table 8.2.2.

Table 8.2.2 Linear Regression Analyses (R^2) of the Kinetic Data for the Various Kinetic Models Studied

		Linear Regression Analysis (R^2)					
		Topochemical			Nucleation	Diffusion	
Salt/ Modification	Condition	1D	2D	3D	PT	1D	3D
IMFBA	100	0.921	0.896	0.887	0.886	0.958	0.901
	Hv	0.948	0.915	0.901	0.867	0.989	0.921
	Lt	0.884	0.807	0.779	0.721	0.967	0.816
IMFBB	100	0.993	0.956	0.940	0.889	0.978	0.966
	Hv	0.976	0.926	0.901	0.841	0.968	0.938
	Lt	0.760	0.752	0.734	0.680	0.680	0.754
IMFBC	100	-	0.991	0.985	0.963	0.928	0.992
	Hv	0.998	0.976	0.958	0.896	0.949	0.982
	Lt	0.873	0.843	0.793	0.784	0.700	0.871
IMFBTOL	100	0.921	0.934	0.823	0.848	0.800	0.954
	Hv	0.741	0.662	0.635	0.584	0.833	0.671
IMMHCLHY	100	0.997	0.953	0.916	0.795	0.967	0.964
	Hv	0.920	0.571	0.380	0.591	0.914	0.653
	Lt	0.975	0.780	0.605	0.758	0.923	0.936
IMMMES	Hv	0.957	0.615	0.425	0.910	0.922	0.713
IMTHCLHYA	Hv	0.893	0.541	0.736	0.647	0.980	-
IMTHCLHYC	100	0.921	0.906	0.897	0.872	0.910	0.910
	Hv	0.837	0.815	0.807	0.790	0.873	0.819
IMTHCLHYE	Hv	0.655	0.721	0.664	0.467	0.852	0.875

All samples stored at 25°C to 50°C and at elevated humidities, demonstrated excellent stability after 24 weeks storage, with no loss in potency or degradation observed. This demonstrates that slight changes in colour are not always accompanied by chemical decomposition.

At elevated temperatures, the four different phases of IM free base gave quite different stability profiles. These data are summarised in Figures 8.2.1 to 8.2.4. At 70°C, IMFBB and IMFBTOL gave quantitative recoveries, whilst IMFBA and IMFBC gave slight drops in potency, 96.2% and 97.0% label, respectively. These drops in potency were accompanied by quite complex degradation profiles. For IMFBA, there were several very polar degradation products eluting on the solvent front and four partially retained degradation products at RRt 0.45 (1.41%), RRt 0.51 (0.91%), RRt 0.64 (1.47%) and RRt 0.79 (0.48%). For IMFBC, there were no non-retained degradation products, three more polar degradation products at RRt 0.53 (1.04%), RRt 0.61 (0.69%) and RRt 0.74 (0.61%). In addition, one less polar degradation product at RRt 1.20 (0.1%) was observed.

At 100°C, IMFBB and IMFBC have half-lives of about 24 weeks and similar kinetic profiles. Both phases gave good correlation coefficients for all of the models studied (Table 8.2.2) and similar degradation profiles (Table 8.2.3).

IMFBA and IMFBTOL showed markedly different degradation profiles from one another and from the other phases. IMFBA has a half-life of about 10 weeks; after this stage there is a marked change in the reaction rate. This could be indicative of a phase change, but the level of decomposition in the sample precluded any investigations. The data gave good fits for both of

the diffusion models and for the 1D advancement of a phase boundary (zero order kinetics).

IMFBTOL has a half-life of about 16 weeks and at the completion of the studies at 24 weeks, had a similar potency (6.0%) to that of IMFBA (9.4%). Despite the fact that IMFBTOL melts at a considerably higher temperature than the storage temperature of 100°C, the sample had, in fact, partially melted. The DSC heating curve (Figure 8.3.4) gives no indication of a desolvation endotherm at about 100°C, however, crimping of the DSC pan often leads to these endotherms either being masked or occurring at very much higher temperatures. Loss of solvent followed by partial melting would seem to be a logical explanation and is substantiated by the high correlation coefficient for the 3D diffusion model, which gave the best fit of all of the models studied.

A comparison of the degradation profiles at or about the half-life, shows, in all cases, a very complex pattern which is summarised in Table 8.2.3.

It is interesting to note that the relative chemical stabilities at 100°C: IMFBB = IMFBC > IMFBA > IMFBTOL are not the same as the thermodynamic stabilities (see Section 8.3).

All four phases of IM free base showed evidence of light instability. The most stable phase is IMFBTOL, which is additional evidence for the destabilising role of desolvation. IMFBTOL showed a slight drop in potency to 97.4% label and several more polar degradation products. IMFBB and IMFBC showed similar recoveries of 92.1 and 93.4% label, respectively. None of the kinetic models gave a good correlation for the data. The degradation profiles were, in both cases, very complex and are summarised in Table 8.2.4. The

least stable of the phases was IMFBA which gave a recovery of 83.4% label and again, a very complex degradation profile which was very similar to that of IMFBB. The only kinetic model which gave a high correlation for the data was the 1D diffusion model.

The photolytic instability was even more pronounced when stored under UV light and the comparative stability was in the order IMFBTOL > IMFBC > IMFBA > IMFBB. The stability profile of IMFBB when stored under UV light was very similar to that of the 100°C sample, with a half-life of 24 weeks. As with the 100°C sample, the kinetic data gave a good correlation for all of the kinetic models. The degradation profiles are, however, different, but equally complex. The UV light samples gave a major, less polar degradation product at RRt 1.48 and several non-retained peaks at RRt <0.4 (Table 8.2.5). IMFBA and IMFBC showed similar recoveries with potencies of 60.7 and 63.9% label, respectively and both gave good fits for all of the kinetic models studied. Degradation profiles were similar, although IMFBC showed a higher percentage of less polar degradation products.

The significance of desolvation to salt stability is again demonstrated for the monoprotonated salts. Both IMMHCLHY (175.0-177.8°C) and IMMMES (203.0-204.0°C) have similar melting points, but whereas IMMMES demonstrates excellent thermal stability, IMMHCLHY shows a much reduced shelf-life, with a half-life of about 25 weeks (Figures 8.2.5 and 8.2.6). Dehydration, followed by degradation of the anhydrous phase, appears to be a likely explanation.

IMMMES shows only a small drop in potency (97.9% label) at 100°C accompanied by three more polar degradation products with a total value of 0.8%.

Both the light and UV light samples for IMMMES gave similar degradation profiles, several more polar degradation products were observed in the latter sample, but all were at low levels (≤ 0.2%). The data for the UV light samples gave good correlations for the nucleation, 1D diffusion and 1D phase boundary advancement (zero order) models.

The monochloride salt gave good correlations for the 100°C kinetic data with all models, except the Prout Tompkins nucleation model. This salt showed light instability when stored under window light or UV light and the kinetic profiles were similar, giving highest correlation for either 1D diffusion or 1D phase advancement models. In both cases, there were major degradation products observed at RRt 0.70 and 1.15, in addition to a number of other products at smaller levels. The profiles for thermal and light degradation were very similar.

The various phases of the trichloride were stable when stored between 25°C and 70°C and at high relative humidities (Figures 8.2.7-8.2.9). Despite small colour changes, no degradation was observed in any of these samples.

Storage at 100°C resulted in an apparent increase in potency for the IMTHCLHYA. This occurred after the 4 week timepoint and remains constant at this level for the whole duration of the study. This may be explained by dehydration of the sample (Theory 103.3%, Found 104.7% label) which is accompanied by small levels of degradation (Table 8.2.3).

A similar process occurs for IMTHCLHYE samples which lose one mole of water after 4 weeks. The process of dehydration continues in a gradual fashion until at the end of the study an additional two moles of water have

been removed (Theory 109.9%, Found 110.6%); this is again accompanied by small levels of degradation.

For the IMTHCLHYC samples, the rate of decomposition at 100°C is far in excess of the rate of desolvation. The recovery after the 4 week timepoint decreased to 93.6% of label with evidence of degradation. The 70°C data for IMTHCLHYC does show an increase in potency, commensurate with the loss of one mole of water.

There is an obvious change in the rate of decomposition after 8 weeks, accompanied by a phase change, which manifests itself as partial melting of the sample. This phase change is presumably formation of the anhydrate followed by its immediate melting, IMTHCLHYC has a half-life of 14 weeks at 100°C. Despite the fact that there are two competing reactions taking place simultaneously, the data fit several of the kinetic models satisfactorily, giving the highest correlation for the diffusion models and the 1D phase advancement model. The degradation profile at about the half-life is very complex (Table 8.2.3), with major degradation products at RRt 0.46, 0.60, 0.76 and 0.85.

The trichloride phases show good light stability. Only IMTHCLHYA shows a slight drop in potency (97.6% label) with evidence of three more polar degradation products at RRt 0.42, 0.46 and 0.70.

IMTHCLHYC and IMTHCLHYE samples gave slightly elevated recoveries (100.5 and 102.5% label) which, together, with the presence of several degradation products indicates that partial desolvation is occurring.

The trichloride salts were slightly less stable towards UV light than towards window light. IMTHCLHYA samples show recoveries of 89.1% label with a large number of more polar degradation products.

IMTHCLHYE samples show recoveries of 93.5% label, with a very similar degradation profile, to that observed for IMTHCLHYA. The least photolytically stable phase is IMTHCLHYC with a recovery of 62.5% label. A very complex degradation profile was observed with degradation products eluting at RRt 0.46, 0.51, 0.60 and 0.70, the major degradation product is less polar eluting at RRt 1.15.

The UV light data for the three phases of the trichloride salt, do not fit any of the kinetic models particularly well. The best correlations in all cases are for either the 1 or 3D diffusion models. This is again supporting evidence for the role of the water molecules in stabilising this compound.

IMTHCLHYE samples show recoveries of 93.5% label, with a very similar degradation profile, to that observed for IMTHCLHYA. The least photolytically stable phase is IMTHCLHYC with a recovery of 62.5% label. A very complex degradation profile was observed with degradation products eluting at RRt 0.46, 0.51, 0.60 and 0.70, the major degradation product is less polar eluting at RRt 1.15.

The UV light data for the three phases of the trichloride salt, do not fit any of the kinetic models particularly well. The best correlations in all cases are for either the 1 or 3D diffusion models. This is again supporting evidence for the role of the water molecules in stabilising this compound.

Table 8.2.3 Degradation Profiles for Salts and Modifications of IM at 100°C

Salt/ Modification	Degradation Peaks, RRt (% Area Normalised)														
	NR	More Polar									IM	Less Polar			
	0.40	0.42	0.46	0.51	0.54	0.60	0.65	0.70	0.75	0.85	1.00	1.15	1.32	1.48	2.07
IMFBA[1]	4.5	2.1	1.6		1.2	2.4	5.1		1.0	1.5	61.5	2.4	0.9	1.5	2.1
IMFBB[2]	5.9	2.4	4.0	2.0	1.8	6.6	0.6	3.6	2.4	0.6	48.2	0.6			
IMFBC[2]	2.7	1.4	3.1		2.9	3.3		6.0			50.2	4.3			
IMFBTOL[3]	3.3		1.9	1.5	1.2	5.8		4.4		0.5	53.6	0.1			
IMMHCLHY[4]	16.7	0.2	4.9			4.0		8.6		0.6	46.2	5.9		0.5	
IMMMES[5]	0.5	0.2		0.1							97.9				
IMTHCLHYA[5]	0.7	0.8	1.9								104.7				
IMTHCLHYC[5]	2.9		7.8			1.8		5.7		3.7	61.0				
IMTHCLHYE[5]		0.20	0.4		0.5						110.6		0.1		

Notes: In all cases, degradation profiles were compiled at the timepoint nearest to the half-life. In cases where the half-life was not reached, profiling was determined at the end of the study.

1. $T_{60} \equiv$ 8 weeks 2. $T_{60} \equiv$ 24 weeks 3. $T_{60} \equiv$ 16 weeks 4. $T_{60} \equiv$ 28 weeks 5. end of the study

NR = Not Retained

Table 8.2.4 Degradation Profiles for Salts and Modifications of IM, when Stored under Window Light

Salt/ Modification	Degradation Peaks, RRt (% Area Normalised)														
	NR	More Polar									IM	Less Polar			
	<0.40	0.42	0.46	0.51	0.54	0.60	0.65	0.70	0.75	0.85	1.00	1.15	1.32	1.48	2.07
IMFBA	4.2	0.3	1.5	0.2		0.8			0.2	0.7	85.2			0.1	
IMFBB	3.6	0.4	1.4	0.7		0.3		0.1	0.5	0.5	92.1			0.1	
IMFBC	1.3	0.2	0.2	0.1	0.8	0.1	0.2	0.5		0.1	93.4	0.4			0.1
IMFBTOL	1.9	1.1	0.7								97.4				
IMMHCLHY	4.8	0.1	0.2					1.4	0.5		83.2	4.1			
IMMMES	1.0							0.3	0.1		94.5				
IMTHCLHYA	1.0	0.4	0.5					0.1			97.6				
IMTHCLHYC				0.9		0.6	0.2	0.5	0.2		100.5	2.9			
IMTHCLHYE	1.1		0.3	0.6		0.5					102.6				

Notes: In all cases, degradation profiles were compared at the timepoint nearest to the half-life. In cases where the half-life was not reached, profiling was determined at the end of the study.

NR = Not Retained

Table 8.2.5 Degradation Profiles for Salts and Modifications of IM, when Stored under UV Light

Salt/ Modification	Degradation Peaks. RRt (% Area Normalised) NR	More Polar								IM	Less Polar			
	<0.40	0.42	0.46	0.51	0.54	0.60	0.65	0.70	0.75	0.85	1.00	1.15	1.32	1.48	2.07
IMFBA[1]	13.9	0.7	2.8	0.5			2.0	0.2	2.1	0.3	60.7			0.7	
IMFBB[2]	21.0	1.6	3.6	0.9	0.3		0.5		3.2	0.9	49.6			5.4	
IMFBC[2]	12.1	1.2	1.4	0.8	3.2	0.9	0.6	2.4		0.3	63.9	2.8	0.3		1.9
IMFBTOL[2]	7.6	1.8	1.0				1.0	1.3			78.6				
IMMHCLHY[3]	12.9	0.1	0.1					3.5	0.7		64.2	5.4		0.1	
IMMMES[3]	2.8		0.1	0.2	0.1			0.5	0.1		91.0				
IMTHCLHYA[2]	2.7	0.9	1.6		0.4	0.5		0.9	0.7	0.3	89.1				
IMTHCLHYC[2]	16.6		2.1	4.0		1.9	1.1	2.2		1.1	62.5	6.4	1.0	0.8	
IMTHCLHYE[2]	2.4		0.3		0.9	0.4		0.2	0.2	0.1	93.5		0.6		

Notes: In all cases, degradation profiles were compared at the timepoint nearest to the half-life. In cases where the half-life was not reached, profiling was determined at the end of the study.
1. $T_{50} \equiv 20$ weeks 2. $T_{50} \equiv 24$ weeks 3. $T_{50} \equiv 28$ weeks
NR = Not Retained

Figure 8.2.1 Stability Data for IMFBA

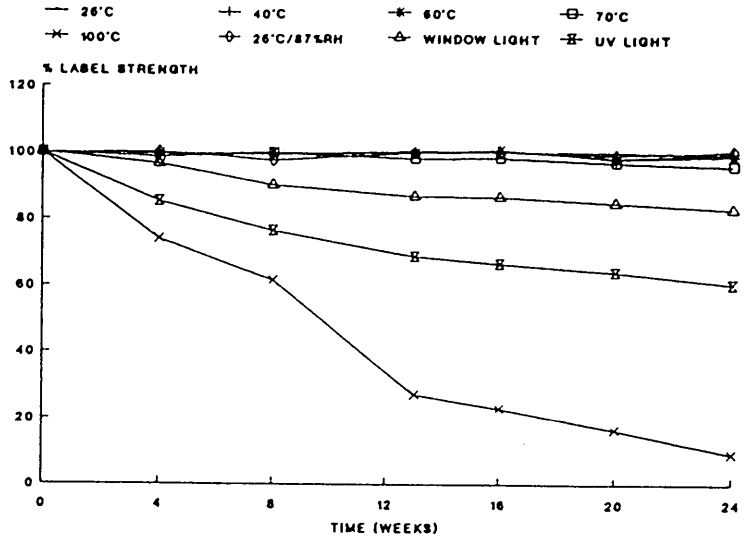

TIMEPOINT	CONDITION (% Label)							
(Weeks)	25	40	50	70	100	RH	Lt	Hν
4	99.8	99.8	99.6	98.6	74.0	100.2	96.4	85.2
8	99.8	99.6	100.2	100.0	61.5	97.8	90.2	76.6
13	100.8	100.4	100.2	98.4	27.1	100.2	87.0	69.0
16	100.4	100.7	101.0	98.6	23.0	100.4	86.9	66.8
20	100.6	98.7	98.6	97.4	16.6	99.8	85.2	64.3
24	100.0	100.2	99.4	96.2	9.4	101.0	83.4	60.7

Figure 8.2.2 Stability Data for IMFBB

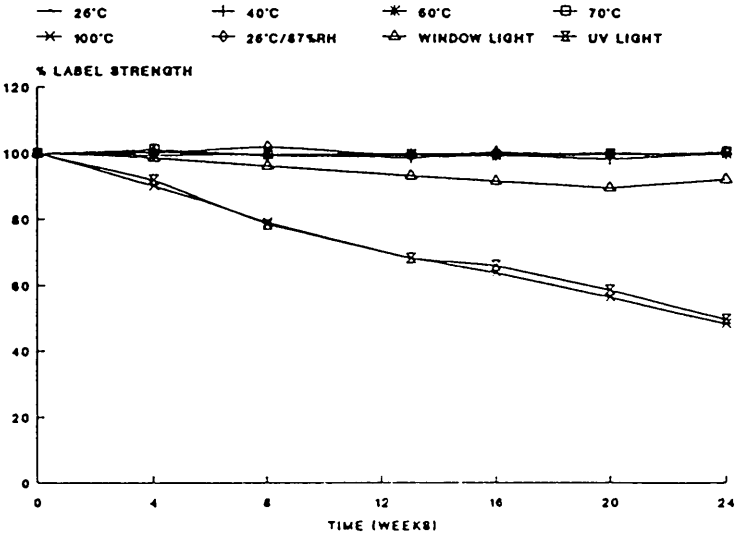

TIMEPOINT	CONDITION (% Label)							
(Weeks)	25	40	50	70	100	RH	Lt	Hν
4	100.2	101.2	99.3	101.2	90.0	100.4	98.6	91.8
8	99.8	99.2	99.6	99.6	79.3	101.9	96.0	78.4
13	99.9	98.6	99.7	99.4	68.2	99.3	93.0	68.2
16	99.7	99.2	99.0	99.4	63.8	100.4	91.4	66.0
20	100.1	98.2	99.6	99.8	56.3	99.6	89.4	58.6
24	99.7	99.7	99.8	100.4	48.2	100.4	92.1	49.6

Figure 8.2.3 Stability Data for IMFBC

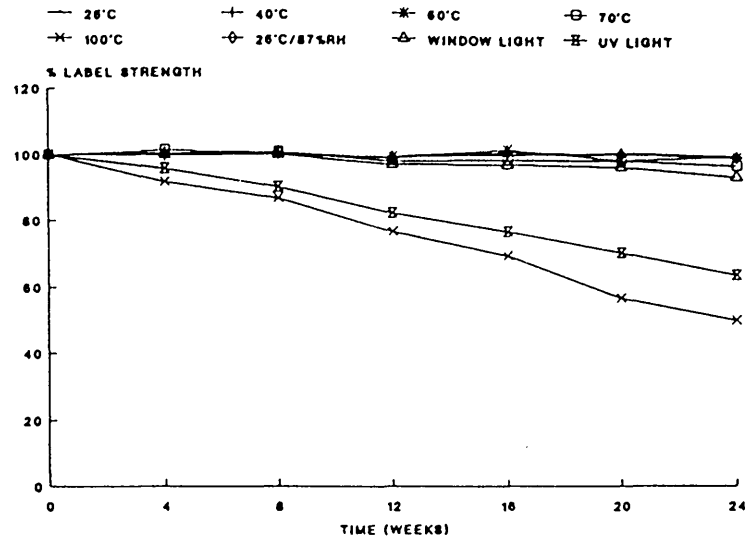

TIMEPOINT	CONDITION (% Label)							
(Weeks)	25	40	50	70	100	RH	Lt	Hυ
4	100.0	99.8	100.4	101.4	91.7	100.4	99.7	95.6
8	99.9	100.4	100.2	101.0	86.8	101.0	99.9	90.3
12	99.6	99.5	99.6	98.2	76.9	99.2	97.2	82.4
16	100.0	99.8	101.6	98.4	69.6	100.7	97.0	76.8
20	101.0	100.4	98.6	98.4	57.0	100.5	96.6	70.5
24	99.9	99.6	99.5	97.0	50.2	99.4	93.4	63.9

Figure 8.2.4 Stability Data for IMFBTOL

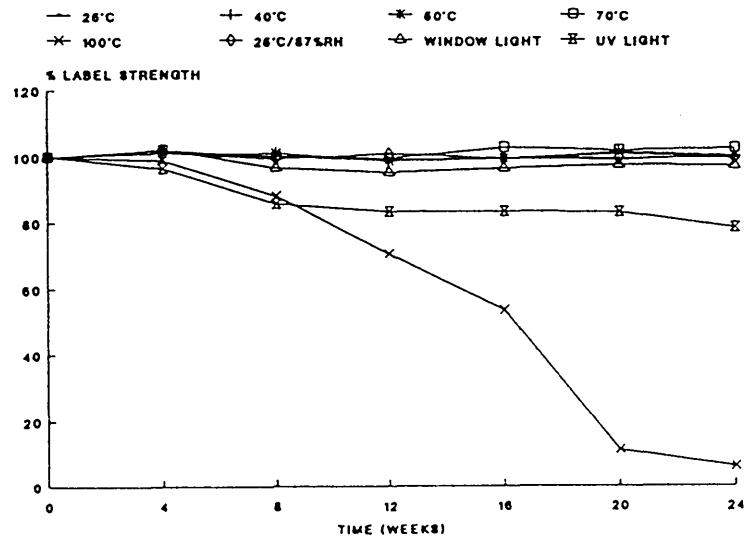

TIMEPOINT	CONDITION (% Label)							
(Weeks)	25	40	50	70	100	RH	Lt	Hυ
4	101.1	101.1	101.2	102.2	99.0	101.2	102.2	96.6
8	100.2	100.2	101.1	100.2	88.2	99.4	96.8	85.8
12	99.1	98.8	98.7	99.6	70.6	100.9	95.2	83.5
16	99.3	99.4	99.4	102.8	53.6	99.6	96.6	83.4
20	98.9	100.7	101.4	102.0	11.2	99.6	97.6	83.3
24	100.2	99.8	100.3	102.6	6.0	99.6	97.4	78.6

Figure 8.2.5 Stability Data for IMMMES

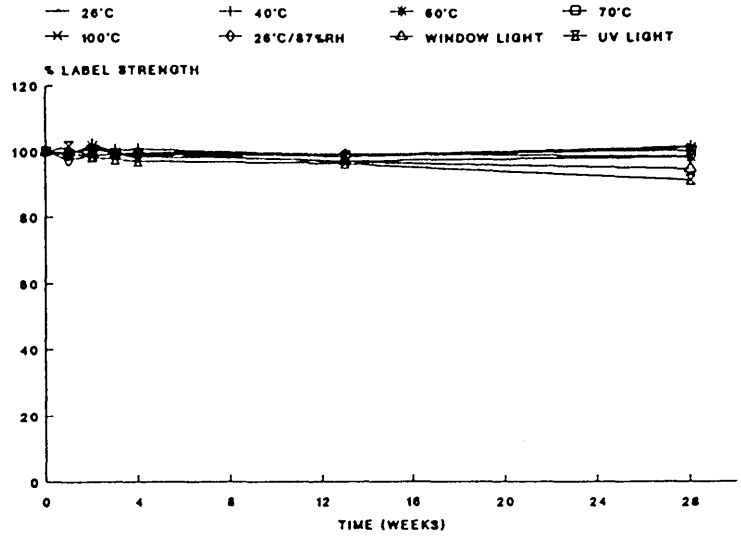

TIMEPOINT	CONDITION (% Label)							
(Weeks)	25	40	50	70	100	RH	Lt	Hυ
1	99.8	99.3	98.8	99.4	99.0	97.4	99.9	101.6
2	101.0	102.2	101.8	100.6	98.7	98.5	99.3	98.2
3	99.5	100.4	99.8	99.4	98.9	99.4	98.8	97.6
4	99.8	100.7	99.4	99.6	98.2	98.5	99.2	97.0
13	99.5	99.2	98.4	99.0	97.4	99.2	97.0	96.2
28	100.0	101.3	101.0	100.0	97.9	98.4	94.5	91.0

Figure 8.2.6 Stability Data for IMMHCLHY

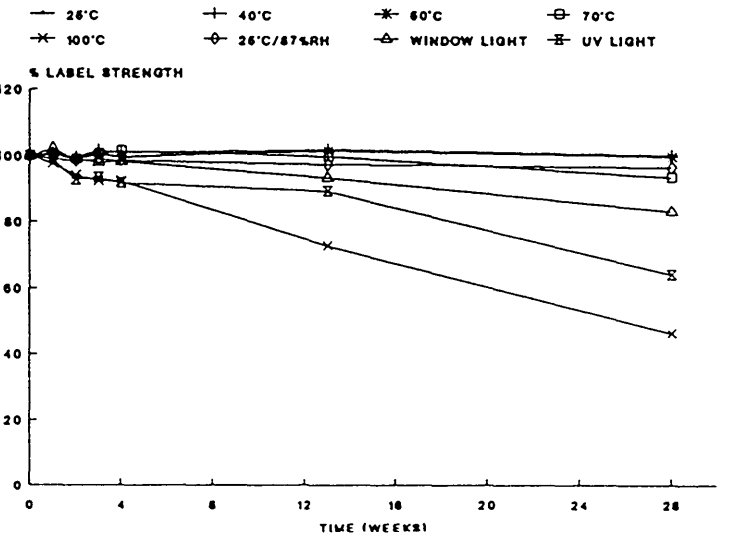

TIMEPOINT	CONDITION (% Label)							
(Weeks)	25	40	50	70	100	RH	Lt	Hυ
1	100.0	100.8	100.4	100.4	97.6	99.0	102.2	99.0
2	99.1	99.6	98.9	99.0	94.1	98.4	98.9	92.7
3	100.2	101.6	100.5	100.6	92.3	98.8	98.0	93.2
4	99.4	101.0	99.6	101.4	92.2	98.5	98.2	91.6
13	102.0	101.9	101.4	99.8	72.7	97.4	93.3	89.2
28	100.0	100.3	99.8	93.4	46.2	96.4	83.2	64.2

Figure 8.2.7 Stability Data for IMTHCLHYA

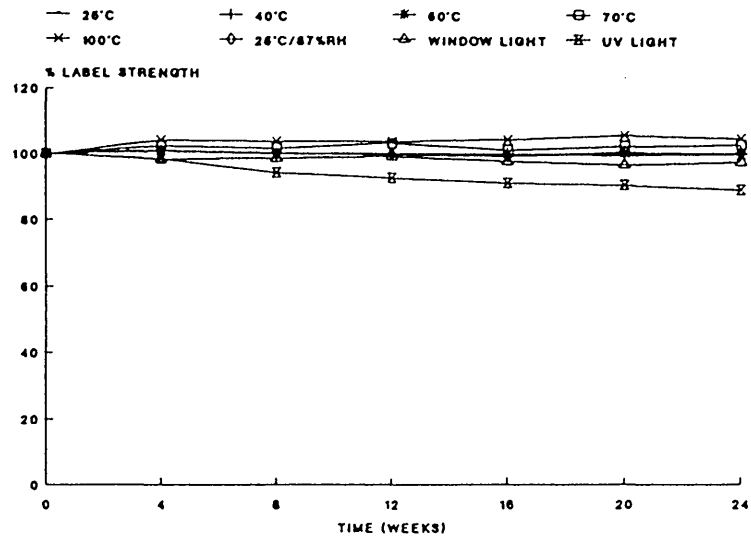

TIMEPOINT	CONDITION (% Label)							
(Weeks)	25	40	50	70	100	RH	Lt	Hν
4	101.0	100.8	100.7	102.4	104.2	101.0	98.4	98.4
8	100.2	100.0	99.9	101.6	103.8	100.0	98.6	94.0
12	99.6	99.9	100.2	103.1	103.8	99.9	99.0	92.5
16	99.0	99.7	99.9	101.0	104.2	99.2	97.5	90.8
20	100.2	99.4	100.0	102.4	105.8	100.7	96.8	90.4
24	100.1	100.3	99.8	102.8	104.7	100.2	97.6	89.1

Figure 8.2.8 Stability Data for IMTHCLHYC

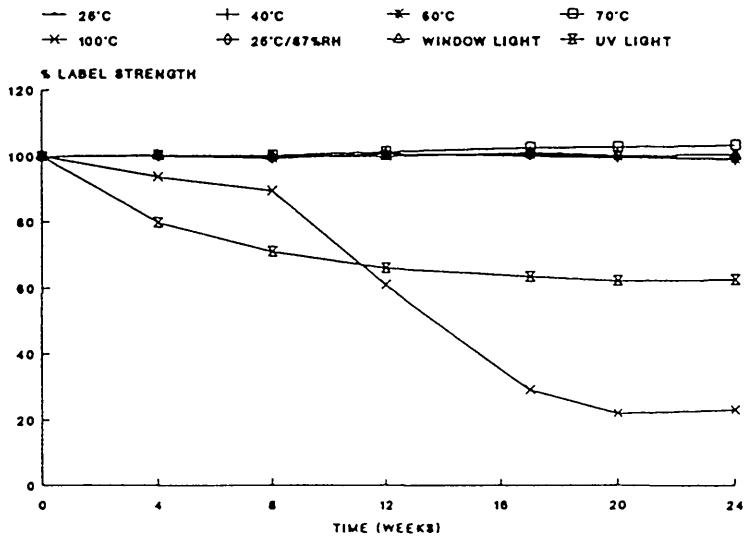

TIMEPOINT	CONDITION (% Label)							
(Weeks)	25	40	50	70	100	RH	Lt	Hν
4	100.4	100.0	100.4	100.3	93.6	100.2	100.0	79.8
8	99.2	99.4	99.4	100.4	89.5	99.6	100.0	70.9
12	100.7	100.6	100.6	101.4	61.0	100.6	99.7	66.0
17	99.8	100.5	100.3	102.6	29.0	100.4	101.1	63.3
20	99.4	99.5	99.8	102.7	22.0	99.9	100.4	62.1
24	99.2	99.0	99.2	103.3	23.0	99.3	100.5	62.5

Figure 8.2.9 Stability Data for IMTHCLHYE

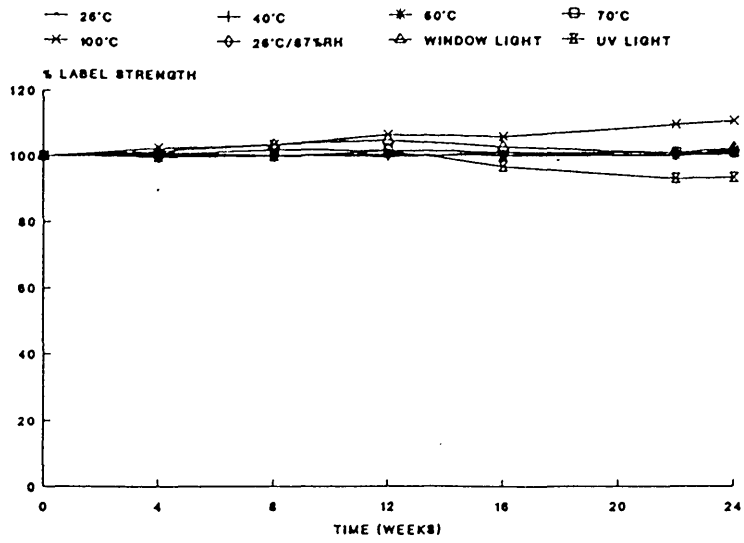

TIMEPOINT	CONDITION (% Label)							
(Weeks)	25	40	50	70	100	RH	Lt	Hv
4	101.0	100.4	99.4	100.6	102.4	99.3	101.4	99.7
8	100.4	100.4	100.2	102.0	103.5	100.0	103.5	100.0
12	99.6	100.0	100.5	101.7	106.4	100.4	104.7	101.6
16	100.8	100.0	99.8	101.0	105.6	99.8	102.5	96.4
22	100.0	100.0	99.9	100.9	109.4	100.1	101.0	93.1
24	100.3	101.9	101.6	100.7	110.6	101.0	102.6	93.5

Figure 8.2.10 Comparison of Thermal Stability (100°C) of Salts and Modifications of IM

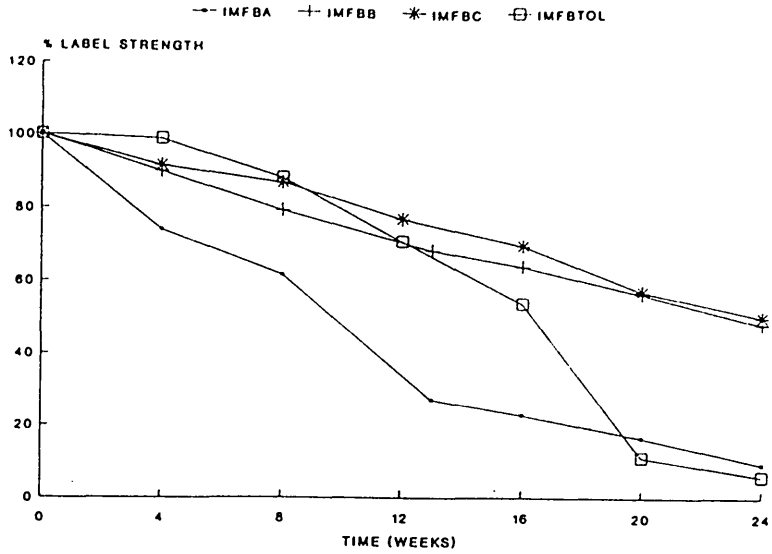

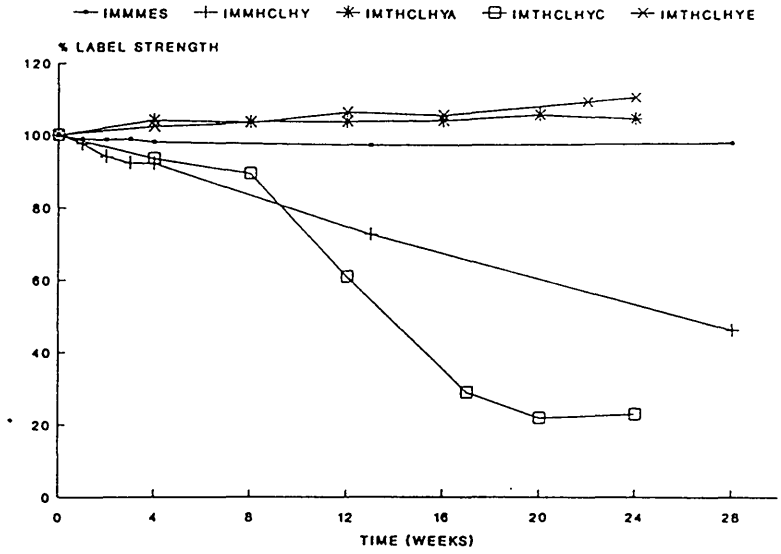

Figure 8.2.11 Comparison of Window Light Stability of Salts and Modifications of IM

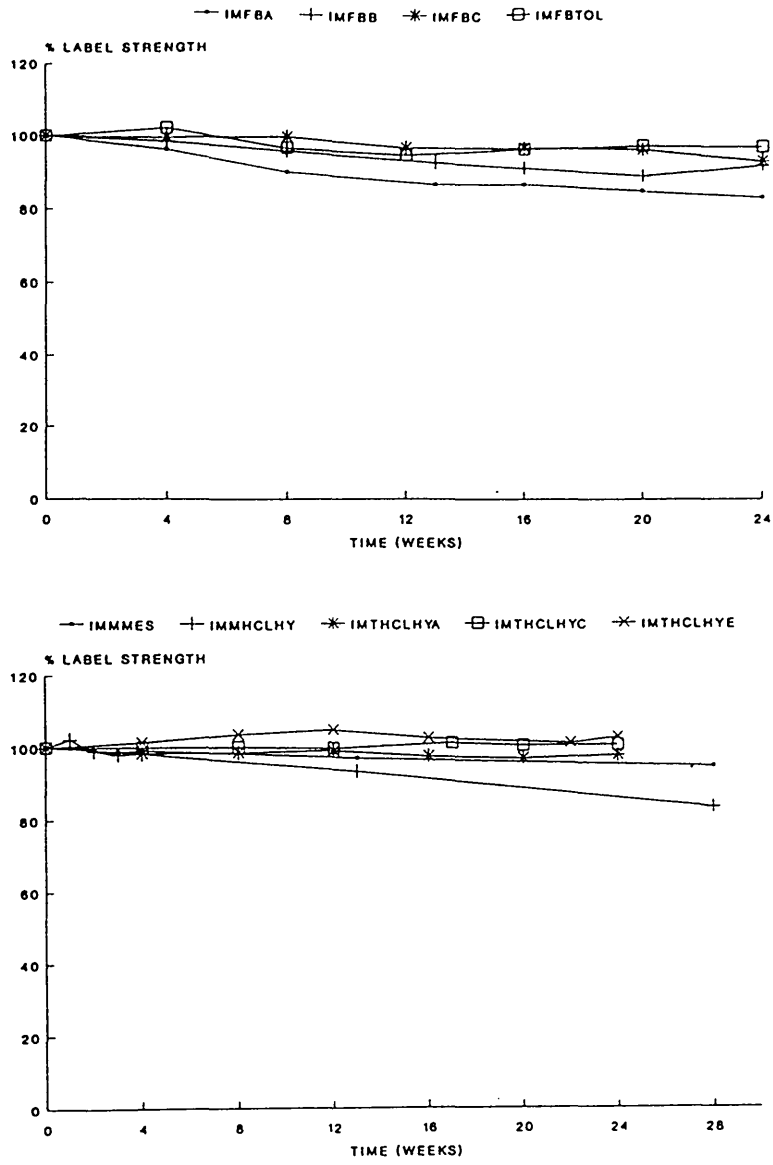

Figure 8.2.12 Comparison of UV Light Stability of Salts and Modifications of IM

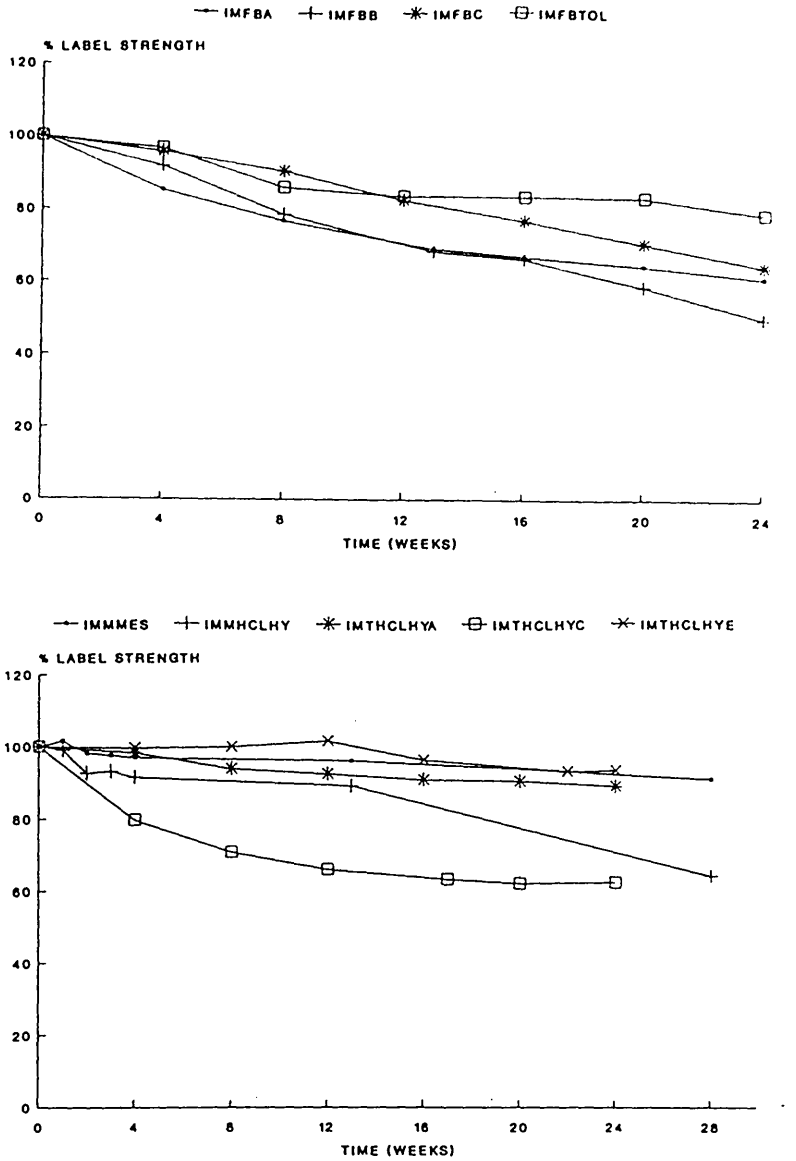

8.3 Van't Hoff Solubility Investigations on Salts and Modifications of IM

The data and Van't Hoff solubility plots are summarised in Figures 8.3.1 to 8.3.3 respectively for the neutral, mono and triprotonated species. Linear regression analyses (using least squares fit) were performed on the data and are summarised together with the heat of solution (ΔH_s) values, in Table 8.3.1.

Table 8.3.1 Summary of Linear Regression and Heat of Solution (ΔH_s) Data for Salts and Modifications of IM

Salts/ Modifications	Linear Regression Analysis			ΔH_s
	R^2	a	b	KJ mol^{-1}
IMFBA	0.974	0.646	-1139.5	9.47
IMFBC	0.967	-0.221	-852.0	7.08
IMMMES	0.995	6.340	-2671.7	22.21
IMTHCLHYC	0.994	-11.064	2532.9	-21.06

a = intercept, b = slope

The free energy change (ΔG_T) associated with the transitions between the various phases of the free base and trichloride salt of IM, were calculated directly from the molar solubility (C_s) measurements at 25°C, via equation (1).

$$\Delta G_T = RT \ln \frac{C_s(A)}{C_s(B)} \quad \ldots\ldots\ldots \quad (1)$$

where R = Universal Gas Constant, T = Absolute Temperature and $C_s(A)$ and $C_s(B)$ are the respective molar solubilities of the two phases A and B.

Aguiar and Zelmer[3], postulated that when the free energy differences between polymorphs or solvates are small then it is unlikely that there will be differences in the bioavailability of the drug as it is probable that the forms will interconvert *in vivo*.

A difference in biological activity between solid oral preparations of their polymorphs was demonstrated for Chloramphenicol palmitate, but not Mefanamic acid. The respective free energy differences are 3.24 and 1.05 $KJ.mol^{-1}$.

Subsequent work[4,5] has tended to confirm the hypothesis of Aguiar and Zelmer.

For the polymorphs and solvates of the free base, the data are summarised in Scheme 1.

Scheme 1 Gibbs Free Energy Differences Between Polymorphs of IMFB ($KJ\ mol^{-1}$) at 25°C in Ethanol

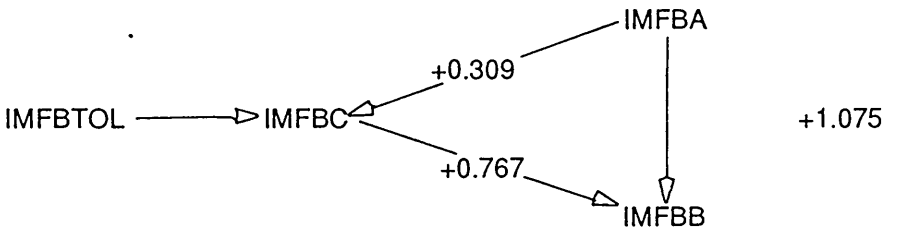

The toluene solvate (IMFBTOL) converted directly into Phase C (IMFBC), following suspension and agitation in ethanol at 4°C and thus could not be directly studied.

The free energy differences at 25°C between Phases A, B and C are minimal, with the largest difference (1.075 $KJ.mol^{-1}$, Phase B to Phase A) being of the same order as found between the various polymorphs of Mefanamic acid. Bioavailability differences between the various polymorphs of IMFB are thus unlikely.

The relative thermodynamic stabilities of the polymorphic forms at 25°C are Form A > C > B, these findings are supported by the DSC data (Figure 2.1.2) which indicates that the metastable Form B converts into the more stable Form A when heated above 188°C.

It should be noted from the Van't Hoff solubility plot (Figure 8.3.1) that at 4°C the relative thermodynamic stabilities are Forms B > A > C. This plot also confirms the metastable nature of Form B, the change in the slope at 25°C being indicative of a phase change into the more stable Form A.

Form A (ΔH_s = 9.47 KJ.mol^{-1}) subsequently converts into the thermodynamically more stable Form C (ΔH_s = 7.08 KJ.mol^{-1}), the transition temperature is about 56°C.

Behme *et al*[6] advocated the classification of polymorphs as monotropic or enantiotropic, as an aid to the understanding of polymorphic systems. For monotropic solids, the higher melting form has the lower free energy at all temperatures and is, therefore, more stable at every temperature. The relative stabilities of enantiotropic solids depends on the temperature of the system relative to the transition temperature.

All three polymorphs of IMFB were characterised as enantiotropic on the basis of Burger and Rambergers[7] heat of transition rule. This rule states in part that if an endothermal transition, resultant upon a solid-solid phase transition, is observed at some temperature, then it may be assumed that there is a transition point below it and that the two forms are related enantiotropically. Endothermic phase transitions were observed for Phases B to A (see Figure 2.1.2) and Phases C to A (see Figure 8.3.4). In addition, the Van't Hoff solubility plot shows a

transition between Phases A and C and Phases B and A.

A very similar polymorphic system to IMFB was described by Behme *et al*[6], in their investigations into the polymorphism of Gepirone Hydrochloride. In an exactly analogous fashion, the DSC investigations showed a low melting form (Form I) converting into a high melting form (Form II) via a solid-solid phase transition. All forms characterised during these investigations were enantiotropic.

Due to the exceptionally high solubility (250.3 $mg.ml^{-1}$), of the monochloride salt (IMMHCLHY) at 4°C, additional solubility readings at 25°C, 40°C and 48°C could not be determined due to lack of solute.

The monomesylate salt (IMMMES) demonstrated the highest ΔH_s (22.21 $KJ.mol^{-1}$) of all the salts and modifications of IM studied.

The Van't Hoff solubility plot of sesquifumarate salt (IMSFUM), shows evidence of a transition from a thermodynamically less stable to a more stable form. The transition temperature is about 25°C.

The free energy differences at 25°C for the solvates of the trichloride are summarised in Scheme 2.

Scheme 2 Gibbs Free Energy Differences Between Solvates of IMTHCl ($KJ.mol^{-1}$) at 25°C in Ethanol

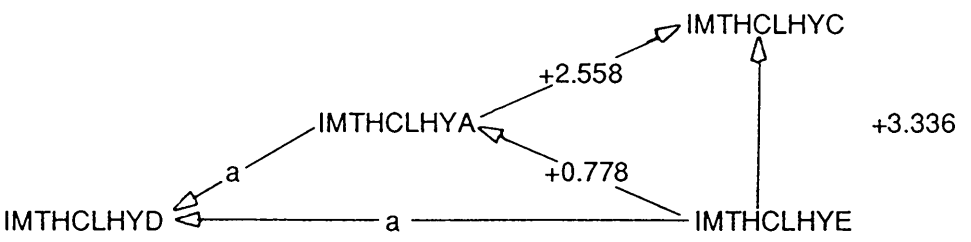

From the crystallographic investigations (Table 7.1) it was found that Phases A and E, converted into Phase D on standing[a]. This data coupled with the Van't Hoff solubility data suggests that the relative thermodynamic stabilities are Phase D > E > A > C at 25°C.

Although the hypothesis of Aguiar and Zelmer[3] would suggest that there will be no differences in the bioavailability of Phases A and E, due to free energy differences of < 1 $KJ.mol^{-1}$. It would also indicate that Phase C will not be bioequivalent with either Phase A or E. However, it must be noted that this thermodynamic data was generated in ethanol, due to the freely soluble (> 10 $mg.ml^{-1}$) nature of these phases in water. Kaplan[8] suggested that provided the solubility of the drug is in excess of 10 $mg.ml^{-1}$ at <pH 7, then no bioavailability problems were to be expected. This is because the kinetics of absorption for freely soluble drugs (see Section 1) are trans-membrane rate limited. Dissolution rate limited kinetics only apply for poorly soluble drugs (< 1 $mg.ml^{-1}$).

The change of slope observed at 25°C for Phases A and E is probably indicative of a phase change, possibly to the more stable Phase D.

As observed previously for GUMASCHY and GUDMES (see Section 4.3), Phase C demonstrates an inverse relationship between temperature and molar solubility and a resultant exothermic heat of solution. As stated previously, this could be indicative of the molecule adopting a conformation corresponding to an isolated, rather than a solvated molecule. As the temperature decreases, the intramolecular hydrogen bonds weaken and the solubility increases.

Figure 8.3.1 Van't Hoff Solubility Plots for the Various Polymorphs of the Free Base of IM

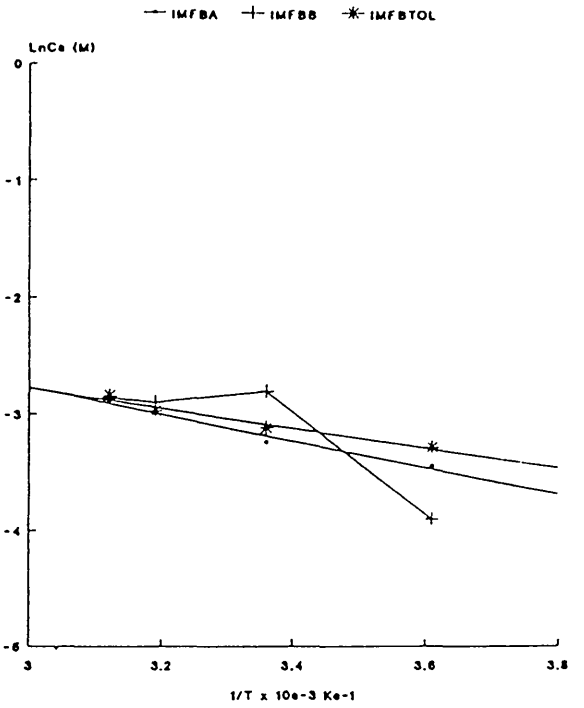

	10^3 Inverse of Absolute Temperature (K^{-1})			
SALT	3.61	3.36	3.19	3.12
IMFBA	-3.44	-3.24	-2.99	-2.88
IMFBB	-3.90	-2.80	-2.90	-2.86
IMFBTOL	-3.28	-3.11	-2.97	-2.84

(Figures quoted are Ln of Molar concentration)

Figure 8.3.2 Van't Hoff Solubility Plots for the Monoprotonated Salts of IM

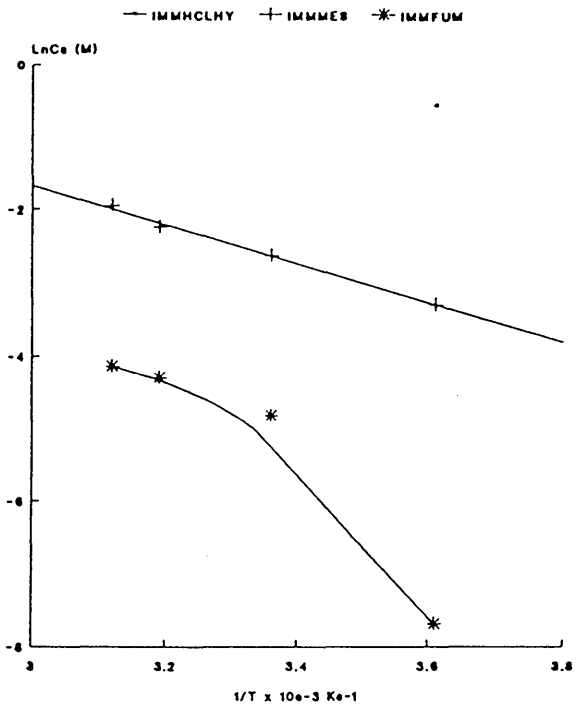

SALT	10^3 Inverse of Absolute Temperature (K^{-1}) 3.61	3.36	3.19	3.12
IMMHCLHY	-0.66	NA	NA	NA
IMMMES	-3.30	-2.63	-2.24	-1.96
IMMFUM	-7.68	-4.83	-4.30	-4.14

Figure 8.3.3 Van't Hoff Solubility Plots for the Various Phases of the Trichloride Salt of IM

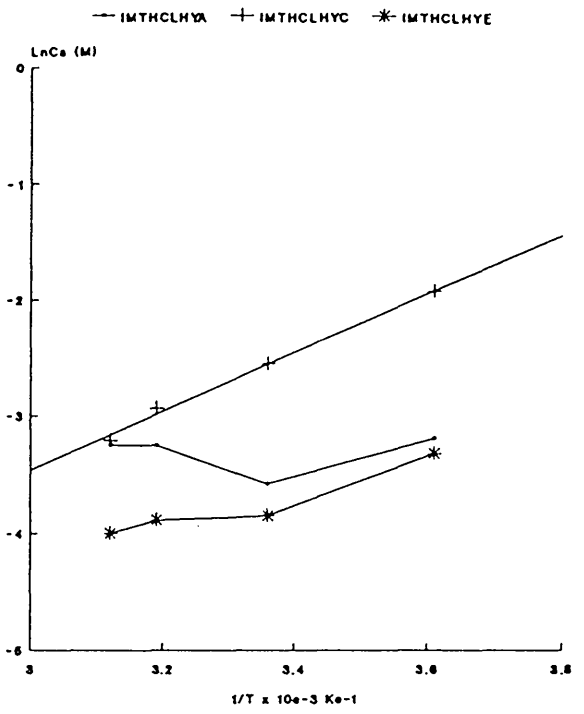

	10^3 Inverse of Absolute Temperature (K^{-1})			
SALT	3.61	3.36	3.19	3.12
IMTHCLHYA	-3.19	-3.68	-3.26	-3.26
IMTHCLHYC	-1.93	-2.66	-2.93	-3.21
IMTHCLHYE	-3.94	-3.89	-3.46	-3.23

Figure 8.3.4 DSC Heating Curves for (i) IMFBB and (ii) IMFBC, Showing in Both Cases Evidence of Solid-Solid Phase Transitions and Subsequent Melting as Phase A

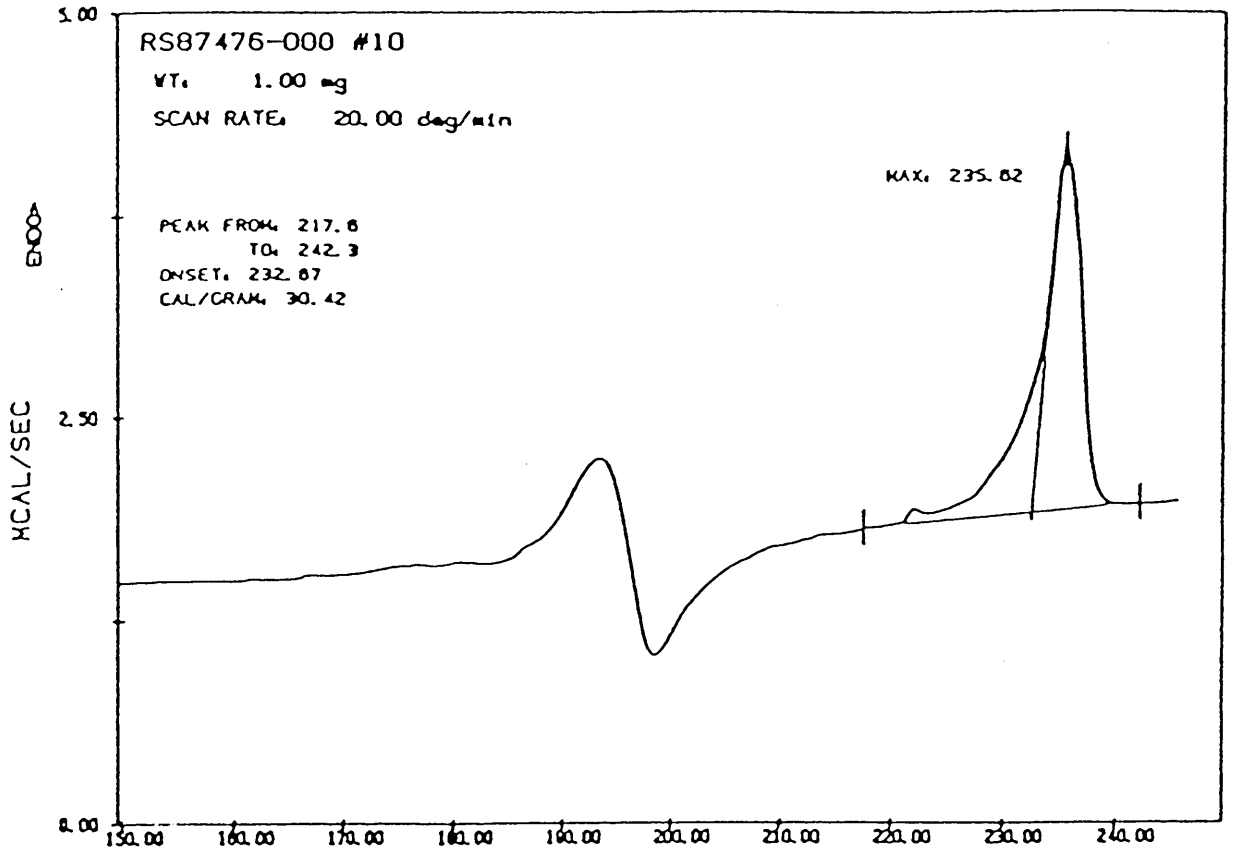

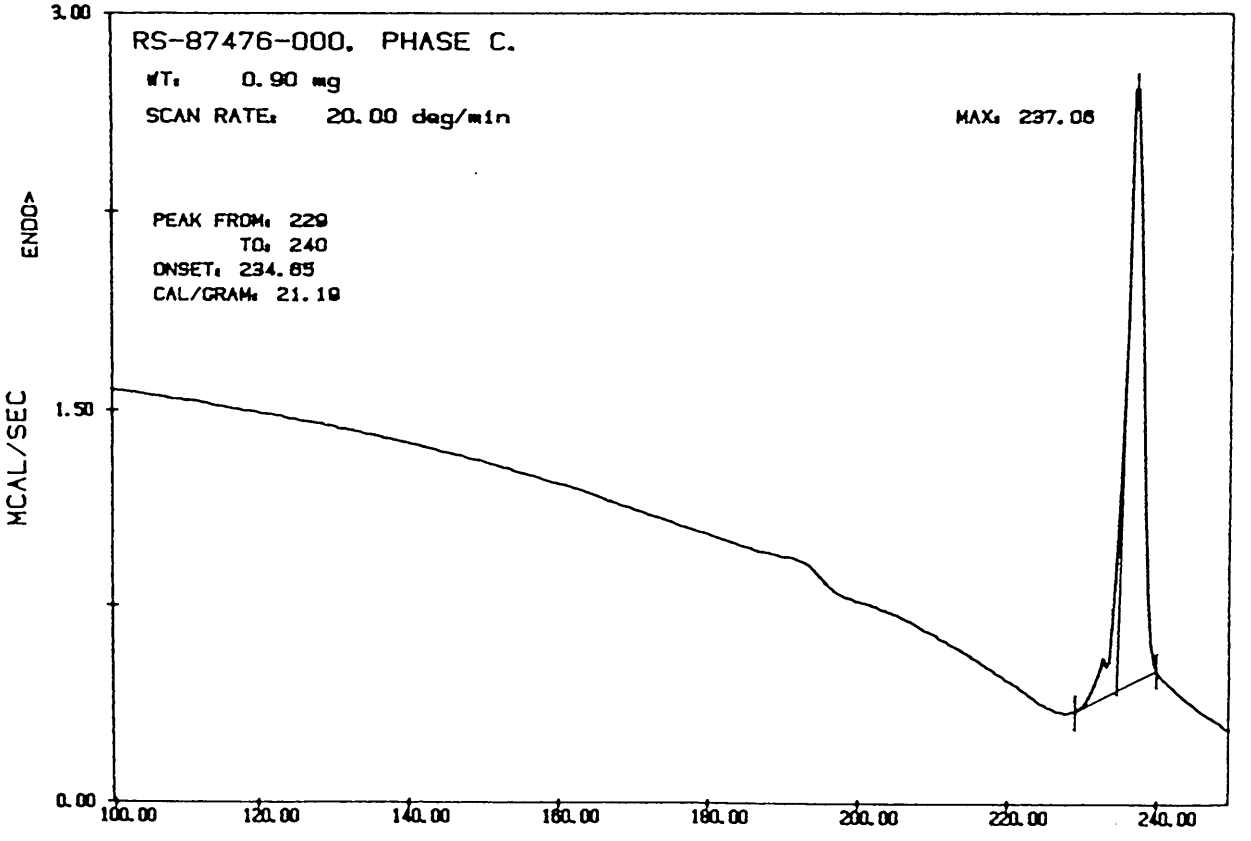

8.4 Physicochemical Properties of Salts and Modifications of IM

The physicochemical properties of the salts and modifications of IM are summarised in Table 8.4.1.

The very low aqueous solubility of all of the modifications of the free base of IM would restrict their use in conventional solid oral dosage forms. However, their potential use should not be totally discounted, as at a later stage in product development a sustained release formulation may be deemed desirable. In this case, the low aqueous solubility may be considered advantageous. This approach of utilising the slow release characteristics of slightly soluble salts of a drug substance has previously been used successfully for Methadone[9] and Amitryptyline[10].

With chloride salts there is frequently an 'overkill' on acid strength which leads to a very low pH for an aqueous solution. These problems can be particularly acute for di- and trichlorides (or the sulphate analogues). Other problems arise as a result of the polar nature of chloride salts. Their hydrophilic nature leads to hygroscopicity problems. This was encountered for both the mono- and trichlorides of IM. This can often result in processing difficulties, *eg* powder flow, and reduce the stability of compounds prone to hydrolysis; the latter effect can be exacerbated by the very low pH of the surface bound water.

The low aqueous solubility of the fumarate salt and the isolation problems associated with the sulphate and oxalate salts (plus the toxicity of the latter salt) would be major impediments to their further use. Therefore, based on the good solubility, non-hygroscopic

nature and excellent stability, the monomesylate salt would be a prime candidate for future development.

Again, as with GU, the salts and modifications of IM have a marked propensity for displaying polymorphism and pseudopolymorphism.

Table 8.4.1 Comparison of Physicochemical Data on Salts of IM

Salt/ Modification	MP	% Yield	Hygroscopicity	Adsorption Desorption Isotherms	Stability	Solubility ($mg.ml^{-1}$)	Comments
Modification							
IMFBA	236.1-238.4	92.4	All 1	I, closed	25-70,RH,(5), 100(1),Lt(4), Hv(3)		Low aqueous solubility and toxicity of toluene solvate are problems.
IMFBB	186.4-188.6	90.6	All 1	I, closed	25-70,RH,Lt(5), 100(2),Hv(2)	All <0.001 in water	
IMFBC	219.1-220.4	93.1	-	-	25-70,RH,Lt(5), 100(3),Hv(3)		
IMFBTOL	201.8-204.2	67.8	All 1	II, closed	25-70,RH,Lt(5), 100(1),Hv(3)		
Monoprotonated							
IMMHCLHY	175.0-177.8	82.3	20%(1), 87%-52%(2)	II, open	25-70,RH(5), 100(2),Hv(3), Lt(4)	>10 in water	Hygroscopicity is a problem.
IMMHCLAC	-	61.9	-	-	-	-	Not isolatable on a large scale.

Table 8.4.1 Comparison of Physicochemical Data on Salts of IM

Salt/ Modification	MP	% Yield	Hygroscopicity	Adsorption Desorption Isotherms	Stability	Solubility ($mg.ml^{-1}$)	Comments
Monoprotonated							
IMMMES	203.0-204.0	85.6	All 1	II, closed	All 5	>10 in water	Excellent.
Triprotonated							
IMTHCLHYA	188.1-190.9	89.2	87%(3), 75%-20%(1)	III, open	25-100,RH,Lt(5), Hv(4)		Hygroscopicity is a problem, undergoes a phase transition at 25°C (-D?).
IMTHCLHYB	-	73.2	-	-	-	All >10 in water	Mixture of two phases IMTHCLHYB and IMTHCLHYE. Therefore not isolatable on a large scale.
IMTHCLHYC	189.8-191.8	69.3	87%(4), 75%(3), 52%(2), 20%(1)	III, open	25-70,RH,Lt(5), 100(2), Hv(3)		Hygroscopicity is a major problem.

Table 8.4.1 Comparison of Physicochemical Data on Salts of IM

Salt/ Modification	MP	% Yield	Hygroscopicity[A]	Adsorption Desorption Isotherms	Stability[B]	Solubility ($mg.ml^{-1}$)	Comments
Triprotonated							
IMTHCLHYD	-	-	-	-	-		Stable form. Not isolatable on a large scale.
IMTHCLHYE	207.7-210.8	61.4	87%-52%(3), 20%(2)	II, open	All 5	>10 in water	Hygroscopicity is a problem. Undergoes a phase transition at 25°C (D?).
IMTSULF	-	61.8	-	-	-	-	Not isolatable on a large scale.
IMTOXA	-	51.4	-	-	-	-	Not isolatable on a large scale.
IMSFUM	-	83.4	All 1	II, closed	-	<0.001	Low aqueous solubility is a problem

Notes

A. Hygroscopicity classed as follows:

1. 0% - 5% w/w; Non-hygroscopic
2. 5% - 10% w/w; Moderate hygroscopicity
3. 10% - 20% w/w; Medium hygroscopicity
4. >20% w/w; High hygroscopicity

B. Stability classed as follows:

1. 0% - 20% label; Very poor stability
2. 20% - 50% label; Poor stability
3. 50% - 80% label; Moderate stability
4. 80% - 90% label; Medium stability
5. 90% - 100% label; Good stability

8.5 References

1. BRUNAUER, S, DEMING, L S, DEMING W E and TELLER, E, J Amer Chem Soc, 62, 1723, 1940

2. UMPRAYN, K and MENDES, R W, Drug Dev Ind Pharm, 13, 653, 1987

3. AGUIAR, A J and ZELMER, J E, J Pharm Sci, 58, 983, 1969

4. YOKOYAMA, T, UMEDA, T, KURODA, K, SATO, K and TAKAGISHI, Y, Chem Parm Bull, 27, 1476, 1979

5. KOZJECK, F and GOLIC, L, Acta Pharm Jugosl, 35, 275, 1985, through BUXTON, P C, LYNCH, R J and ROE, J M, Int J Pharmac, 42, 135, 1988

6. BEHME, R J, BROOKE, D, FARNEY, R F and KENSLER, T T, J Pharm Sci, 74, 1041, 1985

7. BURGER, A and RAMBERGER, R, Mikrochimica Acta, II, 259, 1979

8. KAPLAN, S A, Drug Metab Rev, 1, 15, 1972

9. CHOULIS, N H, ABELLANA-INTAPHAN, L and NARANG, P K, Pharmazie, 33, 5, 1978

10. FEKETE, P I, ORBAN, E and ELEKES, I, Pharm Pharmacol, 34, 12, 1982

SECTION 9 : CRYSTALLOGRAPHIC DATA FOR IM

9.1 IMFBTOL

Crystal Data

Small coloured plates from toluene, 0.25 x 0.25 x 0.04 mm.

$C_{29}H_{32}N_4.C_7H_8$, Mr = 529.8, orthorhombic, Pbca (No.61), a = 27.054 (7), b = 22.701 (6), c = 9.580 (3) Å, V = 5833.4 Å^3, Z = 8, V/Z = 729 Å^3.

Lattice parameters refined from accurately measured 2θ values (30.6-32.0°) for 40 reflections.

Dc = 1.19 g.cm^{-3}, μ = 0.37 cm^{-1}, F(000) = 2272.0, T = 290 K.

Data Collection and Processing

Stoë STADI-4 diffractometer, MoK_α, λ = 0.71073 Å. 5120 independent data ($2 \leq \theta \leq 22°$, $-29 \leq h \leq 29$, $-24 \leq k \leq 24$, $0 \leq l \leq 10$) yielding 2146 data with $I \geq 2.5\ \sigma(I)$. No measurable crystal decay or movement.

Structure Solution and Refinement

Solution by direct methods (SHELX 86).

$\varpi^{-1} = \sigma^2(F) + 0.000218F^2$, R = 0.0855, wR = 0.0932, S = 1.273 based on 332 parameters. Maximum and minimum ripple in difference electron density map : 0.53 and -0.26 e.Å^{-3}.

The disordered toluene solvent is located on an inversion centre and is modelled as two inter-penetrating ring systems. The toluene was refined isotropically, the methyl group and all of the ring hydrogens could not be located. Ten low angle reflections were omitted from the refinement.

Structure Discussion

Selected bond lengths, angles and torsion angles are given in Tables 9.9.1-9.9.3. A drawing of the molecular structure and molecular packing as viewed along the c-axis is given in Figure 9.1. The packing may be described as interpenetrating bilayers of IM

running parallel to the a-axis, separated by a monolayer of solvent molecules. The imidazole 'pyrrole' nitrogen, N(3) forms a bifurcated hydrogen bond, giving closest contact with N(1) and a very long contact with N(7) of the same molecule. These distances, together with some of the close intermolecular contacts are summarised in Table 9.1.

Table 9.1 Hydrogen Bonding and Other Close Intermolecular Contacts

a) Hydrogen Bonding

Donor	Acceptor	Symmetry	D-H	H...A	D...A
N(3)-H(3)...	N(1)	x,1½-y,½+z	0.87	2.02(5)	2.839(7)
	N(7)	x,1½-y,½+z	0.87	2.85(5)	3.419(7)

b) C...C Contacts Closer than 3.75Å

C(4').....C(4S)	1-x,½+y,½-z	3.57(2)
C(17).....C(21)	-½+x,y,½-z	3.62(1)
C(4M).....C(9)	x,y,-1+z	3.65(1)
C(17').....C(2M)	-½+x,1½-y,1-z	3.67(2)
C(6).....C(6S)	1-x,½+y,½-z	3.69(2)
C(16').....C(2M)	-½+x,1½-y,1-z	3.70(2)

c) C...N Contacts Closer than 3.75Å

C(21).....N(3)	x,1½-y,½+z	3.502(9)
C(25).....N(1)	x,1½-y,-½+z	3.645(9)
C(4M).....N(1)	x,1½-y,-½+z	3.669(8)
C(4).....N(1)	x,1½-y,-½+z	3.682(8)
C(2).....N(3)	x,1½-y,½+z	3.693(8)
C(5).....N(3)	x,1½-y,½+z	3.744(8)

Figure 9.1 Molecular Structure and Molecular Packing (as viewed along the c-axis) of IMFBTOL

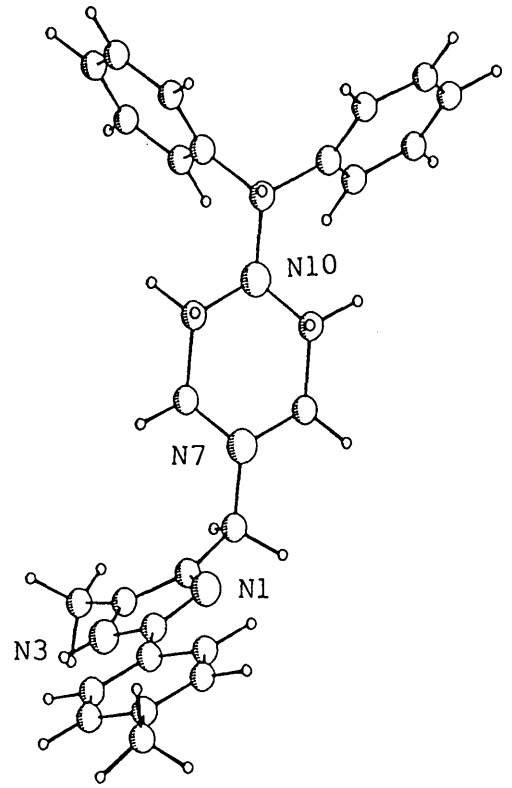

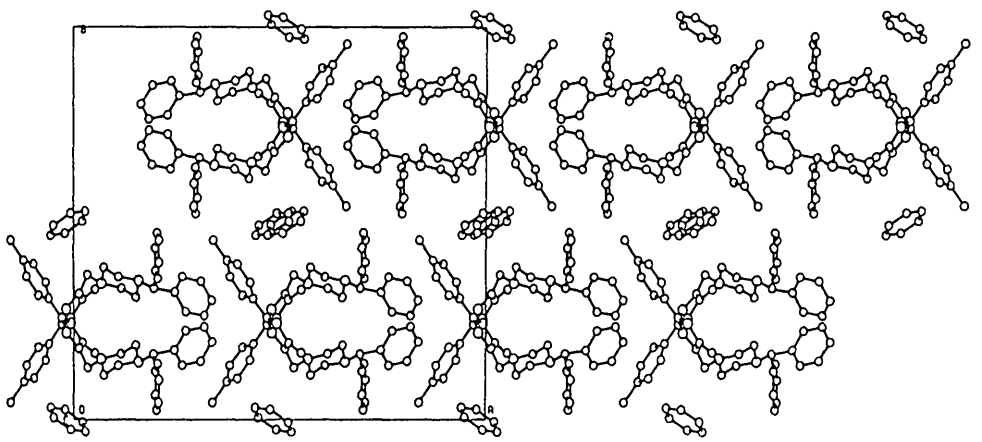

9.2 IMMMES

Crystal Data

Large colourless plates from a 50:50 v/v mixture of methanol and ethyl acetate, 0.80 x 0.74 x 0.07 mm. $C_{29}H_{33}N_4^+.CH_3SO_3^-$, Mr = 548.7, monoclinic, $P2_1/n$ alternative setting of $P2_1/c$ (No.14), a = 9.498 (7), b = 31.647 (2), c = 10.103 (9) Å, β = 106.23 (6)°, V = 2916.0 Å^3, Z = 4, V/Z = 729 Å^3.
Lattice parameters refined from accurately measured 2θ values (25.3° - 29.2°) for 12 reflections.
Dc = 1.25 g.cm^{-3}, μ = 12.22 cm^{-1}, F(000) = 1168, T = 290 K.

Data Collection and Refinement

Stoë STADI-4 diffractometer, CuK_α, λ = 1.5418 Å. 4591 independent data ($2 \leq \theta \leq 66.8°$, $-11 \leq h \leq 11$, $0 \leq k \leq 37$, $0 \leq l \leq 12$) yielding 2080 data with $I \geq 2.5\ \sigma(I)$. No measurable crystal decay or movement.

Structure Solution and Refinement

Solution by direct methods (SHELX 86).
$\varpi^{-1} = \sigma^2(F) + 0.000253F^2$, R = 0.0479, wR = 0.0534, S = 0.933 based on 374 parameters. Maximum shift/esd in last cycle = -0.102. Maximum and minimum ripple in difference electron density map : 0.18 and -0.24 e.Å^{-3}.

Structure Discussion

Selected bond lengths, angles and torsion angles are given in Tables 9.9.1-9.9.3. A drawing of the molecular structure and molecular packing as viewed along the a-axis is given in Figure 9.2. The packing may be described as corrugated monolayers of IM, packing along the b-axis, the direction of the IM molecules alternating from one layer to the next. The mesylate anions are located near the piperazine ring of each IM molecule and alternate from one side of the layer to the other.

The salt hydrogen bond is formed between the mesylate oxygen, O(2S) and the piperazine nitrogen , N(7), and an additional hydrogen bond is formed between the imidazole nitrogen, N(3) and the mesylate oxygen, O(1S) of a second anion. These distances, together with some of the close intermolecular contacts are summarised in Table 9.2.

Table 9.2 Hydrogen Bonding and Other Close Intermolecular Contacts

a) Hydrogen Bonding

Donor	Acceptor	Symmetry	D-H	H...A	D...A
O(2S)-H(7)..	N(7)*	x,y,z	0.79	1.93(5)	2.754(5)
N(3)-H(3)...	O(1S)	-1 + x,y,z	0.81	1.96(5)	2.792(6)

* salt H-bond

b) C...C Contacts Shorter than 3.75Å

C(19')....C(20)	½ + x,½-y,-½ + z	3.638(8)
C(18).....C(2M)	½-x,½ + y,½-z	3.664(10)
C(21).....C(1S)	x,y,z	3.652(9)
C(22).....C(22)	-x,-y,1-z	3.689(8)
C(17).....C(2M)	½-x,½ + y,½-z	3.722(11)
C(19')....C(21)	½ + x,½-y,-½ + z	3.740(8)
C(19).....C(2M)	½-x,½ + y,½-z	3.756(9)

c) C...N Contacts Shorter than 3.75Å

C(1S).....N(1)	x,y,z	3.497(8)
C(12).....N(3)	½ + x,½-y,½ + z	3.721(7)
C(19).....N(1)	½ + x,½-y,-½ + z	3.744(7)

d) C...O Contacts Shorter than 3.75Å

C(9).....O(3S)	-½ + x,½-y,-½ + z	3.192(6)
C(12).....O(3S)	x,y,z	3.231(7)
C(4M).....O(2S)	-½ + x,½-y,½ + z	3.296(6)
C(8).....O(2S)	x,y,z	3.456(6)
C(6).....O(1S)	-½ + x,½-y,½ + z	3.467(6)
C(25).....O(1S)	-1 + x,y,z	3.484(7)

d) C...O Contacts Shorter than 3.75Å (cont'd)

C(12).....O(2S)	x,y,z	3.503(6)
C(4M).....O(1S)	-½ + x, ½-y, ½ + z	3.544(6)
C(4M).....O(3S)	-1 + x,y,z	3.580(7)
C(6).....O(2S)	x,y,z	3.593(6)
C(9).....O(2S)	x,y,z	3.610(6)
C(11).....O(2S)	x,y,z	3.664(6)
C(4).....O(1S)	-1 + x,y,z	3.676(6)
C(5).....O(2S)	x,y,z	3.688(6)
C(11).....O(3S)	x,y,z	3.708(6)
C(4M).....O(1S)	-1 + x,y,z	3.745(6)

Figure 9.2 Molecular Structure and Molecular Packing (as viewed along the a-axis) of IMMMES

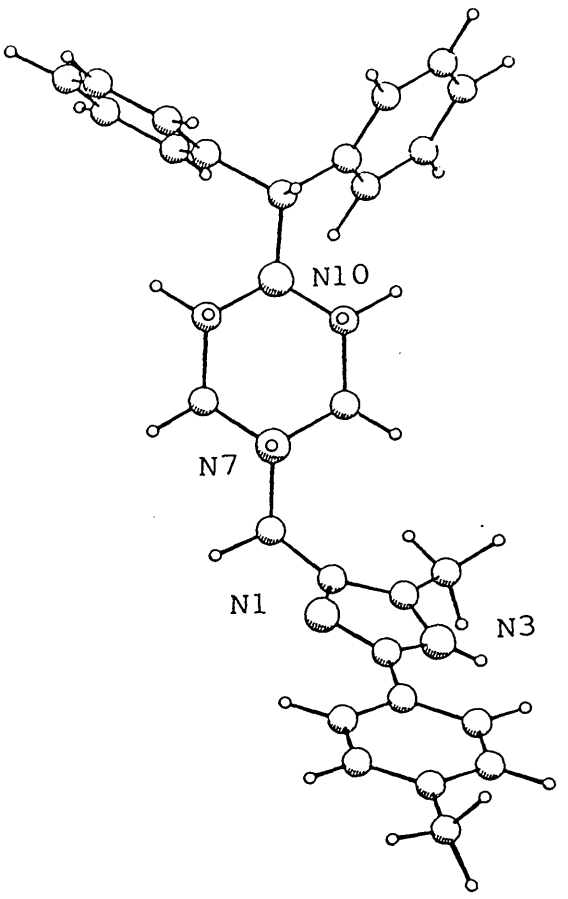

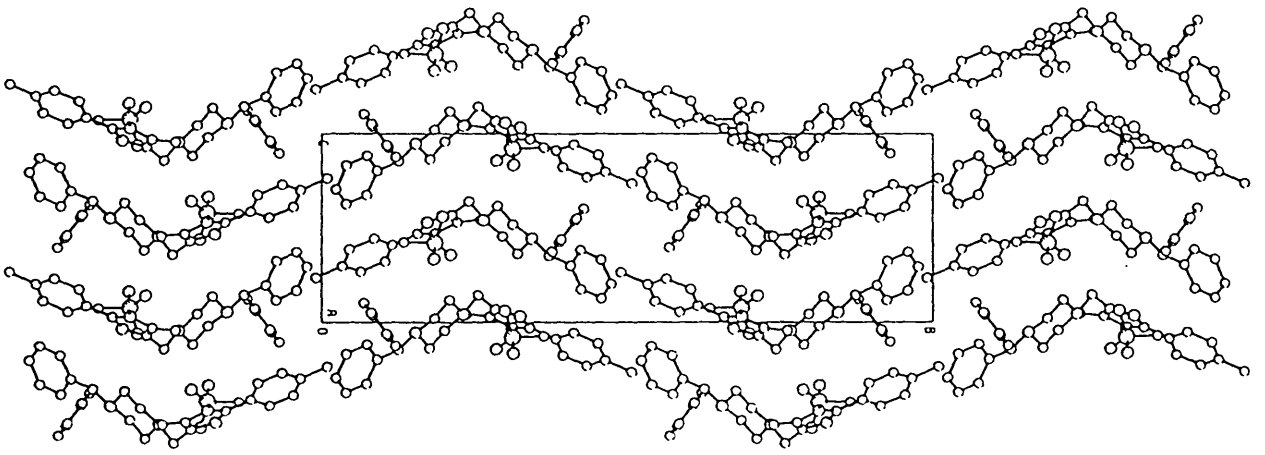

9.3 IMMHCLAC

Crystal Data

Large colourless plates from a 50% aqueous acetone, 0.80 x 0.76 x 0.08 mm.

$C_{29}H_{33}N_4^+.Cl^-.C_3H_6O$, Mr = 532.2, triclinic, $P\bar{1}$ (No.2)

a = 9.062 (5), b = 11.968 (6), c = 15.781 (7), Å, α = 71.24 (2), β = 77.96 (2), γ = 69.23 (2)°, V = 1503.8 Å^3, Z = 2, V/Z = 752 Å^3.

Lattice parameters refined from accurately measured 2θ values (7.79° - 11.01°) for 23 reflections.

Dc = 1.19 g.cm^{-3}, μ = 1.19 cm^{-1}, F(000) = 524.0, T = 290 K.

Data Collection and Refinement

Stoë STADI-4 diffractometer, MoK_α, λ = 0.71069 Å. 4573 independent data ($2 \leq \theta \leq 22°$, $-9 \leq h \leq 9$, $-11 \leq k \leq 12$, $0 \leq l \leq 16$) yielding 2821 data with $I \geq 2.5\ \sigma(I)$. No measurable crystal decay or movement.

Structure Solution and Refinement

Solution by direct methods (SHELX 86).

$\varpi^{-1} = \sigma^2(F) + 0.00050F^2$, R = 0.0499, wR = 0.0655, S = 1.253 based on 377 parameters. Maximum shift/esd in last cycle = 0.803. Maximum and minimum ripple in difference electron density map : 0.20 and -0.27 e.Å^{-3}. Disorder was apparent in the tolyl methyl group and was modelled as two alternative positions for the three hydrogens. All of the major shifts associated with the structure were attributable to the disordered methyl group.

Structure Discussion

Selected bond lengths, angles and torsion angles are given in Tables 9.9.1-9.9.3. A drawing of the molecular structure and molecular packing as viewed along the a-axis is given in Figure 9.3. It is dominated by hydrogen bonding and ring stacking.

Conformationally, the molecule is quite dissimilar from other IM structures, mainly involving rotations about the single non-ring bond at C(5)-C(6). The molecular packing may be described as parallel bilayers of IM cations, stacking in a head-tail fashion along each layer and with each layer being aligned in opposite directions. Each bilayer is separated by a channel occupied by the anions and solvent molecules. The chloride anion is central to the hydrogen bonding being joined to two different cation molecules. These distances are summarised in Table 9.3, together with some close intermolecular contacts. The main hydrophobic contacts are between phenyl and tolyl ring systems through an inversion centre.

Table 9.3 Hydrogen Bonding and Other Close Intermolecular Contacts

a) Hydrogen Bonding

Donor	Acceptor	Symmetry	D-H	H...A	D...A
N(3)-H(3)...	Cl(1)	x,y,z	0.83	2.34(4)	3.167(3)
Cl(1)-H(7)..	N(7)*	-x,1-y,-z	0.90	2.17(4)	3.067(3)

* salt H-bond

b) C...C Contacts Shorter than 3.75Å

C(9).....C(1A)	-1+x,y,z	3.426(7)
C(17').....C(25)	x,1+y,-1+z	3.470(7)
C(2).....C(15)	-1-x,2-y,-z	3.580(5)
C(24).....C(3A)	-x,1-y,-z	3.595(7)
C(9).....C(3A)	-1+x,y,z	3.635(7)
C(4M).....C(22)	1+x,y,z	3.642(6)
C(15').....C(23)	-1-x,2-y,-z	3.695(6)
C(17').....C(24)	x,1+y,-1+z	3.704(7)
C(4M).....C(1A)	x,y,z	3.719(7)
C(15).....C(20)	-1-x,2-y,-z	3.741(5)
C(16').....C(23)	-1-x,2-y,-z	3.742(6)

c) C...N Contacts Shorter than 3.75Å

C(8).....N(1)	-1-x,2-y,-z	3.574(5)
C(15).....N(1)	-1-x,2-y,-z	3.637(5)

d) C...O Contacts Shorter than 3.75Å

C(6).....O(1A)	-x,2-y,-z	3.498(5)
C(9).....O(1A)	-1 + x,y,z	3.603(5)
C(4M).....O(1A)	x,y,z	3.607(6)
C(8).....O(1A)	-1 + x,y,z	3.638(5)
C(6).....O(1A)	x,y,z	3.738(6)

Figure 9.3 Molecular Structure and Molecular Packing (as viewed along the a-axis) of IMMHCLAC

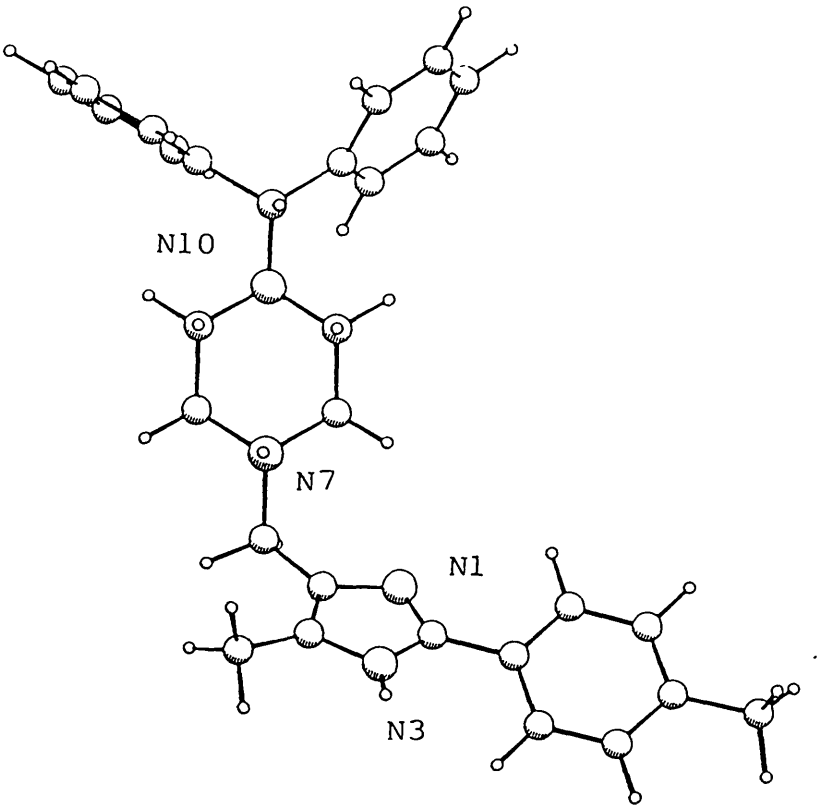

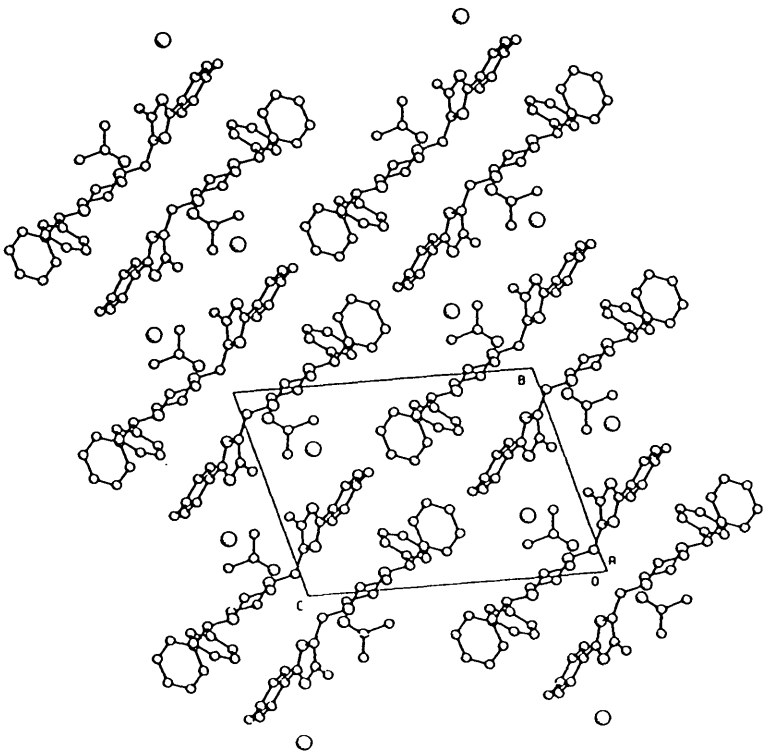

9.4 IMTHCLHYA

Crystal Data

Colourless prisms from 50% methanolic ethyl acetate, 0.52 x 0.40 x 0.26 mm.

$C_{29}H_{35}N_4^{3+}.3Cl^-.H_2O$, Mr = 565.0, monoclinic, $P2_1/n$ (No.14), a = 14.491 (8), b = 13.070 (8), c = 15.269 (8) Å, β = 99.72 (4)°, V = 2850.3 Å^3, Z = 4, V/Z = 713 Å^3.

Lattice parameters refined from accurately measured 2θ values (12.4° - 16.3°) for 20 reflections.

Dc = 1.31 g.cm^{-3}, μ = 30.11 cm^{-1}, F(000) = 1184, T = 290 K.

Data Collection and Refinement

Stoë STADI-4 diffractometer, CuK_α, λ = 1.5418 Å. 3418 independent data ($2 < \theta < 56°$, $0 \leq h \leq 15$, $0 \leq k \leq 14$, $-16 \leq l \leq 16$) yielding 2508 data with $I \geq 2.5\ \sigma(I)$. No measurable crystal decay or movement.

Structure Solution and Refinement

Solution by direct methods (SHELX 84).

$\varpi^{-1} = \sigma^2(F) + 0.00031F^2$, R = 0.0385, wR = 0.0510, S = 1.217 based on 368 parameters. Maximum shift/esd on last cycle = -0.109. Maximum and minimum ripple in difference electron density map : 0.24 and -0.26 e.Å^{-3}. Disorder was apparent in solvent molecule. The water oxygen was refined with a site occupancy of one third. No hydrogens located for disordered water molecule.

Structure Discussion

Selected bond lengths, angles and torsion angles are given in Tables 9.9.1-9.9.3. A drawing of the molecular structure and molecular packing as viewed along the a-axis is given in Figure 9.4. The molecular packing may be described as off-set, parallel bilayers of cations running diagonally across the projected unit cell. The anions straddle the resulting channel between these bilayers. The hydrogen bonding and other

close intermolecular contacts are summarised in Table 9.4. The principal hydrophobic contacts are between phenyl and tolyl ring systems through an inversion centre.

Table 9.4 Hydrogen Bonding and Other Close Intermolecular Contacts

a) Hydrogen Bonding

Donor	Acceptor	Symmetry	D-H	H...A	D...A
N(3)-H(3)...	Cl(1)	-x,-y,-z	1.08	2.26(4)	3.109(3)
Cl(1)-H(10).	N(10)*	½-x,½+y,½-z	0.96	2.12(4)	3.067(3)
O(1)-H(1W)..	Cl(2)	x,y,z	-	-	3.356(12)
Cl(2)-H(1)..	N(1)*	x,y,z	0.86	2.04(3)	3.053(3)
O(1)-H(2W)..	Cl(3)	½+x,-½-y,½+z	-	-	3.189(12)
Cl(3)-H(7)..	N(7)*	½+x,-½-y,½+z	0.92	2.08(4)	2.990(3)

* salt H-bonds

b) C...C Contacts Shorter than 3.75Å

C(18).....C(25)	-x,-y,1-z	3.337(6)
C(4).....C(25)	-x,-y,1-z	3.437(5)
C(4M).....C(24)	-x,-y,-z	3.453(6)
C(19').....C(21)	-x,-y,1-z	3.491(5)
C(19).....C(25)	-x,-y,1-z	3.506(5)
C(18).....C(24)	-x,-y,1-z	3.524(6)
C(4M).....C(25)	-x,-y,-z	3.591(5)
C(19').....C(22)	-x,-y,1-z	3.641(6)
C(18').....C(22)	-x,-y,1-z	3.655(6)
C(19).....C(20)	-x,-y,1-z	3.719(5)
C(18').....C(21)	-x,-y,1-z	3.730(6)
C(4).....C(24)	-x,-y,-z	3.733(5)
C(14').....C(22)	-x,-y,1-z	3.734(5)
C(17').....C(22)	-x,-y,1-z	3.736(7)
C(17).....C(24)	-x,-y,1-z	3.741(6)
C(9).....C(17)	-½+x,-½-y,-½+z	3.746(6)

c) C...N Contacts Shorter than 3.75Å

C(25).....N(3)	-x,-y,-z	3.506(5)

d) C...O Contacts Shorter than 3.75Å

C(11).....O(1)	x,y,z	3.149(13)
C(19').....O(1)	-x,-y,1-z	3.274(13)
C(2M).....O(1)	-½ + x, ½-y,-½ + z	3.325(13)
C(12).....O(1)	x,y,z	3.485(13)
C(17).....O(1)	½-x,-½ + y,1½-z	3.515(13)
C(16).....O(1)	½-x,-½ + y,1½-z	3.543(13)
C(24).....O(1)	-½ + x, ½-y,-½ + z	3.580(13)
C(18').....O(1)	-x,-y,1-z	3.741(13)

Figure 9.4 Molecular Structure and Molecular Packing (as viewed along the a-axis) of IMTHCLHYA

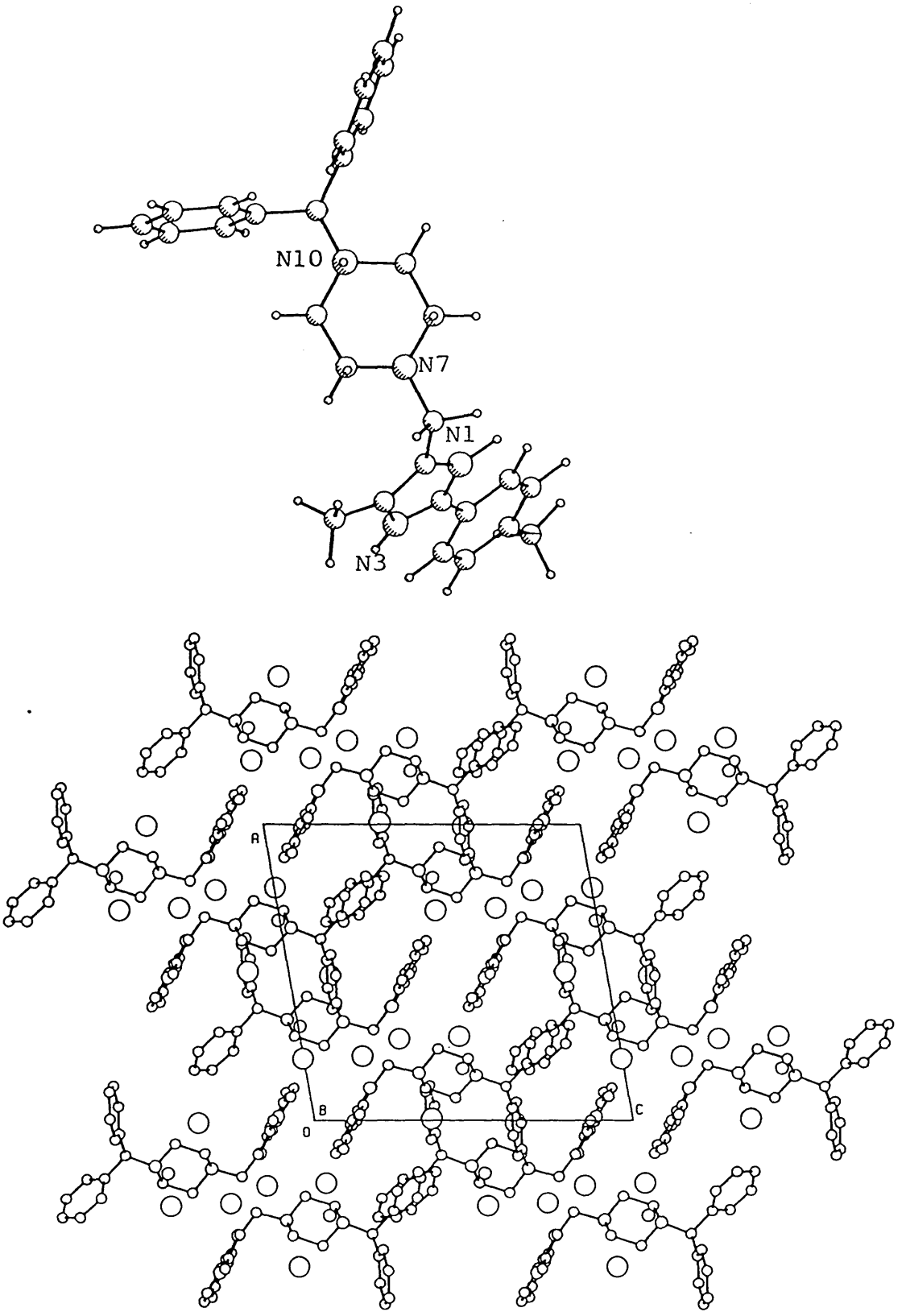

9.5 IMTHCLHYB

Crystal Data

Colourless needles from isopropanol, 0.58 x 0.09 x 0.06 mm.

$C_{29}H_{35}N_4^{3+}.3Cl^-.2H_2O$, Mr = 583.0, triclinic, $P\bar{1}$ (No.2), a = 6.970 (5), b = 15.000 (18), c = 16.340 (36) Å, α = 118.01 (3), β = 91.64 (13), γ = 101.40 (8)°, V = 1512.7 Å^3, Z = 2, V/Z = 756 Å^3.

Lattice parameters refined from accurately measured 2Θ values (18.2° - 24.2°) for 14 reflections.

Dc = 1.28 g.cm^{-3}, μ = 2.86 cm^{-1}, F(000) = 592, T = 290 K.

Data Collection and Refinement

Stoë STADI-4 diffractometer, MoK_α, λ = 0.71073 Å. 3932 independent data ($2 < \Theta < 22°$, $-7 \leq h \leq 7$, $-16 \leq k \leq 16$, $0 \leq l \leq 17$) yielding 1970 data with $I \geq 2.5\ \sigma(I)$. No measurable crystal decay or movement.

Structure Solution and Refinement

Solution by direct methods (SHELX 86).

$w^{-1} = \sigma^2(F) + 0.000243F^2$, R = 0.0683, wR = 0.0691, S = 1.252 based on 374 parameters. Maximum shift/esd on last cycle = -0.136. Maximum and minimum ripple in difference electron density map : 0.33 and -0.28 e.Å^{-3}. Disorder was apparent in solvent molecules. No hydrogens located for either disordered water molecule.

Structure Discussion

Selected bond lengths, angles and torsion angles are given in Tables 9.9.1-9.9.3. A drawing of the molecular structure and molecular packing as viewed along the a-axis is given in Figure 9.5. The molecular packing may be described as parallel monolayers of IM cations, stacking in a head to tail fashion along each layer and with each layer being aligned in opposite directions. The channels between layers are occupied

by anions and solvent molecules. The packing is similar to that previously described in Section 9.3 for IMMHCLAC. The chloride anions are central to the packing being hydrogen bonded to two different cation molecules. The hydrogen bonding and other close intermolecular contacts are summarised in Table 9.5. The principal hydrophobic contacts are imidazole-phenyl along the a-axis, phenyl-phenyl and phenyl-tolyl through an inversion centre.

Table 9.5 Hydrogen Bonding and Other Close Intermolecular Contacts

a) Hydrogen Bonding

Donor	Acceptor	Symmetry	D-H	H...A	D...A
N(1)-H(1)...	Cl(2)	-x,2-y,1-z	1.01	2.29(9)	3.070(9)
Cl(2)-H(7)..	N(7)*	-x,2-y,1-z	1.01	2.13(8)	3.098(8)
Cl(1)-H(10).	N(10)*	1+x,y,z	0.97	2.09(8)	3.058(7)
Cl(3)-H(3)..	N(3)*	x,y,z	0.88	2.04(8)	3.017(9)
O(1) ..	Cl(2)	1+x,y,z	-	-	3.208(9)

* salt H-bonds

b) C...C Contacts Shorter than 3.75Å

C(4).....C(22)	-1+x,y,z	3.394(14)
C(5).....C(22)	-1+x,y,z	3.428(14)
C(17')....C(17')	-1-x,1-y,1-z	3.469(20)
C(17')....C(21)	-x,2-y,1-z	3.592(17)
C(4).....C(23)	-1+x,y,z	3.593(15)
C(17).....C(24)	-1+x,-1+y,z	3.631(17)
C(16).....C(24)	-1+x,-1+y,z	3.657(17)
C(16')....C(21)	-x,2-y,1-z	3.671(17)

c) C...N Contacts Shorter than 3.75Å

C(2M).....N(3)	1+x,y,z	3.546(14)
C(23).....N(3)	1+x,y,z	3.601(14)

d) C...O Contacts Shorter than 3.75Å

C(6).....O(1)	-x,2-y,1-z	3.339(13)
C(8).....O(1)	-x,2-y,1-z	3.512(12)
C(19')....O(1)	x,y,z	3.529(14)
C(6).....O(2)	x,y,z	3.546(14)
C(12).....O(2)	x,y,z	3.552(13)
C(4M).....O(2)	x,y,z	3.590(14)
C(15')....O(1)	-1 + x,y,z	3.668(14)
C(9).....O(1)	x,y,z	3.745(12)

Figure 9.5 Molecular Structure and Molecular Packing (as viewed along the a-axis) of IMTHCLHYB

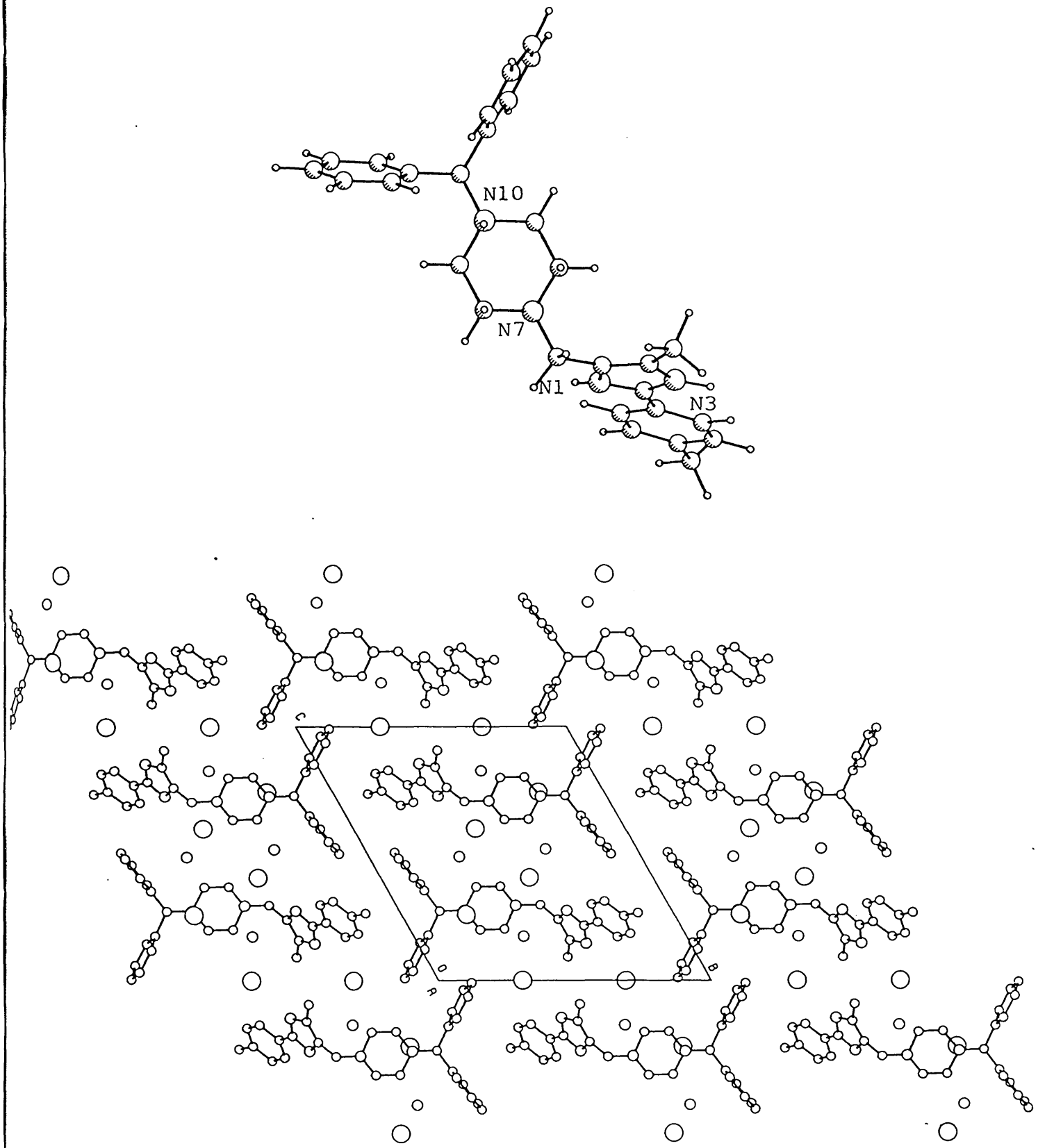

9.6 IMTHCLHYC

Crystal Data

Colourless plates from 50% aqueous acetone, 0.85 x 0.70 x 0.10 mm.

$C_{29}H_{35}N_4^{3+}.3Cl^-.5H_2O$, M = 637.0, monoclinic, C2/c (No.15), a = 23.580 (3), b = 17.176 (2), c = 17.164 (2) Å, β = 105.88 (1)°, V = 6686.4 Å^3, z = 8, V/z = 833 Å^3.

Lattice parameters refined from accurately measured 2θ values (10.0° - 11.3°) for 30 reflections.

Dc = 1.25 g.cm^{-3}, μ = 2.60 cm^{-1}, F(000) = 2368,

T = 290 k.

Data Collection and Processing

Stoë STADI-4 diffractometer, MoK_α, λ = 0.71073 Å. 3167 independent data ($2 < \theta < 22°$, $-25 \leq h \leq 25$, $0 \leq k \leq 18$, $0 \leq l \leq 18$) yielding 1355 data with $I \geq 2.5 \sigma(I)$.

Structure Solution and Refinement

Solution by direct methods (SHELX 86) after incorporating the positions of Cl(1) and Cl(2) into the matrix. No weighting scheme employed, R = 0.0848, wR = 0.1035, S = 9.513 based on 376 parameters. Maximum shift/esd on last cycle = 1.514. Maximum and minimum ripple in difference electron density map : 0.47 and -0.30 e.Å^{-3}.

Refinement not completed, anions and water molecules all disordered. High thermal parameters for Cl(2) and O(3), O(4) and O(5). Cl(1) badly disordered and modelled in three segments, about a special position, with partial site occupancies of 0.5, 0.18 and 0.32, the two smaller fragments were refined isotropically. Water oxygens O(3), O(4) and O(5) all modelled with partial site occupancy of 0.5. No hydrogens were located on any of the water oxygens.

Structure Discussion

Selected bond lengths, angles and torsion angles are given in Tables 9.9.1-9.9.3. Molecular structure and molecular packing diagram (as viewed along the b-axis) are shown in Figure 9.6. The hydrogen bonding and other close intermolecular contacts are summarised in Table 9.6. The principal hydrophobic contacts are phenyl-tolyl and imidazole-tolyl through an inversion centre.

Table 9.6 Hydrogen Bonding and Other Close Intermolecular Contacts

a) Hydrogen Bonding

Donor	Acceptor	Symmetry	D-H	H...A	D...A
N(1)-H(1)...	O(1)	x,y,z	1.08	2.83(2)	3.29(2)
Cl(1)-H(3)..	N(3)*	½ + x, ½-y,z	1.08	2.08(5)	3.11(2)
Cl(2)-H(10).	N(10)*	½-x, ½-y,-z	1.08	1.98(1)	3.03(2)
N(7)-H(7)...	O(1)	x,y,z	1.08	1.66(2)	2.73(2)
Cl(5)-H(7)..	N(7)*	x,y,z	1.08	3.34(3)	3.65(3)
O(3).....	O(5)	x,y,z	-	-	2.48(6)
O(3).....	O(4)	½-x,-½ + y, ½-z	-	-	2.78(5)
O(1).....	O(5)	x,y,z	-	-	3.27(5)

* salt H-bonds

b) C...C Contacts Shorter than 3.75Å

C(19).....C(21)	½-x, ½-y,-z	3.42(4)
C(20).....C(20)	1-x,1-y,-z	3.44(3)
C(2).....C(20)	1-x,1-y,-z	3.47(3)
C(19).....C(22)	½-x, ½-y,-z	3.49(4)
C(2).....C(21)	1-x,1-y,-z	3.55(3)
C(4).....C(22)	1-x,1-y,-z	3.56(3)
C(4).....C(23)	1-x,1-y,-z	3.56(3)
C(18')....C(24)	½-x, ½-y,-z	3.57(4)
C(5).....C(23)	1-x,1-y,-z	3.58(3)
C(15).....C(2M)	x,-1 + y,z	3.62(4)
C(19')....C(23)	½-x, ½-y,-z	3.63(4)

b) C...C Contacts Shorter than 3.75Å continued

C(18).....C(25)	½-x,-½ +y,-½-z	3.66(4)
C(5).....C(24)	1-x,1-y,-z	3.66(3)
C(18')....C(23)	½-x,½-y,-z	3.67(4)
C(2).....C(25)	1-x,1-y,-z	3.67(3)
C(19')....C(24)	½-x,½-y,-z	3.73(4)
C(18).....C(22)	½-x,½-y,-z	3.74(4)
C(18).....C(21)	½-x,½-y,-z	3.75(4)

c) C...N Contacts Shorter than 3.75Å

C(21).....N(3)	1-x,1-y,-z	3.44(3)
C(22).....N(3)	1-x,1-y,-z	3.45(3)
C(25).....N(1)	1-x,1-y,-z	3.56(3)
C(24).....N(1)	1-x,1-y,-z	3.56(3)

d) C...O Contacts Shorter than 3.75Å

C(8).....O(2)	½-x,½-y,-z	3.20(3)
C(4).....O(2)	½-x,½-y,-z	3.25(3)
C(11).....O(3)	x,y,z	3.33(4)
C(16')....O(2)	½-x,-½ +y,½-z	3.37(4)
C(8).....O(1)	x,y,z	3.39(3)
C(11).....O(5)	x,y,z	3.40(6)
C(9).....O(1)	x,y,z	3.48(3)
C(4).....O(4)	½-x,½-y,-z	3.54(4)
C(12).....O(1)	x,y,z	3.55(3)
C(2M).....O(5)	x,1-y,-½ +z	3.56(6)
C(12).....O(4)	½ +x,-½ +y,z	3.57(4)
C(6).....O(1)	x,y,z	3.59(3)
C(12).....O(5)	x,y,z	3.60(6)

Figure 9.6 Molecular Structure and Molecular Packing (as viewed along the b-axis) of IMTHCLHYC

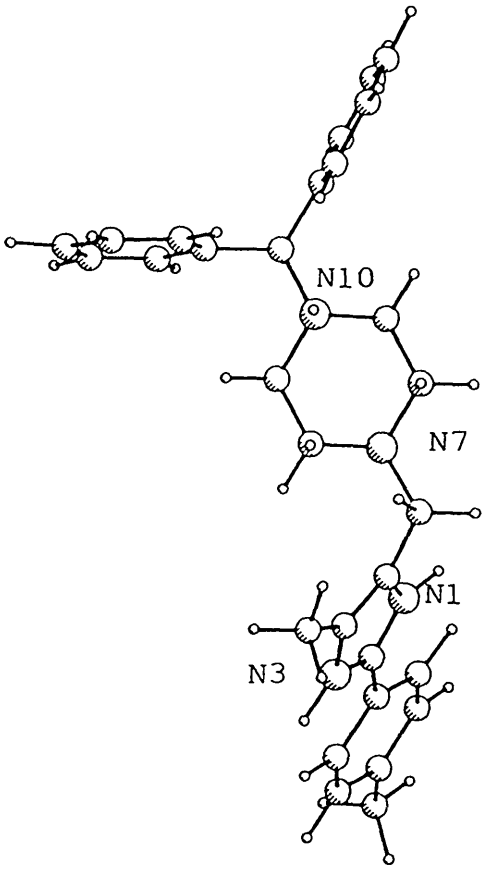

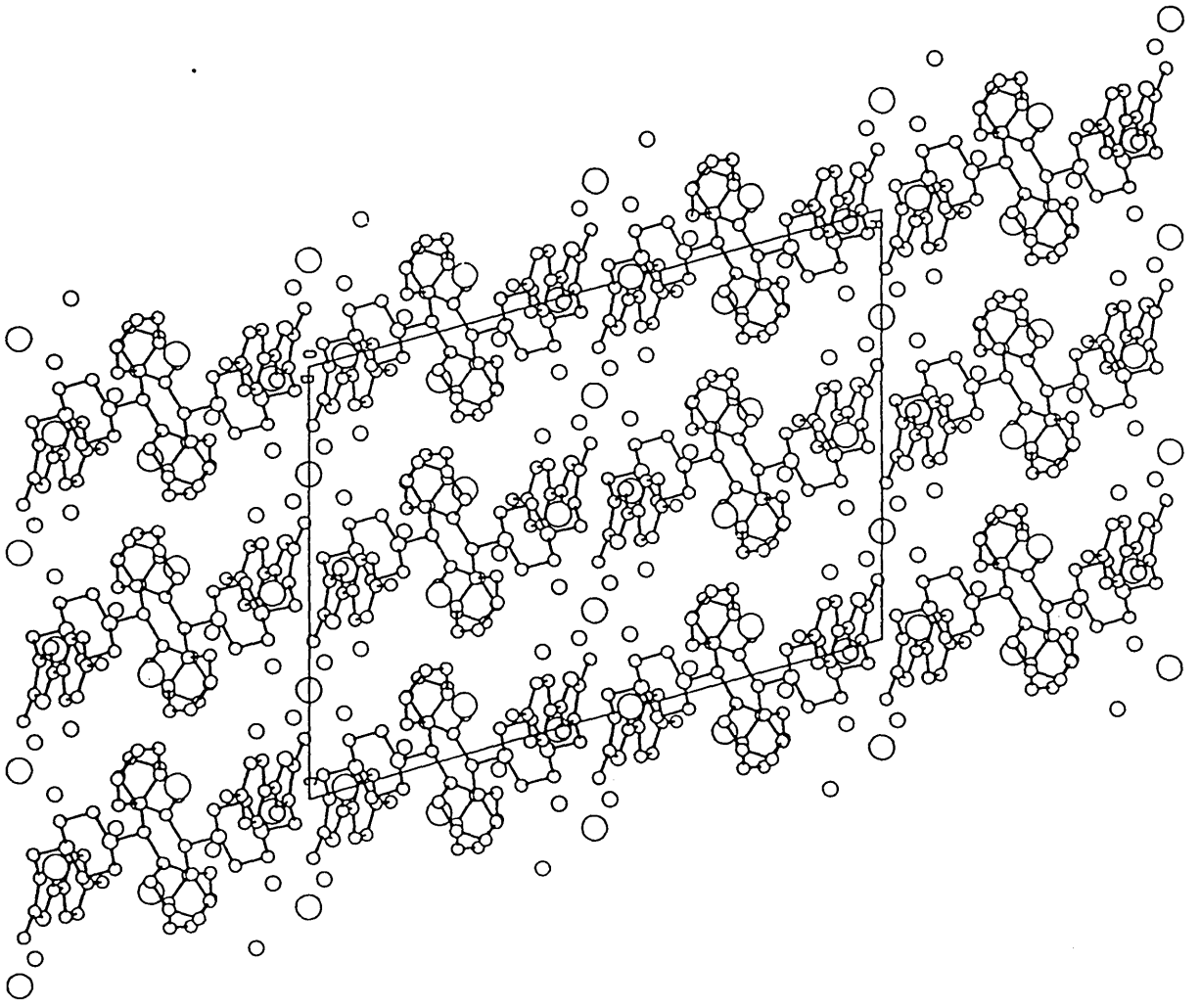

9.7 IMTHCLHYD

Crystal Data

Colourless plates from water, also formed from aqueous suspensions of Phases A or E, 1.12 x 0.60 x 0.20 mm.
$C_{29}H_{35}N_4^{3+}.3Cl^-.5H_2O$, M = 637.0, monoclinic, C2/c (No.15),
a = 26.624 (3), b = 9.412 (1), c = 28.890 (5), Å,
β = 112.355 (8)°, V = 6695.8 Å^3, Z = 8, V/Z = 840 Å^3.
Lattice parameters refined from accurately measured 2θ values (23.0° - 26.2°) for 26 reflections.
Dc = 1.26 g.cm^{-3}, μ = 2.67 cm^{-1}, F(000) = 2648,
T = 258 K.

Data Collection and Processing

St0ë STADI-4 diffractometer, MoK_α, λ = 0.71073 Å. 3599 independent data ($2 < \theta < 22°$, $0 \leq h \leq 28$, $0 \leq k \leq 10$, $0 \leq l \leq 31$) yielding 2506 data with $I \geq 3.0\ \sigma(I)$.

Structure Solution and Refinement

Solution by direct methods (SHELX 86).
$\varpi^{-1} = \sigma^2(F) + 0.000154F^2$, R = 0.1107, wR = 0.1273,
S = 1.153 based on 434 parameters. Maximum shift/esd on last cycle = 0.946. Maximum and minimum ripple in difference electron density map : 0.49 and -0.59 e.Å^{-3}.

Refinement not completed, anions and water molecules disordered and all show high thermal parameters. Two partial fragments of a water molecule refined with partial site occupancy of 0.25 each (O(6) and O(6A)). The O(6A) fragment was also refined isotropically. Hydrogen on N(1) was located and refined, but was removed when distance contracted to <0.5 Å. Hydrogen on remaining imidazole nitrogen is also contracting, N(3)-H(3) = 0.72 Å and all major shifts/esd in last cycle were associated with these two atoms. No hydrogens were located on any of the water oxygens.

6 low angle reflections were omitted from the refinement, a DIFABS absorption correction was applied to the data, but made no significant difference. A new data set was collected from another crystal, but this showed no improvement on the existing data and was rejected.

Structure Discussion

Selected bond lengths, angles and torsion angles are given in Tables 9.9.1-9.9.3. Molecular structure and molecular packing diagram (as viewed along the b-axis) are shown in Figure 9.7. The molecular packing may be described as interleaved layers of tolyl and phenyl rings running parallel to c. The anions and water molecules occupy the remaining channels. The hydrogen bonding and other close intermolecular contacts are summarised in Table 9.7. The principal hydrophobic contacts are imidazole-tolyl and phenyl-phenyl through an inversion centre.

Table 9.7 Hydrogen Bonding and Other Close Intermolecular Contacts

a) Hydrogen Bonding

Donor	Acceptor	Symmetry	D-H	H...A	D...A
Cl(1)-H(7)...	N(7)*	x,y,z	0.67	2.36	3.02(1)
Cl(2)-H(3)...	N(3)*	x,y,z	0.72	2.22	2.94(1)
Cl(3)-H(10)..	N(10)*	½-x,-½+y,½-z	0.74	2.38	3.09(1)
N(1)-H(1)....	O(1)		-	-	2.68(1)

* salt H-bonds

b) C...C Contacts Shorter than 3.75Å

C(4M).....C(22)	½-x,½-y,1-z	3.686(16)
C(4M).....C(23)	½-x,½-y,1-z	3.694(17)
C(15).....C(17)	1-x,1-y,2-z	3.724(20)
C(16).....C(16)	1-x,1-y,2-z	3.727(19)
C(15).....C(16)	1-x,1-y,2-z	3.737(18)

c) C...N Contacts Shorter than 3.75Å

C(20).....N(3)	½-x,½-y,1-z	3.602(14)
C(21).....N(3)	½-x,½-y,1-z	3.742(14)

d) C...O Contacts Shorter than 3.75Å

C(12).....O(3)	1-x,y,1½-z	3.363(20)
C(4M).....O(3)	-½+x,½+y,z	3.461(20)
C(4M).....O(5)	½-x,½+y,1½-z	3.476(19)
C(18')....O(1)	x,1-y,½+z	3.497(18)
C(17')....O(6A)	1-x,1-y,1-z	3.50(5)
C(5).....O(1)	1-x,-y,1-z	3.518(15)
C(9).....O(6A)	x,1-y,½+z	3.52(5)
C(16')....O(6A)	x,1-y,½+z	3.53(5)
C(16')....O(6A)	1-x,1-y,1-z	3.55(5)
C(8).....O(4)	1-x,1-y,1-z	3.553(17)
C(4M).....O(1)	1-x,1-y,1-z	3.557(16)
C(21).....O(1)	1-x,-y,1-z	3.560(16)
C(6).....O(1)	1-x,-y,1-z	3.585(15)
C(16')....O(6)	1-x,1-y,1-z	3.603(22)

Figure 9.7 Molecular Structure and Molecular Packing (as viewed along the b-axis) of IMTHCLHYD

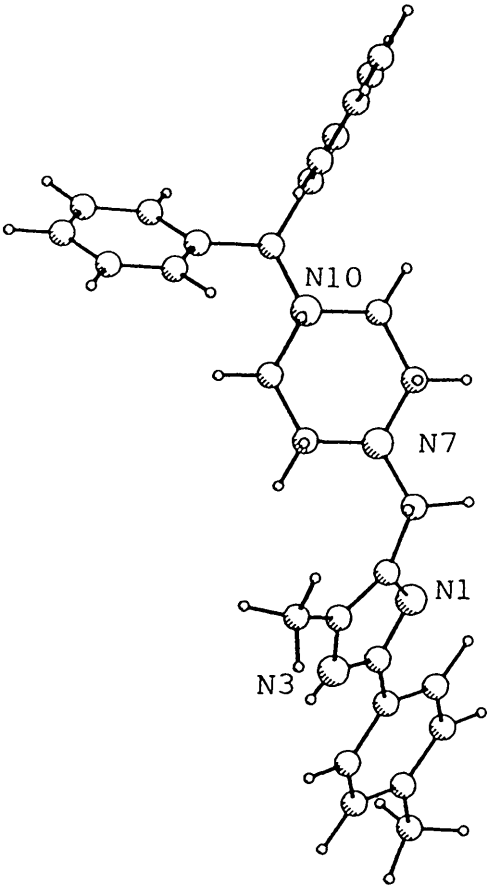

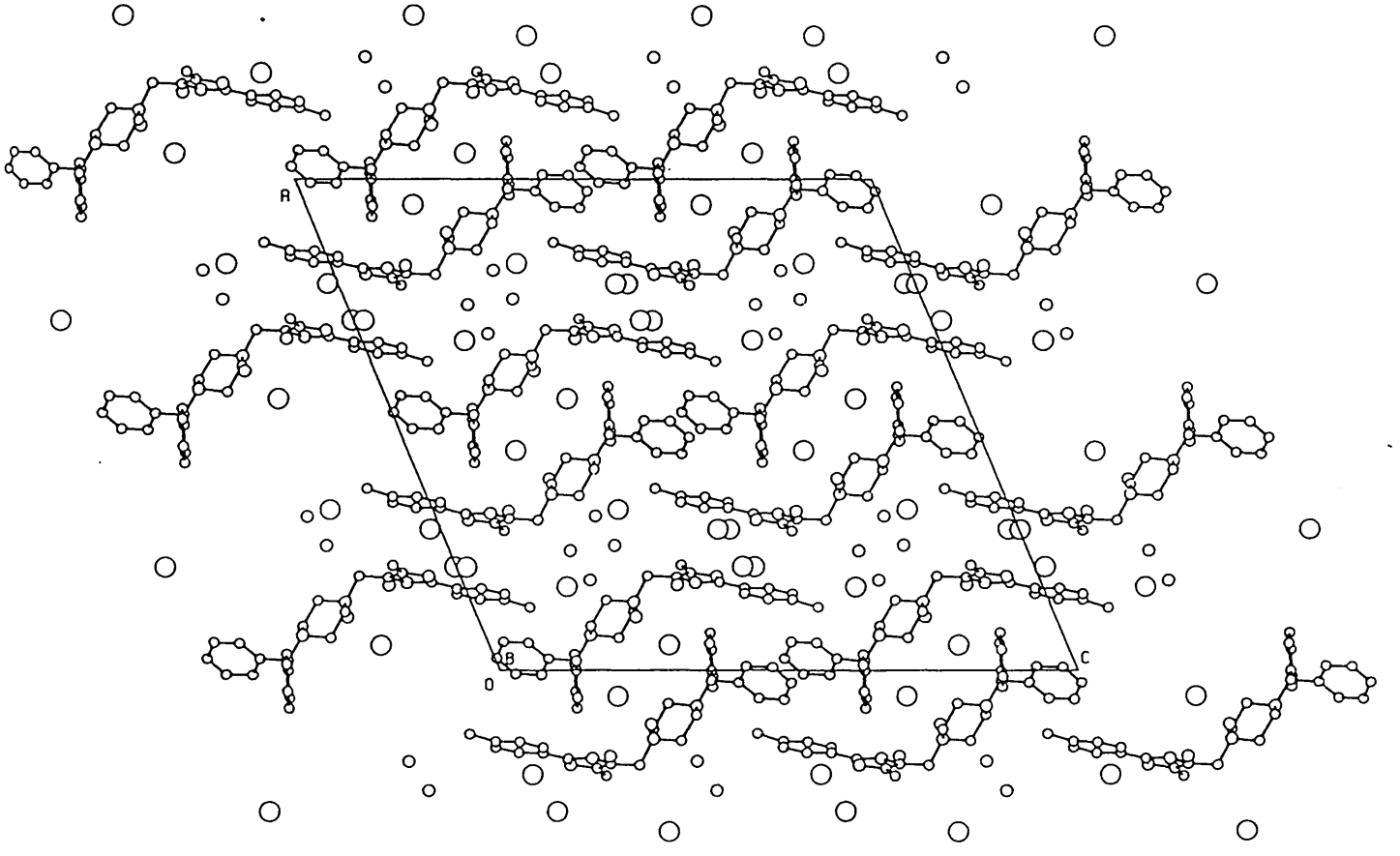

9.8 IMTHCLHYE

Crystal Data

Colourless plates from isopropanol (also from 50% v/v acetonitrile/hexane), 0.76 x 0.84 x 0.24 mm.
$C_{29}H_{35}N_4^{3+}.3Cl^-.5H_2O$, Mr = 637.0, triclinic, $P\bar{1}$ (No.2), a = 9.217 (1), b = 14.146 (2), c = 14.270 (2) Å, α = 70.88 (1), β = 87.54 (1), γ = 74.03 (1)°, V = 1706.3 Å^3, Z = 2, V/Z = 847 Å^3.
Lattice parameters refined from accurately measured 2θ values (31.0° - 31.9°) for 40 reflections.
Dc = 1.24 g.cm^{-3}, μ = 2.9 cm^{-1}, F(000) = 592, T = 290 K.

Data Collection and Processing

Stoë STADI-4 diffractometer, MoK$_\alpha$, λ = 0.71073 Å. 5127 independent data ($2 < \theta < 23°$, $-9 \leq h \leq 10$, $-14 \leq k \leq 15$, $0 \leq l \leq 16$) yielding 3849 data with $I \geq 3.0\ \sigma(I)$.

Structure Solution and Refinement

Solution by direct methods (SHELX 86).
$\varpi^{-1} = \sigma^2(F) + 0.000792F^2$, R = 0.0806, wR = 0.1238, S = 0.989 based on 410 parameters. Maximum shift/esd on last cycle = 0.035. Maximum and minimum ripple in difference electron density map : 0.70 and -0.61 e.Å^{-3}.

Anions and water molecules were all disordered, Cl(3), O(4) and O(5) were refined isotropically and these oxygens had high thermal parameters. Cl(3) was badly disordered and in an analogous fashion to Phase C was modelled in three parts with partial site occupancies of 0.4, 0.1 and 0.4. The water oxygen O(5) was modelled in a similar fashion with each of the parts having one third site occupancy. The remaining disordered water oxygen, O(4), was modelled in two parts with site occupancies of 0.75 and 0.25. No hydrogens were located on any of the water oxygens.

24 low angle reflections were omitted from the refinement. A DIFABS absorption correction was applied to the data, but made no significant difference. A new data set was collected from another crystal, but this showed no improvement on the existing data and was rejected.

Structure Discussion

Selected bond lengths, angles and torsion angles are given in Tables 9.9.1-9.9.3. Molecular structure and molecular packing diagram (as viewed along the a-axis) are shown in Figure 9.8. The cations form dimeric units around an inversion centre, with large channels parallel to b being occupied with anions and water molecules. The hydrogen bonding and other close intermolecular contacts are summarised in Table 9.8. The principal hydrophobic contacts are phenyl-tolyl and imidazole-tolyl through an inversion centre.

Table 9.8 Hydrogen Bonding and Other Close Intermolecular Contacts

a) Hydrogen Bonding

Donor	Acceptor	Symmetry	D-H	H...A	D...A
Cl(1)-H(3)...	N(3)*	x,y,z	0.72	2.39(15)	3.092(4)
N(1)-H(1)....	O(1)	2-x,-y,1-z	0.94	1.65	2.756(8)
Cl(3)-H(7)...	N(7)*	2-x,-y,1-z	0.96	2.04(5)	2.993(7)
Cl(2)-H(10)..	N(10)*	x,y,z	0.68	2.36(5)	3.019(4)
O(42).....	O(52)	x,y,z	-	-	2.83(4)
O(41).....	O(51)	x,y,z	-	-	2.88(3)
O(2).....	O(3)	x,y,-1+z	-	-	2.89(1)
O(3).....	O(3)	1-x,-y,2-z	-	-	2.90(1)
O(1).....	O(41)	1-x,-y,1-z	-	-	3.03(2)

* salt H-bonds

b) C...C Contacts Shorter than 3.75Å

C(19).....C(21)	2-x,-y,1-z	3.396(7)
C(2).....C(21)	1-x,1-y,1-z	3.446(6)
C(20).....C(20)	1-x,1-y,1-z	3.506(6)
C(19).....C(22)	2-x,-y,1-z	3.540(7)
C(5).....C(23)	1-x,1-y,1-z	3.550(6)
C(4).....C(22)	1-x,1-y,1-z	3.555(7)
C(2).....C(20)	1-x,1-y,1-z	3.604(6)
C(20).....C(21)	1-x,1-y,1-z	3.626(6)
C(2).....C(22)	1-x,1-y,1-z	3.633(6)
C(18')....C(24)	2-x,-y,1-z	3.648(9)
C(18).....C(22)	2-x,-y,1-z	3.650(8)
C(15).....C(2M)	1+x,-1+y,1+z	3.677(8)

c) C...N Contacts Shorter than 3.75Å

C(22).....N(3)	1-x,1-y,1-z	3.431(6)
C(21).....N(3)	1-x,1-y,1-z	3.549(6)
C(24).....N(1)	1-x,1-y,1-z	3.608(6)
C(23).....N(1)	1-x,1-y,1-z	3.709(6)
C(25).....N(1)	1-x,1-y,1-z	3.735(6)

d) C...O Contacts Shorter than 3.75Å

C(12).....O(5)	x,y,z	3.236(24)
C(4M).....O(5)	x,y,z	3.252(24)
C(9).....O(5)	1+x,y,z	3.267(24)
C(4).....O(5)	x,y,z	3.400(24)
C(9).....O(4)	1+x,y,z	3.400(25)
C(4M).....O(3)	x,y,z	3.438(10)
C(4M).....O(3)	1-x,-y,2-z	3.506(10)
C(9).....O(4)	1+x,y,z	3.520(17)
C(16')....O(2)	2-x,-y,1-z	3.525(9)
C(18')....O(5)	1+x,y,z	3.532(25)
C(19')....O(5)	1+x,y,z	3.535(24)
C(6).....O(1)	2-x,-y,1-z	3.549(8)
C(19).....O(1)	x,y,z	3.556(9)
C(5).....O(1)	2-x,-y,1-z	3.566(8)
C(18).....O(1)	x,y,z	3.574(9)
C(8).....O(3)	1+x,y,z	3.583(9)

Figure 9.8 Molecular Structure and Molecular Packing (as viewed along the b-axis) of IMTHCLHYE

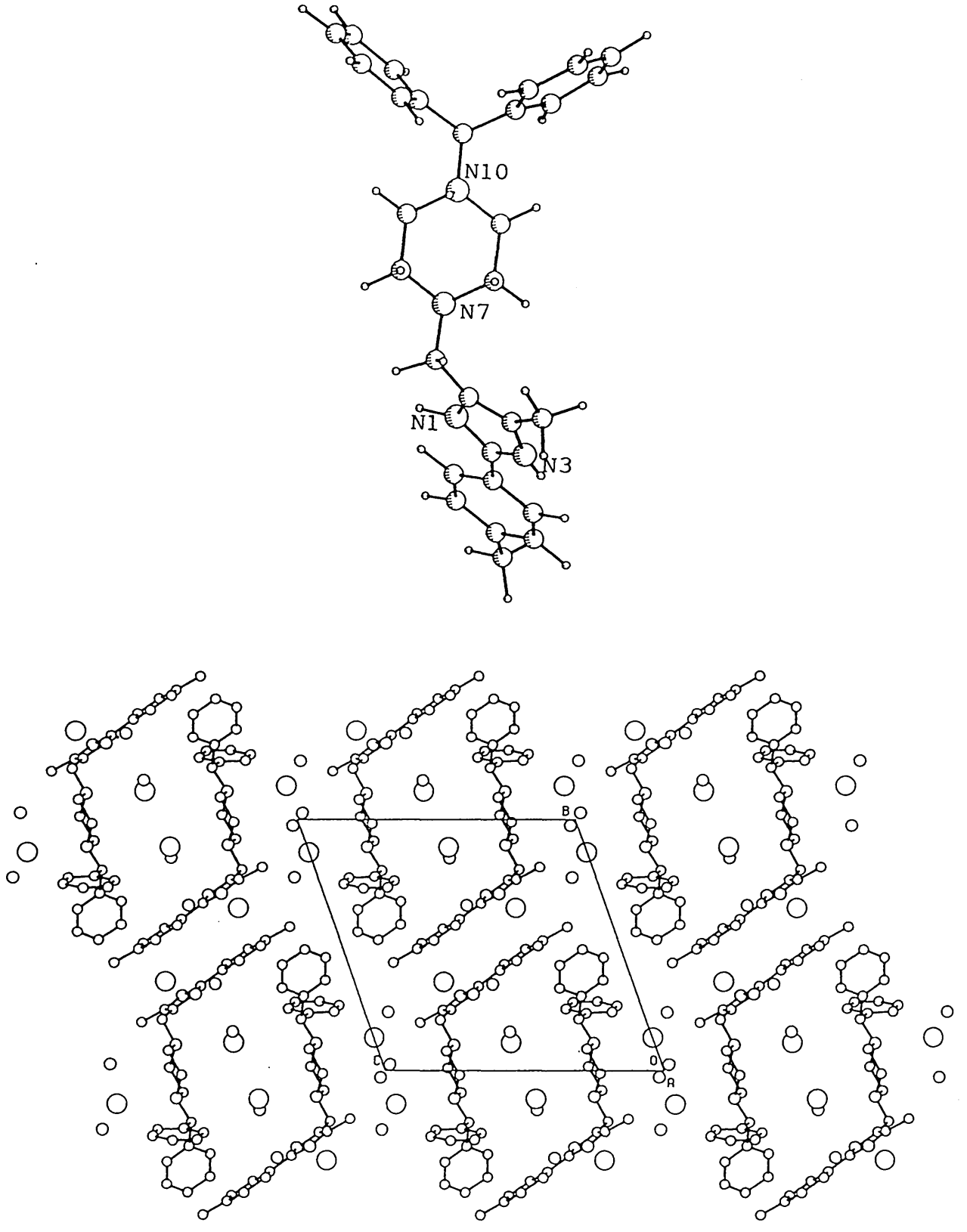

Table 9.9.1 Selected Bond Lengths for All IM Structures

	FBTOL	MHCL	MMES	THCLA	THCLB	THCLC	THCLD	THCLE
N(1) - C(2)	1.338(8)	1.321(4)	1.315(6)	1.333(4)	1.347(13)	1.32(3)	1.337(14)	1.335(5)
N(1) - C(5)	1.382(8)	1.388(4)	1.383(6)	1.384(4)	1.370(13)	1.42(3)	1.381(13)	1.364(5)
C(2) - N(3)	1.363(8)	1.350(5)	1.366(6)	1.350(5)	1.337(13)	1.37(3)	1.345(14)	1.318(5)
C(2) - C(20)	1.454(9)	1.469(5)	1.464(7)	1.454(5)	1.455(14)	1.45(3)	1.454(15)	1.448(6)
N(3) - C(4)	1.385(9)	1.366(5)	1.366(6)	1.378(5)	1.400(13)	1.38(3)	1.380(14)	1.364(6)
C(4) - C(4')	1.489(9)	1.493(5)	1.475(7)	1.491(5)	1.463(14)	1.51(3)	1.482(15)	1.488(7)
C(4) - C(5)	1.359(9)	1.364(5)	1.374(7)	1.359(5)	1.353(13)	1.37(3)	1.355(14)	1.336(6)
C(5) - C(6)	1.482(9)	1.482(5)	1.481(7)	1.484(5)	1.504(13)	1.51(3)	1.484(14)	1.488(6)
C(6) - N(7)	1.461(8)	1.514(5)	1.524(6)	1.521(4)	1.518(12)	1.52(3)	1.495(13)	1.508(5)
N(7) - C(8)	1.457(9)	1.493(5)	1.499(6)	1.490(5)	1.484(12)	1.45(3)	1.481(13)	1.500(6)
N(7) - C(12)	1.449(8)	1.485(5)	1.497(7)	1.489(4)	1.498(11)	1.51(3)	1.472(14)	1.479(6)
C(8) - C(9)	1.501(10)	1.504(5)	1.511(7)	1.517(5)	1.519(12)	1.49(3)	1.510(14)	1.505(6)
C(9) - N(10)	1.469(9)	1.467(5)	1.468(6)	1.489(4)	1.491(11)	1.51(3)	1.506(13)	1.491(6)
N(10) - C(11)	1.453(9)	1.463(5)	1.464(6)	1.510(4)	1.511(11)	1.44(3)	1.498(14)	1.493(6)
N(10) - C(13)	1.466(9)	1.476(4)	1.481(6)	1.540(4)	1.533(11)	1.52(3)	1.485(13)	1.524(5)
C(11) - C(12)	1.509(10)	1.507(5)	1.514(7)	1.513(5)	1.510(12)	1.51(3)	1.529(15)	1.531(6)
C(13) - C(14)	1.532(10)	1.516(5)	1.514(7)	1.515(5)	1.526(12)	1.50(3)	1.506(14)	1.504(6)
C(13) - C(14')	1.521(10)	1.523(5)	1.514(7)	1.523(5)	1.496(13)	1.52(3)	1.537(14)	1.525(6)
C(14) - C(15)	1.344(11)	1.373(5)	1.358(8)	1.383(5)	1.372(14)	1.41(4)	1.383(16)	1.377(7)
C(14) - C(19)	1.383(12)	1.389(6)	1.387(8)	1.397(5)	1.376(13)	1.33(4)	1.395(16)	1.376(6)
C(15) - C(16)	1.383(13)	1.374(6)	1.381(10)	1.389(6)	1.386(16)	1.34(4)	1.362(18)	1.379(8)
C(16) - C(17)	1.368(14)	1.369(7)	1.403(11)	1.379(7)	1.372(16)	1.34(5)	1.400(21)	1.367(9)
C(17) - C(18)	1.342(15)	1.351(8)	1.358(12)	1.367(7)	1.348(17)	1.38(4)	1.338(21)	1.347(9)
C(18) - C(19)	1.382(14)	1.387(7)	1.380(10)	1.386(6)	1.383(16)	1.30(4)	1.399(19)	1.377(8)
C(14') - C(15')	1.367(12)	1.384(5)	1.386(8)	1.372(6)	1.389(14)	1.38(3)	1.381(15)	1.362(7)
C(14') - C(19')	1.373(13)	1.379(6)	1.379(8)	1.390(5)	1.379(15)	1.39(3)	1.391(16)	1.372(7)
C(15') - C(16')	1.371(15)	1.383(6)	1.395(9)	1.391(7)	1.398(17)	1.37(4)	1.363(16)	1.412(8)
C(16') - C(17')	1.336(20)	1.371(7)	1.380(10)	1.372(7)	1.357(19)	1.40(4)	1.371(18)	1.354(9)
C(17') - C(18')	1.321(22)	1.358(8)	1.371(10)	1.371(7)	1.369(19)	1.35(4)	1.371(19)	1.328(10)
C(18') - C(19')	1.389(18)	1.397(7)	1.367(9)	1.393(6)	1.383(17)	1.34(4)	1.379(18)	1.406(9)
C(20) - C(21)	1.387(9)	1.388(5)	1.380(7)	1.383(5)	1.363(14)	1.37(3)	1.388(15)	1.371(6)
C(20) - C(25)	1.375(9)	1.389(5)	1.394(7)	1.386(5)	1.401(15)	1.40(3)	1.383(16)	1.381(6)
C(21) - C(22)	1.375(10)	1.384(6)	1.380(8)	1.386(6)	1.389(15)	1.34(4)	1.351(16)	1.373(7)
C(22) - C(23)	1.387(11)	1.379(6)	1.378(8)	1.374(6)	1.386(16)	1.39(4)	1.371(18)	1.376(7)
C(23) - C(23')	1.516(12)	1.509(6)	1.482(9)	1.511(6)	1.508(16)	1.52(4)	1.510(18)	1.498(8)
C(23) - C(24)	1.387(11)	1.375(6)	1.390(8)	1.394(6)	1.367(17)	1.41(4)	1.403(18)	1.349(7)
C(24) - C(25)	1.370(11)	1.380(5)	1.378(8)	1.380(6)	1.385(16)	1.39(3)	1.348(17)	1.380(7)

Table 9.9.2 Selected Bond Angles for All IM Structures

	FBTOL	MHCL	MMES	THLCA	THCLB	THCLC	THCLD	THCLE
C(2) - N(1) - C(5)	106.8(5)	104.8(3)	105.5(4)	110.3(3)	109.6(8)	109.4(17)	109.7(8)	109.3(3)
N(1) - C(2) - N(3)	108.9(5)	110.9(3)	110.7(4)	106.0(3)	107.1(9)	106.3(18)	106.8(9)	106.6(3)
N(1) - C(2) - C(20)	127.1(6)	125.8(3)	125.1(4)	126.5(3)	125.4(9)	125.7(19)	127.3(10)	126.4(4)
N(3) - C(2) - C(20)	124.0(6)	123.2(3)	124.2(4)	127.5(3)	127.5(9)	128.0(19)	125.8(10)	127.0(4)
C(2) - N(3) - C(4)	109.0(5)	108.9(3)	108.5(4)	110.7(3)	109.4(8)	111.6(17)	109.8(9)	110.4(4)
N(3) - C(4) - C(4')	120.4(6)	122.7(3)	121.9(4)	121.9(3)	122.0(8)	122.8(18)	121.5(9)	121.6(4)
N(3) - C(4) - C(5)	105.1(6)	104.6(3)	104.7(4)	106.0(3)	106.1(8)	105.1(18)	106.6(9)	106.4(4)
C(4') - C(4) - C(5)	134.4(6)	132.6(3)	133.5(5)	132.1(3)	131.9(9)	132.0(20)	131.8(9)	131.9(4)
N(1) - C(5) - C(4)	110.2(5)	110.8(3)	110.6(4)	107.0(3)	107.7(8)	107.5(18)	107.0(9)	107.3(4)
N(1) - C(5) - C(6)	120.1(5)	122.1(3)	120.7(4)	119.9(3)	119.8(8)	121.5(18)	123.1(9)	121.3(3)
C(4) - C(5) - C(6)	129.7(6)	127.1(3)	128.7(4)	132.6(3)	132.2(9)	130.9(20)	129.8(9)	131.4(4)
C(5) - C(6) - N(7)	112.0(5)	112.1(3)	112.5(4)	109.6(3)	111.3(7)	111.4(16)	113.5(8)	113.8(3)
C(6) - N(7) - C(8)	112.6(5)	112.6(3)	112.1(4)	111.1(3)	110.6(7)	111.0(15)	111.8(8)	109.5(3)
C(6) - N(7) - C(12)	110.6(5)	112.5(3)	111.5(4)	112.95(25)	111.1(7)	110.4(15)	110.6(8)	112.1(3)
C(8) - N(7) - C(12)	109.7(5)	109.0(3)	110.0(4)	109.3(3)	109.7(7)	107.8(15)	109.6(8)	109.5(3)
N(7) - C(8) - C(9)	110.7(6)	110.0(3)	110.5(4)	110.7(3)	109.5(7)	109.7(17)	111.6(8)	110.6(4)
C(8) - C(9) - N(10)	110.5(6)	111.4(3)	110.8(4)	112.4(3)	110.8(7)	114.4(16)	111.6(8)	112.2(4)
C(9) - N(10) - C(11)	106.5(5)	109.1(3)	107.9(4)	109.9(3)	108.6(6)	108.2(15)	107.4(8)	109.4(3)
C(9) - N(10) - C(13)	112.4(5)	109.4(3)	109.3(4)	110.68(25)	111.5(6)	112.7(15)	111.9(8)	110.5(3)
C(11) - N(10) - C(13)	112.4(5)	112.0(3)	113.9(4)	109.94(25)	110.5(6)	109.4(16)	110.8(8)	111.6(3)
N(10) - C(11) - C(12)	111.7(6)	110.7(3)	109.8(4)	112.3(3)	111.1(7)	110.5(17)	110.7(8)	111.6(4)
N(7) - C(12) - C(11)	111.2(5)	110.9(3)	111.5(4)	110.1(3)	110.7(7)	111.8(16)	113.0(8)	110.8(4)
N(10) - C(13) - C(14)	110.4(6)	110.8(3)	111.3(4)	111.2(3)	110.2(7)	109.0(18)	111.8(8)	112.4(3)
N(10) - C(13) - C(14')	111.2(6)	111.2(3)	109.7(4)	110.7(3)	112.6(7)	114.1(18)	111.6(8)	111.3(3)
C(14) - C(13) - C(14')	110.8(6)	110.0(3)	111.0(4)	115.0(3)	113.7(7)	115.3(19)	111.6(8)	113.9(3)
C(13) - C(14) - C(15)	121.3(7)	122.4(3)	121.4(5)	123.4(3)	123.0(8)	122.6(22)	123.8(10)	122.7(4)
C(13) - C(14) - C(19)	120.3(7)	119.8(3)	119.6(5)	117.3(3)	118.1(8)	117.3(22)	119.0(10)	119.8(4)
C(15) - C(14) - C(19)	118.4(8)	117.8(4)	119.0(5)	119.2(3)	118.7(9)	120.0(24)	117.1(10)	117.2(4)
C(14) - C(15) - C(16)	120.4(8)	121.4(4)	121.2(6)	119.9(4)	120.6(10)	118(3)	122.3(11)	120.5(5)
C(15) - C(16) - C(17)	121.4(9)	120.1(4)	118.8(7)	120.4(4)	119.2(11)	120(3)	120.3(13)	121.2(6)
C(16) - C(17) - C(18)	118.1(10)	119.7(5)	120.7(8)	119.9(4)	121.0(11)	119(3)	118.2(14)	118.7(6)
C(17) - C(18) - C(19)	121.2(10)	120.7(5)	119.1(7)	120.5(4)	119.6(11)	121(3)	122.4(13)	120.8(6)
C(14) - C(19) - C(18)	120.4(9)	120.2(4)	121.3(6)	120.0(4)	120.8(10)	120(3)	119.7(12)	121.6(5)
C(13) - C(14') - C(15')	122.0(7)	120.9(3)	122.2(5)	123.5(3)	123.0(9)	119.5(21)	124.8(9)	123.0(4)
C(13) - C(14') - C(19')	120.3(7)	120.3(3)	119.4(5)	117.5(3)	118.0(9)	120.7(20)	116.6(9)	118.0(4)
C(15') - C(14') - C(19')	117.7(8)	118.8(4)	118.4(5)	119.0(4)	119.0(9)	119.7(22)	118.6(10)	118.9(5)
C(14') - C(15') - C(16')	119.8(9)	120.7(4)	120.1(5)	121.1(4)	120.2(10)	117.4(24)	120.6(10)	120.0(5)
C(15') - C(16') - C(17')	122.8(12)	119.8(4)	120.5(6)	119.6(5)	119.7(12)	121(3)	120.6(11)	120.6(6)
C(16') - C(17') - C(18')	117.6(14)	120.5(5)	118.7(6)	120.1(5)	120.5(13)	119(3)	119.9(12)	119.1(6)
C(17') - C(18') - C(19')	122.6(14)	120.0(5)	121.2(6)	120.5(4)	120.6(12)	119(3)	119.8(12)	122.0(6)
C(14') - C(19') - C(18')	119.4(10)	120.2(4)	121.2(6)	119.7(4)	120.0(11)	122.1(24)	120.4(11)	119.3(5)
C(2) - C(20) - C(21)	119.4(6)	120.2(3)	120.1(4)	119.9(3)	121.0(9)	120.7(20)	119.5(10)	119.8(4)
C(2) - C(20) - C(25)	123.2(6)	121.3(3)	121.9(4)	121.1(3)	121.2(9)	117.5(19)	122.8(10)	120.1(4)
C(21) - C(20) - C(25)	117.4(6)	118.4(3)	118.0(5)	118.9(3)	117.8(9)	121.8(20)	117.7(10)	120.1(4)
C(20) - C(21) - C(22)	120.9(6)	119.9(3)	121.2(5)	120.4(4)	121.0(10)	119.1(22)	119.2(10)	119.2(4)
C(21) - C(22) - C(23)	121.6(7)	121.9(4)	121.2(5)	121.4(4)	121.1(10)	123.6(25)	123.8(11)	121.4(5)
C(22) - C(23) - C(23')	120.6(7)	121.3(4)	120.9(5)	121.6(4)	122.3(10)	124.0(23)	122.8(11)	120.9(5)
C(22) - C(23) - C(24)	117.1(7)	117.6(4)	117.6(5)	117.8(4)	118.2(11)	116.3(24)	116.9(12)	118.5(5)
C(23') - C(23) - C(24)	122.3(7)	121.0(4)	121.5(5)	120.6(4)	119.4(10)	119.5(23)	120.3(11)	120.5(5)
C(23) - C(24) - C(25)	120.9(7)	121.7(4)	121.6(5)	121.4(4)	120.9(11)	122.3(23)	119.7(12)	121.7(5)
C(20) - C(25) - C(24)	122.1(7)	120.5(3)	120.3(5)	120.1(4)	121.0(10)	116.7(21)	122.7(11)	119.0(4)

Table 9.9.3 Selected Torsion Angles for All IM Structures

				FBTOL	MHCL	MMES	THCLA	THCLB	THCLC	THCLD	THCLD
- N(1)	- C(2)	- N(3)		0.7(7)	0.1(4)	0.1(5)	-1.1(4)	1.0(11)	-1.4(23)	-1.5(12)	-0.1(4)
- N(1)	- C(2)	- C(20)		179.9(6)	179.4(3)	178.9(5)	177.1(3)	-179.2(9)	-179.1(20)	178.0(10)	-179.3(4)
- N(1)	- C(5)	- C(4)		-0.1(7)	0.4(4)	-0.2(5)	0.7(4)	-0.6(11)	1.6(24)	2.4(11)	-0.3(5)
- N(1)	- C(5)	- C(6)		177.7(6)	-179.6(3)	-179.7(4)	-172.3(3)	-175.0(8)	177.3(19)	179.5(9)	-177.8(4)
- C(2)	- N(3)	- C(4)		-1.1(7)	-0.4(4)	0.1(6)	1.0(4)	-1.0(11)	0.7(23)	0.1(12)	0.3(5)
- C(2)	- N(3)	- C(4)		179.6(6)	-179.8(3)	-178.8(5)	-177.2(3)	179.2(10)	178.4(20)	-179.4(10)	179.6(4)
- C(2)	- C(20)	- C(21)		-4.6(10)	22.9(5)	14.8(8)	-5.7(5)	7.2(16)	0(3)	2.3(17)	-4.4(6)
- C(2)	- C(20)	- C(25)		176.2(6)	-155.8(4)	-166.5(5)	178.0(3)	-170.8(10)	-177.4(20)	-177.6(11)	175.6(4)
- C(2)	- C(20)	- C(21)		174.5(6)	-157.9(3)	-166.6(5)	172.1(3)	-173.0(10)	-176.6(21)	-178.3(11)	176.4(4)
- C(2)	- C(20)	- C(25)		-4.6(10)	23.4(5)	12.2(8)	-4.2(6)	9.0(16)	5(3)	1.8(18)	-3.6(7)
- N(3)	- C(4)	- C(4')		-179.6(6)	-176.2(3)	-179.8(4)	178.5(3)	-179.1(9)	177.5(19)	-179.5(9)	177.7(4)
- N(3)	- C(4)	- C(5)		1.1(7)	0.6(4)	-0.2(5)	-0.5(4)	0.6(11)	0.3(23)	1.3(12)	-0.4(5)
- C(4)	- C(5)	- N(1)		-0.6(7)	-0.6(4)	0.2(5)	-0.1(4)	-0.1(10)	-1.1(23)	-2.2(11)	0.4(5)
- C(4)	- C(5)	- C(6)		-178.1(6)	179.4(3)	179.7(5)	171.7(3)	173.5(9)	-176.2(21)	-179.1(10)	177.6(4)
- C(4)	- C(5)	- N(1)		-179.8(7)	175.8(4)	179.8(5)	-179.0(4)	179.6(10)	-177.9(21)	178.7(10)	-177.5(5)
- C(4)	- C(5)	- C(6)		2.6(13)	-4.2(6)	-0.7(9)	-7.3(7)	-6.9(18)	6(4)	1.8(19)	-0.3(8)
- C(5)	- C(6)	- N(7)		-67.6(7)	-79.6(4)	86.5(5)	85.0(4)	-75.8(10)	79.7(23)	88.3(11)	-80.0(5)
- C(5)	- C(6)	- N(7)		109.7(8)	100.4(4)	-93.0(6)	-85.9(4)	111.4(11)	-105(3)	-95.2(13)	103.1(5)
- C(6)	- N(7)	- C(8)		157.0(5)	70.6(4)	65.0(5)	89.4(3)	165.1(7)	67.6(20)	67.1(10)	166.1(3)
- C(6)	- N(7)	- C(12)		-79.8(6)	-165.8(3)	-171.2(4)	-147.4(3)	-72.8(9)	-172.9(16)	-170.5(8)	-72.3(4)
- N(7)	- C(8)	- C(9)		-179.9(5)	-177.7(3)	177.4(4)	-175.4(3)	-177.8(7)	178.6(16)	177.9(8)	-178.8(3)
- N(7)	- C(8)	- C(9)		56.4(7)	56.8(4)	52.8(5)	59.3(4)	59.4(9)	57.5(20)	55.0(10)	57.9(4)
- N(7)	- C(12)	- C(11)		-179.6(5)	177.3(3)	-178.4(4)	176.2(3)	179.4(7)	178.3(16)	-178.2(8)	-179.3(3)
- N(7)	- C(12)	- C(11)		-54.7(7)	-57.1(4)	-53.4(5)	-59.6(3)	-58.0(9)	-60.3(20)	-54.5(11)	-57.6(4)
- C(8)	- C(9)	- N(10)		-61.0(7)	-58.9(4)	-58.8(5)	-56.9(4)	-61.0(9)	-57.9(21)	-59.1(10)	-57.8(5)
- C(9)	- N(10)	- C(11)		60.9(7)	59.0(4)	63.0(5)	52.6(4)	58.7(9)	55.4(21)	59.0(10)	55.7(5)
- C(9)	- N(10)	- C(13)		-175.5(6)	-178.2(3)	-172.7(4)	174.2(3)	-179.4(7)	176.6(17)	-179.3(8)	178.9(3)
- N(10)	- C(11)	- C(12)		-59.6(7)	-58.4(4)	-62.4(5)	-53.2(4)	-56.8(9)	-54.5(20)	-57.1(10)	-54.8(4)
- N(10)	- C(11)	- C(12)		176.9(5)	-179.7(3)	176.2(4)	-175.3(3)	-179.4(7)	-177.7(16)	-179.6(8)	-177.4(3)
- N(10)	- C(13)	- C(14)		-179.3(6)	64.5(4)	-166.6(4)	175.6(3)	-178.8(7)	53.9(22)	-175.3(8)	-173.9(3)
- N(10)	- C(13)	- C(14')		57.4(7)	-172.9(3)	70.1(5)	46.5(3)	53.1(9)	-175.7(17)	59.0(11)	57.0(4)
- N(10)	- C(13)	- C(14)		-59.1(7)	-174.4(3)	-45.9(5)	-62.8(3)	-57.9(9)	174.4(18)	-55.5(11)	-52.0(4)
- N(10)	- C(13)	- C(14')		177.6(6)	-51.8(4)	-169.2(4)	168.1(3)	174.0(7)	-55.2(23)	178.8(8)	179.0(3)
- C(11)	- C(12)	- N(7)		58.3(7)	58.8(4)	58.9(5)	57.4(4)	57.0(9)	60.1(21)	57.3(11)	57.3(5)
- C(13)	- C(14)	- C(15)		-45.3(9)	30.3(5)	-63.6(6)	-58.7(4)	-69.9(11)	67(3)	-66.1(13)	-77.9(5)
- C(13)	- C(14)	- C(19)		135.2(7)	-151.8(4)	115.6(5)	124.4(3)	114.2(9)	-109.6(24)	118.1(11)	107.7(4)
- C(13)	- C(14)	- C(15)		78.3(9)	-93.0(4)	58.9(7)	68.1(4)	57.6(12)	-62(3)	59.6(14)	49.8(6)
- C(13)	- C(14)	- C(19)		-101.3(8)	84.8(4)	-121.9(5)	-108.8(4)	-118.3(9)	120.6(25)	-116.2(11)	-124.6(4)
- C(13)	- C(14')	- C(15')		40.4(10)	-63.3(4)	31.4(6)	73.0(4)	50.6(12)	-57(3)	35.9(14)	50.7(6)
- C(13)	- C(14')	- C(19')		-140.8(8)	118.4(4)	-150.1(5)	-106.3(4)	-129.2(9)	125.9(22)	-144.2(10)	-132.4(4)
- C(13)	- C(14')	- C(15')		-82.7(9)	59.8(4)	-92.1(6)	-54.1(5)	-75.7(11)	69(3)	-89.9(12)	-77.6(5)
- C(13)	- C(14')	- C(19')		96.1(9)	-118.5(4)	86.4(6)	126.6(4)	104.5(10)	-106(3)	90.0(11)	99.4(5)
- C(14)	- C(15)	- C(16)		178.5(8)	178.2(4)	179.8(6)	-174.4(4)	-176.3(9)	-178(3)	-179.3(11)	-173.8(5)
- C(14)	- C(15)	- C(16)		-2.0(13)	0.4(6)	0.6(9)	2.4(6)	-0.4(15)	-1(4)	-3.5(18)	0.7(7)
- C(14)	- C(19)	- C(18)		-178.7(8)	-178.0(4)	-179.4(6)	174.9(4)	176.2(9)	-179.1(25)	177.2(11)	173.3(5)
- C(14)	- C(19)	- C(18)		1.8(13)	-0.1(6)	-0.2(9)	-2.1(6)	0.2(15)	3(4)	1.1(17)	-1.4(7)
- C(15)	- C(16)	- C(17)		1.7(14)	-0.7(7)	-1.1(10)	-0.6(6)	1.0(17)	-3(5)	3.9(20)	0.6(9)
- C(16)	- C(17)	- C(18)		-1.1(15)	0.8(8)	1.2(12)	-1.5(7)	-1.3(18)	5(5)	-1.9(22)	-1.3(9)
- C(17)	- C(18)	- C(19)		0.9(16)	-0.5(8)	-0.8(12)	1.8(7)	1.1(18)	-3(5)	-0.4(22)	0.6(9)
- C(18)	- C(19)	- C(14)		-1.3(15)	0.2(8)	0.3(11)	0.0(6)	-0.5(17)	0(4)	0.8(21)	0.7(9)
- C(14')	- C(15')	- C(16')		-179.7(9)	-179.2(4)	178.3(5)	-179.2(4)	179.9(10)	-176.5(23)	179.9(10)	177.3(5)
- C(14')	- C(15')	- C(16')		1.5(13)	-0.9(6)	-0.2(8)	0.1(6)	-0.2(16)	0(4)	0.1(17)	0.4(8)
- C(14')	- C(19')	- C(18')		179.3(10)	179.4(4)	-179.0(5)	178.2(4)	-179.1(10)	176.2(24)	-178.3(11)	-177.5(5)
- C(14')	- C(19')	- C(18')		-1.9(14)	1.0(6)	-0.5(9)	-1.1(6)	1.1(16)	0(4)	1.5(17)	-0.4(8)
- C(15')	- C(16')	- C(17')		-0.6(18)	0.0(7)	0.8(10)	0.8(7)	-1.2(18)	0(4)	-1.1(18)	0.1(9)
- C(16')	- C(17')	- C(18')		0.2(22)	0.8(8)						
- C(17')	- C(18')	- C(19')		-0.6(23)	-0.7(8)	-0.7(10)	-0.6(8)	1.7(20)	-1(4)	0.6(19)	-0.5(10)
- C(18')	- C(19')	- C(14')		1.5(20)	-0.2(8)	0.1(10)	-0.4(8)	-0.8(20)	1(4)	1.0(20)	0.5(11)
- C(20)	- C(21)	- C(22)		179.7(6)	-179.9(3)	0.6(10)	1.3(7)	-0.6(19)	0(4)	-2.1(19)	0.1(10)
- C(20)	- C(21)	- C(22)		-1.1(10)	-1.2(5)	-179.5(5)	-176.6(3)	179.7(10)	-174.3(22)	-179.0(10)	178.4(4)
- C(20)	- C(25)	- C(24)		-179.6(7)	179.8(3)	1.6(8)	-0.3(6)	-2.2(15)	3(4)	0.9(16)	-1.6(7)
- C(20)	- C(25)	- C(24)		1.3(10)	1.1(5)	179.9(5)	176.3(4)	179.9(10)	175.8(21)	178.6(11)	-179.0(4)
- C(21)	- C(22)	- C(23)		0.1(11)	0.2(6)	-1.3(8)	-0.1(6)	1.8(16)	-2(3)	-1.3(18)	1.0(7)
- C(22)	- C(23)	- C(23')		-178.7(7)	-176.8(4)	0.2(9)	1.0(6)	2.0(16)	-3(4)	0.5(18)	-0.1(7)
- C(22)	- C(23)	- C(24)		0.8(11)	0.9(6)	179.0(6)	177.9(4)	-179.4(10)	177.5(24)	176.5(12)	-175.5(5)
- C(23)	- C(24)	- C(25)		-0.6(12)	-1.0(6)	-2.3(9)	-1.4(6)	-1.3(17)	1(4)	-1.5(19)	2.4(8)
- C(23)	- C(24)	- C(25)		178.9(7)	176.7(4)	2.6(9)	1.1(6)	0.9(17)	0(4)	1.1(19)	-3.2(8)
- C(24)	- C(25)	- C(20)		-0.4(12)	0.1(6)	-178.6(6)	-178.2(4)	179.0(10)	-176.2(23)	-176.9(12)	174.8(5)
						-0.9(8)	-0.4(6)	-1.2(17)	0(4)	0.2(19)	1.5(8)

SECTION 10: GENERAL DISCUSSION OF IM STRUCTURES

10.1 Introduction

IM is a tribasic piperazinyl imidazole which can theoreticaly exist as a monoanion, neutral species (pKa_3 7.16), monocation (pKa_2 3.93), dication (pKa_1 2.68) and a trication. Two of the ionisation constants are assumed to be associated with the piperazine ring (pKa_1 and pKa_3) and the third with the substituted imidazole group (pKa_2). Only the neutral and cationic species were studied during these investigations. In solution IM can exist as an equilibrium mixture of all of these species, but in practice the relative proportions depend on the ionisation constants and the pH of the medium under consideration. The species composition as a function of pH are shown in Figure 10.1.1 and the sites and order of protonation are shown in Figure 10.1.2.

Figure 10.1.1 Species Composition as a function of pH

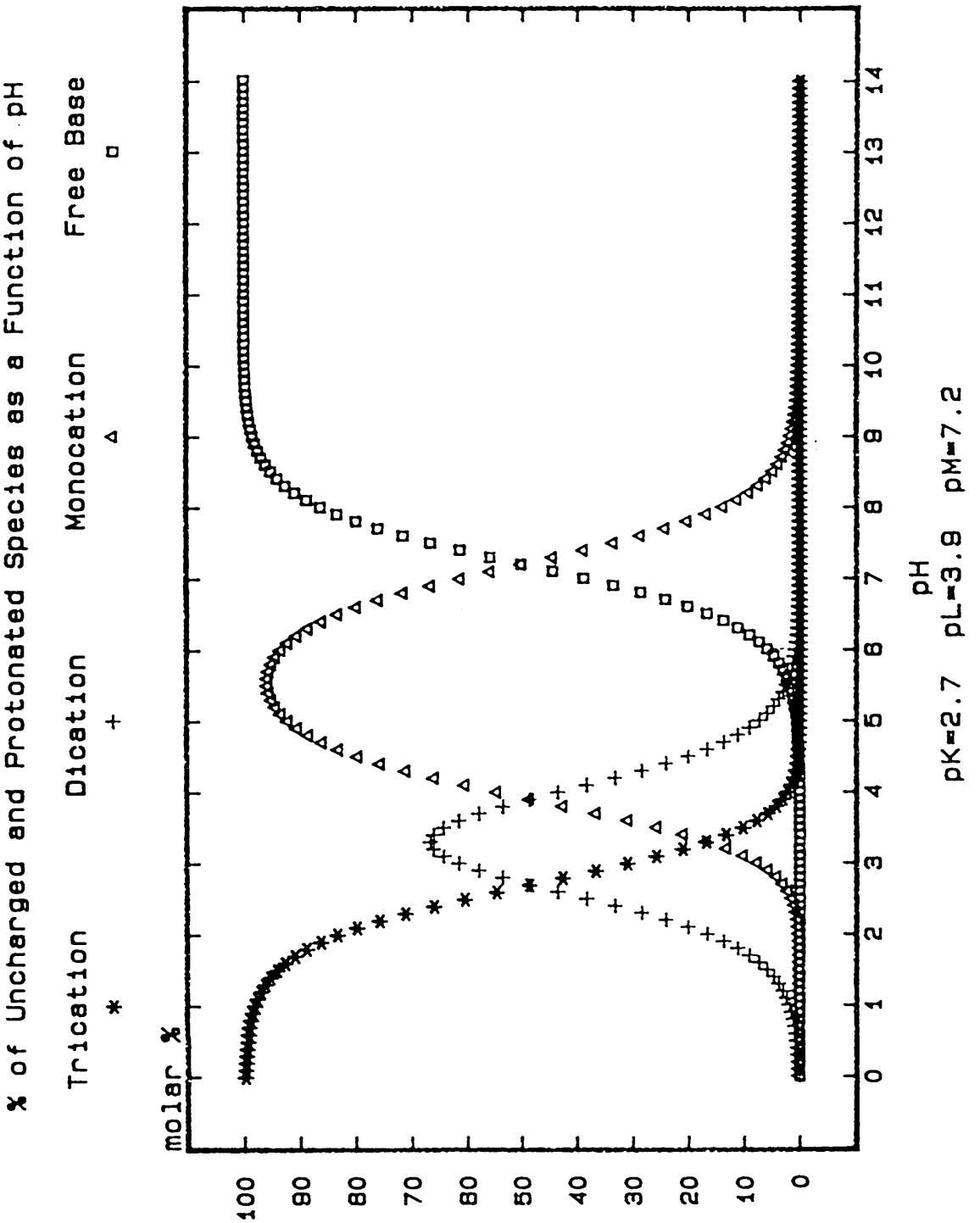

Figure 10.1.2 Sites and Orders of protonation of IM

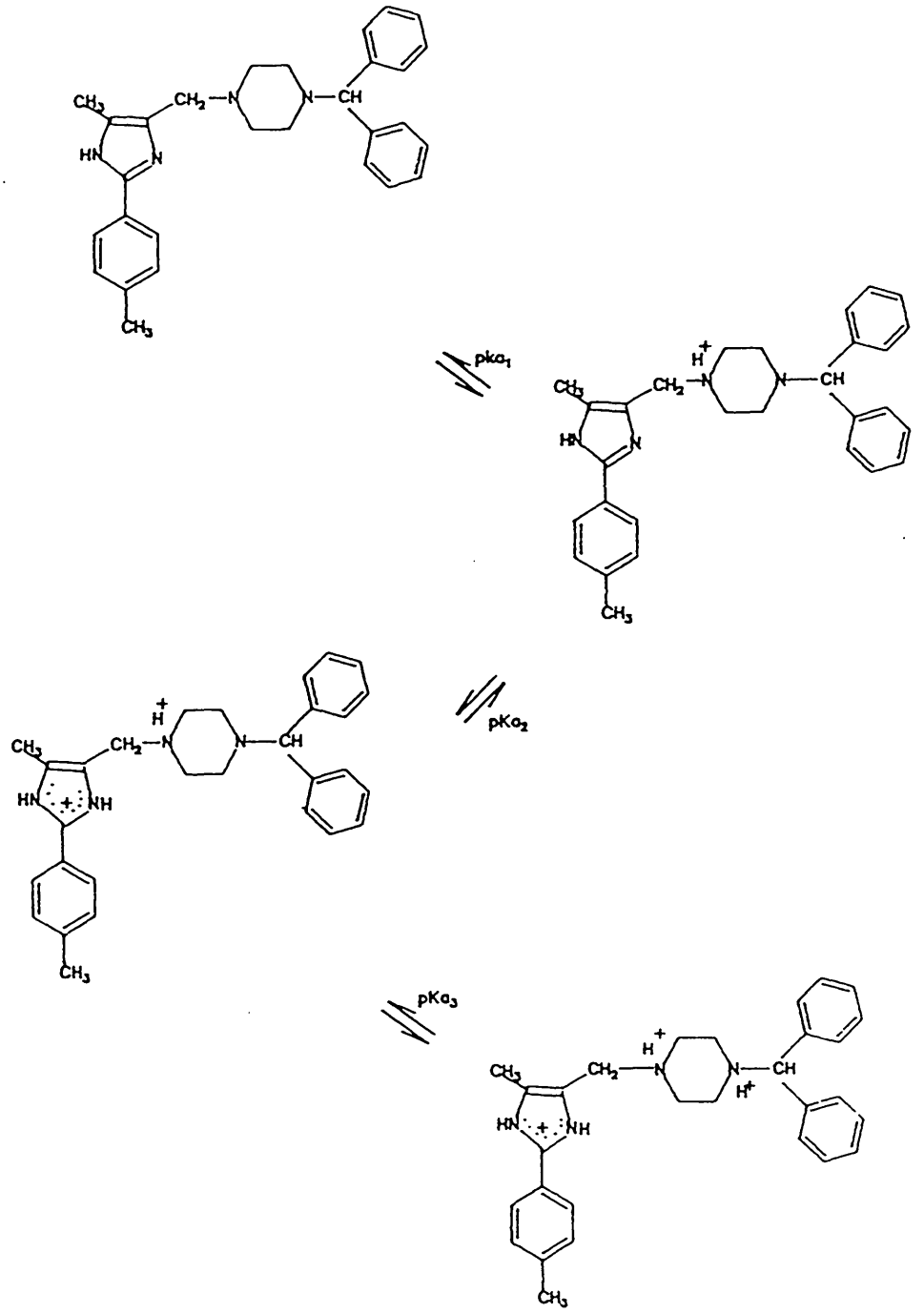

10.2 IM Tautomerism

Unsymmetrically substituted imidazoles exhibit annular tautomerism, between nitrogen atoms, where both tautomers are aromatic[1].
In the recent past annular tautomerism has been considered to require some special explanations, distinct from common prototropy. The chief reason being the very fast rate of proton transfer in annular tautomerism relative to many other types of prototropy. This is due to several factors; firstly, hetero atom-hydrogen bonds are easier to break and form than carbon-hydrogen bonds which are involved in some of the other types of tautomerism. Secondly, the partial or total charges resulting from proton gain or loss are delocalised in an aromatic ring. Thirdly, there are intermolecular associations, which facilitate proton transfer in these systems, as shown in Figure 10.2.1.

Figure 10.2.1 Imidazole inter-molecular associations

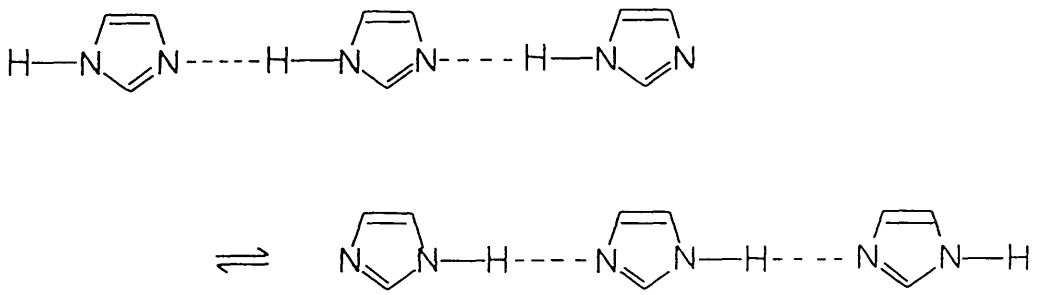

The two tautomers are referred to as the N^{π}-H (proximal) and N^{τ}-H (distal) forms, with reference to the largest of the substituents, on the 4 or 5 position of the imidazole ring. ^{13}C NMR is probably the method of choice to study

the position of the tautomeric equilibria in imidazole compounds, when derivatives representing the frozen forms of the two tautomeric possibilities are not available. Reynold *et al*[2] using these techniques concluded for the first time that the tautomeric equilibria of histidine and its 1-and 3-methyl analogues is shifted towards the distal (τ) form.

Figure 10.2.2 Structure of Histidine

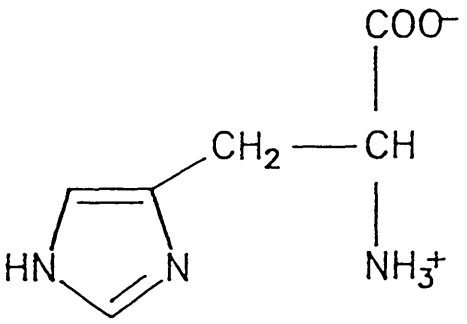

The same technique has been applied to several peptides and proteins, in most cases it has been found that the N^{τ}-H tautomer is predominant[3,4] with the occasional meaningful exception[5].
Charlton[6,7] qualitatively suggested that when considering 4 (5)-substituted imidazoles, that electron donating groups will favour the 5-substituted tautomer and electron withdrawing groups the 4-substituted tautomer.

Figure 10.2.3 Tautomerism of Monosubstituted Imidazole

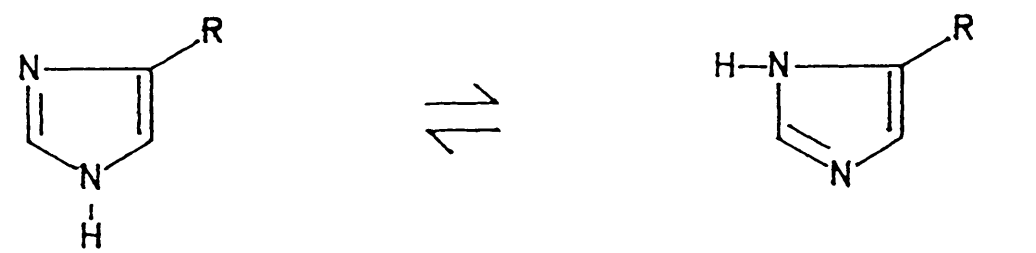

4–SUBSTITUTED (DISTAL)

5–SUBSTITUTED (PROXIMAL)

Confirmation of this hypothesis was produced by Pedroso *et al*[8], who demonstrated that the tautomeric equilibria in N^{α}-acetyl-5-nitrohistidine methyl ester was 98% in favour of the N^{π}-H tautomer. The same group of workers confirmed these findings during investigations of [5-nitro-L-histidine]α-thyroliberin[9], showing without ambiguity that the tautomeric equilibrium in the peptide is strongly shifted to the N^{π}-tautomer. They also postulated that the position of the tautomeric equilibrium determines the extent of biological activity, and that the N^{π}-H tautomer shows much reduced biological activity. This confirmed the earlier work of Deslauriers *et al*[10] on the unsubstituted peptide, thyroliberin, which showed the N^{τ}-H tautomer to be the predominant tautomeric form. Staabe and Mannschreck[11] used isotopic studies to confirm the site of deuterium uptake by 4(5)-bromoimidazole and its 2-methyl analogues. They concluded that the 4-bromo structure was the predominant structure for these compounds, again confirming Charlton's hypothesis.

X-ray crystallographic studies have produced conflicting findings. The structure of the imidazole-containing amino acid L-histidine was determined by Madden[12,13]. The tautomeric preference was found to be for the N^{τ}-H form. By contrast, histamine (the product of enzymatic decarboxylation of histidine) was found to exist in the N^{π}-form[14]. Interestingly when histamine acts as a bidentate ligand, with a metal, then these complexes are derivatives of the 4-substituted imidazole ie the N^{τ}-H form.[15,16,17 and 18]

Worth *et al*[19] have shown the importance of hydration energy on the position of the tautomeric equilibrium. A combination of quantum mechanical and molecular dynamics simulations on 4(5)-methyl imidazole have shown that the aqueous phase favours the N^{π}-H tautomer more than the gas phase.

In the present work, both the neutral and the monocationic species of IM may demonstrate annular tautomerism of the type previously described. (see Figure 10.2.4)
In the free base (IMFBTOL) and monocation (IMMMES and IMMHCLAC) structures of IM studied; all showed unambigously the N^{τ}-H tautomer, with reference to the largest substituent (R_3)

Figure 10.2.4 Tautomeric Equilibria of IM

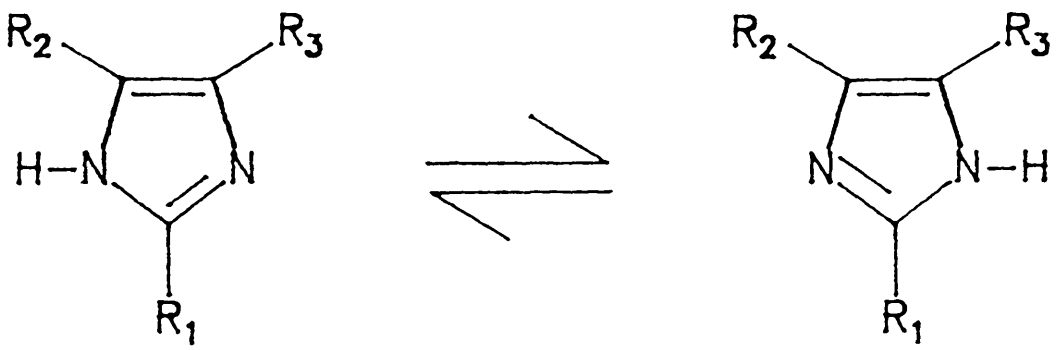

where R_1 = tolyl
R_2 = methyl
R_3 = methyl diphenyl piperazine

In all cases a single hydrogen was located on N(3) and N(1)-C(2) is shorter than N(3)-C(2), in most cases significantly so. A summary of the relevant crystallographic data are given in Table 10.2.1.

Table 10.2.1 Imidazole Bond Lengths, Tautomeric Preference and Dihedral Angle between Imidazole and Tolyl Rings in Free Base and Monoprotonated Structures of IM

Structure	Imidazole In-ring Bond Lengths (Å)					Out-ring	Tautomer	Dihedral
	N(1)-C(2)	C(2)-N(3)	N(3)-C(4)	C(4)-C(5)	C(5)-N(1)	C(2)-C(20)		Angle (ø,°)
Free Base								
IMFBTOL	1.338(8)	1.363(8)	1.385(9)	1.359(9)	1.382(8)	1.454(9)	Distal	4.57
Monoprotonated								
IMMMES	1.315(6)	1.366(6)	1.366(6)	1.374(7)	1.383(6)	1.464(7)	Distal	13.42
IMMHCLAC	1.321(4)	1.350(5)	1.366(5)	1.364(5)	1.388(4)	1.469(5)	Distal	23.27
	$\bar{x}$1.325(12)	$\bar{x}$1.360(8)	$\bar{x}$1.372(11)	$\bar{x}$1.366(8)	$\bar{x}$1.384(3)	$\bar{x}$1.462(8)		

The imidazole rings are in all cases planar, within experimental error; IMFBTOL (σ = 0.0043Å), IMMMES (σ = 0.0008Å) and IMMHCLAC (σ = 0.0024Å)

10.3 Imidazolium Cation

Protonation of the tautomerisable imidazole yields only one cation and as with the guanidinium ion (see Section 6.3), it is the conjugate acid (BH^+) of both of the tautomeric bases (B1 and B2). Some of the structural implications of its aromatic character are the two essentially equivalent C-N bonds and the strictly planar geometry of the cation. The C-N bond lengths, inter-planar angle (ϕ) between the imidazolium cation and tolyl ring and the root mean square deviation (σ) of the cation from planarity, for all of the imidazolium cations are summarised in Table 10.3.1.

An interesting feature of the molecular geometry is the observed co-planarity of the imidazolium and tolyl rings. This may arise from the combination of a hyper-conjugation effect of the 4-methyl group (located on the tolyl ring), linked to the powerful electron sink capabilities of the imidazolium ion, causing significant double bond character of the inter-ring bond (C(2)-C(20)), resulting co-planarity and charge stabilisation. The possible resonance hybrids are given in Figure 10.3.1.

Table 10.3.1 Imidazole Bond, Lengths, Planarity (σ) and Dihedral Angle between Imidazolium and Tolyl Rings in Triprotonated Structures of IM

Structure	Imidazole In-ring Bond Lengths (Å)					Out-ring	Planarity	Dihedral
	N(1)-C(2)	C(2)-N(3)	N(3)-C(4)	C(4)-C(5)	C(5)-N(1)	C(2)-C(20)	(σ,Å)	Angle (ø,°)
Triprotonated								
IMTHCLHYA	1.333(4)	1.350(5)	1.378(5)	1.359(5)	1.384(4)	1.454(5)	0.0040	7.30
IMTHCLHYB	1.347(13)	1.337(13)	1.400(13)	1.353(13)	1.370(13)	1.455(14)	0.0038	8.21
IMTHCLHYC	1.32(3)	1.37(3)	1.38(3)	1.37(3)	1.42(3)	1.45(3)	0.0060	4.03
IMTHCLHYD	1.337(14)	1.345(14)	1.380(14)	1.355(14)	1.381(13)	1.454(15)	0.0091	3.20
IMTHCLHYE	1.335(5)	1.318(5)	1.364(6)	1.336(6)	1.364(5)	1.448(6)	0.0047	4.06
Mean	1.334(10)	1.344(19)	1.380(13)	1.348(11)	1.382(20)	1.452(3)		5.4

Figure 10.3.1 Potential Resonance Hybrids for Imidazolium Cations

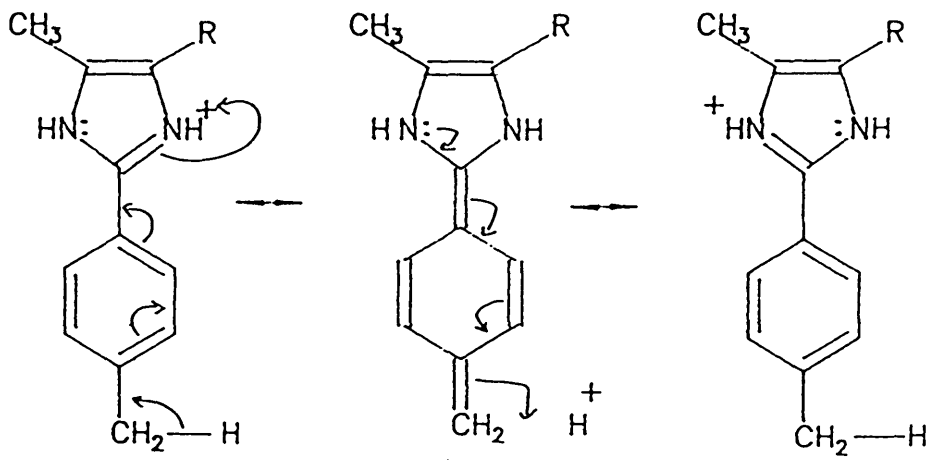

By reference to Table 10.3.1 it can be seen that the mean C(1)-N(1) and C(1)-N(2) bond lengths are equivalent and there is significant double bond character on the inter-ring bond, 1.452(3)Å; as compared with a typical phenyl-carbon, out of ring bond, in toluene of 1.53(1)Å[20]. In the free base and monoprotonated structures this hyper-conjugation effect may still occur, but it is energetically less favoured, as the resonance hybrids require two separate charges and not one as in the triprotonated forms. In the free base (IMFBTOL) co-planarity (ø=4.54°) and the consequent shortening of the inter-ring bond (1.454(9)Å) was observed. This structure is potentially stabilised by the type of inter-molecular association shown in Figure 10.2.1. This was observed in the H-bonding scheme for IMFBTOL (see Table 9.1). This inter-molecular association was not observed for the monomesylate (Table 9.2) or the monochloride (Table 9.3) and as such the degree of coplanarity ($ø_{MES}$=13.42°, $ø_{HCL}$=23.27°) and consequent shortening of the inter-ring bond (MES=1.464(7) and HCL=1.469(5) Å) is reduced.

10.4 IM Conformation

The conformation of salts and modifications of IM remains essentially the same, irrespective of the state of ionisation. Only the monoprotonated chloride (IMMHCLAC) showed any evidence of conformational changes (see Figure 9.3) and these involved rotations about the non-ring bonds, C(5)-C(6) and C(6)-N(7) and a slight twisting about C(2)-C(20). All phenyl rings are planar within experimental error. The piperazine ring exists in a half chair conformation significantly flattened towards N(7) in the free base and monoprotonated structures and towards N(10), but not significantly so, in the triprotonated structures.

This may be illustrated using the absolute in-ring torsion angles about N(10) (but excluding N(7)) and about N(7) (but excluding N(10)). These values are summarised in Table 10.4.1, together with the puckering parameters of Cremer and Pople[21] (starting from either nitrogen atom and reducing ϕ and Θ to first quadrant angles).

Table 10.4.1 IM Puckering Parameters and In-ring Piperazine Torsion Angles

Salt/ Modification	Puckering Parameters Q	q2	q3	ø	Θ	Torsion Angles (°) x̄ N(7)	x̄ N(10)
Free Base							
IMFBTOL	0.585	0.044	-0.583	26.9	-4.3	55.56	60.24
Monoprotonated							
IMMMES	0.590	0.060	-0.587	-0.4	-5.8	53.10	62.69
IMMHCLAC	0.585	0.003	-0.585	29.5	-0.35	58.71 x̄55.90	57.00 x̄59.84
Triprotonated							
IMTHCLHYA	0.572	0.047	0.570	-7.5	4.7	59.49	52.90
IMTHCLHYB	0.595	0.023	0.595	-81.2	2.2	58.70	57.74
IMTHCLHYC	0.575	0.035	0.573	29.2	3.5	58.32	54.47
IMTHCLHYD	0.574	0.018	-0.574	2.5	-1.8	57.76	55.24
IMTHCLHYE	0.577	0.038	0.575	16.7	3.7	54.71 x̄57.80 (1.84)	58.01 x̄55.67 (2.18)

Interestingly, there appears to be no difference between the free base torsion angles and the mean torsion angles for the monoprotonated structures; both are flattened towards N(7). This is in agreement with the findings for the GU structures (Section 6.4).

As explained previously, in the GU structures the positive charge is extensively delocalised over the whole guanidinium cation. This results in marginal build up of charge on the appropriate piperazine nitrogen, N(11) and only small differences in the levels of charge, between the free base and monoprotonated structures.

However, in the case of the corresponding IM structures, there is again no charge present in the free base structure, but in the monoprotonated structures the charge is located on the appropriate piperazine nitrogen, N(7). To circumvent this localisation of charge, the in-

ring and out-ring C-N bond lengths significantly lengthen (see Table 10.4.2) in the monoprotonated structures, to spread the charge over four atoms.

Table 10.4.2 IM In-ring and Out-ring Piperazine Bond Lengths

Structure	Out-ring Bond Lengths (Å)		In-ring Bond Lengths (Å)		
	N(7)-C(6)	N(10)-C(13)	x̄N(7)-C(8) /C(12)	x̄N(10)-C(9) /C(11)	C(8)-C(9) x̄C(11)-C(12)
Free Base					
IMFBTOL	1.461	1.466	1.453	1.469	1.505
Monoprotonated					
IMMMES	1.524	1.481	1.498	1.466	1.513
IMMHCLAC	1.514	1.476	1.489	1.465	1.506
	x̄1.519	x̄1.479	x̄1.494	x̄1.466	x̄1.510
Triprotonated					
IMTHCLHYA	1.521	1.540	1.490	1.500	1.515
IMTHCLHYB	1.518	1.533	1.491	1.501	1.515
IMTHCLHYC	1.52	1.522	1.498	1.498	1.498
IMTHCLHYD	1.495	1.485	1.477	1.502	1.520
IMTHCLHYE	1.508	1.524	1.490	1.492	1.518
	x̄1.512	x̄1.521	x̄1.489	x̄1.499	x̄1.513

In the triprotonated structures, the presence of a second charge on the piperazine nitrogen, N(10), results in a small flattening towards N(10), as the ring tries to maximise the separation of the two positive charges. However the flattening is not significant and in the case of IMTHCLHYE (one of the more disordered structures, see Section 9.7) the ring is actually flattened towards N(7). Again, as was the case for GU structures, the flattening of the ring is accompanied by significant lengthening of both the in-ring and out-ring C-N bond lengths at the appropriate side of the ring, as shown in Table 10.4.2.

10 References

1. ELGUERO, J, MARZIN, C, KATRITZKY, A R and LINDA, P in 'The Tautomerism of Heterocycles', p266-278, 1976 Academic Press, New York

2. REYNOLD, W F, PEAT, I R, FREEDMAN, M H and LYERLA, J R, J Amer Chem Soc, 95, 328, 1973

3. ALLERHAND, A, Acc Chem Res, 11, 469, 1978

4. WILDBUR, D J and ALLERHAND, A, J Biol Chem, 252, 4968, 1977

5. UGURBIL, K, NORTON, R S, ALLERHAND, A and BERSOHN, R, Biochemistry, 16, 886, 1977

6. CHARLTON, M, J Org Chem, 30, 3346, 1965

7. CHARLTON, M, J Chem Soc (B), 1240, 1969

8. PEDROSO, E, GRANDAS, A, LUDEVID, M-D and GIRALT, E, J Heterocyclic Chem, 23, 921, 1986

9. GIRALT, E, LUDEVID, M-D and PEDROSO, E, Bioorganic Chemistry, 14, 405, 1986

10. DESLAURIERS, R, McGREGOR, W H, SARANTAKIS, D and SMITH, C P, Biochemistry , 13, 3443, 1974

11. STAABE, H A and MANNSCHRECK, A, Angew Chem, 75, 300, 1963

12. MADDEN, J J, McGANDY, E L and SEEMAN, N C, Acta Cryst, B28, 2377, 1972(a)

13. MADDEN, J J, McGANDY, E L and SEEMAN, N C, *ibid*, B28, 2382, 1972(b)

14. BONNET, J J and IBERS, J A, J Amer Chem Soc 95,4829, 1973

15. BONNET, J J and JEANIN, Y, Acta Cryst, B26, 318, 1970(a)

16. BONNETT, J J and JEANIN, Y, C R Acad Sci, Ser C, 271, 1329, 1970(b)

17. BONNETT J J and JEANIN Y, Bull Soc Fr Minearal, Cristallogr, 93, 287, 1970(c)

18. BONNETT J J and JEANIN Y, *ibid*, 95, 61, 1972

19. WORTH, G A, KING, P M and RICHARDS, W G, Biochimica et Biophysica Acta, 993, 134, 1989

20. Typical Bond Lengths in 'Handbook of Chemistry and Physics', 67th Ed, pF-158, 1986, CRC Press, Flordia

21. CREMER, D and POPLE, J A, J Amer Chem Soc, 97, 1354, 1975

APPENDIX A

Table A.1 Positional and thermal parameters for GUFBHY

	x	y	z	U_{eq}
C(1)	-0.1772(6)	0.4780(5)	0.10601(20)	0.027(3)
N(2)	-0.0369(5)	0.4194(5)	0.10414(18)	0.034(3)
N(3)	-0.2865(4)	0.4156(4)	0.13016(16)	0.0311(25)
N(11)	-0.1992(4)	0.6068(4)	0.07663(15)	0.0260(23)
C(12)	-0.1154(5)	0.6362(5)	0.02702(20)	0.031(3)
C(13)	-0.1147(5)	0.7999(5)	0.01274(21)	0.030(3)
N(14)	-0.2682(4)	0.8547(4)	0.00660(16)	0.0276(24)
C(15)	-0.3343(5)	0.8419(5)	0.06096(19)	0.030(3)
C(16)	-0.3454(5)	0.6789(5)	0.07559(20)	0.030(3)
C(21)	-0.2542(5)	0.3101(5)	0.17275(20)	0.031(3)
C(22)	-0.3428(6)	0.1846(6)	0.17430(22)	0.039(3)
C(23)	-0.3159(6)	0.0820(6)	0.21658(23)	0.045(4)
Cl(23)	-0.42595(19)	-0.07601(18)	0.21875(8)	0.0811(13)
C(24)	-0.2036(6)	0.1000(6)	0.25873(23)	0.044(4)
C(25)	-0.1178(5)	0.2247(6)	0.25591(20)	0.039(3)
Cl(25)	0.03077(17)	0.24906(17)	0.30557(6)	0.0554(9)
C(26)	-0.1415(6)	0.3310(5)	0.21504(19)	0.032(3)
C(31)	-0.2732(5)	0.9985(5)	-0.01910(21)	0.027(3)
C(32)	-0.2543(5)	1.0064(5)	-0.07703(21)	0.029(3)
O(32)	-0.2422(4)	0.8734(4)	-0.10421(14)	0.0473(24)
C(3M)	-0.2165(7)	0.8741(6)	-0.16209(22)	0.054(4)
C(33)	-0.2520(5)	1.1415(5)	-0.10443(21)	0.032(3)
C(34)	-0.2680(5)	1.2710(5)	-0.07466(22)	0.032(3)
O(34)	-0.2553(4)	1.4026(4)	-0.10297(15)	0.0412(24)
C(35)	-0.2904(5)	1.2673(5)	-0.01818(21)	0.032(3)
C(36)	-0.2923(5)	1.1300(5)	0.00937(20)	0.031(3)
O(1W)	0.4307(5)	0.3921(4)	0.06999(19)	0.051(3)
H(2A)	0.0463	0.4908	0.1022	0.0500
H(2B)	-0.0201	0.3430	0.1228	0.0500
H(12A)	-0.0027	0.5995	0.0353	0.0500
H(12B)	-0.1656	0.5761	-0.0082	0.0500
H(13A)	-0.0622	0.8161	-0.0260	0.0500
H(13B)	-0.0543	0.8596	0.0459	0.0500
H(15A)	-0.2653	0.8979	0.0928	0.0500
H(15B)	-0.4433	0.8907	0.0583	0.0500
H(16A)	-0.4191	0.6254	0.0447	0.0500
H(16B)	-0.3890	0.6685	0.1163	0.0500
H(22)	-0.4319	0.1676	0.1427	0.0500
H(24)	-0.1849	0.0202	0.2919	0.0500
H(25)	-0.0740	0.4291	0.2156	0.0500
H(3M1)	-0.2164	0.7601	-0.1751	0.0500
H(3M2)	-0.1103	0.9229	-0.1687	0.0500
H(3M3)	-0.3021	0.9329	-0.1864	0.0500
H(33)	-0.2379	1.1455	-0.1488	0.0500
H(34)	-0.3152	1.4747	-0.0871	0.0500
H(35)	-0.3063	1.3682	0.0046	0.0500
H(36)	-0.3090	1.1270	0.0536	0.0500
H(1W)	0.4103	0.3222	0.0557	0.0500
H(2W)	0.5156	0.3885	0.0907	0.0500

	U_{11}	U_{22}	U_{33}	U_{23}	U_{13}	U_{12}
C(1)	0.030(3)	0.024(3)	0.027(3)	-0.006(3)	-0.006(3)	0.002(3)
N(2)	0.030(3)	0.028(3)	0.045(3)	0.014(2)	0.003(2)	0.010(2)
N(3)	0.031(3)	0.024(2)	0.038(3)	0.011(2)	0.002(2)	-0.002(2)
N(11)	0.024(2)	0.025(2)	0.029(2)	0.006(2)	0.001(2)	0.005(2)
C(12)	0.032(3)	0.030(3)	0.031(3)	0.008(3)	0.003(2)	0.004(3)
C(13)	0.021(3)	0.032(3)	0.038(3)	0.008(2)	0.002(2)	0.006(2)
N(14)	0.025(2)	0.023(2)	0.035(3)	0.009(2)	0.002(2)	0.004(2)
C(15)	0.029(3)	0.029(3)	0.032(3)	0.004(3)	0.007(2)	0.000(2)
C(16)	0.030(3)	0.029(3)	0.031(3)	0.007(2)	0.000(3)	0.005(2)
C(21)	0.030(3)	0.032(3)	0.030(3)	0.007(3)	0.005(3)	0.006(3)
C(22)	0.034(3)	0.039(3)	0.044(4)	0.014(3)	-0.005(3)	-0.002(3)
C(23)	0.043(4)	0.038(3)	0.052(4)	0.011(3)	0.004(3)	-0.005(3)
Cl(23)	0.077(1)	0.060(1)	0.104(2)	0.042(1)	-0.016(1)	-0.027(1)
C(24)	0.046(4)	0.042(3)	0.044(4)	0.012(3)	0.003(3)	0.007(3)
C(25)	0.039(3)	0.048(4)	0.030(3)	0.001(3)	-0.003(3)	0.008(3)
Cl(25)	0.055(1)	0.066(1)	0.044(1)	0.010(1)	-0.015(1)	0.004(1)
C(26)	0.038(3)	0.033(3)	0.025(3)	0.005(3)	0.000(3)	0.005(3)
C(31)	0.023(3)	0.027(3)	0.030(3)	0.001(3)	0.000(2)	0.003(2)
C(32)	0.028(3)	0.024(3)	0.036(4)	-0.006(3)	0.000(3)	0.000(2)
O(32)	0.078(3)	0.029(2)	0.035(2)	-0.007(2)	0.005(2)	0.002(2)
C(3M)	0.072(4)	0.048(4)	0.040(4)	-0.010(3)	0.003(3)	0.016(3)
C(33)	0.032(3)	0.027(3)	0.035(3)	0.003(3)	0.003(3)	0.004(2)
C(34)	0.027(3)	0.030(3)	0.037(3)	0.009(3)	0.000(3)	-0.001(3)
O(34)	0.047(2)	0.029(2)	0.049(3)	0.010(2)	0.015(2)	0.007(2)
C(35)	0.032(3)	0.022(3)	0.040(3)	-0.002(3)	-0.003(3)	0.003(2)
C(36)	0.031(3)	0.032(3)	0.030(3)	0.002(3)	0.002(2)	0.001(3)
O(1W)	0.040(3)	0.030(2)	0.083(4)	-0.007(2)	-0.014(2)	0.003(2)

Table A.2 Positional and thermal parameters for GUFBIP

	x	y	z	U_{eq}
C(1)	0.1918(7)	0.5033(6)	0.5602(5)	0.029(5)
N(2)	0.1362(6)	0.5382(5)	0.6568(5)	0.039(4)
N(3)	0.2742(5)	0.5816(5)	0.5263(4)	0.031(4)
N(11)	0.1558(5)	0.3755(4)	0.4973(4)	0.028(4)
C(12)	0.0213(6)	0.2908(5)	0.4882(5)	0.029(5)
C(13)	0.0270(7)	0.1554(6)	0.4558(5)	0.034(5)
N(14)	0.0851(5)	0.1145(4)	0.3493(4)	0.028(4)
C(15)	0.2220(6)	0.1998(5)	0.3681(6)	0.033(5)
C(16)	0.2157(7)	0.3341(5)	0.3944(5)	0.033(5)
C(21)	0.3424(6)	0.7036(6)	0.6058(5)	0.028(5)
C(22)	0.3459(6)	0.8077(6)	0.5769(6)	0.035(5)
C(23)	0.4207(7)	0.9273(6)	0.6523(6)	0.034(5)
Cl(23)	0.42201(21)	1.05676(17)	0.61543(16)	0.0547(14)
C(24)	0.4942(7)	0.9478(6)	0.7552(6)	0.036(5)
C(25)	0.4909(6)	0.8435(7)	0.7828(5)	0.036(5)
Cl(25)	0.58501(21)	0.86378(20)	0.91120(17)	0.0666(17)
C(26)	0.4181(6)	0.7220(6)	0.7105(5)	0.032(5)
C(31)	0.0789(6)	-0.0163(6)	0.3123(5)	0.027(5)
C(32)	-0.0433(7)	-0.1090(6)	0.2518(5)	0.030(5)
O(32)	-0.1486(4)	-0.0643(4)	0.2291(4)	0.040(3)
C(3M)	-0.2677(7)	-0.1548(7)	0.1544(6)	0.046(6)
C(33)	-0.0539(7)	-0.2360(6)	0.2196(5)	0.029(5)
C(34)	0.0597(7)	-0.2728(6)	0.2438(5)	0.032(5)
O(34)	0.0404(5)	-0.4002(4)	0.2134(4)	0.042(4)
C(35)	0.1824(7)	-0.1850(6)	0.2971(5)	0.032(5)
C(36)	0.1915(7)	-0.0571(6)	0.3323(5)	0.034(5)
C(1A)	0.4889(8)	0.4071(7)	0.6790(8)	0.073(8)
C(2A)	0.6241(8)	0.4772(7)	0.7553(6)	0.053(6)
O(2A)	0.7297(5)	0.4334(4)	0.7009(4)	0.048(4)
C(3A)	0.6328(11)	0.4572(10)	0.8664(7)	0.103(10)
C(1B)	-0.1860(10)	0.2378(9)	0.0418(7)	0.081(8)
C(2B)	-0.1165(8)	0.1646(8)	0.0881(6)	0.056(6)
O(2B)	-0.1194(6)	0.2025(5)	0.2073(4)	0.059(4)
C(3B)	0.0258(11)	0.1770(12)	0.0684(8)	0.143(13)
H(2A)	0.0795	0.4851	0.6842	0.0500
H(2B)	0.1452	0.6136	0.6851	0.0500
H(12A)	-0.0128	0.3200	0.5695	0.0500
H(12B)	-0.0498	0.2955	0.4236	0.0500
H(13A)	-0.0751	0.0937	0.4423	0.0500
H(13B)	0.0902	0.1489	0.5245	0.0500
H(15A)	0.2843	0.1969	0.4392	0.0500
H(15B)	0.2666	0.1701	0.2922	0.0500
H(16A)	0.1535	0.3373	0.3233	0.0500
H(16B)	0.3176	0.3961	0.4080	0.0500
H(22)	0.2906	0.7955	0.4958	0.0500
H(24)	0.5526	1.0418	0.8125	0.0500
H(26)	0.4195	0.6423	0.7342	0.0500
H(3M1)	-0.3320	-0.0966	0.1472	0.0500
H(3M2)	-0.3168	-0.2195	0.1927	0.0500
H(3M3)	-0.2515	-0.2077	0.0704	0.0500
H(33)	-0.1500	-0.3063	0.1759	0.0500
H(34)	0.1059	-0.4154	0.2328	0.0500
H(35)	0.2715	-0.2146	0.3119	0.0500
H(36)	0.2882	0.0123	0.3762	0.0500
H(1A1)	0.4068	0.4325	0.7214	0.0500
H(1A2)	0.4746	0.3069	0.6553	0.0500
H(1A3)	0.4889	0.4300	0.6032	0.0500
H(2A1)	0.6361	0.5759	0.7716	0.0500
H(2AO)	0.7336	0.4397	0.6339	0.0500
H(3A1)	0.5570	0.4981	0.9065	0.0500
H(3A2)	0.7327	0.5100	0.9174	0.0500
H(3A3)	0.6102	0.3600	0.8595	0.0500
H(1B1)	-0.1925	0.2115	-0.0495	0.0500
H(1B2)	-0.1345	0.3377	0.0842	0.0500
H(1B3)	-0.2876	0.2174	0.0619	0.0500
H(2B1)	-0.1713	0.0659	0.0425	0.0500
H(2BO)	-0.0956	0.1561	0.2309	0.0500
H(3B1)	0.0271	0.1465	-0.0222	0.0500
H(3B2)	0.1021	0.1491	0.1090	0.0500
H(3B3)	0.0477	0.2787	0.1044	0.0500

	U_{11}	U_{22}	U_{33}	U_{23}	U_{13}	U_{12}
C(1)	0.030(4)	0.029(4)	0.022(4)	0.008(3)	0.002(3)	0.013(3)
N(2)	0.044(4)	0.027(3)	0.037(4)	0.007(3)	0.019(3)	0.010(3)
N(3)	0.031(3)	0.021(3)	0.034(4)	0.008(3)	0.010(3)	0.008(3)
N(11)	0.032(3)	0.020(3)	0.026(3)	0.004(3)	0.010(3)	0.007(3)
C(12)	0.029(4)	0.022(4)	0.029(4)	0.006(3)	0.006(3)	0.006(3)
C(13)	0.036(4)	0.034(4)	0.024(4)	0.012(3)	0.009(3)	0.012(3)
N(14)	0.026(3)	0.019(3)	0.030(3)	0.005(2)	0.008(3)	0.004(3)
C(15)	0.031(4)	0.022(4)	0.035(4)	0.005(3)	0.010(3)	0.004(3)
C(16)	0.031(4)	0.024(4)	0.036(4)	0.008(3)	0.014(3)	0.008(3)
C(21)	0.021(4)	0.024(4)	0.032(4)	0.006(3)	0.007(3)	0.010(3)
C(22)	0.027(4)	0.038(5)	0.031(4)	0.010(4)	0.011(3)	0.012(3)
C(23)	0.030(4)	0.022(4)	0.040(5)	0.008(4)	0.015(4)	0.007(3)
Cl(23)	0.072(1)	0.029(1)	0.052(1)	0.015(1)	0.019(1)	0.013(1)
C(24)	0.029(4)	0.029(4)	0.035(5)	-0.001(3)	0.003(4)	0.003(3)
C(25)	0.025(4)	0.045(5)	0.029(4)	0.008(4)	0.001(3)	0.017(4)
Cl(25)	0.059(1)	0.070(1)	0.047(1)	0.010(1)	-0.017(1)	0.016(1)
C(26)	0.025(4)	0.028(4)	0.034(4)	0.005(3)	0.002(3)	0.010(3)
C(31)	0.026(4)	0.024(4)	0.026(4)	0.008(3)	0.007(3)	0.007(3)
C(32)	0.032(4)	0.029(4)	0.022(4)	0.010(3)	0.008(3)	0.013(4)
O(32)	0.029(3)	0.033(3)	0.046(3)	0.009(2)	-0.002(2)	0.012(2)
C(3M)	0.028(4)	0.053(5)	0.041(5)	0.006(4)	-0.003(4)	0.014(4)
C(33)	0.031(4)	0.026(4)	0.020(4)	0.003(3)	0.000(3)	0.006(3)
C(34)	0.049(5)	0.018(4)	0.023(4)	0.009(3)	0.010(4)	0.008(4)
O(34)	0.041(3)	0.026(3)	0.047(3)	0.010(2)	0.003(3)	0.013(2)
C(35)	0.035(4)	0.017(4)	0.036(4)	0.007(3)	0.004(4)	0.006(3)
C(36)	0.032(4)	0.037(5)	0.024(4)	0.010(3)	0.003(3)	0.009(4)
C(1A)	0.052(6)	0.054(6)	0.100(8)	0.035(5)	0.018(6)	0.019(5)
C(2A)	0.056(6)	0.047(5)	0.048(5)	0.016(4)	0.020(5)	0.028(4)
O(2A)	0.052(3)	0.050(3)	0.036(3)	0.021(3)	0.015(3)	0.028(3)
C(3A)	0.110(8)	0.125(9)	0.067(7)	0.055(7)	0.051(7)	0.059(7)
C(1B)	0.098(8)	0.091(7)	0.042(6)	0.035(5)	0.014(5)	0.034(6)
C(2B)	0.056(6)	0.063(5)	0.033(5)	0.008(4)	0.009(4)	0.014(4)
O(2B)	0.084(4)	0.049(4)	0.036(3)	0.014(3)	0.022(3)	0.038(3)
C(3B)	0.096(9)	0.250(16)	0.062(7)	0.067(9)	0.040(7)	0.089(10)

Table A.3 Positional and thermal parameters for GUFBIB

	x	y	z	U_{eq}
C(1)	0.1887(6)	0.5025(6)	0.5636(5)	0.032(5)
N(2)	0.1415(6)	0.5331(5)	0.6578(5)	0.042(4)
N(3)	0.2677(5)	0.5822(4)	0.5289(4)	0.034(4)
N(11)	0.1530(5)	0.3788(4)	0.4994(4)	0.033(4)
C(12)	0.0191(6)	0.2950(5)	0.4902(5)	0.034(4)
C(13)	0.0261(6)	0.1621(5)	0.4592(5)	0.032(4)
N(14)	0.0783(5)	0.1268(4)	0.3565(4)	0.031(4)
C(15)	0.2149(6)	0.2087(5)	0.3721(6)	0.038(5)
C(16)	0.2085(6)	0.3429(5)	0.3996(5)	0.035(4)
C(21)	0.3414(6)	0.6992(5)	0.6049(5)	0.031(4)
C(22)	0.3419(6)	0.8042(5)	0.5761(5)	0.033(4)
C(23)	0.4212(7)	0.9186(5)	0.6475(6)	0.041(5)
Cl(23)	0.41982(21)	1.04984(16)	0.61086(16)	0.0579(14)
C(24)	0.5026(7)	0.9349(6)	0.7460(6)	0.039(5)
C(25)	0.5009(6)	0.8300(6)	0.7711(5)	0.042(5)
Cl(25)	0.60564(21)	0.84368(20)	0.89246(17)	0.0716(16)
C(26)	0.4240(6)	0.7135(6)	0.7038(5)	0.040(5)
C(31)	0.0735(6)	-0.0027(5)	0.3186(5)	0.030(4)
C(32)	-0.0486(6)	-0.0910(6)	0.2610(5)	0.032(4)
O(32)	-0.1547(4)	-0.0437(4)	0.2384(4)	0.043(3)
C(3M)	-0.2726(7)	-0.1282(6)	0.1618(5)	0.046(5)
C(33)	-0.0608(6)	-0.2170(5)	0.2279(5)	0.034(5)
C(34)	0.0532(6)	-0.2556(5)	0.2532(5)	0.030(4)
O(34)	0.0330(5)	-0.3819(4)	0.2235(4)	0.043(3)
C(35)	0.1757(7)	-0.1709(5)	0.3049(5)	0.037(5)
C(36)	0.1851(6)	-0.0452(6)	0.3389(5)	0.035(5)
C(1A)	0.4896(8)	0.3883(7)	0.6445(7)	0.071(7)
C(2A)	0.6264(10)	0.4540(8)	0.7339(7)	0.085(8)
O(2A)	0.7385(4)	0.4208(4)	0.6893(4)	0.050(4)
C(3A)	0.6190(11)	0.4214(10)	0.8334(10)	0.106(4)
C(4A')	0.7380(18)	0.5150(16)	0.9236(14)	0.075(5)
C(4A")	0.525(3)	0.4802(23)	0.9035(21)	0.132(9)
C(1B')	-0.217(4)	0.215(3)	0.018(3)	0.132(11)
C(2B)	-0.1183(10)	0.1671(9)	0.0913(9)	0.089(3)
O(2B)	-0.1192(6)	0.2174(5)	0.2073(4)	0.060(4)
C(3B')	0.0186(14)	0.1631(13)	0.0672(11)	0.137(5)
C(4B')	0.071(3)	0.304(3)	0.082(3)	0.186(13)
C(3B")	-0.1499(25)	0.2749(23)	0.0455(19)	0.097(7)
C(4B")	-0.2862(25)	0.2463(22)	0.0363(19)	0.101(8)
H(2AN)	0.0893	0.4837	0.6777	0.0500
H(2BN)	0.1520	0.6154	0.7042	0.0500
H(12A)	-0.0132	0.3208	0.5688	0.0500
H(12B)	-0.0531	0.3026	0.4270	0.0500
H(13A)	-0.0743	0.1012	0.4475	0.0500
H(13B)	0.0927	0.1532	0.5253	0.0500
H(15A)	0.2807	0.2012	0.4395	0.0500
H(15B)	0.2542	0.1819	0.2969	0.0500
H(16A)	0.1445	0.3507	0.3314	0.0500
H(16B)	0.3095	0.4035	0.4128	0.0500
H(22)	0.2812	0.7962	0.4990	0.0500
H(24)	0.5642	1.0255	0.8002	0.0500
H(26)	0.4275	0.6335	0.7274	0.0500
H(3M1)	-0.3396	-0.0731	0.1502	0.0500
H(3M2)	-0.3188	-0.1928	0.2005	0.0500
H(3M3)	-0.2545	-0.1789	0.0823	0.0500
H(33)	-0.1564	-0.2841	0.1833	0.0500
H(34)	0.1017	-0.3949	0.2516	0.0500
H(35)	0.2647	-0.2016	0.3192	0.0500
H(36)	0.2815	0.0212	0.3821	0.0500
H(1A1)	0.4037	0.3984	0.6835	0.0500
H(1A2)	0.4840	0.2911	0.6107	0.0500
H(1A3)	0.4883	0.4272	0.5785	0.0500
H(2A)	0.6410	0.5528	0.7554	0.0500
H(2AO)	0.7380	0.4201	0.6140	0.0500
H(2BO)	-0.0918	0.1876	0.2464	0.0500

	U_{11}	U_{22}	U_{33}	U_{23}	U_{13}	U_{12}
C(1)	0.029(4)	0.026(4)	0.034(4)	0.007(3)	0.001(3)	0.013(3)
N(2)	0.048(4)	0.026(3)	0.044(4)	0.007(3)	0.018(3)	0.007(3)
N(3)	0.031(3)	0.023(3)	0.041(3)	0.013(3)	0.006(3)	0.004(3)
N(11)	0.030(3)	0.023(3)	0.040(3)	0.009(3)	0.011(3)	0.007(2)
C(12)	0.027(4)	0.030(4)	0.037(4)	0.010(3)	0.009(3)	0.006(3)
C(13)	0.033(4)	0.025(4)	0.031(4)	0.008(3)	0.013(3)	0.008(3)
N(14)	0.025(3)	0.019(3)	0.041(3)	0.011(2)	0.004(2)	0.005(2)
C(15)	0.033(4)	0.023(4)	0.051(5)	0.014(3)	0.014(3)	0.003(3)
C(16)	0.031(4)	0.023(4)	0.044(4)	0.009(3)	0.017(3)	0.007(3)
C(21)	0.023(4)	0.028(4)	0.035(4)	0.007(3)	0.007(3)	0.008(3)
C(22)	0.026(4)	0.031(4)	0.035(4)	0.008(3)	0.008(3)	0.006(3)
C(23)	0.035(4)	0.024(4)	0.057(5)	0.012(3)	0.016(4)	0.006(3)
Cl(23)	0.072(1)	0.026(1)	0.064(1)	0.016(1)	0.017(1)	0.004(1)
C(24)	0.034(4)	0.026(4)	0.044(4)	0.000(3)	0.003(3)	0.001(3)
C(25)	0.029(4)	0.045(5)	0.040(4)	0.001(4)	0.003(3)	0.012(3)
Cl(25)	0.062(1)	0.071(1)	0.059(1)	0.008(1)	-0.021(1)	0.016(1)
C(26)	0.032(4)	0.032(4)	0.048(5)	0.012(3)	0.009(4)	0.011(3)
C(31)	0.032(4)	0.022(4)	0.031(4)	0.008(3)	0.009(3)	0.010(3)
C(32)	0.033(4)	0.035(4)	0.023(4)	0.009(3)	0.002(3)	0.017(3)
O(32)	0.032(3)	0.032(3)	0.056(3)	0.013(2)	-0.003(2)	0.011(2)
C(3M)	0.031(4)	0.057(5)	0.036(4)	0.001(4)	-0.008(3)	0.017(4)
C(33)	0.030(4)	0.026(4)	0.039(4)	0.011(3)	0.008(3)	0.008(3)
C(34)	0.041(4)	0.014(4)	0.029(4)	0.005(3)	0.012(3)	0.009(3)
O(34)	0.040(3)	0.026(3)	0.053(3)	0.009(2)	0.005(2)	0.013(2)
C(35)	0.035(4)	0.029(4)	0.042(4)	0.015(3)	0.011(3)	0.013(3)
C(36)	0.027(4)	0.030(4)	0.041(4)	0.012(3)	0.005(3)	0.007(3)
C(1A)	0.049(5)	0.055(5)	0.094(7)	0.022(5)	0.005(5)	0.020(4)
C(2A)	0.096(7)	0.074(6)	0.086(7)	0.047(5)	0.047(6)	0.055(6)
O(2A)	0.045(3)	0.048(3)	0.053(3)	0.022(3)	0.021(3)	0.026(2)
O(2B)	0.081(4)	0.047(3)	0.044(4)	0.014(3)	0.016(3)	0.031(3)

- Table A.4 Positional and thermal parameters for GUHFUM

	x	y	z	U_{eq}
C(1)	0.1648(7)	0.2011(9)	0.3596(6)	0.044(8)
N(2)	0.2208(6)	0.1112(7)	0.4030(5)	0.049(6)
N(3)	0.0826(6)	0.1796(7)	0.2866(5)	0.051(6)
N(11)	0.1856(5)	0.3129(7)	0.3864(5)	0.048(6)
C(12)	0.2790(7)	0.3492(8)	0.4523(6)	0.048(7)
C(13)	0.2603(7)	0.3867(8)	0.5347(6)	0.052(7)
N(14)	0.1939(6)	0.4894(7)	0.5138(5)	0.050(7)
C(15)	0.0973(7)	0.4573(9)	0.4452(6)	0.056(8)
C(16)	0.1114(7)	0.4105(8)	0.3637(6)	0.054(8)
C(21)	0.0347(7)	0.0667(10)	0.2702(8)	0.056(8)
C(22)	0.0125(8)	0.0168(10)	0.1867(7)	0.067(10)
C(23)	-0.0407(9)	-0.0912(13)	0.1703(9)	0.081(11)
Cl(23)	-0.0655(3)	-0.1566(3)	0.0669(3)	0.134(3)
C(24)	-0.0717(9)	-0.1442(11)	0.2323(11)	0.093(12)
C(25)	-0.0487(8)	-0.0929(12)	0.3141(10)	0.082(11)
Cl(25)	-0.0872(3)	-0.1572(3)	0.3920(3)	0.131(3)
C(26)	0.0023(8)	0.0135(11)	0.3328(8)	0.062(9)
C(31)	0.1803(7)	0.5473(10)	0.5680(7)	0.048(9)
C(32)	0.1709(7)	0.6709(10)	0.5680(7)	0.048(9)
O(32)	0.1754(5)	0.7290(7)	0.5154(5)	0.069(6)
C(3M)	0.1888(8)	0.8550(9)	0.5207(7)	0.082(10)
C(33)	0.1593(7)	0.7283(9)	0.6578(8)	0.051(8)
C(34)	0.1550(7)	0.6641(11)	0.7303(7)	0.050(8)
O(34)	0.1424(6)	0.7297(7)	0.7958(4)	0.061(6)
C(35)	0.1661(7)	0.5419(11)	0.7323(7)	0.060(9)
C(36)	0.1779(8)	0.4847(9)	0.6613(8)	0.059(9)
O(1C)	0.1095(5)	0.6114(7)	0.9253(4)	0.067(6)
O(2C)	-0.0493(5)	0.6549(7)	0.8498(5)	0.077(6)
C(2C)	0.0193(11)	0.6072(10)	0.9129(7)	0.066(10)
C(1C)	-0.0205(10)	0.5388(11)	0.9733(8)	0.075(12)
O(1S)	-0.2431(5)	0.6085(7)	0.8253(5)	0.089(6)
C(1S)	-0.312(3)	0.740(4)	0.835(3)	0.0900(0)
C(2S)	-0.2963(14)	0.6964(20)	0.7850(15)	0.0900(0)
C(3S)	-0.2525(13)	0.8202(17)	0.8344(11)	0.0900(0)
C(4S)	-0.3300(18)	0.7978(24)	0.7453(16)	0.0900(0)
H(2A)	0.2838	0.1167	0.4771	0.0500
H(2B)	0.2396	0.0357	0.3842	0.0500
H(3)	0.0488	0.2635	0.2240	0.1488
H(12A)	0.3094	0.4230	0.4277	0.0500
H(12B)	0.3306	0.2757	0.4675	0.0500
H(13A)	0.2265	0.3142	0.5573	0.0500
H(13B)	0.3297	0.4103	0.5858	0.0500
H(15A)	0.0506	0.5353	0.4281	0.0500
H(15B)	0.0621	0.3896	0.4710	0.0500
H(16A)	0.0414	0.3771	0.3186	0.0500
H(16B)	0.1367	0.4819	0.3326	0.0500
H(22)	0.0349	0.0587	0.1370	0.0500
H(24)	-0.1139	-0.2258	0.2168	0.0500
H(26)	0.0172	0.0556	0.3961	0.0500
H(3MA)	0.1910	0.8879	0.4589	0.0500
H(3MB)	0.1280	0.8960	0.5338	0.0500
H(3MC)	0.2577	0.8762	0.5734	0.0500
H(33)	0.1534	0.8241	0.6570	0.0500
H(34)	0.1332	0.6900	0.8304	0.0500
H(35)	0.1656	0.4916	0.7888	0.0500
H(36)	0.1856	0.3891	0.6627	0.0500
H(1C)	-0.0807	0.5446	0.9934	0.0500

	U_{11}	U_{22}	U_{33}	U_{23}	U_{13}	U_{12}
C(1)	0.038(7)	0.046(8)	0.039(6)	-0.004(6)	0.004(5)	-0.010(6)
N(2)	0.050(6)	0.031(5)	0.050(5)	-0.003(5)	-0.003(4)	0.007(5)
N(3)	0.049(6)	0.035(5)	0.053(6)	0.002(5)	-0.004(5)	-0.010(5)
N(11)	0.035(5)	0.039(6)	0.055(6)	-0.014(4)	-0.003(4)	-0.005(4)
C(12)	0.046(6)	0.037(6)	0.051(7)	-0.009(5)	0.008(5)	-0.006(5)
C(13)	0.036(6)	0.044(7)	0.061(7)	-0.007(6)	-0.003(5)	0.004(5)
N(14)	0.053(6)	0.044(6)	0.041(6)	-0.006(5)	0.002(5)	-0.006(5)
C(15)	0.068(8)	0.042(7)	0.046(6)	-0.006(6)	0.010(6)	0.008(6)
C(16)	0.053(7)	0.038(7)	0.055(7)	-0.004(6)	0.000(6)	0.005(6)
C(21)	0.034(6)	0.051(8)	0.065(8)	-0.014(7)	-0.008(7)	0.002(6)
C(22)	0.049(8)	0.067(9)	0.065(9)	0.011(7)	-0.009(7)	0.006(7)
C(23)	0.047(8)	0.064(11)	0.101(11)	-0.034(9)	-0.022(8)	-0.001(7)
Cl(23)	0.107(3)	0.113(3)	0.138(3)	-0.076(3)	-0.021(2)	0.001(2)
C(24)	0.045(8)	0.051(10)	0.146(15)	-0.008(11)	-0.019(9)	-0.013(7)
C(25)	0.035(7)	0.058(10)	0.128(12)	0.006(9)	-0.001(8)	-0.014(7)
Cl(25)	0.090(3)	0.098(3)	0.181(4)	0.041(3)	0.039(3)	-0.037(2)
C(26)	0.030(7)	0.066(10)	0.077(9)	-0.007(8)	0.008(6)	0.003(6)
C(31)	0.043(7)	0.041(8)	0.047(8)	-0.005(7)	-0.002(6)	-0.011(6)
C(32)	0.049(7)	0.043(8)	0.042(8)	0.003(7)	0.009(5)	0.000(6)
O(32)	0.093(6)	0.047(5)	0.057(5)	0.009(4)	0.027(5)	0.005(4)
C(3M)	0.119(11)	0.037(8)	0.074(9)	0.019(6)	0.031(8)	0.003(7)
C(33)	0.052(7)	0.043(7)	0.046(7)	-0.003(7)	0.007(5)	0.002(6)
C(34)	0.043(7)	0.064(9)	0.033(7)	-0.012(7)	0.007(5)	-0.010(6)
O(34)	0.068(5)	0.059(6)	0.045(6)	-0.004(4)	0.015(4)	-0.004(4)
C(35)	0.077(9)	0.042(8)	0.049(9)	-0.002(7)	0.018(7)	-0.007(7)
C(36)	0.067(8)	0.039(7)	0.058(8)	0.003(8)	0.015(6)	-0.001(6)
O(1C)	0.056(5)	0.084(6)	0.049(5)	0.014(4)	0.009(4)	0.002(5)
O(2C)	0.067(6)	0.095(6)	0.054(5)	0.033(5)	0.009(4)	-0.015(5)
C(2C)	0.104(12)	0.053(8)	0.032(7)	0.011(6)	0.026(8)	-0.025(9)
C(1C)	0.075(11)	0.071(10)	0.063(10)	-0.004(8)	0.012(8)	-0.001(9)
O(1S)	0.079(6)	0.056(5)	0.113(7)	0.030(5)	0.021(5)	0.000(5)

Table A.5 Positional and thermal parameters for GUMACE

	x	y	z	U_{eq}
C(1)	0.3781(5)	0.0215(4)	0.37900(21)	0.033(3)
N(2)	0.3902(5)	-0.0673(4)	0.34132(20)	0.045(3)
N(3)	0.3298(5)	-0.0052(4)	0.43320(19)	0.039(3)
N(11)	0.4148(4)	0.1316(3)	0.36341(16)	0.0318(24)
C(12)	0.4268(5)	0.1673(4)	0.30069(20)	0.032(3)
C(13)	0.5860(5)	0.2078(4)	0.29164(20)	0.031(3)
N(14)	0.6217(4)	0.3094(3)	0.33043(16)	0.0291(22)
C(15)	0.6148(5)	0.2733(4)	0.39349(20)	0.035(3)
C(16)	0.4605(5)	0.2263(4)	0.40607(20)	0.035(3)
C(21)	0.2365(5)	0.0607(4)	0.46887(22)	0.031(3)
C(22)	0.2231(5)	0.0216(4)	0.52700(21)	0.036(3)
C(23)	0.1272(6)	0.0783(5)	0.56322(21)	0.037(3)
Cl(23)	0.11001(19)	0.02789(15)	0.63592(6)	0.0664(11)
C(24)	0.0453(5)	0.1765(4)	0.54394(22)	0.037(3)
C(25)	0.0640(5)	0.2159(4)	0.48669(22)	0.036(3)
Cl(25)	-0.02649(16)	0.34472(13)	0.46223(7)	0.0591(10)
C(26)	0.1542(5)	0.1593(4)	0.44792(22)	0.036(3)
C(31)	0.7616(5)	0.3677(4)	0.31986(21)	0.029(3)
C(32)	0.7804(5)	0.4850(4)	0.33859(21)	0.034(3)
O(32)	0.6603(4)	0.5355(3)	0.36451(18)	0.0570(25)
C(3M)	0.6726(7)	0.6546(6)	0.3820(4)	0.105(6)
C(33)	0.9141(5)	0.5456(4)	0.33110(21)	0.036(3)
C(34)	1.0279(5)	0.4902(4)	0.30380(21)	0.033(3)
O(34)	1.1603(4)	0.5477(3)	0.29458(17)	0.0464(24)
C(35)	1.0120(5)	0.3751(4)	0.28345(22)	0.040(3)
C(36)	0.8791(5)	0.3150(4)	0.29218(20)	0.035(3)
C(1S)	0.3036(5)	0.6866(4)	0.4220(3)	0.1037(3)
C(2S)	0.3155(7)	0.5559(5)	0.43813(25)	0.053(4)
O(1S)	0.2462(4)	0.7126(3)	0.37112(16)	0.0427(23)
O(2S)	0.3558(4)	0.7590(3)	0.46001(16)	0.0475(23)
O(1W)	0.4173(4)	0.4400(4)	0.25564(17)	0.052(3)
H(2A)	0.3319	-0.1366	0.3490	0.0500
H(2B)	0.4523	-0.0676	0.3137	0.0500
H(3)	0.3393	-0.0818	0.4461	0.0500
H(12A)	0.3991	0.0932	0.2716	0.0500
H(12B)	0.3495	0.2389	0.2900	0.0500
H(13A)	0.5947	0.2328	0.2454	0.0500
H(13B)	0.6636	0.1368	0.3030	0.0500
H(15A)	0.6973	0.2051	0.4035	0.0500
H(15B)	0.6398	0.3488	0.4219	0.0500
H(16A)	0.3797	0.2973	0.4016	0.0500
H(16B)	0.4640	0.1917	0.4512	0.0500
H(22)	0.2882	-0.0531	0.5439	0.0500
H(24)	-0.0300	0.2204	0.5726	0.0500
H(26)	0.1615	0.1904	0.4025	0.0500
H(3M1)	0.5681	0.6893	0.3964	0.0500
H(3M2)	0.7063	0.7048	0.3441	0.0500
H(3M3)	0.7583	0.6610	0.4183	0.0500
H(33)	0.9278	0.6356	0.3466	0.0500
H(34)	1.1785	0.6035	0.3195	0.0500
H(35)	1.1013	0.3327	0.2611	0.0500
H(36)	0.8669	0.2248	0.2769	0.0500
H(2S1)	0.2200	0.5127	0.4153	0.0500
H(2S2)	0.3030	0.5547	0.4858	0.0500
H(2S3)	0.4171	0.5099	0.4285	0.0500
H(1W)	0.4787	0.4183	0.2918	0.0500
H(2W)	0.3416	0.4717	0.2670	0.0500

	U_{11}	U_{22}	U_{33}	U_{23}	U_{13}	U_{12}
C(1)	0.035(3)	0.030(3)	0.034(3)	-0.001(2)	0.009(2)	-0.005(2)
N(2)	0.065(3)	0.025(3)	0.048(3)	-0.009(2)	0.031(2)	-0.014(2)
N(3)	0.054(3)	0.023(2)	0.042(3)	0.001(2)	0.024(2)	0.002(2)
N(11)	0.040(2)	0.026(2)	0.030(2)	-0.001(2)	0.010(2)	-0.010(2)
C(12)	0.037(3)	0.027(3)	0.031(3)	0.002(2)	0.001(2)	-0.009(2)
C(13)	0.033(3)	0.028(3)	0.033(3)	-0.001(2)	0.005(2)	-0.004(2)
N(14)	0.030(2)	0.022(2)	0.035(2)	0.000(2)	0.005(2)	-0.006(2)
C(15)	0.039(3)	0.034(3)	0.031(3)	-0.002(2)	0.005(2)	-0.008(2)
C(16)	0.047(3)	0.023(3)	0.035(3)	-0.005(2)	0.013(2)	-0.006(2)
C(21)	0.033(3)	0.022(3)	0.040(3)	-0.003(2)	0.006(2)	-0.007(2)
C(22)	0.040(3)	0.033(3)	0.035(3)	0.001(2)	0.006(2)	0.001(3)
C(23)	0.040(3)	0.043(3)	0.029(3)	0.000(2)	0.012(2)	-0.004(3)
Cl(23)	0.085(1)	0.082(1)	0.032(1)	0.005(1)	0.017(1)	0.007(1)
C(24)	0.032(3)	0.043(3)	0.037(3)	-0.010(3)	0.004(2)	-0.003(3)
C(25)	0.026(3)	0.033(3)	0.048(3)	-0.001(3)	-0.001(2)	-0.004(2)
Cl(25)	0.046(1)	0.053(1)	0.078(1)	0.011(1)	0.008(1)	0.015(1)
C(26)	0.033(3)	0.038(3)	0.038(3)	-0.003(3)	0.009(2)	-0.008(3)
C(31)	0.028(3)	0.023(3)	0.037(3)	0.001(2)	0.005(2)	-0.007(2)
C(32)	0.031(3)	0.030(3)	0.042(3)	-0.006(2)	0.008(2)	-0.001(2)
O(32)	0.037(2)	0.034(2)	0.101(3)	-0.027(2)	0.029(2)	-0.008(2)
C(3M)	0.054(4)	0.058(5)	0.206(9)	-0.065(6)	0.070(5)	-0.020(4)
C(33)	0.036(3)	0.029(3)	0.044(3)	-0.006(2)	0.008(2)	-0.006(2)
C(34)	0.025(3)	0.037(3)	0.035(3)	-0.002(2)	0.004(2)	-0.007(2)
O(34)	0.035(2)	0.048(3)	0.057(3)	-0.010(2)	0.020(2)	-0.012(2)
C(35)	0.038(3)	0.041(3)	0.043(3)	-0.006(3)	0.021(2)	0.001(3)
C(36)	0.038(3)	0.030(3)	0.038(3)	-0.002(2)	0.010(2)	0.000(2)
C(1S)	0.033(3)	0.030(3)	0.049(4)	0.001(3)	0.018(3)	-0.005(2)
C(2S)	0.070(4)	0.028(3)	0.062(4)	0.004(3)	0.011(3)	0.006(3)
O(1S)	0.047(2)	0.034(2)	0.046(2)	0.003(2)	0.006(2)	-0.002(2)
O(2S)	0.061(3)	0.033(2)	0.049(2)	-0.004(2)	0.010(2)	-0.002(2)
O(1W)	0.048(3)	0.060(3)	0.048(3)	0.015(2)	0.018(2)	0.020(2)

Table A.6 Positional and thermal parameters for GUMASC

	x	y	z	U_{eq}
C(1)	0.5801(9)	0.1360(7)	0.4374(3)	0.031(4)
N(2)	0.6688(8)	0.1620(7)	0.4875(3)	0.037(4)
N(3)	0.6823(8)	0.0111(7)	0.3981(3)	0.032(4)
N(11)	0.3984(7)	0.2255(6)	0.42558(24)	0.025(3)
C(12)	0.2785(9)	0.1492(7)	0.4053(3)	0.032(4)
C(13)	0.0875(9)	0.2693(7)	0.3793(3)	0.027(4)
N(14)	0.0005(7)	0.3941(5)	0.42770(25)	0.025(3)
C(15)	0.1256(8)	0.4771(7)	0.4316(3)	0.023(4)
C(16)	0.3042(9)	0.3677(7)	0.4657(3)	0.026(4)
C(21)	0.6655(8)	0.0176(7)	0.3250(3)	0.026(4)
C(22)	0.6683(9)	-0.1095(7)	0.2942(3)	0.029(4)
C(23)	0.6493(9)	-0.1003(9)	0.2236(4)	0.039(5)
Cl(23)	0.6453(3)	-0.2580(3)	0.18275(11)	0.0677(16)
C(24)	0.6308(10)	0.0344(9)	0.1843(4)	0.042(5)
C(25)	0.6302(10)	0.1574(9)	0.2171(4)	0.041(5)
Cl(25)	0.6161(3)	0.3233(3)	0.16860(12)	0.0670(16)
C(26)	0.6447(9)	0.1544(8)	0.2861(3)	0.034(5)
C(31)	-0.1938(8)	0.4953(7)	0.4144(3)	0.023(4)
C(32)	-0.2960(9)	0.5966(7)	0.4644(3)	0.030(4)
O(32)	-0.2073(6)	0.5983(5)	0.52312(21)	0.034(3)
C(3M)	-0.2875(11)	0.7297(8)	0.5663(4)	0.044(5)
C(33)	-0.4915(9)	0.6956(7)	0.4564(3)	0.032(4)
C(34)	-0.5793(8)	0.6869(7)	0.3978(3)	0.026(4)
O(34)	-0.7668(6)	0.7798(6)	0.3874(3)	0.040(3)
C(35)	-0.4806(9)	0.5884(7)	0.3472(3)	0.030(4)
C(36)	-0.2893(9)	0.4939(7)	0.3567(3)	0.027(4)
C(1')	-0.8301(8)	-0.2703(7)	-0.0380(3)	0.026(4)
N(2')	-0.9235(9)	-0.3047(7)	-0.0816(3)	0.037(4)
N(3')	-0.9237(8)	-0.1425(6)	0.0014(3)	0.030(4)
N(11')	-0.6484(7)	-0.3520(6)	-0.0285(3)	0.028(4)
C(12')	-0.5212(8)	-0.2743(7)	-0.0139(3)	0.025(4)
C(13')	-0.3429(9)	-0.3861(7)	0.0178(3)	0.033(4)
N(14')	-0.2456(7)	-0.5182(6)	-0.0265(3)	0.031(4)
C(15')	-0.3664(9)	-0.6038(7)	-0.0320(4)	0.033(4)
C(16')	-0.5535(9)	-0.4971(7)	-0.0640(3)	0.032(4)
C(21')	-0.9009(8)	-0.1506(8)	0.0736(3)	0.032(5)
C(22')	-0.9104(9)	-0.0167(8)	0.1046(3)	0.036(5)
C(23')	-0.8694(9)	-0.0289(8)	0.1749(4)	0.032(4)
Cl(23)	-0.8874(3)	0.1294(3)	0.21581(11)	0.0635(16)
C(24')	-0.8693(9)	-0.1596(8)	0.2163(4)	0.038(5)
C(25')	-0.8704(9)	-0.2878(8)	0.1819(4)	0.038(5)
Cl(25)	-0.8544(3)	-0.45258(25)	0.22999(10)	0.0644(16)
C(26')	-0.8820(10)	-0.2850(8)	0.1112(4)	0.038(5)
C(31')	-0.0584(9)	-0.6161(7)	-0.0116(3)	0.030(4)
C(32')	0.0571(9)	-0.7207(8)	-0.0627(3)	0.030(4)
O(32')	-0.0317(6)	-0.7153(5)	-0.12178(22)	0.037(3)
C(3M')	0.0560(11)	-0.8397(9)	-0.1656(4)	0.048(5)
C(33')	0.2422(9)	-0.8171(7)	-0.0502(3)	0.029(4)
C(34')	0.3199(9)	-0.8066(8)	0.0098(3)	0.032(4)
O(34')	0.5086(6)	-0.9016(6)	0.02264(24)	0.044(3)
C(35')	0.2167(10)	-0.7040(7)	0.0586(3)	0.035(5)
C(36')	0.0271(9)	-0.6107(8)	-0.0485(3)	0.034(5)
C(41)	0.1754(11)	-0.2146(9)	-0.3345(4)	0.038(6)
C(42)	0.1587(11)	-0.2444(9)	-0.4025(4)	0.026(5)
C(43)	0.0744(11)	-0.1068(9)	-0.4402(4)	0.029(5)
C(44)	0.0336(11)	0.0208(8)	-0.3913(4)	0.034(5)
C(45)	0.1236(9)	0.1322(7)	-0.4139(3)	0.029(4)
C(46)	0.0727(12)	0.2671(9)	-0.3656(4)	0.031(5)
O(40)	0.1005(7)	-0.0568(6)	-0.32645(24)	0.035(3)
O(41)	0.2438(8)	-0.3027(7)	-0.2853(3)	0.054(4)
O(42)	0.2122(9)	-0.3920(6)	-0.4263(3)	0.047(4)
O(43)	0.0291(7)	-0.0766(5)	-0.50430(25)	0.033(3)
O(45)	0.3259(8)	0.0488(6)	-0.4192(3)	0.034(4)
O(46)	-0.1253(7)	0.3684(6)	-0.3734(3)	0.039(3)
C(81)	-0.3014(10)	-0.0011(9)	-0.1457(4)	0.030(5)
C(82)	-0.3953(12)	0.1106(9)	-0.1966(4)	0.039(6)
C(83)	-0.4121(11)	0.0382(8)	-0.2525(4)	0.030(5)
C(84)	-0.3083(11)	-0.1386(8)	-0.2355(4)	0.035(5)
C(85)	-0.4259(9)	-0.2330(7)	-0.2415(4)	0.033(5)
C(86)	-0.3099(12)	-0.4040(9)	-0.2212(4)	0.035(5)
O(80)	-0.2494(7)	-0.1502(5)	-0.1670(3)	0.039(3)
O(81)	-0.2593(7)	0.0112(6)	-0.0866(3)	0.042(4)
O(82)	-0.4518(12)	0.2668(9)	-0.1908(5)	0.063(6)
O(83)	-0.4863(8)	0.0884(6)	-0.3116(3)	0.056(4)
O(85)	-0.5876(8)	-0.1752(6)	-0.1964(3)	0.044(4)
O(86)	-0.1390(8)	-0.4643(6)	-0.2606(3)	0.047(4)
O(1W)	-0.4794(9)	0.3372(7)	-0.3822(3)	0.046(4)
O(2W)	0.1902(7)	0.4864(7)	-0.1976(3)	0.043(4)

H(2A)	0.8237	0.0899	0.4886	0.0500
H(2B)	0.6039	0.2176	0.5268	0.0500
H(3)	0.7547	-0.0379	0.4140	0.0500
H(12A)	0.3512	0.0704	0.3648	0.0500
H(12B)	0.2535	0.0830	0.4495	0.0500
H(13A)	-0.0054	0.2110	0.3739	0.0500
H(13B)	0.1093	0.3199	0.3298	0.0500
H(15A)	0.1589	0.5121	0.3803	0.0500
H(15B)	0.0553	0.5801	0.4614	0.0500
H(16A)	0.2703	0.3345	0.5172	0.0500
H(16B)	0.3981	0.4262	0.4682	0.0500
H(22)	0.6848	-0.2157	0.3242	0.0500
H(24)	0.6169	0.0406	0.1291	0.0500
H(26)	0.6403	0.2561	0.3108	0.0500
H(3M1)	-0.1672	0.7079	0.5974	0.0500
H(3M2)	-0.3931	0.7045	0.5970	0.0500
H(3M3)	-0.3475	0.8514	0.5478	0.0500
H(33)	-0.5702	0.7765	0.4955	0.0500
H(34)	-0.7742	0.8228	0.4262	0.0500
H(35)	-0.5489	0.5839	0.3009	0.0500
H(36)	-0.2114	0.4149	0.3169	0.0500
H(2A')	-0.8871	-0.3637	-0.1191	0.0500
H(2B')	-1.0284	-0.2732	-0.0852	0.0500
H(3')	-1.0478	-0.0669	-0.0202	0.0500
H(12C)	-0.5949	-0.1812	0.0209	0.0500
H(12D)	-0.4865	-0.2251	-0.0617	0.0500
H(13C)	-0.3755	-0.4295	0.0674	0.0500
H(13D)	-0.2520	-0.3266	0.0244	0.0500
H(15C)	-0.2940	-0.7029	-0.0639	0.0500
H(15D)	-0.3938	-0.6453	0.0168	0.0500

H(16C)	-0.6450	-0.5587	-0.0618	0.0500
H(16D)	-0.5266	-0.4689	-0.1171	0.0500
H(22')	-0.9332	0.0910	0.0748	0.0500
H(24')	-0.8539	-0.1639	0.2713	0.0500
H(26')	-0.8766	-0.3866	0.0861	0.0500
H(3M4)	-0.0423	-0.8178	-0.2064	0.0500
H(3M5)	0.0746	-0.9484	-0.1374	0.0500
H(3M6)	0.1909	-0.8486	-0.1876	0.0500
H(33')	0.3266	-0.9008	-0.0875	0.0500
H(34')	0.6201	-0.9450	-0.0278	0.0500
H(35')	0.2827	-0.6959	0.1048	0.0500
H(36')	-0.0557	-0.5322	0.0878	0.0500
H(44)	-0.1165	0.0947	-0.3888	0.0500
H(45)	0.0680	0.1830	-0.4637	0.0500
H(46C)	0.1578	0.3322	-0.3791	0.0500
H(46D)	0.0976	0.2211	-0.3130	0.0500
H(42)	0.3354	-0.4580	-0.3928	0.0500
H(45O)	0.3869	0.0420	-0.3830	0.0500
H(46O)	-0.1173	0.4533	-0.4246	0.0500
H(84)	-0.1931	-0.1889	-0.2726	0.0500
H(85)	-0.4689	-0.2220	-0.2942	0.0500
H(86C)	-0.3911	-0.4711	-0.2296	0.0500
H(86D)	-0.2778	-0.4142	-0.1673	0.0500
H(82)	-0.4924	0.2944	-0.1676	0.0500
H(85O)	-0.6968	-0.1857	-0.2261	0.0500
H(86O)	-0.1565	-0.5160	-0.2948	0.0500
H(1W1)	-0.4039	0.3369	-0.3613	0.0500
H(1W2)	-0.5010	0.3547	-0.4133	0.0500
H(2W1)	0.1086	0.4858	-0.2055	0.0500

	U_{11}	U_{22}	U_{33}	U_{23}	U_{13}	U_{12}
C(1)	0.034(4)	0.021(4)	0.032(4)	-0.002(3)	-0.001(3)	-0.013(3)
N(2)	0.027(3)	0.045(4)	0.027(3)	-0.006(3)	-0.011(3)	-0.006(3)
N(3)	0.031(4)	0.028(4)	0.029(4)	-0.008(3)	-0.007(3)	-0.004(3)
N(11)	0.020(3)	0.026(3)	0.021(3)	-0.005(2)	-0.004(2)	-0.002(2)
C(12)	0.032(4)	0.025(3)	0.036(4)	-0.010(3)	0.005(3)	-0.014(3)
C(13)	0.022(4)	0.023(4)	0.028(4)	-0.008(3)	0.001(3)	-0.001(3)
N(14)	0.018(3)	0.019(3)	0.032(3)	-0.012(2)	-0.004(2)	-0.004(2)
C(15)	0.016(3)	0.018(3)	0.032(4)	-0.011(3)	0.005(3)	-0.009(3)
C(16)	0.028(4)	0.019(3)	0.022(4)	-0.006(3)	0.003(3)	-0.002(3)
C(21)	0.023(4)	0.030(4)	0.017(3)	0.000(3)	0.000(3)	-0.004(3)
C(22)	0.023(4)	0.021(4)	0.032(4)	-0.005(3)	0.006(3)	0.000(3)
C(23)	0.019(4)	0.044(5)	0.048(5)	-0.022(4)	0.007(3)	-0.011(3)
Cl(23)	0.070(1)	0.068(1)	0.058(1)	-0.035(1)	0.008(1)	-0.039(1)
C(24)	0.033(4)	0.049(5)	0.033(4)	-0.006(4)	-0.001(3)	-0.011(4)
C(25)	0.034(4)	0.049(5)	0.032(4)	-0.004(4)	0.008(3)	-0.019(4)
Cl(25)	0.066(1)	0.061(1)	0.059(1)	0.025(1)	-0.005(1)	-0.025(1)
C(26)	0.032(4)	0.030(4)	0.032(4)	-0.004(3)	0.010(3)	-0.013(3)
C(31)	0.023(4)	0.017(3)	0.027(4)	-0.006(3)	0.006(3)	-0.011(3)
C(32)	0.034(4)	0.025(4)	0.027(4)	-0.003(3)	-0.003(3)	-0.017(3)
O(32)	0.031(3)	0.035(3)	0.026(3)	-0.007(2)	-0.011(2)	-0.004(2)
C(3M)	0.050(5)	0.027(4)	0.042(4)	-0.012(3)	-0.006(4)	-0.005(4)
C(33)	0.034(4)	0.027(4)	0.029(4)	-0.005(3)	-0.006(3)	-0.014(3)
C(34)	0.012(3)	0.017(3)	0.046(4)	-0.004(3)	0.000(3)	-0.007(3)
O(34)	0.027(3)	0.039(3)	0.045(3)	-0.009(2)	-0.011(2)	-0.005(2)
C(35)	0.016(3)	0.032(4)	0.039(4)	-0.002(3)	-0.009(3)	-0.009(3)
C(36)	0.025(4)	0.013(3)	0.038(4)	-0.008(3)	0.000(3)	-0.003(3)

C(1')	0.019(4)	0.028(4)	0.023(4)	0.008(3)	0.004(3)	-0.006(3)
N(2')	0.028(3)	0.034(4)	0.042(4)	-0.012(3)	-0.010(3)	-0.007(3)
N(3')	0.024(3)	0.032(3)	0.024(3)	-0.001(3)	-0.001(2)	-0.002(3)
N(11')	0.021(3)	0.023(3)	0.034(3)	-0.008(2)	-0.001(2)	-0.007(2)
C(12')	0.013(3)	0.027(4)	0.031(4)	-0.014(3)	-0.004(3)	-0.007(3)
C(13')	0.027(4)	0.030(4)	0.039(4)	-0.007(3)	0.003(3)	-0.018(3)
N(14')	0.024(3)	0.030(3)	0.033(3)	-0.004(2)	-0.003(2)	-0.011(3)
C(15')	0.028(4)	0.023(4)	0.043(4)	-0.004(3)	-0.014(3)	-0.008(3)
C(16')	0.030(4)	0.030(4)	0.034(4)	-0.009(3)	0.004(3)	-0.021(3)
C(21')	0.012(3)	0.040(4)	0.039(4)	-0.007(3)	0.006(3)	-0.012(3)
C(22')	0.032(4)	0.044(4)	0.028(4)	-0.008(3)	0.007(3)	-0.026(3)
C(23')	0.023(4)	0.027(4)	0.038(4)	-0.005(3)	0.001(3)	-0.006(3)
Cl(23)	0.069(1)	0.062(1)	0.052(1)	-0.026(1)	0.008(1)	-0.036(1)
C(24')	0.030(4)	0.047(5)	0.029(4)	-0.005(3)	-0.004(3)	-0.013(3)
C(25')	0.027(4)	0.036(4)	0.040(4)	0.018(3)	-0.006(3)	-0.007(3)
Cl(25)	0.084(2)	0.052(1)	0.043(1)	0.016(1)	-0.003(1)	-0.030(1)
C(26')	0.035(4)	0.037(4)	0.037(4)	0.001(3)	-0.006(3)	-0.017(3)
C(31')	0.024(4)	0.029(4)	0.033(4)	0.001(3)	-0.010(3)	-0.010(3)
C(32')	0.023(4)	0.038(4)	0.022(4)	0.000(3)	-0.003(3)	-0.012(3)
O(32')	0.026(3)	0.040(3)	0.033(3)	-0.019(2)	0.005(2)	-0.005(2)
C(3M')	0.044(5)	0.059(5)	0.035(4)	-0.028(4)	0.010(3)	-0.027(4)
C(33')	0.023(4)	0.026(4)	0.029(4)	0.002(3)	0.006(3)	-0.005(3)
C(34')	0.022(4)	0.041(4)	0.024(4)	0.012(3)	-0.001(3)	-0.015(3)
O(34')	0.022(3)	0.064(4)	0.031(3)	0.011(2)	-0.001(2)	-0.005(2)
C(35')	0.048(5)	0.028(4)	0.023(4)	0.002(3)	-0.003(3)	-0.023(3)
C(36')	0.025(4)	0.044(4)	0.029(4)	-0.003(3)	-0.002(3)	-0.018(3)
C(41)	0.037(5)	0.033(5)	0.038(5)	0.014(4)	0.001(4)	-0.021(4)
C(42)	0.018(5)	0.019(4)	0.034(5)	-0.010(4)	-0.002(4)	0.001(4)
C(43)	0.026(4)	0.033(5)	0.025(4)	-0.006(3)	-0.001(3)	-0.015(4)
C(44)	0.027(4)	0.027(4)	0.038(5)	-0.002(4)	0.000(4)	-0.002(3)
C(45)	0.029(4)	0.025(4)	0.028(4)	-0.007(3)	0.005(3)	-0.010(3)
C(46)	0.030(5)	0.026(4)	0.029(4)	-0.003(3)	-0.003(3)	-0.006(4)
O(40)	0.038(3)	0.030(3)	0.031(3)	-0.003(2)	-0.003(2)	-0.015(2)
O(41)	0.059(4)	0.052(4)	0.044(3)	0.012(3)	-0.020(3)	-0.035(3)
O(42)	0.044(4)	0.027(3)	0.060(4)	-0.012(3)	-0.019(3)	-0.006(3)
O(43)	0.020(3)	0.030(3)	0.037(3)	-0.009(2)	-0.001(2)	0.001(2)
O(45)	0.021(3)	0.038(3)	0.036(3)	-0.008(2)	0.004(2)	-0.008(3)
O(46)	0.032(3)	0.027(3)	0.047(3)	-0.004(2)	0.000(2)	-0.005(2)
C(81)	0.017(4)	0.037(5)	0.031(5)	-0.011(4)	-0.002(3)	-0.008(4)
C(82)	0.039(6)	0.025(5)	0.046(5)	-0.004(4)	-0.007(4)	-0.015(4)
C(83)	0.027(4)	0.026(4)	0.032(4)	0.009(3)	-0.007(3)	-0.016(4)
C(84)	0.041(5)	0.026(4)	0.030(5)	0.002(3)	-0.002(4)	-0.013(4)
C(85)	0.033(4)	0.027(4)	0.034(4)	-0.013(3)	0.006(3)	-0.012(3)
C(86)	0.032(5)	0.033(5)	0.034(4)	-0.006(4)	0.005(4)	-0.016(4)
O(80)	0.032(3)	0.028(3)	0.050(3)	-0.004(2)	-0.014(2)	-0.010(2)
O(81)	0.032(3)	0.049(3)	0.034(3)	-0.009(2)	-0.004(2)	-0.011(3)
O(82)	0.050(5)	0.021(4)	0.110(8)	-0.014(4)	-0.025(5)	-0.006(3)
O(83)	0.061(4)	0.048(3)	0.053(4)	0.010(3)	-0.026(3)	-0.031(3)
O(85)	0.032(4)	0.048(4)	0.043(4)	-0.014(3)	0.005(3)	-0.013(3)
O(86)	0.032(3)	0.044(3)	0.055(4)	-0.024(3)	0.005(3)	-0.009(3)
O(1W)	0.037(4)	0.043(3)	0.049(4)	0.003(3)	-0.011(3)	-0.016(3)
O(2W)	0.035(3)	0.041(3)	0.046(3)	0.002(2)	-0.012(3)	-0.020(3)

Table A.7 Positional and thermal parameters for GUMHCL

	x	y	z	U_{eq}
C(1)	0.7726(8)	0.5038(6)	0.3659(6)	0.051(5)
N(2)	0.8880(7)	0.4698(5)	0.3481(5)	0.056(5)
N(3)	0.6411(7)	0.4374(5)	0.3197(5)	0.059(5)
N(11)	0.7833(6)	0.6086(5)	0.4323(4)	0.048(4)
C(12)	0.6546(7)	0.6254(6)	0.4850(6)	0.051(5)
C(13)	0.6659(8)	0.7555(6)	0.5114(6)	0.052(5)
N(14)	0.8012(6)	0.8245(4)	0.5763(4)	0.046(4)
C(15)	0.9261(8)	0.8146(6)	0.5172(6)	0.052(5)
C(16)	0.9252(7)	0.6870(6)	0.4865(6)	0.054(5)
C(21)	0.5950(8)	0.3136(6)	0.2757(6)	0.050(5)
C(22)	0.6410(8)	0.2406(6)	0.3221(6)	0.054(6)
C(23)	0.5860(9)	0.1199(7)	0.2783(7)	0.063(6)
Cl(23)	0.6449(3)	0.02928(19)	0.33637(23)	0.0993(21)
C(24)	0.4894(10)	0.0699(7)	0.1946(7)	0.068(7)
C(25)	0.4438(9)	0.1458(8)	0.1530(7)	0.073(7)
Cl(25)	0.3218(4)	0.08759(25)	0.04560(23)	0.125(3)
C(26)	0.4961(9)	0.2675(7)	0.1922(6)	0.067(7)
C(31)	0.8148(8)	0.9457(6)	0.6195(6)	0.050(5)
C(32)	0.9105(9)	1.0086(6)	0.7064(6)	0.056(6)
O(32)	0.9841(6)	0.9458(4)	0.7432(4)	0.072(4)
C(3M)	1.0701(11)	0.9989(8)	0.8353(7)	0.089(8)
C(33)	0.9304(9)	1.1263(6)	0.7498(6)	0.059(6)
C(34)	0.8526(9)	1.1829(6)	0.7071(6)	0.057(6)
O(34)	0.8804(7)	1.3013(4)	0.7520(4)	0.072(4)
C(35)	0.7533(9)	1.1234(7)	0.6243(7)	0.063(6)
C(36)	0.7362(8)	1.0043(6)	0.5814(6)	0.054(5)
Cl(1S)	0.75707(21)	0.41864(16)	0.60359(17)	0.0656(15)
C(1S)	0.6774(15)	0.6299(15)	0.1466(11)	0.229(20)
C(2S)	0.5296(16)	0.6389(16)	0.1861(11)	0.187(17)
O(2S)	0.4855(7)	0.5627(6)	0.2484(6)	0.104(6)
C(3S)	0.4703(18)	0.7001(15)	0.1558(14)	0.32(3)
C(4S)	1.0670(18)	0.3807(15)	0.0579(13)	0.230(21)
C(5S)	0.9342(15)	0.3060(14)	0.0806(10)	0.141(14)
O(5S)	0.9234(7)	0.2953(5)	0.1776(5)	0.092(5)
C(6S)	0.8104(12)	0.2856(17)	0.0265(11)	0.244(24)
O(1W)	0.1854(12)	0.3089(17)	0.2606(11)	0.101(6)
H(2A)	0.8920	0.4118	0.2836	0.0500
H(2B)	0.9934	0.5082	0.3730	0.0500
H(3)	0.5787	0.4834	0.3053	0.0500
H(12A)	0.6497	0.5960	0.5542	0.0500
H(12B)	0.5565	0.5741	0.4356	0.0500
H(13A)	0.6676	0.7848	0.4424	0.0500
H(13B)	0.5734	0.7669	0.5517	0.0500
H(15A)	1.0261	0.8689	0.5632	0.0500
H(15B)	0.9204	0.8448	0.4493	0.0500
H(16A)	1.0113	0.6812	0.4371	0.0500
H(16B)	0.9432	0.6598	0.5540	0.0500
H(22)	0.7163	0.2762	0.3896	0.0500
H(24)	0.4501	-0.0243	0.1622	0.0500
H(26)	0.4597	0.3244	0.1568	0.0500
H(3M1)	1.0946	0.9253	0.8515	0.0500
H(3M2)	1.1706	1.0686	0.8335	0.0500
H(3M3)	1.0071	1.0312	0.8939	0.0500
H(33)	1.0059	1.1736	0.8163	0.0500
H(34)	0.8248	1.3326	0.7102	0.0500
H(35)	0.6899	1.1671	0.5932	0.0500
H(36)	0.6587	0.9567	0.5159	0.0500
H(1S1)	0.7377	0.5774	0.1670	0.0500
H(1S2)	0.5813	0.5729	0.0975	0.0500
H(1S3)	0.7455	0.6910	0.1072	0.0500
H(2S1)	0.6422	0.6622	0.2143	0.0500
H(2S)	0.4000	0.5824	0.2794	0.0500
H(3S1)	0.3810	0.7164	0.1977	0.0500
H(3S2)	0.4946	0.7522	0.1005	0.0500
H(3S3)	0.4399	0.6076	0.1171	0.0500
H(4S1)	1.1803	0.4266	0.0852	0.0500
H(4S2)	1.0500	0.3857	-0.0193	0.0500
H(4S3)	0.9988	0.4212	0.1060	0.0500
H(5S1)	0.9834	0.2479	0.0320	0.0500
H(5S)	0.9139	0.2851	0.2481	0.0500
H(6S1)	0.8091	0.2802	-0.0542	0.0500
H(6S2)	0.7551	0.1993	0.0383	0.0500
H(6S3)	0.7554	0.3462	0.0630	0.0500
H(1W2)	0.0769	0.2925	0.2568	0.0500

	U_{11}	U_{22}	U_{33}	U_{23}	U_{13}	U_{12}
C(1)	0.044(5)	0.039(4)	0.063(5)	0.022(4)	0.008(4)	0.009(4)
N(2)	0.040(4)	0.040(4)	0.077(5)	0.007(3)	0.011(4)	0.012(3)
N(3)	0.047(4)	0.037(4)	0.082(5)	0.004(3)	-0.006(4)	0.015(3)
N(11)	0.038(3)	0.031(3)	0.064(4)	0.007(3)	0.012(3)	0.007(3)
C(12)	0.038(4)	0.038(4)	0.068(5)	0.010(4)	0.016(4)	0.011(3)
C(13)	0.041(4)	0.035(4)	0.071(5)	0.009(4)	0.009(4)	0.012(3)
N(14)	0.042(4)	0.030(3)	0.057(4)	0.009(3)	0.014(3)	0.009(3)
C(15)	0.042(4)	0.033(4)	0.071(5)	0.012(4)	0.010(4)	0.009(3)
C(16)	0.036(4)	0.042(4)	0.074(6)	0.012(4)	0.012(4)	0.008(4)
C(21)	0.050(5)	0.038(4)	0.055(5)	0.009(4)	0.011(4)	0.013(4)
C(22)	0.046(5)	0.046(5)	0.057(5)	0.007(4)	0.016(4)	0.010(4)
C(23)	0.062(5)	0.041(5)	0.075(6)	0.015(4)	0.022(5)	0.016(4)
Cl(23)	0.093(2)	0.056(1)	0.136(2)	0.041(1)	0.004(2)	0.021(1)
C(24)	0.075(6)	0.044(5)	0.067(6)	0.004(5)	-0.003(5)	0.007(5)
C(25)	0.063(6)	0.061(6)	0.075(7)	0.005(5)	0.001(5)	0.003(5)
Cl(25)	0.138(3)	0.089(2)	0.106(2)	0.004(2)	-0.054(2)	-0.005(2)
C(26)	0.070(6)	0.050(5)	0.067(6)	0.013(5)	-0.002(5)	0.013(4)
C(31)	0.058(5)	0.042(4)	0.044(5)	0.015(4)	0.015(4)	0.021(4)
C(32)	0.075(6)	0.037(4)	0.046(5)	0.012(4)	0.011(4)	0.020(4)
O(32)	0.088(4)	0.043(3)	0.075(4)	0.010(3)	-0.016(3)	0.028(3)
C(3M)	0.110(8)	0.057(6)	0.083(7)	0.016(5)	-0.015(7)	0.022(6)
C(33)	0.064(5)	0.039(5)	0.063(5)	0.014(4)	0.008(4)	0.013(4)
C(34)	0.069(6)	0.034(4)	0.063(6)	0.014(4)	0.019(5)	0.022(4)
O(34)	0.096(5)	0.036(3)	0.071(4)	0.009(3)	0.007(3)	0.024(3)
C(35)	0.065(6)	0.043(5)	0.076(6)	0.021(4)	0.009(5)	0.025(4)
C(36)	0.049(5)	0.040(4)	0.063(5)	0.013(4)	0.009(4)	0.012(4)
Cl(1S)	0.055(1)	0.047(1)	0.087(2)	0.025(1)	0.013(1)	0.020(1)
C(1S)	0.116(11)	0.310(22)	0.273(20)	0.221(19)	0.123(13)	0.123(14)
C(2S)	0.116(10)	0.282(20)	0.174(14)	0.172(15)	0.075(10)	0.119(13)
O(2S)	0.075(4)	0.105(5)	0.132(6)	0.067(5)	0.044(4)	0.053(4)
C(3S)	0.263(22)	0.313(26)	0.439(33)	0.318(27)	0.242(24)	0.240(22)
C(4S)	0.122(13)	0.345(26)	0.160(15)	0.125(17)	0.050(12)	-0.019(15)
C(5S)	0.100(10)	0.202(16)	0.094(10)	0.053(10)	0.036(8)	0.041(11)
O(5S)	0.110(5)	0.091(4)	0.056(4)	0.023(4)	0.035(4)	0.029(4)
C(6S)	0.151(16)	0.407(32)	0.160(16)	0.174(19)	0.078(13)	0.117(19)
O(1W)	0.083(5)	0.081(4)	0.124(6)	0.038(4)	0.018(4)	0.027(4)

Table A.8 Positional and thermal parameters for GUDMES

	x	y	z	U_{eq}
C(1)	0.2599(5)	0.8766(8)	0.9065(7)	0.034(5)
N(2)	0.3243(5)	0.9473(8)	1.0135(6)	0.041(5)
N(3)	0.1928(5)	0.7494(7)	0.8930(5)	0.041(5)
N(11)	0.2608(4)	0.9274(7)	0.8108(5)	0.030(4)
C(12)	0.1699(5)	0.9080(9)	0.7048(6)	0.034(5)
C(13)	0.1973(5)	0.8453(8)	0.5939(6)	0.034(5)
N(14)	0.2807(4)	0.9614(7)	0.5927(5)	0.031(4)
C(15)	0.3723(5)	0.9837(8)	0.7059(6)	0.032(5)
C(16)	0.3435(5)	1.0412(8)	0.8160(5)	0.029(5)
C(21)	0.1622(5)	0.7159(9)	0.9859(6)	0.036(5)
C(22)	0.1665(5)	0.5606(9)	1.0069(7)	0.046(6)
C(23)	0.1304(6)	0.5355(11)	1.0967(8)	0.055(7)
Cl(23)	0.13818(20)	0.3412(3)	1.12710(23)	0.0994(24)
C(24)	0.0931(6)	0.6580(12)	1.1623(7)	0.061(7)
C(25)	0.0938(6)	0.8098(11)	1.1382(7)	0.063(7)
Cl(25)	0.04596(25)	0.9662(4)	1.2177(3)	0.125(3)
C(26)	0.1260(6)	0.8431(10)	1.0506(7)	0.047(6)
C(31)	0.3112(5)	0.9053(9)	0.4876(6)	0.030(5)
C(32)	0.3448(5)	1.0276(8)	0.4436(6)	0.033(5)
O(32)	0.3480(4)	1.1866(6)	0.5054(4)	0.055(4)
C(3M)	0.3838(7)	1.3164(9)	0.4655(7)	0.059(7)
C(33)	0.3761(5)	0.9821(9)	0.3472(6)	0.037(6)
C(34)	0.3753(5)	0.8161(9)	0.2957(6)	0.033(5)
O(34)	0.4059(4)	0.7786(6)	0.2001(4)	0.044(4)
C(35)	0.3466(5)	0.6957(8)	0.3432(6)	0.039(5)
C(36)	0.3141(5)	0.7430(9)	0.4383(6)	0.043(6)
S(1)	0.48578(15)	0.36958(24)	0.16446(17)	0.0406(15)
O(1S)	0.4813(4)	0.2087(6)	0.0869(4)	0.048(4)
O(2S)	0.4001(4)	0.4597(6)	0.1114(4)	0.052(4)
O(3S)	0.4973(5)	0.3601(7)	0.2834(4)	0.076(5)
C(1S)	0.5961(6)	0.4820(10)	0.1736(7)	0.059(7)
S(2)	0.11905(16)	0.35370(25)	0.60692(18)	0.0436(15)
O(4S)	0.2023(4)	0.2551(6)	0.6489(5)	0.059(4)
O(5S)	0.1440(4)	0.5233(6)	0.6734(4)	0.059(4)
O(6S)	0.0232(4)	0.2856(8)	0.6020(6)	0.100(6)
C(2S)	0.1087(7)	0.3527(11)	0.4622(7)	0.067(7)
H(2A)	0.3610	1.0330	1.0297	0.0500
H(2B)	0.3342	0.8857	1.0747	0.0500
H(3)	0.1745	0.6883	0.8386	0.0500
H(12A)	0.1396	1.0260	0.7020	0.0500
H(12B)	0.1135	0.8201	0.7074	0.0500
H(13A)	0.2232	0.7239	0.5943	0.0500
H(13B)	0.1307	0.8376	0.5148	0.0500
H(14)	0.2502	1.0550	0.5868	0.0500
H(15A)	0.4283	1.0750	0.7060	0.0500
H(15B)	0.4044	0.8670	0.7086	0.0500
H(16A)	0.4088	1.0439	0.8955	0.0500
H(16B)	0.3190	1.1638	0.8188	0.0500
H(22)	0.1959	0.4630	0.9574	0.0500
H(24)	0.0648	0.6342	1.2297	0.0500
H(26)	0.1234	0.9646	1.0324	0.0500
H(3M1)	0.3681	1.4290	0.5315	0.0500
H(3M2)	0.4584	1.2994	0.4603	0.0500
H(3M3)	0.3312	1.3249	0.3792	0.0500
H(33)	0.4013	1.0760	0.3115	0.0500
H(34)	0.4049	0.6837	0.1670	0.0500
H(35)	0.3495	0.5663	0.3063	0.0500
H(36)	0.2902	0.6490	0.4749	0.0500
H(1S)	0.5986	0.6071	0.2237	0.0500
H(2S)	0.6664	0.4315	0.2138	0.0500
H(3S)	0.5864	0.4825	0.0821	0.0500
H(4S)	0.0502	0.4237	0.4184	0.0500
H(5S)	0.1824	0.4077	0.4721	0.0500
H(6S)	0.0959	0.2271	0.4089	0.0500

	U_{11}	U_{22}	U_{33}	U_{23}	U_{13}	U_{12}
C(1)	0.032(5)	0.032(5)	0.035(5)	0.001(4)	0.020(4)	-0.004(4)
N(2)	0.046(5)	0.040(5)	0.029(4)	0.009(3)	0.012(4)	-0.013(3)
N(3)	0.044(5)	0.033(4)	0.039(4)	0.003(3)	0.025(4)	-0.010(4)
N(11)	0.023(4)	0.034(4)	0.028(3)	0.012(3)	0.005(3)	-0.007(3)
C(12)	0.023(4)	0.040(5)	0.034(4)	0.012(4)	0.013(4)	-0.001(4)
C(13)	0.025(5)	0.035(5)	0.033(4)	0.005(3)	0.004(4)	-0.010(4)
N(14)	0.026(4)	0.029(4)	0.033(4)	0.007(3)	0.013(3)	0.006(3)
C(15)	0.020(4)	0.035(4)	0.035(4)	0.015(3)	0.006(4)	-0.004(3)
C(16)	0.024(4)	0.035(5)	0.022(4)	0.004(3)	0.006(3)	-0.010(4)
C(21)	0.035(5)	0.043(5)	0.025(4)	0.010(4)	0.013(4)	-0.012(4)
C(22)	0.042(5)	0.035(5)	0.051(5)	0.014(4)	0.008(4)	-0.008(4)
C(23)	0.039(6)	0.050(6)	0.063(6)	0.035(5)	-0.001(5)	-0.016(5)
Cl(23)	0.109(2)	0.072(2)	0.095(2)	0.052(2)	0.012(2)	-0.025(2)
C(24)	0.051(6)	0.080(8)	0.044(5)	0.021(5)	0.017(5)	-0.018(5)
C(25)	0.053(6)	0.075(7)	0.054(6)	0.008(5)	0.035(5)	-0.004(5)
Cl(25)	0.136(3)	0.123(3)	0.108(2)	0.010(2)	0.095(2)	0.032(2)
C(26)	0.045(5)	0.047(5)	0.041(5)	0.010(4)	0.020(4)	0.001(4)
C(31)	0.029(5)	0.031(5)	0.026(4)	0.012(4)	0.010(3)	-0.001(4)
C(32)	0.038(5)	0.027(5)	0.027(4)	0.002(4)	0.011(4)	0.003(4)
O(32)	0.078(4)	0.031(3)	0.049(3)	0.006(3)	0.036(3)	0.000(3)
C(3M)	0.073(7)	0.030(5)	0.063(6)	0.012(4)	0.029(5)	-0.008(5)
C(33)	0.038(5)	0.033(5)	0.034(5)	0.010(4)	0.014(4)	0.004(4)
C(34)	0.023(4)	0.043(5)	0.029(4)	0.010(4)	0.008(4)	0.008(4)
O(34)	0.050(4)	0.039(3)	0.034(3)	0.000(3)	0.020(3)	0.004(3)
C(35)	0.052(5)	0.024(4)	0.035(4)	0.006(4)	0.023(4)	0.006(4)
C(36)	0.048(5)	0.037(5)	0.038(5)	0.015(4)	0.020(4)	0.004(4)
S(1)	0.044(1)	0.033(1)	0.037(1)	0.002(1)	0.016(1)	-0.002(1)
O(1S)	0.050(4)	0.035(3)	0.044(3)	-0.009(3)	0.014(3)	0.000(3)
O(2S)	0.035(3)	0.045(4)	0.059(4)	0.004(3)	0.006(3)	0.008(3)
O(3S)	0.110(5)	0.068(4)	0.043(4)	0.024(3)	0.043(4)	0.024(4)
C(1S)	0.039(5)	0.062(6)	0.059(6)	0.007(5)	0.007(5)	-0.020(5)
S(2)	0.036(1)	0.034(1)	0.048(1)	0.005(1)	0.008(1)	0.001(1)
O(4S)	0.051(4)	0.051(4)	0.062(4)	0.017(3)	0.012(3)	0.026(3)
O(5S)	0.082(4)	0.031(3)	0.042(3)	-0.005(3)	0.005(3)	-0.008(3)
O(6S)	0.044(4)	0.113(6)	0.126(6)	0.048(5)	0.028(4)	-0.015(4)
C(2S)	0.077(7)	0.073(7)	0.035(5)	0.009(5)	0.014(5)	0.027(5)

Table A.9 Positional and thermal parameters for GUDHCL

	x	y	z	U_{eq}
C(1)	-0.9749(10)	0.7322(7)	-0.0341(6)	0.033(7)
N(2)	-0.9823(9)	0.7500(6)	-0.1185(5)	0.038(6)
N(3)	-1.0486(9)	0.7779(5)	0.0187(5)	0.036(6)
N(11)	-0.8953(8)	0.6686(5)	-0.0011(5)	0.032(5)
C(12)	-0.9080(9)	0.6331(6)	0.0837(6)	0.033(6)
C(13)	-0.7562(10)	0.6396(7)	0.1420(6)	0.038(7)
N(14)	-0.6335(7)	0.5979(5)	0.0960(5)	0.028(5)
C(15)	-0.6270(9)	0.6285(6)	0.0047(5)	0.036(6)
C(16)	-0.7863(10)	0.6246(6)	-0.0477(6)	0.036(6)
C(21)	-1.1721(11)	0.8296(7)	-0.0146(6)	0.036(7)
C(22)	-1.1622(11)	0.9123(7)	-0.0021(6)	0.044(8)
C(23)	-1.2810(12)	0.9614(7)	-0.0357(7)	0.051(8)
Cl(23)	-1.2631(3)	1.06290(20)	-0.0239(3)	0.091(3)
C(24)	-1.4140(11)	0.9276(8)	-0.0800(7)	0.049(8)
C(25)	-1.4212(11)	0.8464(8)	-0.0894(6)	0.046(8)
Cl(25)	-1.5908(3)	0.80345(21)	-0.14309(20)	0.0661(23)
C(26)	-1.3041(10)	0.7936(7)	-0.0580(6)	0.041(7)
C(31)	-0.4782(11)	0.6008(6)	0.1490(6)	0.033(7)
C(32)	-0.4025(11)	0.6727(7)	0.1671(6)	0.040(7)
O(32)	-0.4751(7)	0.7425(5)	0.1403(4)	0.048(5)
C(3M)	-0.4170(13)	0.8180(7)	0.1736(8)	0.061(9)
C(33)	-0.2516(10)	0.6718(7)	0.2115(6)	0.032(6)
C(34)	-0.1879(11)	0.5978(7)	0.2363(6)	0.039(7)
O(34)	-0.0405(7)	0.6016(5)	0.2794(5)	0.048(5)
C(35)	-0.2623(11)	0.5261(7)	0.2213(6)	0.036(7)
C(36)	-0.4114(11)	0.5275(7)	0.1755(6)	0.040(7)
Cl(S1)	0.0994(3)	0.82434(18)	0.20731(16)	0.0495(18)
Cl(S2)	0.2463(3)	0.42732(19)	0.08099(21)	0.0621(20)
O(1S)	0.1223(9)	0.0340(5)	0.7641(6)	0.077(6)
H(2A)	-0.9628	0.7021	-0.1836	0.0500
H(2B)	-1.0116	0.8014	-0.1357	0.0500
H(3)	-1.0056	0.7881	0.0752	0.0500
H(12A)	-0.9957	0.6642	0.1139	0.0500
H(12B)	-0.9387	0.5705	0.0752	0.0500
H(13A)	-0.7266	0.7021	0.1529	0.0500
H(13B)	-0.7650	0.6107	0.2039	0.0500
H(14)	-0.7019	0.5227	0.0872	0.0500
H(15A)	-0.5877	0.6901	0.0076	0.0500
H(15B)	-0.5483	0.5920	-0.0269	0.0500
H(16A)	-0.8219	0.5626	-0.0554	0.0500
H(16B)	-0.7825	0.6513	-0.1112	0.0500
H(22)	-1.0610	0.9380	0.0342	0.0500
H(24)	-1.5090	0.9651	-0.1062	0.0500
H(26)	-1.3146	0.7293	-0.0665	0.0500
H(3M1)	-0.4936	0.8640	0.1446	0.0500
H(3M2)	-0.3031	0.8282	0.1563	0.0500
H(3M3)	-0.4139	0.8199	0.2438	0.0500
H(33)	-0.1882	0.7268	0.2255	0.0500
H(34)	-0.0032	0.5492	0.2829	0.0500
H(35)	-0.2087	0.4701	0.2437	0.0500
H(36)	-0.4735	0.4722	0.1611	0.0500
H(1S)	0.0542	0.4715	0.3117	0.0500

	U_{11}	U_{22}	U_{33}	U_{23}	U_{13}	U_{12}
C(1)	0.024(6)	0.059(8)	0.016(5)	0.004(6)	-0.004(5)	0.000(6)
N(2)	0.036(5)	0.045(6)	0.033(6)	0.001(5)	0.007(4)	0.016(5)
N(3)	0.034(5)	0.042(6)	0.031(5)	-0.005(5)	0.001(4)	0.017(5)
N(11)	0.026(5)	0.040(6)	0.029(5)	-0.003(4)	0.002(4)	0.009(4)
C(12)	0.028(6)	0.041(7)	0.029(6)	0.000(5)	0.001(5)	0.001(5)
C(13)	0.034(6)	0.054(7)	0.027(6)	0.000(5)	0.010(5)	0.007(5)
N(14)	0.020(4)	0.031(5)	0.032(5)	0.001(4)	-0.008(4)	0.004(4)
C(15)	0.021(5)	0.057(8)	0.029(6)	0.007(5)	0.002(5)	-0.007(5)
C(16)	0.037(6)	0.044(7)	0.027(6)	0.001(5)	0.007(5)	0.005(6)
C(21)	0.033(7)	0.044(8)	0.030(6)	0.003(6)	0.005(5)	0.010(6)
C(22)	0.029(6)	0.058(9)	0.046(7)	0.002(7)	0.008(5)	-0.001(6)
C(23)	0.028(6)	0.046(8)	0.079(8)	0.013(7)	0.022(6)	0.009(6)
Cl(23)	0.052(2)	0.045(2)	0.177(4)	0.018(2)	0.037(2)	0.006(2)
C(24)	0.030(6)	0.052(9)	0.066(8)	0.021(7)	0.012(6)	0.021(7)
C(25)	0.037(7)	0.071(10)	0.030(7)	0.006(6)	0.003(5)	-0.005(7)
Cl(25)	0.037(2)	0.097(3)	0.062(2)	0.011(2)	-0.008(1)	-0.001(2)
C(26)	0.027(6)	0.064(9)	0.034(6)	0.003(6)	0.008(5)	0.013(6)
C(31)	0.035(6)	0.022(7)	0.041(6)	-0.004(6)	0.011(5)	0.000(6)
C(32)	0.040(7)	0.039(8)	0.040(6)	0.004(6)	0.012(5)	0.007(6)
O(32)	0.046(4)	0.036(5)	0.059(5)	0.005(5)	-0.002(4)	0.006(4)
C(3M)	0.064(8)	0.032(8)	0.081(9)	-0.005(8)	-0.014(7)	0.010(7)
C(33)	0.022(6)	0.040(8)	0.034(6)	-0.002(6)	0.011(5)	-0.004(5)
C(34)	0.033(7)	0.058(9)	0.027(6)	-0.005(6)	0.002(5)	0.001(7)
O(34)	0.022(4)	0.058(6)	0.061(5)	-0.002(5)	-0.015(4)	0.008(4)
C(35)	0.029(6)	0.039(8)	0.043(7)	0.005(6)	-0.010(5)	0.001(6)
C(36)	0.041(7)	0.039(8)	0.040(6)	0.006(6)	0.014(6)	0.005(6)
Cl(S1)	0.063(2)	0.051(2)	0.034(2)	-0.007(2)	0.007(1)	-0.005(2)
Cl(S2)	0.049(2)	0.044(2)	0.091(2)	-0.008(2)	0.000(2)	-0.006(2)
O(1S)	0.056(5)	0.070(7)	0.105(7)	-0.004(6)	0.015(5)	-0.014(5)

APPENDIX B

Table B.1 Positional and thermal parameters for IMFBTOL

	x	y	z	U_{eq}
N(1)	0.51868(18)	0.78088(23)	0.1961(5)	0.057(3)
C(2)	0.53032(22)	0.7414(3)	0.0977(6)	0.052(4)
N(3)	0.50645(21)	0.7559(3)	-0.0228(5)	0.059(4)
C(4)	0.47794(23)	0.8056(3)	0.0002(7)	0.060(4)
C(4')	0.44746(25)	0.8310(3)	-0.1144(7)	0.079(5)
C(5)	0.48631(23)	0.8205(3)	0.1356(6)	0.056(4)
C(6)	0.46490(24)	0.8689(3)	0.2200(7)	0.060(4)
N(7)	0.43106(19)	0.84697(22)	0.3269(5)	0.059(3)
C(8)	0.42513(25)	0.8880(3)	0.4426(7)	0.075(5)
C(9)	0.39020(24)	0.8636(4)	0.5497(7)	0.078(5)
N(10)	0.34112(19)	0.85389(23)	0.4881(5)	0.065(4)
C(11)	0.3477(3)	0.8115(3)	0.3761(7)	0.074(5)
C(12)	0.38319(24)	0.8337(3)	0.2667(7)	0.072(5)
C(13)	0.3047(3)	0.8344(3)	0.5916(7)	0.072(5)
C(14)	0.2544(3)	0.8242(3)	0.5221(8)	0.073(5)
C(15)	0.2355(3)	0.8632(4)	0.4312(10)	0.094(6)
C(16)	0.1906(3)	0.8525(4)	0.3671(10)	0.107(7)
C(17)	0.1636(3)	0.8031(5)	0.3965(11)	0.104(7)
C(18)	0.1823(4)	0.7643(4)	0.4882(12)	0.115(8)
C(19)	0.2272(4)	0.7742(4)	0.5529(10)	0.096(6)
C(14')	0.30025(25)	0.8784(4)	0.7105(8)	0.073(5)
C(15')	0.3006(3)	0.9379(4)	0.6877(10)	0.095(6)
C(16')	0.2967(4)	0.9759(5)	0.7984(16)	0.141(10)
C(17')	0.2920(5)	0.9575(8)	0.9303(17)	0.165(14)
C(18')	0.2913(5)	0.9001(8)	0.9528(12)	0.176(13)
C(19')	0.2947(4)	0.8592(5)	0.8455(10)	0.124(8)
C(20)	0.56327(22)	0.6912(3)	0.1119(6)	0.054(4)
C(21)	0.58902(23)	0.6831(3)	0.2357(7)	0.064(4)
C(22)	0.6203(3)	0.6359(3)	0.2526(6)	0.077(5)
C(23)	0.6274(3)	0.5948(3)	0.1475(10)	0.083(6)
C(23')	0.6613(3)	0.5424(4)	0.1699(10)	0.113(7)
C(24)	0.6020(3)	0.6036(4)	0.0235(9)	0.090(6)
C(25)	0.57100(25)	0.6508(3)	0.0072(7)	0.073(5)
C(1S)	0.5218(6)	0.5250(7)	0.4356(12)	0.119(9)
C(2S)	0.5581(6)	0.5301(7)	0.5382(12)	0.111(6)
C(3S)	0.5508(6)	0.5048(7)	0.6693(12)	0.113(6)
C(4S)	0.5071(6)	0.4745(7)	0.6978(12)	0.153(8)
C(5S)	0.4708(6)	0.4694(7)	0.5952(12)	0.169(13)
C(6S)	0.4781(6)	0.4947(7)	0.4641(12)	0.140(8)

H(3)	0.5065	0.7351	-0.0994	0.0500
H(41)	0.4253	0.8670	-0.0769	0.0500
H(42)	0.4234	0.7977	-0.1578	0.0500
H(43)	0.4709	0.8472	-0.1975	0.0500
H(61)	0.4449	0.8983	0.1516	0.0500
H(62)	0.4946	0.8926	0.2703	0.0500
H(81)	0.4607	0.8956	0.4907	0.0500
H(82)	0.4106	0.9291	0.4035	0.0500
H(91)	0.3870	0.8943	0.6352	0.0500
H(92)	0.4044	0.8222	0.5881	0.0500
H(111)	0.3620	0.7709	0.4194	0.0500
H(112)	0.3123	0.8032	0.3277	0.0500
H(121)	0.3682	0.8732	0.2202	0.0500
H(122)	0.3877	0.8004	0.1873	0.0500
H(131)	0.3173	0.7932	0.6352	0.0500
H(15)	0.2556	0.9032	0.4080	0.0500
H(16)	0.1765	0.8839	0.2922	0.0500
H(17)	0.1283	0.7954	0.3473	0.0500
H(18)	0.1619	0.7247	0.5119	0.0500
H(19)	0.2411	0.7429	0.6280	0.0500
H(15')	0.3040	0.9549	0.5829	0.0500
H(16')	0.2975	1.0227	0.7781	0.0500
H(17')	0.2889	0.9885	1.0154	0.0500
H(18')	0.2879	0.8844	1.0567	0.0500
H(19')	0.2931	0.8126	0.8680	0.0500
H(21)	0.5845	0.7143	0.3196	0.0500
H(22)	0.6398	0.6306	0.3502	0.0500
H(231)	0.6705	0.5233	0.0710	0.0500
H(232)	0.6427	0.5105	0.2336	0.0500
H(233)	0.6943	0.5566	0.2216	0.0500
H(24)	0.6068	0.5728	-0.0615	0.0500
H(25)	0.5520	0.6565	-0.0911	0.0500

	U_{11}	U_{22}	U_{33}	U_{23}	U_{13}	U_{12}
N(1)	0.061(3)	0.070(3)	0.039(3)	-0.003(3)	0.002(3)	0.001(3)
C(2)	0.050(4)	0.069(4)	0.037(4)	0.006(4)	-0.003(3)	-0.012(4)
N(3)	0.066(3)	0.079(4)	0.031(3)	-0.006(3)	-0.001(3)	-0.008(3)
C(4)	0.059(4)	0.071(4)	0.049(4)	0.005(4)	-0.002(4)	-0.003(4)
C(4')	0.084(5)	0.098(6)	0.055(4)	0.007(4)	-0.020(4)	0.012(5)
C(5)	0.057(4)	0.069(4)	0.041(4)	0.008(4)	-0.006(3)	-0.004(4)
C(6)	0.067(4)	0.057(4)	0.055(4)	0.000(4)	-0.001(4)	0.006(4)
N(7)	0.063(4)	0.069(4)	0.045(3)	-0.006(3)	-0.001(3)	0.009(3)
C(8)	0.061(4)	0.094(5)	0.069(5)	-0.027(5)	-0.018(4)	0.009(4)
C(9)	0.065(5)	0.116(6)	0.053(4)	-0.018(4)	-0.006(4)	0.020(4)
N(10)	0.062(3)	0.075(4)	0.058(3)	-0.011(3)	-0.002(3)	0.004(3)
C(11)	0.074(5)	0.081(5)	0.066(5)	-0.010(4)	0.004(4)	-0.008(4)
C(12)	0.079(5)	0.085(5)	0.052(4)	-0.018(4)	-0.004(4)	-0.012(4)
C(13)	0.078(5)	0.066(5)	0.072(5)	0.001(4)	0.010(5)	0.011(4)
C(14)	0.067(5)	0.065(5)	0.086(6)	-0.017(5)	0.017(5)	-0.010(4)
C(15)	0.073(5)	0.079(5)	0.131(8)	0.018(6)	-0.021(6)	-0.011(5)
C(16)	0.087(6)	0.107(7)	0.128(8)	0.008(6)	-0.019(6)	-0.014(6)
C(17)	0.087(6)	0.113(8)	0.113(8)	-0.036(7)	0.007(6)	-0.027(7)
C(18)	0.100(7)	0.089(8)	0.154(10)	-0.009(7)	0.029(7)	-0.033(6)
C(19)	0.103(6)	0.090(7)	0.096(6)	0.002(5)	0.018(6)	-0.006(5)
C(14')	0.062(5)	0.092(6)	0.066(5)	-0.010(5)	0.001(4)	0.021(4)
C(15')	0.098(6)	0.087(6)	0.099(7)	-0.025(6)	0.027(5)	-0.013(5)
C(16')	0.111(8)	0.113(8)	0.201(13)	-0.090(10)	0.045(9)	-0.007(6)
C(17')	0.106(9)	0.246(19)	0.141(13)	-0.132(15)	-0.013(9)	0.036(11)
C(18')	0.202(14)	0.264(18)	0.062(7)	-0.043(11)	-0.024(7)	0.130(15)
C(19')	0.163(10)	0.137(8)	0.072(6)	0.003(7)	0.005(6)	0.081(7)
C(20)	0.050(4)	0.071(4)	0.039(4)	-0.003(4)	-0.002(3)	-0.003(4)
C(21)	0.066(4)	0.071(5)	0.056(4)	-0.001(4)	0.001(4)	0.012(4)
C(22)	0.075(5)	0.088(5)	0.066(5)	0.003(5)	-0.013(4)	-0.001(5)
C(23)	0.063(5)	0.084(5)	0.102(7)	-0.013(6)	-0.002(5)	0.006(4)
C(23')	0.090(6)	0.100(6)	0.148(8)	-0.025(6)	-0.030(6)	0.017(5)
C(24)	0.081(5)	0.097(6)	0.091(6)	-0.033(5)	-0.011(5)	0.019(5)
C(25)	0.071(5)	0.091(5)	0.056(4)	-0.015(4)	-0.011(4)	0.005(4)

Table B.2 Positional and thermal parameters for IMMHCL

	x	y	z	U_{eq}
N(1)	-0.3253(3)	0.76723(25)	0.08025(17)	0.0459(20)
C(2)	-0.3011(4)	0.6497(3)	0.12644(20)	0.0401(23)
N(3)	-0.1460(3)	0.5837(3)	0.11711(18)	0.0437(20)
C(4)	-0.0638(4)	0.6608(3)	0.06178(20)	0.0428(23)
C(4')	0.1097(4)	0.6157(4)	0.03290(25)	0.060(3)
C(5)	-0.1761(4)	0.7742(3)	0.03995(20)	0.0435(23)
C(6)	-0.1508(4)	0.8921(3)	-0.01827(21)	0.0492(24)
N(7)	-0.1946(3)	0.92281(25)	-0.11262(17)	0.0417(19)
C(8)	0.3694(4)	0.9594(3)	0.11541(22)	0.0535(24)
C(9)	-0.4048(4)	0.9835(3)	-0.20996(22)	0.0528(25)
N(10)	-0.3446(3)	1.08207(24)	-0.27302(17)	0.0434(19)
C(11)	-0.1729(4)	1.0457(3)	-0.27119(22)	0.0488(24)
C(12)	-0.1336(4)	1.0220(3)	-0.17733(22)	0.0482(24)
C(13)	-0.3867(4)	1.1051(3)	-0.36409(21)	0.0495(24)
C(14)	-0.5652(4)	1.1548(3)	-0.36600(22)	0.0487(24)
C(15)	-0.6635(4)	1.2253(4)	-0.31059(25)	0.060(3)
C(16)	-0.8246(5)	1.2722(4)	-0.3151(3)	0.080(4)
C(17)	-0.8903(6)	1.2500(5)	-0.3764(4)	0.087(4)
C(18)	-0.7964(7)	1.1807(5)	-0.4317(4)	0.096(4)
C(19)	-0.6337(6)	1.1325(4)	-0.4275(3)	0.080(4)
C(14')	-0.3090(4)	1.1952(3)	-0.43388(21)	0.050(3)
C(15')	-0.3463(4)	1.3161(4)	-0.42988(24)	0.060(3)
C(16')	-0.2769(5)	1.3980(4)	-0.4940(3)	0.075(3)
C(17')	-0.1699(6)	1.3593(6)	-0.5623(3)	0.089(4)
C(18')	-0.1330(5)	1.2415(6)	-0.5682(3)	0.089(4)
C(19')	-0.2029(5)	1.1583(4)	-0.50373(25)	0.072(3)
C(20)	-0.4233(4)	0.5952(3)	0.18200(20)	0.0427(23)
C(21)	-0.5814(4)	0.6521(3)	0.16600(23)	0.0519(25)
C(22)	-0.6959(4)	0.6003(4)	0.21863(25)	0.060(3)
C(23)	-0.6583(5)	0.4927(3)	0.28777(24)	0.059(3)
C(23')	-0.7833(5)	0.4337(4)	0.3415(3)	0.081(4)
C(24)	-0.5018(4)	0.4384(3)	0.30399(23)	0.056(3)
C(25)	-0.3851(4)	0.4879(3)	0.25242(22)	0.0510(25)
Cl(1)	0.04614(12)	0.30024(8)	0.19211(6)	0.0616(7)
O(1A)	0.2799(4)	0.8626(3)	-0.0817(3)	0.119(3)
C(1A)	0.3529(6)	0.7996(4)	-0.1322(4)	0.068(4)
C(2A)	0.4809(6)	0.6830(4)	-0.1022(4)	0.100(4)
C(3A)	0.3173(6)	0.8371(5)	-0.2273(4)	0.103(5)
H(3)	-0.0995	0.5086	0.1392	0.0500
H(41')	0.1602	0.6881	0.0250	0.0500
H(42')	0.1280	0.5929	-0.0300	0.0500
H(43')	0.1652	0.5343	0.0840	0.0500
H(61)	-0.2231	0.9664	0.0116	0.0500
H(62)	-0.0272	0.8842	-0.0224	0.0500
H(7)	-0.1455	0.8551	-0.1328	0.0500
H(81)	0.4136	0.8855	0.0712	0.0500
H(82)	0.4271	0.0428	0.0934	0.0500
H(91)	-0.5317	1.0109	-0.2109	0.0500
H(92)	-0.3490	0.8993	-0.2311	0.0500
H(111)	-0.1165	0.9621	-0.2931	0.0500
H(112)	-0.1293	1.1194	-0.3162	0.0500
H(121)	-0.1871	1.1065	-0.1563	0.0500
H(122)	-0.0063	0.9939	-0.1778	0.0500
H(131)	-0.3427	1.0176	-0.3810	0.0500
H(15)	-0.6131	1.2444	-0.2624	0.0500
H(16)	-0.8994	1.3265	-0.2702	0.0500
H(17)	-1.0168	1.2879	-0.3806	0.0500
H(18)	-0.8484	1.1626	-0.4797	0.0500
H(19)	-0.5600	1.0777	-0.4724	0.0500
H(15')	-0.4305	1.3468	-0.3761	0.0500
H(16')	-0.3066	1.4921	-0.4901	0.0500
H(17')	-0.1148	1.4231	-0.6120	0.0500
H(18')	-0.0497	1.2121	-0.6227	0.0500
H(19')	-0.1734	1.0647	-0.5086	0.0500
H(21)	-0.6149	0.7365	0.1124	0.0500
H(22)	-0.8184	0.6456	0.2054	0.0500
H(231)	-0.8978	0.5028	0.3431	0.0500
H(232)	-0.7540	0.3875	0.4098	0.0500
H(233)	-0.7889	0.3661	0.3116	0.0500
H(234)	-0.8608	0.4357	0.2972	0.0500
H(235)	-0.8528	0.4824	0.3904	0.0500
H(236)	-0.7271	0.3381	0.3762	0.0500
H(24)	-0.4693	0.3550	0.3586	0.0500
H(25)	-0.2632	0.4429	0.2669	0.0500
H(2A1)	0.4563	0.6227	-0.1061	0.0500
H(2A2)	0.5976	0.6763	-0.1405	0.0500
H(2A3)	0.5105	0.6428	-0.0233	0.0500
H(3A1)	0.4256	0.8146	-0.2714	0.0500
H(3A2)	0.2559	0.9354	-0.2467	0.0500
H(3A3)	0.2424	0.7856	-0.2303	0.0500

	U_{11}	U_{22}	U_{33}	U_{23}	U_{13}	U_{12}
N(1)	0.046(2)	0.040(2)	0.038(2)	-0.011(1)	0.002(1)	-0.009(1)
C(2)	0.042(2)	0.034(2)	0.033(2)	-0.010(1)	-0.002(1)	-0.006(2)
N(3)	0.047(2)	0.031(1)	0.041(2)	-0.006(1)	-0.006(1)	-0.008(1)
C(4)	0.041(2)	0.042(2)	0.034(2)	-0.009(2)	-0.005(2)	-0.012(2)
C(4')	0.047(2)	0.061(2)	0.054(2)	-0.012(2)	-0.003(2)	-0.016(2)
C(5)	0.048(2)	0.038(2)	0.033(2)	-0.010(1)	-0.002(2)	-0.013(2)
C(6)	0.052(2)	0.044(2)	0.040(2)	-0.011(2)	-0.004(2)	-0.017(2)
N(7)	0.038(2)	0.032(1)	0.042(2)	-0.009(1)	0.001(1)	-0.007(1)
C(8)	0.037(2)	0.044(2)	0.049(2)	0.003(2)	0.001(2)	0.014(2)
C(9)	0.046(2)	0.049(2)	0.049(2)	0.002(2)	-0.005(2)	-0.021(2)
N(10)	0.034(2)	0.040(2)	0.041(2)	-0.005(1)	0.000(1)	-0.009(1)
C(11)	0.039(2)	0.045(2)	0.044(2)	0.000(2)	0.001(2)	-0.011(2)
C(12)	0.037(2)	0.043(2)	0.049(2)	0.000(2)	-0.002(2)	-0.016(2)
C(13)	0.050(2)	0.043(2)	0.042(2)	-0.012(2)	-0.003(2)	-0.011(2)
C(14)	0.049(2)	0.041(2)	0.044(2)	-0.005(2)	-0.008(2)	-0.018(2)
C(15)	0.039(2)	0.068(3)	0.059(2)	-0.025(2)	-0.007(2)	-0.010(2)
C(16)	0.048(3)	0.086(3)	0.084(3)	-0.025(3)	-0.008(2)	-0.013(2)
C(17)	0.057(3)	0.078(3)	0.103(4)	0.001(3)	-0.029(3)	-0.028(3)
C(18)	0.090(4)	0.088(3)	0.099(4)	-0.017(3)	-0.051(3)	-0.036(3)
C(19)	0.085(3)	0.072(3)	0.072(3)	-0.028(2)	-0.021(2)	-0.028(2)
C(14')	0.040(2)	0.059(2)	0.035(2)	-0.006(2)	-0.004(2)	-0.011(2)
C(15')	0.056(2)	0.060(3)	0.046(2)	-0.004(2)	-0.003(2)	-0.023(2)
C(16')	0.071(3)	0.073(3)	0.064(3)	0.010(2)	-0.024(2)	-0.039(2)
C(17')	0.068(3)	0.127(5)	0.049(3)	0.022(3)	-0.021(2)	-0.059(3)
C(18')	0.059(3)	0.136(5)	0.039(2)	-0.009(3)	0.008(2)	-0.030(3)
C(19')	0.056(3)	0.089(3)	0.047(2)	-0.022(2)	0.004(2)	-0.013(2)
C(20)	0.044(2)	0.037(2)	0.037(2)	-0.013(2)	-0.003(2)	-0.012(2)
C(21)	0.046(2)	0.047(2)	0.047(2)	-0.014(2)	-0.004(2)	-0.006(2)
C(22)	0.041(2)	0.067(3)	0.056(2)	-0.019(2)	-0.001(2)	-0.014(2)
C(23)	0.057(3)	0.057(2)	0.053(2)	-0.020(2)	0.006(2)	-0.027(2)
C(23')	0.064(3)	0.081(3)	0.080(3)	-0.018(2)	0.007(2)	-0.038(2)
C(24)	0.057(3)	0.050(2)	0.047(2)	-0.007(2)	-0.002(2)	-0.020(2)
C(25)	0.049(2)	0.046(2)	0.044(2)	-0.004(2)	-0.008(2)	-0.015(2)
Cl(1)	0.0719(7)	0.0424(5)	0.0498(5)	-0.0136(4)	-0.0035(4)	-0.0023(4)
O(1A)	0.108(3)	0.086(2)	0.140(3)	-0.068(2)	0.048(2)	-0.041(2)
C(1A)	0.072(3)	0.068(3)	0.111(4)	-0.043(3)	0.028(3)	-0.043(3)
C(2A)	0.093(4)	0.079(4)	0.107(4)	-0.041(3)	0.014(3)	-0.033(3)
C(3A)	0.074(4)	0.080(3)	0.136(5)	-0.044(3)	0.001(3)	-0.025(3)

Table B.3 Positional and thermal parameters for IMMMES

	x	y	z	U_{eq}
N(1)	0.0725(4)	0.17421(12)	0.5340(4)	0.050(3)
C(2)	-0.0574(5)	0.15842(15)	0.4723(5)	0.046(3)
N(3)	-0.1651(4)	0.18732(13)	0.4692(4)	0.0469(25)
C(4)	-0.1012(5)	0.22352(15)	0.5317(5)	0.047(3)
C(4')	-0.1887(5)	0.26093(15)	0.5454(5)	0.056(3)
C(5)	0.0465(5)	0.21485(14)	0.5717(5)	0.045(3)
C(6)	0.1694(5)	0.24261(15)	0.6440(5)	0.050(3)
N(7)	0.2348(4)	0.26671(12)	0.5448(4)	0.046(3)
C(8)	0.1278(5)	0.29733(15)	0.4575(5)	0.052(3)
C(9)	0.1988(5)	0.32197(15)	0.3652(5)	0.050(3)
N(10)	0.3275(4)	0.34521(12)	0.4470(4)	0.0485(25)
C(11)	0.4353(5)	0.31426(15)	0.5216(5)	0.050(3)
C(12)	0.3726(5)	0.28928(17)	0.6197(5)	0.051(3)
C(13)	0.3825(5)	0.37319(15)	0.3550(5)	0.049(3)
C(14)	0.5339(5)	0.38997(16)	0.4266(6)	0.052(3)
C(15)	0.5576(6)	0.41547(19)	0.5389(6)	0.070(4)
C(16)	0.6959(9)	0.43059(23)	0.6041(7)	0.094(5)
C(17)	0.8136(8)	0.4186(3)	0.5538(10)	0.104(6)
C(18)	0.7915(7)	0.39313(24)	0.4416(10)	0.098(6)
C(19)	0.6518(6)	0.37877(17)	0.3783(7)	0.071(4)
C(14')	0.2752(5)	0.40898(15)	0.3044(5)	0.047(3)
C(15')	0.1903(6)	0.42552(17)	0.3834(6)	0.068(4)
C(16')	0.0958(7)	0.45927(20)	0.3338(7)	0.088(5)
C(17')	0.0846(7)	0.47615(20)	0.2053(7)	0.083(5)
C(18')	0.1691(8)	0.45939(22)	0.1283(7)	0.087(5)
C(19')	0.2630(6)	0.42661(19)	0.1768(6)	0.072(4)
C(20)	-0.0640(5)	0.11603(14)	0.4124(5)	0.048(3)
C(21)	0.0258(6)	0.08602(16)	0.4445(6)	0.059(4)
C(22)	0.0038(6)	0.04595(17)	0.3888(6)	0.068(4)
C(23)	-0.1265(7)	0.03448(17)	0.2987(6)	0.067(4)
C(23')	-0.1505(7)	-0.00839(18)	0.2374(7)	0.095(5)
C(24)	-0.2406(6)	0.06422(17)	0.2699(5)	0.061(4)
C(25)	-0.2195(6)	0.10438(16)	0.3245(5)	0.056(4)
S	0.43235(14)	0.18677(4)	0.42091(15)	0.0544(8)
O(1S)	0.5348(4)	0.18511(12)	0.3361(4)	0.0700(25)
O(2S)	0.3053(4)	0.21263(12)	0.3594(3)	0.0648(24)
O(3S)	0.5012(4)	0.19886(13)	0.5608(4)	0.080(3)
C(1S)	0.3682(7)	0.13525(18)	0.4280(9)	0.104(6)

H(3)	-0.2576	0.1857	0.4402	0.0500
H(41')	-0.1415	0.2858	0.6159	0.0500
H(42')	-0.2865	0.2587	0.5756	0.0500
H(43')	-0.2321	0.2817	0.4604	0.0500
H(61)	0.1296	0.2651	0.7054	0.0500
H(62)	0.2541	0.2234	0.7105	0.0500
H(7)	0.2606	0.2502	0.4929	0.0500
H(81)	0.0348	0.2801	0.3946	0.0500
H(82)	0.0914	0.3190	0.5236	0.0500
H(91)	0.1203	0.3441	0.3047	0.0500
H(92)	0.2325	0.3003	0.2972	0.0500
H(111)	0.4623	0.2930	0.4487	0.0500
H(112)	0.5332	0.3305	0.5793	0.0500
H(121)	0.3400	0.3111	0.6877	0.0500
H(122)	0.4470	0.2662	0.6801	0.0500
H(13)	0.3916	0.3550	0.2673	0.0500
H(15)	0.4665	0.4241	0.5778	0.0500
H(16)	0.7133	0.4513	0.6921	0.0500
H(17)	0.9228	0.4296	0.6049	0.0500
H(18)	0.8822	0.3843	0.4025	0.0500
H(19)	0.6338	0.3584	0.2893	0.0500
H(15')	0.1974	0.4123	0.4836	0.0500
H(16')	0.0310	0.4723	0.3964	0.0500
H(17')	0.0106	0.5020	0.1661	0.0500
H(18')	0.1613	0.4723	0.0276	0.0500
H(19')	0.3289	0.4143	0.1141	0.0500
H(21)	0.1308	0.0941	0.5146	0.0500
H(22)	0.0918	0.0232	0.4162	0.0500
H(231)	-0.0583	-0.0279	0.2372	0.0500
H(232)	-0.2075	-0.0137	0.1331	0.0500
H(233)	-0.2057	-0.0324	0.2781	0.0500
H(24)	-0.3468	0.0556	0.2031	0.0500
H(25)	-0.3084	0.1269	0.2990	0.0500
H(11S)	0.3209	0.1330	0.3178	0.0500
H(12S)	0.2819	0.1342	0.4785	0.0500
H(13S)	0.4426	0.1092	0.4632	0.0500

	U_{11}	U_{22}	U_{33}	U_{23}	U_{13}	U_{12}
N(1)	0.050(3)	0.043(2)	0.054(3)	0.003(2)	0.020(2)	-0.003(2)
C(2)	0.042(3)	0.043(3)	0.049(3)	0.007(2)	0.019(3)	-0.001(3)
N(3)	0.041(2)	0.045(2)	0.052(3)	0.001(2)	0.018(2)	-0.004(2)
C(4)	0.049(3)	0.045(3)	0.044(3)	0.002(2)	0.020(2)	0.001(2)
C(4')	0.054(3)	0.049(3)	0.060(3)	-0.007(3)	0.022(3)	0.003(3)
C(5)	0.045(3)	0.045(3)	0.042(3)	0.001(2)	0.014(2)	-0.008(2)
C(6)	0.052(3)	0.052(3)	0.043(3)	0.001(2)	0.013(3)	-0.002(3)
N(7)	0.050(2)	0.039(2)	0.047(2)	-0.005(2)	0.017(2)	-0.003(2)
C(8)	0.042(3)	0.045(3)	0.063(3)	0.007(3)	0.008(3)	-0.003(2)
C(9)	0.049(3)	0.044(3)	0.048(3)	0.002(2)	0.001(3)	-0.007(2)
N(10)	0.045(2)	0.042(2)	0.053(2)	-0.001(2)	0.010(2)	-0.006(2)
C(11)	0.039(3)	0.045(3)	0.060(3)	0.004(3)	0.007(2)	-0.003(2)
C(12)	0.040(3)	0.052(3)	0.053(3)	-0.007(3)	-0.001(2)	-0.009(2)
C(13)	0.047(3)	0.051(3)	0.048(3)	-0.003(3)	0.019(3)	-0.007(3)
C(14)	0.047(3)	0.048(3)	0.056(3)	0.006(3)	0.013(3)	-0.004(2)
C(15)	0.059(4)	0.075(4)	0.067(4)	-0.003(3)	0.013(3)	-0.018(3)
C(16)	0.100(6)	0.098(5)	0.068(4)	0.003(4)	-0.003(4)	-0.039(5)
C(17)	0.052(4)	0.121(7)	0.123(7)	0.043(6)	-0.008(5)	-0.025(5)
C(18)	0.057(4)	0.090(5)	0.139(7)	0.021(5)	0.032(5)	0.002(4)
C(19)	0.057(4)	0.059(3)	0.092(4)	0.010(3)	0.026(3)	-0.002(3)
C(14')	0.048(3)	0.044(3)	0.047(3)	0.000(2)	0.015(3)	-0.005(2)
C(15')	0.078(4)	0.058(3)	0.066(4)	0.014(3)	0.029(3)	0.013(3)
C(16')	0.086(5)	0.078(4)	0.097(5)	0.002(4)	0.041(4)	0.026(4)
C(17')	0.085(5)	0.067(4)	0.085(5)	0.024(4)	0.007(4)	0.012(4)
C(18')	0.103(5)	0.097(5)	0.054(4)	0.030(4)	0.021(4)	0.014(4)
C(19')	0.067(4)	0.088(5)	0.057(4)	0.012(4)	0.022(3)	0.010(3)
C(20)	0.050(3)	0.040(3)	0.051(3)	0.005(2)	0.023(3)	-0.004(2)
C(21)	0.052(3)	0.048(3)	0.073(4)	0.000(3)	0.023(3)	-0.007(3)
C(22)	0.062(4)	0.050(3)	0.087(4)	0.002(3)	0.026(4)	0.007(3)
C(23)	0.084(4)	0.050(3)	0.063(4)	-0.003(3)	0.028(3)	-0.008(3)
C(23')	0.116(6)	0.050(4)	0.107(5)	-0.023(4)	0.020(5)	-0.004(4)
C(24)	0.068(4)	0.052(3)	0.057(3)	-0.006(3)	0.016(3)	-0.008(3)
C(25)	0.054(3)	0.049(3)	0.061(3)	0.008(3)	0.017(3)	0.000(3)
S	0.0482(7)	0.0482(7)	0.0624(9)	0.0029(7)	0.0169(7)	-0.0027(7)
O(1S)	0.048(2)	0.078(3)	0.081(3)	0.005(2)	0.027(2)	0.003(2)
O(2S)	0.061(2)	0.073(2)	0.057(2)	0.000(2)	0.020(2)	0.020(2)
O(3S)	0.081(3)	0.092(3)	0.055(2)	0.005(2)	0.002(2)	0.000(2)
C(1S)	0.097(5)	0.047(4)	0.169(7)	0.002(4)	0.077(5)	-0.008(3)

Table B.4 Positional and thermal parameters for IMTHCLA

	x	y	z	U_{eq}
N(1)	0.11112(19)	0.00351(20)	0.19234(18)	0.0345(17)
C(2)	0.03196(24)	0.0325(3)	0.14058(22)	0.0359(21)
N(3)	-0.01453(22)	-0.05444(22)	0.11369(19)	0.0384(18)
C(4)	0.03485(24)	-0.1388(3)	0.14983(22)	0.0375(21)
C(4')	-0.0017(3)	-0.2449(3)	0.1327(3)	0.0482(24)
C(5)	0.11443(23)	-0.10202(25)	0.19977(22)	0.0342(20)
C(6)	0.19029(22)	-0.1514(3)	0.26316(21)	0.0368(21)
N(7)	0.16291(18)	-0.15495(21)	0.35497(18)	0.0327(17)
C(8)	0.1107(3)	-0.2506(3)	0.36728(24)	0.0396(23)
C(9)	0.07685(23)	-0.2496(3)	0.45602(22)	0.0380(21)
N(10)	0.15483(19)	-0.23576(21)	0.53213(18)	0.0341(16)
C(11)	0.21184(25)	-0.1427(3)	0.51695(23)	0.0416(21)
C(12)	0.24465(23)	-0.1457(3)	0.42804(22)	0.0394(21)
C(13)	0.11657(22)	-0.2242(3)	0.61980(22)	0.0365(20)
C(14)	0.19541(23)	-0.2183(3)	0.69863(22)	0.0375(21)
C(15)	0.2617(3)	-0.2944(3)	0.71983(25)	0.0504(25)
C(16)	0.3270(3)	-0.2874(4)	0.7975(3)	0.066(3)
C(17)	0.3267(3)	-0.2045(4)	0.8533(3)	0.066(3)
C(18)	0.2632(3)	-0.1274(4)	0.8313(3)	0.064(3)
C(19)	0.1973(3)	-0.1333(3)	0.75427(25)	0.0494(25)
C(14')	0.04288(25)	-0.3055(3)	0.62697(23)	0.0409(23)
C(15')	0.0636(3)	-0.4068(3)	0.6436(3)	0.065(3)
C(16')	-0.0067(4)	-0.4781(4)	0.6485(4)	0.084(4)
C(17')	-0.0984(4)	-0.4470(4)	0.6352(3)	0.079(4)
C(18')	-0.1204(3)	-0.3462(4)	0.6183(3)	0.069(3)
C(19')	-0.0501(3)	-0.2743(3)	0.61489(25)	0.053(3)
C(20)	0.00139(23)	0.1371(3)	0.12016(22)	0.0369(21)
C(21)	0.0525(3)	0.2179(3)	0.16199(25)	0.0478(24)
C(22)	0.0214(3)	0.3176(3)	0.1465(3)	0.056(3)
C(23)	-0.0611(3)	0.3389(3)	0.0907(3)	0.055(3)
C(23')	-0.0970(4)	0.4472(4)	0.0760(3)	0.086(4)
C(24)	-0.1118(3)	0.2571(3)	0.0484(3)	0.059(3)
C(25)	-0.0814(3)	0.1575(3)	0.0630(3)	0.0501(25)
Cl(1)	0.21215(6)	0.08997(7)	-0.00227(6)	0.0496(6)
Cl(2)	0.26017(8)	0.09631(8)	0.31259(7)	0.0655(7)
Cl(3)	0.50595(7)	-0.48895(8)	0.87009(7)	0.0614(7)
O(1)	0.1786(9)	0.0946(8)	0.4945(9)	0.121(10)

H(1)	0.1649	0.0550	0.2240	0.0500
H(3)	-0.0677	-0.0569	0.0792	0.0500
H(41')	0.0529	-0.3002	0.1529	0.0500
H(42')	-0.0280	-0.2552	0.0632	0.0500
H(43')	-0.0576	-0.2592	0.1696	0.0500
H(61)	0.2012	-0.2283	0.2412	0.0500
H(62)	0.2541	-0.1079	0.2661	0.0500
H(7)	0.1192	-0.1035	0.3544	0.0500
H(81)	0.1538	-0.3106	0.3607	0.0500
H(82)	0.0599	-0.2575	0.3195	0.0500
H(91)	0.0423	-0.3214	0.4642	0.0500
H(92)	0.0277	-0.1876	0.4561	0.0500
H(10)	0.1937	-0.2952	0.5309	0.0500
H(111)	0.1693	-0.0753	0.5195	0.0500
H(112)	0.2724	-0.1389	0.5669	0.0500
H(121)	0.2904	-0.2107	0.4262	0.0500
H(122)	0.2823	-0.0762	0.4193	0.0500
H(131)	0.0804	-0.1520	0.6200	0.0500
H(15)	0.2628	-0.3591	0.6761	0.0500
H(16)	0.3783	-0.3473	0.8142	0.0500
H(17)	0.3766	-0.2005	0.9144	0.0500
H(18)	0.2644	-0.0616	0.8742	0.0500
H(19)	0.1474	-0.0720	0.7373	0.0500
H(15')	0.1357	-0.4316	0.6532	0.0500
H(16')	0.0109	-0.5574	0.6625	0.0500
H(17')	-0.1533	-0.5021	0.6363	0.0500
H(18')	-0.1928	-0.3222	0.6075	0.0500
H(19')	-0.0678	-0.1947	0.6029	0.0500
H(21)	0.1170	0.2033	0.2070	0.0500
H(22)	0.0629	0.3798	0.1769	0.0500
H(231)	-0.0945	0.4688	0.0079	0.0500
H(232)	-0.1685	0.4506	0.0855	0.0500
H(233)	-0.0549	0.4985	0.1195	0.0500
H(24)	-0.1763	0.2718	0.0034	0.0500
H(25)	-0.1223	0.0954	0.0297	0.0500

	U_{11}	U_{22}	U_{33}	U_{23}	U_{13}	U_{12}
N(1)	0.033(2)	0.035(2)	0.034(2)	0.004(1)	0.004(1)	-0.003(1)
C(2)	0.034(2)	0.043(2)	0.030(2)	0.002(2)	0.005(2)	-0.001(2)
N(3)	0.034(2)	0.042(2)	0.036(2)	0.001(1)	-0.003(1)	-0.003(2)
C(4)	0.039(2)	0.038(2)	0.034(2)	-0.001(2)	0.004(2)	-0.001(2)
C(4')	0.048(2)	0.044(2)	0.051(2)	-0.002(2)	0.002(2)	-0.005(2)
C(5)	0.036(2)	0.033(2)	0.032(2)	0.001(2)	0.007(2)	0.000(2)
C(6)	0.037(2)	0.036(2)	0.037(2)	0.003(2)	0.007(2)	0.002(2)
N(7)	0.031(2)	0.028(2)	0.037(2)	0.003(1)	0.002(1)	0.003(1)
C(8)	0.040(2)	0.037(2)	0.040(2)	-0.002(2)	0.002(2)	-0.010(2)
C(9)	0.032(2)	0.043(2)	0.037(2)	0.004(2)	-0.002(2)	-0.007(2)
N(10)	0.033(2)	0.031(2)	0.037(2)	0.003(1)	0.002(1)	0.001(1)
C(11)	0.044(2)	0.039(2)	0.038(2)	0.003(2)	-0.002(2)	-0.013(2)
C(12)	0.034(2)	0.042(2)	0.040(2)	0.004(2)	-0.002(2)	-0.007(2)
C(13)	0.035(2)	0.038(2)	0.035(2)	-0.005(2)	0.007(2)	0.000(2)
C(14)	0.034(2)	0.043(2)	0.035(2)	0.003(2)	0.007(2)	0.000(2)
C(15)	0.047(2)	0.057(3)	0.045(2)	0.000(2)	0.005(2)	0.006(2)
C(16)	0.049(3)	0.091(4)	0.054(3)	0.012(3)	0.003(2)	0.017(2)
C(17)	0.048(3)	0.108(4)	0.040(3)	-0.002(3)	0.002(2)	-0.008(3)
C(18)	0.056(3)	0.082(3)	0.051(3)	-0.021(2)	0.006(2)	-0.014(3)
C(19)	0.045(2)	0.050(2)	0.051(3)	-0.006(2)	0.007(2)	-0.003(2)
C(14')	0.041(2)	0.043(2)	0.037(2)	-0.005(2)	0.009(2)	-0.004(2)
C(15')	0.055(3)	0.046(3)	0.092(3)	-0.003(2)	0.019(2)	-0.007(2)
C(16')	0.086(4)	0.049(3)	0.116(4)	-0.008(3)	0.031(3)	-0.019(3)
C(17')	0.075(4)	0.086(4)	0.075(3)	-0.021(3)	0.024(3)	-0.043(3)
C(18')	0.046(3)	0.098(4)	0.061(3)	-0.005(3)	0.011(2)	-0.014(3)
C(19')	0.042(2)	0.067(3)	0.048(2)	0.005(2)	0.011(2)	-0.006(2)
C(20)	0.037(2)	0.041(2)	0.032(2)	0.006(2)	0.008(2)	0.002(2)
C(21)	0.049(2)	0.044(2)	0.048(2)	-0.002(2)	0.000(2)	0.005(2)
C(22)	0.065(3)	0.041(2)	0.058(3)	-0.006(2)	0.002(2)	0.005(2)
C(23)	0.062(3)	0.046(3)	0.056(3)	0.011(2)	0.014(2)	0.015(2)
C(23')	0.104(4)	0.057(3)	0.093(4)	0.008(3)	0.007(3)	0.026(3)
C(24)	0.049(2)	0.059(3)	0.066(3)	0.018(2)	-0.001(2)	0.013(2)
C(25)	0.046(2)	0.048(3)	0.053(3)	0.010(2)	0.000(2)	0.001(2)
Cl(1)	0.0449(5)	0.0493(6)	0.0516(6)	0.0023(5)	-0.0018(4)	-0.0121(4)
Cl(2)	0.0654(7)	0.0512(6)	0.0735(7)	0.0089(5)	-0.0139(6)	-0.0203(5)
Cl(3)	0.0587(7)	0.0485(6)	0.0758(7)	-0.0001(5)	0.0162(5)	-0.0168(5)
O(1)	0.115(9)	0.068(7)	0.163(12)	-0.015(7)	-0.050(8)	0.008(7)

Table B.5 Positional and thermal parameters for IMTHCLB

	x	y	z	U_{eq}
N(1)	0.1169(11)	1.1196(5)	0.2739(6)	0.058(7)
C(2)	0.1953(14)	1.1509(6)	0.2153(7)	0.051(7)
N(3)	0.0523(11)	1.1216(5)	0.1449(6)	0.057(6)
C(4)	-0.1206(13)	1.0689(6)	0.1584(6)	0.050(7)
C(4')	-0.3022(13)	1.0261(6)	0.0916(7)	0.062(8)
C(5)	-0.0765(12)	1.0687(5)	0.2394(6)	0.044(7)
C(6)	-0.2016(12)	1.0333(6)	0.2963(7)	0.055(7)
N(7)	-0.1510(10)	0.9412(5)	0.2937(5)	0.045(6)
C(8)	-0.2347(12)	0.9233(5)	0.3684(6)	0.049(7)
C(9)	-0.1752(11)	0.8333(5)	0.3666(6)	0.045(7)
N(10)	-0.2535(9)	0.7408(4)	0.2750(5)	0.042(5)
C(11)	-0.1737(12)	0.7588(5)	0.1980(6)	0.049(7)
C(12)	-0.2265(11)	0.8497(5)	0.2002(6)	0.042(6)
C(13)	-0.1967(11)	0.6489(5)	0.2724(6)	0.043(6)
C(14)	-0.2750(11)	0.5559(5)	0.1772(6)	0.045(7)
C(15)	-0.4723(13)	0.5099(7)	0.1478(8)	0.067(9)
C(16)	-0.5343(15)	0.4223(7)	0.0628(8)	0.071(9)
C(17)	-0.3958(17)	0.3809(7)	0.0089(7)	0.066(8)
C(18)	-0.2015(17)	0.4253(7)	0.0364(8)	0.076(10)
C(19)	-0.1400(13)	0.5130(7)	0.1210(7)	0.056(8)
C(14')	-0.2540(13)	0.6342(6)	0.3533(6)	0.049(7)
C(15')	-0.4426(13)	0.6327(7)	0.3787(7)	0.075(9)
C(16')	-0.4668(16)	0.6166(8)	0.4551(9)	0.100(11)
C(17')	-0.3455(21)	0.6045(8)	0.5034(9)	0.101(12)
C(18')	-0.1588(19)	0.6066(7)	0.4792(8)	0.093(11)
C(19')	-0.1117(15)	0.6219(7)	0.4046(8)	0.083(10)
C(20)	0.3982(13)	1.2065(6)	0.2283(7)	0.053(8)
C(21)	0.5342(14)	1.2222(6)	0.2985(7)	0.061(8)
C(22)	0.7261(15)	1.2750(7)	0.3105(7)	0.069(8)
C(23)	0.7680(14)	1.3159(6)	0.2534(9)	0.073(9)
C(23')	0.9978(14)	1.3726(7)	0.2642(8)	0.088(10)
C(24)	0.6519(15)	1.3014(7)	0.1835(8)	0.083(10)
C(25)	0.4587(14)	1.2484(7)	0.1709(8)	0.079(9)
Cl(1)	0.3079(3)	0.73959(17)	0.25723(19)	0.0721(21)
Cl(2)	-0.2707(3)	0.95159(19)	0.59600(19)	0.0740(21)
Cl(3)	0.0195(4)	1.18810(20)	-0.00023(20)	0.0861(24)
O(1)	0.2921(10)	0.8328(5)	0.4851(6)	0.108(7)
O(2)	-0.6855(13)	0.9065(7)	0.1728(7)	0.140(10)

H(1)	0.1952	1.1226	0.3189	0.0500
H(3)	0.0666	1.1420	0.0949	0.0500
H(41')	-0.4298	1.0078	0.1219	0.0500
H(42')	-0.2927	0.9573	0.0298	0.0500
H(43')	-0.3307	1.0778	0.0663	0.0500
H(61)	-0.1770	1.0930	0.3680	0.0500
H(62)	-0.3552	1.0144	0.2681	0.0500
H(7)	-0.0036	0.9643	0.3147	0.0500
H(81)	-0.1787	0.9891	0.4357	0.0500
H(82)	-0.3939	0.9084	0.3567	0.0500
H(91)	-0.2340	0.8215	0.4219	0.0500
H(92)	-0.0159	0.8484	0.3774	0.0500
H(10)	-0.3952	0.7350	0.2703	0.0500
H(111)	-0.0148	0.7709	0.2070	0.0500
H(112)	-0.2357	0.6935	0.1311	0.0500
H(121)	-0.3852	0.8360	0.1871	0.0500
H(122)	-0.1610	0.8626	0.1466	0.0500
H(131)	-0.0374	0.6630	0.2804	0.0500
H(15)	-0.5801	0.5428	0.1909	0.0500
H(16)	-0.6897	0.3866	0.0396	0.0500
H(17)	-0.4430	0.3120	-0.0569	0.0500
H(18)	-0.0939	0.3927	-0.0072	0.0500
H(19)	0.0157	0.5483	0.1434	0.0500
H(15')	-0.5556	0.6425	0.3394	0.0500
H(16')	-0.6322	0.6193	0.4761	0.0500
H(17')	-0.3805	0.5908	0.5609	0.0500
H(18')	-0.0466	0.5966	0.5188	0.0500
H(19')	0.0362	0.6240	0.3863	0.0500
H(21)	0.4900	1.1934	0.3455	0.0500
H(22)	0.8338	1.2845	0.3655	0.0500
H(231)	1.0822	1.3789	0.3236	0.0500
H(232)	0.9988	1.4462	0.2743	0.0500
H(233)	1.0615	1.3323	0.2022	0.0500
H(24)	0.6950	1.3317	0.1375	0.0500
H(25)	0.3528	1.2390	0.1161	0.0500

	U_{11}	U_{22}	U_{33}	U_{23}	U_{13}	U_{12}
N(1)	0.063(6)	0.046(4)	0.051(7)	0.029(5)	0.007(5)	0.014(4)
C(2)	0.061(6)	0.044(5)	0.035(7)	0.023(5)	0.007(6)	0.022(5)
N(3)	0.061(5)	0.051(4)	0.050(6)	0.034(4)	0.019(5)	0.020(4)
C(4)	0.066(6)	0.048(5)	0.025(7)	0.019(5)	0.001(5)	0.028(5)
C(4')	0.072(6)	0.057(6)	0.039(7)	0.022(5)	0.002(6)	0.017(5)
C(5)	0.047(5)	0.033(4)	0.037(7)	0.015(4)	0.001(5)	0.011(4)
C(6)	0.050(5)	0.054(5)	0.049(7)	0.033(5)	0.010(5)	0.013(4)
N(7)	0.036(4)	0.045(4)	0.042(6)	0.031(4)	0.004(4)	0.003(3)
C(8)	0.061(5)	0.035(4)	0.034(7)	0.013(4)	0.006(5)	0.006(4)
C(9)	0.048(5)	0.036(5)	0.036(7)	0.016(5)	-0.001(4)	0.001(4)
N(10)	0.032(3)	0.037(4)	0.041(5)	0.017(4)	0.007(4)	0.008(3)
C(11)	0.057(5)	0.049(5)	0.027(6)	0.021(5)	0.020(5)	0.011(4)
C(12)	0.043(5)	0.039(5)	0.029(6)	0.014(5)	0.006(4)	0.009(4)
C(13)	0.043(5)	0.036(5)	0.038(6)	0.018(5)	0.007(4)	0.010(4)
C(14)	0.046(5)	0.040(5)	0.040(7)	0.026(5)	0.011(5)	0.014(4)
C(15)	0.047(6)	0.048(6)	0.075(10)	0.021(6)	-0.003(6)	0.002(5)
C(16)	0.061(6)	0.057(6)	0.067(9)	0.028(6)	-0.023(6)	-0.001(5)
C(17)	0.087(8)	0.045(5)	0.038(7)	0.006(5)	-0.004(6)	0.012(6)
C(18)	0.089(8)	0.064(7)	0.055(9)	0.027(7)	0.027(7)	0.022(6)
C(19)	0.052(5)	0.058(6)	0.039(7)	0.020(6)	0.010(5)	0.009(5)
C(14')	0.055(6)	0.041(5)	0.033(6)	0.015(5)	0.003(5)	0.006(4)
C(15')	0.049(6)	0.084(7)	0.074(8)	0.057(6)	0.013(6)	0.009(5)
C(16')	0.097(9)	0.094(8)	0.088(11)	0.064(8)	0.037(8)	0.017(7)
C(17')	0.118(10)	0.082(8)	0.083(11)	0.064(8)	0.025(9)	0.012(8)
C(18')	0.115(10)	0.085(8)	0.059(9)	0.052(7)	-0.019(8)	0.014(7)
C(19')	0.071(7)	0.076(7)	0.081(10)	0.049(7)	0.007(7)	0.019(6)
C(20)	0.056(6)	0.040(5)	0.047(8)	0.022(5)	0.006(6)	0.012(4)
C(21)	0.062(6)	0.064(6)	0.041(7)	0.034(5)	0.007(5)	0.013(5)
C(22)	0.073(7)	0.061(6)	0.053(8)	0.025(6)	0.005(6)	0.023(5)
C(23)	0.060(6)	0.049(6)	0.087(10)	0.030(6)	0.018(7)	0.021(5)
C(23')	0.071(7)	0.070(7)	0.097(11)	0.044(7)	0.022(7)	0.023(6)
C(24)	0.063(6)	0.088(7)	0.080(10)	0.062(7)	0.018(6)	0.016(6)
C(25)	0.063(6)	0.072(6)	0.081(10)	0.054(7)	0.002(6)	0.009(5)
Cl(1)	0.036(1)	0.075(2)	0.080(2)	0.038(2)	0.016(1)	0.018(1)
Cl(2)	0.061(1)	0.084(2)	0.055(2)	0.042(2)	0.002(1)	0.010(1)
Cl(3)	0.079(2)	0.096(2)	0.064(2)	0.053(2)	0.021(2)	0.031(2)
O(1)	0.067(4)	0.106(5)	0.098(7)	0.027(5)	0.019(5)	0.013(4)
O(2)	0.131(7)	0.142(7)	0.099(9)	0.062(7)	-0.017(6)	0.016(6)

Table B.6 Positional and thermal parameters for IMTHCLC

	x	y	z	U_{eq}
N(1)	0.4453(7)	0.3611(10)	0.0109(10)	0.047(13)
C(2)	0.4413(8)	0.4126(12)	-0.0482(14)	0.047(16)
N(3)	0.4592(7)	0.3748(9)	-0.1065(11)	0.053(13)
C(4)	0.4741(9)	0.2981(11)	-0.0851(13)	0.046(16)
C(4')	0.4929(11)	0.2422(12)	-0.1398(14)	0.081(20)
C(5)	0.4648(9)	0.2883(13)	-0.0111(14)	0.054(18)
C(6)	0.4760(8)	0.2189(11)	0.0463(12)	0.050(16)
N(7)	0.4179(7)	0.1786(8)	0.0426(10)	0.046(12)
C(8)	0.3907(9)	0.1417(11)	-0.0369(13)	0.053(16)
C(9)	0.3347(9)	0.1011(11)	-0.0378(12)	0.047(15)
N(10)	0.3434(7)	0.0399(8)	0.0287(10)	0.042(12)
C(11)	0.3723(10)	0.0764(12)	0.1075(12)	0.055(16)
C(12)	0.4294(9)	0.1161(11)	0.1078(12)	0.055(16)
C(13)	0.2846(10)	0.0032(12)	0.0288(14)	0.065(19)
C(14)	0.2521(11)	-0.0274(14)	-0.0557(14)	0.058(19)
C(15)	0.2733(12)	-0.0911(14)	-0.0904(18)	0.091(24)
C(16)	0.2416(16)	-0.1136(16)	-0.1672(20)	0.10(3)
C(17)	0.1899(14)	-0.0782(18)	-0.2075(16)	0.084(24)
C(18)	0.1717(11)	-0.0143(18)	-0.1730(18)	0.082(24)
C(19)	0.2024(11)	0.0099(14)	-0.0996(16)	0.062(19)
C(14')	0.2912(10)	-0.0541(12)	0.0988(14)	0.058(18)
C(15')	0.3289(12)	-0.1172(14)	0.1076(15)	0.073(22)
C(16')	0.3309(14)	-0.1694(14)	0.1686(18)	0.11(3)
C(17')	0.2959(13)	-0.1602(16)	0.2200(16)	0.083(24)
C(18')	0.2597(13)	-0.0973(19)	0.2108(16)	0.10(3)
C(19')	0.2574(10)	-0.0456(14)	0.1516(15)	0.069(20)
C(20)	0.4237(9)	0.4935(11)	-0.0476(14)	0.044(15)
C(21)	0.4099(10)	0.5236(12)	0.0182(15)	0.071(20)
C(22)	0.3688(11)	0.5967(15)	0.0137(16)	0.083(23)
C(23)	0.3629(11)	0.6460(14)	-0.0525(18)	0.077(21)
C(23')	0.3568(11)	0.7278(12)	-0.0597(15)	0.083(22)
C(24)	0.3989(10)	0.6148(14)	-0.1183(17)	0.079(22)
C(25)	0.4198(10)	0.5386(13)	-0.1176(13)	0.061(18)
Cl(1)	0.00000(0)	0.0630(5)	0.25000(0)	0.077(7)
Cl(2)	0.0625(5)	0.5692(5)	-0.0043(5)	0.170(10)
Cl(3)	0.0625(3)	0.5692(3)	-0.0043(4)	0.073(5)
Cl(4)	0.50000(0)	0.2576(19)	0.25000(0)	0.119(20)
Cl(5)	0.4573(13)	0.2505(16)	0.2539(17)	0.014(9)
O(1)	0.3330(7)	0.2808(9)	0.0561(11)	0.110(16)
O(2)	0.0439(6)	0.3717(16)	0.1732(11)	0.205(25)
O(3)	0.4097(14)	0.0922(25)	0.3115(16)	0.11(3)
O(4)	0.0267(19)	0.4572(19)	0.1959(20)	0.13(4)
O(5)	0.366(3)	0.216(3)	0.2447(25)	0.23(6)

H(1)	0.4353	0.3725	0.0670	0.0500
H(3)	0.4615	0.4016	-0.1625	0.0500
H(41)	0.5022	0.1859	-0.1102	0.0500
H(42)	0.5327	0.2639	-0.1506	0.0500
H(43)	0.4572	0.2365	-0.1979	0.0500
H(61)	0.4981	0.2386	0.1086	0.0500
H(62)	0.5046	0.1780	0.0288	0.0500
H(7)	0.3882	0.2226	0.0525	0.0500
H(81)	0.4216	0.1000	-0.0477	0.0500
H(82)	0.3802	0.1856	-0.0846	0.0500
H(91)	0.3036	0.1442	0.0300	0.0500
H(92)	0.3159	0.0730	-0.0969	0.0500
H(10)	0.3705	-0.0063	0.0167	0.0500
H(111)	0.3827	0.0325	0.1552	0.0500
H(112)	0.3424	0.1191	0.1192	0.0500
H(121)	0.4502	0.1424	0.1675	0.0500
H(122)	0.4593	0.0731	0.0965	0.0500
H(13)	0.2568	0.0476	0.0425	0.0500
H(15)	0.3140	-0.1217	-0.0573	0.0500
H(16)	0.2573	-0.1620	-0.1950	0.0500
H(17)	0.1643	-0.0990	-0.2681	0.0500
H(18)	0.1311	0.0166	-0.2060	0.0500
H(19)	0.1870	0.0597	-0.0735	0.0500
H(15')	0.3558	-0.1248	0.0676	0.0500
H(16')	0.3604	-0.2190	0.1758	0.0500
H(17')	0.2974	-0.2020	0.2678	0.0500
H(18')	0.2329	-0.0895	0.2508	0.0500
H(19')	0.2280	0.0040	0.1452	0.0500
H(21)	0.4144	0.4882	0.0720	0.0500
H(22)	0.3766	0.6190	0.0651	0.0500
H(231)	0.3572	0.7539	-0.1169	0.0500
H(232)	0.3834	0.7628	-0.0086	0.0500
H(233)	0.3112	0.7248	-0.0589	0.0500
H(24)	0.3949	0.6508	-0.1715	0.0500
H(25)	0.4318	0.5155	-0.1686	0.0500

	U_{11}	U_{22}	U_{33}	U_{23}	U_{13}	U_{12}
N(1)	0.059(12)	0.039(11)	0.041(12)	0.005(11)	0.025(10)	0.002(10)
C(2)	0.036(14)	0.048(15)	0.053(16)	0.010(14)	0.021(13)	0.003(11)
N(3)	0.059(13)	0.036(12)	0.062(13)	0.010(10)	0.031(11)	0.003(9)
C(4)	0.054(16)	0.039(14)	0.035(15)	0.013(12)	0.002(13)	0.008(12)
C(4')	0.108(22)	0.048(15)	0.079(18)	0.000(13)	0.042(17)	0.024(14)
C(5)	0.057(17)	0.038(15)	0.057(17)	0.006(13)	0.004(14)	0.006(12)
C(6)	0.037(14)	0.047(14)	0.059(16)	0.004(12)	0.012(12)	0.005(12)
N(7)	0.035(12)	0.022(9)	0.079(14)	0.001(10)	0.027(11)	0.007(8)
C(8)	0.056(16)	0.034(12)	0.058(17)	0.012(12)	0.009(14)	0.004(13)
C(9)	0.047(15)	0.051(14)	0.036(13)	0.006(12)	0.011(12)	0.010(12)
N(10)	0.043(12)	0.025(9)	0.049(12)	0.002(9)	0.001(10)	0.007(8)
C(11)	0.069(17)	0.040(13)	0.049(16)	0.005(12)	0.014(14)	0.014(14)
C(12)	0.071(17)	0.037(13)	0.046(15)	0.009(11)	0.009(13)	0.005(12)
C(13)	0.058(17)	0.038(13)	0.093(21)	0.010(15)	0.035(16)	0.000(13)
C(14)	0.051(17)	0.060(17)	0.055(18)	0.020(15)	0.014(17)	0.022(14)
C(15)	0.101(23)	0.048(17)	0.103(25)	0.027(16)	0.007(21)	0.034(16)
C(16)	0.136(31)	0.073(20)	0.087(25)	0.040(19)	0.034(23)	0.010(21)
C(17)	0.087(24)	0.081(23)	0.065(21)	0.001(19)	0.000(20)	0.021(19)
C(18)	0.067(21)	0.098(25)	0.068(22)	0.027(19)	0.006(19)	0.020(18)
C(19)	0.048(17)	0.081(18)	0.047(18)	0.003(15)	0.004(14)	0.002(16)
C(14')	0.068(18)	0.037(14)	0.065(17)	0.008(13)	0.034(15)	0.007(13)
C(15')	0.127(25)	0.004(16)	0.084(20)	0.024(15)	0.054(19)	0.005(17)
C(16')	0.161(30)	0.050(18)	0.110(25)	0.011(18)	0.078(25)	0.008(17)
C(17')	0.100(24)	0.075(21)	0.065(20)	0.010(15)	0.025(19)	0.037(17)
C(18')	0.113(26)	0.112(26)	0.072(21)	0.010(19)	0.068(20)	0.019(20)
C(19')	0.058(17)	0.077(19)	0.069(19)	0.001(16)	0.036(16)	0.002(14)
C(20)	0.049(14)	0.019(12)	0.057(15)	0.001(12)	0.018(13)	0.006(10)
C(21)	0.095(21)	0.034(14)	0.080(19)	0.008(13)	0.043(17)	0.010(14)
C(22)	0.093(22)	0.058(19)	0.094(23)	0.017(16)	0.050(18)	0.002(16)
C(23)	0.070(19)	0.043(16)	0.109(24)	0.014(17)	0.030(18)	0.010(14)
C(23')	0.091(21)	0.049(18)	0.093(22)	0.008(14)	0.013(17)	0.023(14)
C(24)	0.077(20)	0.047(17)	0.099(23)	0.006(16)	0.015(17)	0.006(15)
C(25)	0.073(18)	0.051(15)	0.054(17)	0.003(13)	0.028(15)	0.007(13)
Cl(1)	0.100(8)	0.067(6)	0.063(6)	0.000(0)	0.048(6)	0.000(0)
Cl(2)	0.244(12)	0.127(7)	0.130(8)	0.032(6)	0.096(8)	0.077(7)
Cl(3)	0.082(5)	0.001(4)	0.128(6)	0.003(4)	0.049(5)	0.014(4)
O(1)	0.100(14)	0.063(11)	0.154(18)	0.006(11)	0.046(13)	0.028(10)
O(2)	0.095(16)	0.414(39)	0.098(16)	0.142(21)	0.043(13)	0.007(20)
O(3)	0.074(24)	0.228(45)	0.026(18)	0.016(24)	0.003(18)	0.020(28)
O(4)	0.205(46)	0.080(27)	0.086(27)	0.019(21)	0.069(28)	0.021(27)
O(5)	0.340(74)	0.247(56)	0.105(36)	0.140(39)	0.120(44)	0.066(54)

Table B.7 Positional and thermal parameters for IMTHCLD

	x	y	z	U_{eq}
N(1)	0.3204(3)	0.2156(9)	0.5969(3)	0.046(6)
C(2)	0.3198(4)	0.2720(11)	0.5542(4)	0.049(8)
N(3)	0.3066(4)	0.4100(9)	0.5545(3)	0.051(7)
C(4)	0.2994(4)	0.4410(10)	0.5982(4)	0.045(7)
C(4')	0.2843(4)	0.5857(11)	0.6085(4)	0.066(8)
C(5)	0.3092(4)	0.3195(11)	0.6253(4)	0.043(7)
C(6)	0.3065(3)	0.2910(10)	0.6749(4)	0.047(7)
N(7)	0.3601(3)	0.3044(9)	0.7175(3)	0.047(6)
C(8)	0.3800(4)	0.4530(10)	0.7245(3)	0.046(7)
C(9)	0.4332(4)	0.4668(11)	0.7688(3)	0.046(7)
N(10)	0.4280(3)	0.4190(9)	0.8165(3)	0.051(7)
C(11)	0.4098(4)	0.2672(10)	0.8095(4)	0.057(8)
C(12)	0.3565(4)	0.2518(11)	0.7641(3)	0.052(7)
C(13)	0.4800(4)	0.4340(11)	0.8604(3)	0.045(7)
C(14)	0.4760(4)	0.3749(11)	0.9073(4)	0.053(7)
C(15)	0.4434(5)	0.4324(13)	0.9301(4)	0.071(9)
C(16)	0.4411(5)	0.3771(15)	0.9729(4)	0.084(11)
C(17)	0.4748(6)	0.2635(18)	0.9971(5)	0.093(12)
C(18)	0.5078(5)	0.2092(15)	0.9763(5)	0.083(11)
C(19)	0.5093(5)	0.2612(12)	0.9315(5)	0.075(9)
C(14')	0.5000(4)	0.5886(11)	0.8676(4)	0.050(8)
C(15')	0.4667(4)	0.7065(12)	0.8584(4)	0.057(8)
C(16')	0.4682(5)	0.8399(12)	0.8660(4)	0.062(9)
C(17')	0.5434(6)	0.8595(14)	0.8636(4)	0.074(10)
C(18')	0.5773(5)	0.7443(15)	0.8933(5)	0.083(10)
C(19')	0.5559(4)	0.6090(13)	0.8846(4)	0.065(9)
C(20)	0.3311(4)	0.2002(12)	0.5146(4)	0.053(8)
C(21)	0.3426(4)	0.0558(12)	0.5188(4)	0.055(8)
C(22)	0.3539(4)	-0.0098(13)	0.4823(4)	0.069(9)
C(23)	0.3553(4)	0.0582(16)	0.4408(4)	0.068(9)
C(23')	0.3711(5)	-0.0157(14)	0.4020(4)	0.090(11)
C(24)	0.3428(5)	0.2036(15)	0.4364(4)	0.074(10)
C(25)	0.3312(4)	0.2698(12)	0.4725(4)	0.065(9)
Cl(1)	0.44790(18)	0.1830(5)	0.66697(19)	0.156(5)
Cl(2)	0.26753(21)	0.6431(5)	0.48185(21)	0.159(5)
Cl(3)	0.1710(3)	0.0766(8)	0.67723(25)	0.219(7)
O(1)	0.6753(5)	0.0521(11)	0.3704(4)	0.093(6)
O(2)	0.3144(5)	0.1337(12)	0.2775(4)	0.126(10)
O(3)	0.7450(5)	0.1070(21)	0.7096(6)	0.201(17)
O(4)	0.6091(5)	0.1708(15)	0.2758(5)	0.167(12)
O(5)	0.2635(6)	0.3688(16)	0.8779(6)	0.149(13)
O(6)	0.50000(0)	0.062(3)	0.25000(0)	0.305(22)
O(6A)	0.4813(17)	0.207(5)	0.2424(21)	0.141(16)

H(3)	0.3005	0.4665	0.5362	0.0500
H(41')	0.2719	0.5846	0.6401	0.0500
H(42')	0.2508	0.6265	0.5765	0.0500
H(43')	0.3180	0.6582	0.6168	0.0500
H(61)	0.2786	0.3658	0.6605	0.0500
H(62)	0.2916	0.1843	0.6747	0.0500
H(7)	0.3813	0.2721	0.7144	0.0500
H(81)	0.3857	0.4874	0.6912	0.0500
H(82)	0.3500	0.5197	0.7306	0.0500
H(91)	0.4458	0.5767	0.7727	0.0500
H(92)	0.4634	0.4022	0.7623	0.0500
H(10)	0.4078	0.4715	0.8171	0.0500
H(111)	0.4406	0.2030	0.8039	0.0500
H(112)	0.4038	0.2312	0.8426	0.0500
H(121)	0.3254	0.3112	0.7711	0.0500
H(122)	0.3455	0.1408	0.7594	0.0500
H(131)	0.5099	0.3714	0.8527	0.0500
H(15)	0.4189	0.5242	0.9135	0.0500
H(16)	0.4133	0.4211	0.9681	0.0500
H(17)	0.4743	0.2209	1.0316	0.0500
H(18)	0.5341	0.1220	0.9948	0.0500
H(19)	0.5361	0.2136	0.9157	0.0500
H(15')	0.4232	0.6928	0.8452	0.0500
H(16')	0.4616	0.9309	0.8580	0.0500
H(17')	0.5600	0.9657	0.8898	0.0500
H(18')	0.6208	0.7594	0.9076	0.0500
H(19')	0.5825	0.5184	0.8911	0.0500
H(21)	0.3424	-0.0033	0.5507	0.0500
H(22)	0.3624	-0.1223	0.4860	0.0500
H(231)	0.3548	-0.1215	0.3960	0.0500
H(232)	0.4146	-0.0210	0.4147	0.0500
H(233)	0.3555	0.0424	0.3675	0.0500
H(24)	0.3425	0.2624	0.4042	0.0500
H(25)	0.3216	0.3817	0.4683	0.0500
H(1S1)	0.6668	0.0604	0.3431	0.0500
H(1S2)	0.7023	0.0560	0.3677	0.0500
H(2S1)	0.3486	0.1050	0.2842	0.0500
H(2S2)	0.2949	0.1228	0.2327	0.0500
H(3S1)	0.7316	0.2062	0.6917	0.0500
H(3S2)	0.7675	0.0876	0.7443	0.0500
H(4S1)	0.5939	0.0635	0.2600	0.0500
H(5S1)	0.2719	0.3378	0.8419	0.0500
H(5S2)	0.2977	0.3328	0.8627	0.0500

	U_{11}	U_{22}	U_{33}	U_{23}	U_{13}	U_{12}
N(1)	0.050(5)	0.037(5)	0.039(5)	-0.006(4)	0.010(4)	-0.002(4)
C(2)	0.039(6)	0.044(7)	0.049(7)	0.009(6)	0.000(5)	-0.002(5)
N(3)	0.051(5)	0.032(6)	0.055(7)	0.014(4)	0.008(5)	0.004(4)
C(4)	0.045(6)	0.039(7)	0.042(6)	-0.002(5)	0.014(5)	0.002(5)
C(4')	0.079(8)	0.038(7)	0.068(8)	-0.002(6)	0.029(7)	0.013(6)
C(5)	0.038(6)	0.036(7)	0.044(6)	-0.001(5)	0.007(5)	-0.005(5)
C(6)	0.035(6)	0.034(6)	0.063(7)	-0.003(5)	0.018(5)	-0.003(5)
N(7)	0.046(6)	0.038(6)	0.053(6)	-0.003(4)	0.026(5)	0.004(4)
C(8)	0.056(6)	0.034(6)	0.044(6)	0.000(5)	0.026(6)	0.010(5)
C(9)	0.057(6)	0.042(6)	0.038(6)	0.005(5)	0.023(5)	-0.009(5)
N(10)	0.057(6)	0.036(6)	0.053(5)	0.003(5)	0.027(5)	-0.003(4)
C(11)	0.076(7)	0.037(7)	0.051(7)	0.003(5)	0.031(6)	-0.004(6)
C(12)	0.068(7)	0.035(6)	0.045(6)	-0.010(5)	0.027(6)	-0.016(5)
C(13)	0.038(6)	0.046(7)	0.045(6)	0.002(5)	0.016(5)	0.000(5)
C(14)	0.059(7)	0.050(7)	0.043(6)	0.002(6)	0.022(6)	-0.018(6)
C(15)	0.086(9)	0.065(8)	0.053(7)	0.012(7)	0.034(7)	-0.002(7)
C(16)	0.098(10)	0.088(11)	0.060(8)	-0.005(8)	0.044(8)	-0.023(9)
C(17)	0.102(11)	0.109(13)	0.049(8)	0.025(8)	0.017(8)	-0.033(10)
C(18)	0.071(9)	0.079(10)	0.077(10)	0.035(8)	0.006(8)	-0.013(8)
C(19)	0.071(8)	0.057(8)	0.083(9)	0.012(8)	0.031(7)	0.006(7)
C(14')	0.062(7)	0.044(7)	0.038(6)	0.002(5)	0.022(5)	-0.009(6)
C(15')	0.053(6)	0.047(8)	0.063(8)	-0.002(6)	0.026(6)	-0.006(6)
C(16')	0.067(8)	0.049(8)	0.058(8)	-0.001(6)	0.019(6)	-0.006(6)
C(17')	0.101(10)	0.067(9)	0.045(7)	-0.006(7)	0.031(7)	-0.029(8)
C(18')	0.061(8)	0.072(10)	0.101(10)	-0.003(8)	0.027(7)	-0.017(8)
C(19')	0.056(8)	0.057(8)	0.074(8)	-0.006(6)	0.031(6)	-0.001(6)
C(20)	0.045(6)	0.046(8)	0.052(7)	0.001(6)	0.000(5)	0.000(6)
C(21)	0.069(7)	0.048(8)	0.043(7)	0.009(6)	0.028(6)	0.009(6)
C(22)	0.065(8)	0.057(8)	0.074(9)	-0.001(7)	0.026(7)	0.009(6)
C(23)	0.051(7)	0.090(11)	0.050(8)	-0.012(8)	0.011(6)	-0.002(7)
C(23')	0.103(10)	0.095(11)	0.056(8)	-0.003(7)	0.032(8)	0.001(8)
C(24)	0.084(9)	0.082(11)	0.050(8)	0.008(7)	0.034(7)	0.005(8)
C(25)	0.077(8)	0.042(7)	0.063(8)	0.011(6)	0.027(7)	0.001(6)
Cl(1)	0.118(3)	0.145(4)	0.186(5)	-0.064(4)	0.075(3)	-0.016(3)
Cl(2)	0.175(4)	0.093(3)	0.184(5)	0.037(3)	0.075(4)	0.027(3)
Cl(3)	0.224(6)	0.195(6)	0.213(6)	0.046(5)	0.110(5)	0.035(5)
O(1)	0.133(9)	0.040(5)	0.093(7)	0.008(6)	0.057(8)	0.009(6)
O(2)	0.156(10)	0.110(9)	0.098(8)	0.016(7)	0.049(8)	0.023(8)
O(3)	0.122(11)	0.265(21)	0.192(15)	-0.098(16)	0.061(10)	0.044(12)
O(4)	0.167(11)	0.141(11)	0.148(11)	0.062(9)	0.016(9)	-0.013(9)
O(5)	0.123(9)	0.163(13)	0.154(14)	0.003(9)	0.090(10)	-0.017(9)
O(6)	0.108(19)	0.124(25)	0.068(16)	0.000(0)	0.036(15)	0.000(0)

Table B.8 Positional and thermal parameters for IMTHCLE

	x	y	z	U_{eq}
N(1)	0.6941(4)	0.30269(24)	0.58605(22)	0.0407(20)
C(2)	0.5461(4)	0.3360(3)	0.5565(3)	0.0403(23)
N(3)	0.4740(4)	0.2982(3)	0.6345(3)	0.0500(22)
C(4)	0.5716(5)	0.2410(3)	0.7146(3)	0.052(3)
C(4')	0.5176(6)	0.1925(5)	0.8139(4)	0.085(4)
C(5)	0.7099(4)	0.2437(3)	0.6840(3)	0.0424(24)
C(6)	0.6606(4)	0.1992(3)	0.7382(3)	0.0462(24)
N(7)	0.9542(3)	0.10178(24)	0.71987(23)	0.0418(20)
C(8)	1.1147(5)	0.0784(3)	0.7562(3)	0.053(3)
C(9)	1.2116(5)	-0.0173(3)	0.7366(4)	0.054(3)
N(10)	1.1552(4)	-0.11030(25)	0.78460(23)	0.0413(20)
C(11)	0.9943(4)	-0.0867(3)	0.7506(3)	0.052(3)
C(12)	0.8958(5)	0.0111(3)	0.7695(3)	0.052(3)
C(13)	1.2547(4)	-0.2048(3)	0.7616(3)	0.0474(25)
C(14)	1.1930(4)	-0.2977(3)	0.7991(3)	0.0476(25)
C(15)	1.2076(6)	-0.3593(4)	0.8974(3)	0.070(3)
C(16)	1.1619(7)	-0.4492(4)	0.9265(4)	0.083(4)
C(17)	1.1026(6)	-0.4802(4)	0.8591(5)	0.082(4)
C(18)	1.0865(6)	-0.4199(4)	0.7629(4)	0.079(4)
C(19)	1.1302(5)	-0.3293(4)	0.7328(4)	0.062(3)
C(14')	1.4193(5)	-0.2272(3)	0.7949(3)	0.050(3)
C(15')	1.4625(5)	-0.2349(4)	0.8878(4)	0.069(4)
C(16')	1.6174(6)	-0.2602(5)	0.9152(5)	0.086(4)
C(17')	1.7242(6)	-0.2768(4)	0.8497(6)	0.085(4)
C(18')	1.6814(6)	-0.2697(5)	0.7593(6)	0.096(5)
C(19')	1.5283(6)	-0.2448(4)	0.7293(4)	0.079(4)
C(20)	0.4846(4)	0.3999(3)	0.4575(3)	0.0430(24)
C(21)	0.5768(5)	0.4378(3)	0.3856(3)	0.054(3)
C(22)	0.5158(5)	0.4961(4)	0.2914(3)	0.062(3)
C(23)	0.3645(5)	0.5170(3)	0.2678(3)	0.060(3)
C(23')	0.3014(8)	0.5741(5)	0.1632(4)	0.095(5)
C(24)	0.2747(5)	0.4822(4)	0.3404(4)	0.066(3)
C(25)	0.3316(5)	0.4225(4)	0.4357(4)	0.060(3)
Cl(1)	0.13464(13)	0.35283(11)	0.67675(10)	0.0775(10)
Cl(2)	1.12969(17)	-0.13246(12)	1.00197(9)	0.0842(10)
Cl(31)	1.0617(9)	-0.1057(4)	0.4889(4)	0.1119(16)
Cl(32)	0.9904(22)	-0.1322(14)	0.4882(13)	0.092(4)
Cl(33)	1.1626(8)	-0.0947(4)	0.4843(3)	0.0892(12)
Cl(34)	1.245(3)	-0.0675(13)	0.4834(12)	0.085(4)
O(1)	1.0470(6)	-0.3460(7)	0.4987(4)	0.162(6)
O(2)	0.1411(6)	0.2347(4)	-0.0849(4)	0.131(5)
O(3)	0.3401(7)	0.0254(5)	0.9755(6)	0.176(6)
O(41)	0.1943(18)	0.1546(12)	0.4924(11)	0.230(6)
O(42)	0.294(3)	0.1508(17)	0.5235(16)	0.118(6)
O(51)	0.500(3)	0.0610(18)	0.5748(16)	0.168(8)
O(52)	0.613(3)	0.0787(21)	0.5238(20)	0.184(9)
O(53)	0.5593(25)	-0.0021(17)	0.7320(16)	0.165(7)
H(1)	0.7723	0.3271	0.5503	0.0500
H(3)	0.3936	0.3046	0.6380	0.0500
H(41)	0.6014	0.1713	0.6733	0.0500
H(42)	0.4682	0.1219	0.6173	0.0500
H(43)	0.4167	0.2438	0.6311	0.0500
H(61)	0.9222	0.2571	0.7151	0.0500
H(62)	0.8436	0.1809	0.6166	0.0500
H(7)	0.9404	0.1105	0.6511	0.0500
H(81)	1.1580	0.1436	0.7179	0.0500
H(82)	1.1181	0.0657	0.6350	0.0500
H(91)	1.3253	-0.0333	0.7656	0.0500
H(92)	1.2121	-0.0026	0.6576	0.0500
H(10)	1.1626	-0.1199	0.6340	0.0500
H(111)	0.9690	-0.0746	0.6720	0.0500
H(112)	0.9515	-0.1519	0.7903	0.0500
H(121)	0.6958	-0.0021	0.6465	0.0500
H(122)	0.7618	0.0272	0.7409	0.0500
H(131)	1.2526	-0.1862	0.6619	0.0500
H(15)	1.2550	-0.3370	0.9521	0.0500
H(16)	1.1733	-0.4961	1.0041	0.0500
H(17)	1.0694	-0.5516	0.8624	0.0500
H(18)	1.0388	-0.4426	0.7086	0.0500
H(19)	1.1148	-0.2819	0.6554	0.0500
H(15')	1.3763	-0.2218	0.9406	0.0500
H(16')	1.6511	-0.2664	0.9890	0.0500
H(17')	1.8425	-0.2955	0.8706	0.0500
H(18')	1.7667	-0.2635	0.7074	0.0500
H(19')	1.4969	-0.2397	0.6554	0.0500
H(21)	0.6958	0.4221	0.4026	0.0500
H(1)	0.5682	0.5261	0.2347	0.0500
H(231)	0.3799	0.6099	0.1173	0.0500
H(232)	0.1955	0.6314	0.1595	0.0500
H(233)	0.2797	0.5166	0.1304	0.0500
H(24)	0.1548	0.5016	0.3236	0.0500
H(25)	0.2582	0.3939	0.4923	0.0500

	U_{11}	U_{22}	U_{33}	U_{23}	U_{13}	U_{12}
N(1)	0.035(2)	0.040(2)	0.034(2)	-0.007(1)	-0.004(1)	-0.001(1)
C(2)	0.036(2)	0.036(2)	0.039(2)	-0.012(2)	-0.003(2)	-0.001(2)
N(3)	0.034(2)	0.048(2)	0.050(2)	-0.002(2)	-0.003(2)	-0.004(2)
C(4)	0.044(2)	0.048(2)	0.046(2)	0.000(2)	0.000(2)	-0.004(2)
C(4')	0.062(3)	0.103(4)	0.055(3)	0.017(3)	0.003(2)	-0.016(3)
C(5)	0.044(2)	0.033(2)	0.038(2)	-0.006(2)	-0.004(2)	-0.001(2)
C(6)	0.044(2)	0.046(2)	0.035(2)	-0.011(2)	-0.009(2)	0.002(2)
N(7)	0.036(2)	0.040(2)	0.033(2)	-0.003(1)	-0.005(1)	-0.001(1)
C(8)	0.043(2)	0.038(2)	0.064(3)	-0.007(2)	-0.009(2)	-0.002(2)
C(9)	0.040(2)	0.040(2)	0.065(3)	-0.003(2)	0.000(2)	-0.005(2)
N(10)	0.040(2)	0.041(2)	0.030(2)	-0.005(1)	-0.003(1)	-0.003(1)
C(11)	0.039(2)	0.047(2)	0.058(3)	-0.016(2)	-0.006(2)	-0.005(2)
C(12)	0.042(2)	0.042(2)	0.058(3)	-0.008(2)	-0.002(2)	-0.006(2)
C(13)	0.050(2)	0.044(2)	0.036(2)	-0.011(2)	-0.001(2)	-0.004(2)
C(14)	0.044(2)	0.043(2)	0.044(2)	-0.016(2)	-0.004(2)	-0.001(2)
C(15)	0.095(4)	0.054(3)	0.046(3)	-0.004(2)	-0.012(2)	-0.027(3)
C(16)	0.106(4)	0.060(3)	0.067(3)	-0.005(3)	-0.006(3)	-0.032(3)
C(17)	0.065(3)	0.055(3)	0.111(5)	-0.028(3)	0.013(3)	-0.019(3)
C(18)	0.060(3)	0.077(4)	0.092(4)	-0.049(3)	0.004(3)	-0.018(3)
C(19)	0.047(3)	0.067(3)	0.060(3)	-0.031(2)	0.002(2)	-0.008(2)
C(14')	0.044(2)	0.038(2)	0.056(3)	-0.012(2)	0.000(2)	-0.002(2)
C(15')	0.046(3)	0.075(3)	0.065(3)	-0.015(2)	-0.006(2)	-0.003(2)
C(16')	0.059(3)	0.086(4)	0.088(4)	-0.013(3)	-0.022(3)	-0.008(3)
C(17')	0.039(3)	0.067(3)	0.127(5)	-0.025(3)	-0.005(3)	-0.002(2)
C(18')	0.048(3)	0.087(4)	0.133(6)	-0.047(4)	0.022(3)	-0.004(3)
C(19')	0.062(3)	0.073(3)	0.092(4)	-0.043(3)	0.023(3)	-0.016(3)
C(20)	0.041(2)	0.034(2)	0.043(2)	-0.014(2)	-0.005(2)	0.000(2)
C(21)	0.046(2)	0.058(3)	0.040(2)	-0.012(2)	-0.005(2)	0.001(2)
C(22)	0.066(3)	0.061(3)	0.040(2)	-0.008(2)	-0.003(2)	0.001(2)
C(23)	0.067(3)	0.047(2)	0.048(2)	-0.015(2)	-0.019(2)	0.003(2)
C(23')	0.111(5)	0.084(4)	0.059(3)	-0.009(3)	-0.037(3)	0.004(4)
C(24)	0.050(3)	0.068(3)	0.066(3)	-0.013(2)	-0.026(2)	-0.002(2)
C(25)	0.043(2)	0.058(3)	0.062(3)	-0.007(2)	-0.015(2)	-0.009(2)
Cl(1)	0.046(1)	0.082(1)	0.091(1)	-0.039(1)	0.005(1)	-0.016(1)
Cl(2)	0.093(1)	0.088(1)	0.046(1)	-0.016(1)	0.001(1)	-0.003(1)
O(1)	0.096(3)	0.341(10)	0.092(3)	-0.096(5)	0.043(3)	-0.129(5)
O(2)	0.127(4)	0.134(4)	0.104(4)	-0.030(3)	-0.014(3)	-0.041(3)
O(3)	0.128(5)	0.109(4)	0.231(7)	0.025(4)	-0.055(5)	-0.028(4)